

**Direct Examination of Initiation and Propagation Kinetics of
Zirconocene-Catalyzed Alkene Polymerization**

Thesis by

Sara Bernadine Klamo

In Partial Fulfillment of the Requirements for the
Degree of Doctor of Philosophy

Division of Chemistry and Chemical Engineering
California Institute of Technology
Pasadena, California

2005

(Defended May 27, 2005)

© 2005

Sara Bernadine Klamo

All Rights Reserved

*For Dad, Mom, Rachel, Joe,
Ben, Grandpa, and Ramez.*

Acknowledgements

Graduate school has been a time of great personal growth for me, due to interactions with both outstanding scientists and people. The support of my research advisor, John Bercaw, has made my pursuit of a Ph.D. possible. I have learned a tremendous amount from him during my time in graduate school. I appreciated his management style and thank him for teaching us to think and to become independent scientists. Thank you for the opportunity and to you and Diane for all you have done for the group and for me.

Thank you to my committee – Profs. Harry Gray, Bob Grubbs, Dave MacMillan, and Brian Stoltz for teaching me to learn and think about chemistry in a constructive way. Special thanks to Bob Grubbs for helpful advice; and to Harry Gray for having an open door and caring about me like one of your own students. Also, Dr. Jay Labinger for research suggestions and comments.

I have had a great experience in the Bercaw Group. Former group members, who helped me get started, have been greatly missed. Thank you to Ola Wendt for starting the project that became my thesis. Paul Chirik and Deanna Zubris taught me how to work on the vacuum line. Jeff Yoder was kind to help me with NMR and kinetics when he was busy writing up. Thanks for the Mustang and being a resource for me. Postdocs Cliff Baar, Christoph Balzarek, Reto Dorta, Alan Heyduk, Chris Levy, Alex Muci, and Joseph Sadighi were always available for chemistry questions, moral support, interesting discussions, and good advice. Alan, thanks for teasing me and for letting me cry on your shoulder. Thank you to Annita Zhong and Seva Rostovtsev for inspiring and teaching me, each in your own way. Antek Wong-Foy was a great coworker and an even better friend. I could always count on him for help with chemistry, for trips to get noodles, for nicknames, and to be there for me. Visiting Prof. Tom Livinghouse always provided a good story or a solution to a chemistry problem. Dr. John Scollard, Chris “Theory” Brandow, Lily Ackerman, and Susan Schofer were my buddies in the nook. Johnny patiently helped me with many computer malfunctions. Theory kept things lively in the office and in the lab; a big thank you for all of the recent assistance in the NMR facility. Lily and I shared many experiences, most memorable being TA’s, chemistry discussions in the nook, and the great Green Box repair. Thank you for experimental advice; I will

always admire your patience and unique spirit. Susan was an excellent lab-mate for five years and taught me many vacuum line tricks. I appreciated her easy going ways and her ability to make 213 a fun and hoppin' place to work. Her love of rap and Steely Dan is legendary.

Current group members have made the past year exciting and memorable. Thank you all for encouragement and support during my proposal and thesis writing endeavor. My classmate Endy Min, who made the group a friendlier place, will soon be starting a new adventure as well – good luck! Jonathan Owen had endless enthusiasm for any chemistry discussion and for adventure; it definitely kept me going during the graduate school experience. Thank you also for your patient help with my continuing computer malfunctions. Jeff Byers is the keeper of the vacuum line tradition. Jeff will always be remembered for great group 4 chemistry discussions, the infamous TA experience, and for his appreciation of Nelly. New buddies in the nook are Theo Agapie and Dave Weinberg. I admire Theo's spirit, his work ethic, and his knowledge of chemistry; thank you so much for help with proofreading. Dave has been like my adopted little brother, whose great personality, attitude, and caffeine habit are inspirational. Thanks for letting me share the pre-seminar ritual; one day you will win the lotto. Steve Baldwin is an excellent: Blue Box Czar, early metal coworker, and neighbor and a kind and caring person. Steve shuttled me home many times at night, appreciated the "boat", and helped make my last back-packing trip possible. Bolin Lin's quick mind and friendly nature are admired and appreciated – thanks for teaching me some Chinese culture. Paul Elowe has been my coworker (of uncanny compatibility) in 213 the past two years. I have really enjoyed getting to know him better and talking about our research projects. Thank you for the bitmaps Paul, and bon chance! Postdocs Tom Driver and Parisa Mehrkodavandi have been very generous with their chemistry expertise and time. Thanks to Tom for being chill, for help with chemistry and advice, and for proofreading efforts. Parisa has gone out of her way to help me, both scientifically and personally, and I have enjoyed our hiking adventures. Thank you for: helping me with talks, seemingly endless proofreading, and for providing encouragement when I needed it the most. I could always count on you, as a running buddy and as a friend. Best of luck to new group

members Dr. Patrick Vagner and George Chen – already on his way to becoming a night-owl.

Thank you to surrogate group members: Salvo Carnabuci, Crystal Shih, Yen Nguyen, Anna Folinsky, and Adrian Driver for being fun, kind, and caring people; and to SURFS David Kurtz, Nick Piro, and Smaranda Marinescu for their enthusiasm in the lab. I enjoyed getting to know Heather Weincko and Brian Zeglis – good luck to you both.

Completion of a Ph.D. would not have been possible without the support and assistance of many people. Thank you to undergraduate mentors, Drs. John Montgomery and Darryl Williams, for encouraging me to pursue an advanced degree. Pat Anderson keeps things running smoothly; thanks for being like a “Mom” and taking me shopping. Diane Buchness helped keep me organized and was a patient listener. Thank you to Rick Gerhart, Steve Gould, Lilian Kremar, Joe Drew, Dr. Mike Day, Larry Henling, and Chris Smith for aid in different capacities. Tom Dunn was caring and always ready to lend a hand in the NMR facility. NMR manager, Dr. Scott Ross made my life as a graduate student so much better – thank you for everything.

I was lucky enough to have the support of two great friends. Shane Foister, thank you for always being there for me (and the big one) and for helping me to see the bright side of things. Will Wehbi was a running buddy and a great room-mate. Thank you for listening to me, for teaching me some Arabic, and for encouraging me.

My family has made this all possible. Thank you for all your help and encouragement. My Grandma and Grandpa provided me with courage and inspiration. My parents made many sacrifices for me, provided the resources necessary to get to graduate school, and always supported me in any direction I wanted to pursue. I was lucky enough to spend four years in graduate school with my brother Joe. I will miss our football Saturdays, dinners, trips to Palmdale, and smoothie parties. Thank you for taking care of me when I needed the most help. My sister Rachel and my brother Ben have supported me from across the country with phone calls and kind words.

Finally, thank you to Ramez Elgammal for being my best friend and advocate. You have always been there for me, and your patience and constant encouragement have kept me going during the hardest times. I couldn't have done this without your support and help and I am looking forward to a new beginning with you.

Abstract

Zirconocene precatalysts with sterically bulky alkyl groups were designed in order to obtain models for the propagating species in zirconocene-catalyzed alkene polymerization. Alkyl lithium reagents $\text{Li}(\text{CH}_2\text{CEt}_3)$ and $\text{Li}(\text{CH}_2\text{CMe}_2\text{CH}_2\text{Ph})$ were prepared and utilized in methyl alkylzirconocene synthesis. Dialkyl and methyl alkylzirconocenes of the form $[(\eta^5\text{-C}_5\text{H}_5)(\eta^5\text{-C}_5\text{Me}_5)\text{Zr}(\text{R})_2]$, $[(\eta^5\text{-C}_5\text{H}_5)_2\text{Zr}(\text{R})(\text{CH}_3)]$, and $[(\eta^5\text{-C}_5\text{H}_5)(\eta^5\text{-C}_5\text{Me}_5)\text{Zr}(\text{R})(\text{CH}_3)]$ (where $\text{R} = \text{CH}_2\text{CMe}_3, \text{CH}_2\text{SiMe}_3, \text{CH}_2\text{CEt}_3, \text{CH}_2\text{CMe}_2\text{CH}_2\text{Ph}$) were synthesized and fully characterized by NMR spectroscopy and in some cases X-ray diffraction. The molecular structures determined display the bent-sandwich coordination mode common for zirconocenes. The observed structural parameters are slightly perturbed by the steric influence of the bulky alkyl group.

A direct examination of propagation kinetics for alkene polymerization using the zirconocenium initiator, $[(\eta^5\text{-C}_5\text{H}_5)(\eta^5\text{-C}_5\text{Me}_5)\text{Zr}(\text{CH}_2\text{CMe}_3)]^+[\text{CH}_3\text{B}(\text{C}_6\text{F}_5)_3]^-$, is reported. Propagation rate constants (k_p) for the polymerization of propene and a series of 1-alkenes catalyzed by $[(\eta^5\text{-C}_5\text{H}_5)(\eta^5\text{-C}_5\text{Me}_5)\text{Zr}(\text{CH}_2\text{CHR})_n\text{CH}_2\text{CMe}_3]^+[\text{CH}_3\text{B}(\text{C}_6\text{F}_5)_3]^-$ were measured by ^1H NMR spectroscopy in toluene- d_8 at low temperature. The k_p obtained for propene and other alkenes decreases with increasing chain length and steric influence. The overall activation parameters for propagation determined from an Eyring analysis are $\Delta H^\ddagger = 8.5(3) \text{ kcal}\cdot\text{mol}^{-1}$ and $\Delta S^\ddagger = -25(2) \text{ eu}$. The propagation rate was found to increase in the presence of $[\text{CH}_3\text{B}(\text{C}_6\text{F}_5)_3]^-$ counteranion and in a polar toluene- d_8 -chlorobenzene- d_5 solvent system. The experimental results are most consistent with propagation

mechanism that does not involve the formation of outer-sphere ions for alkene polymerization by this catalyst system.

Propene initiation kinetics have been examined for a series of alkylzirconocene initiators, $[(\eta^5\text{-C}_5\text{H}_5)(\eta^5\text{-C}_5\text{Me}_5)\text{Zr}(\text{R})]^+[\text{CH}_3\text{B}(\text{C}_6\text{F}_5)_3]^-$ ($\text{R} = \text{CH}_3$ (**5**), CH_2CMe_3 (**1**), CH_2SiMe_3 (**4**)). Measurement of k_i for the neopentyl initiator reveals that the rate of initiation is on the order of propagation for this catalyst. This initiator - with a polymeryl like alkyl group - serves as a model of the propagating species in propene polymerization. The catalyst initiation behavior has been investigated and the observed relative rates of propene initiation are not always predicted by ground-state (zirconium-carbon bond strength or extent of ion-pairing) considerations. The catalysts **4** and **5** are both poor initiators with $k_i \ll k_p$ and show less than 50% initiation in the presence of excess propene at $-60\text{ }^\circ\text{C}$ in toluene- d_8 .

TABLE OF CONTENTS

Dedication	iii
Acknowledgements	iv
Abstract	vii
Table of Contents	ix
List of Figures and Tables	x
Chapter 1	1
Dialkyl and Methyl alkylzirconocenes – Precursors to Propagating Species Models in Zirconocene- Catalyzed Alkene Polymerization	
Chapter 2	54
Direct Examination of Propagation Kinetics of Zirconocene-Catalyzed Propene Polymerization	
Chapter 3	109
Direct Examination of Propene Initiation Kinetics Using Mixed-Ring Zirconocene Initiators	
Appendix 1	155
Crystallographic Parameters and Tables	

List of Figures and Tables

Chapter 1

Figure 1. Initiators modeling the propagating catalyst species	5
Figure 2. Influence of ancillary ligation on β -H vs β -Me elimination	7
Figure 3. Molecular structure of 1	10
Figure 4. Molecular structure of 2	12
Figure 5. Molecular structure of 6	18
Figure 6. Steric interactions between Cp* ligand and alkyl β -CH ₂ Ph group in V	22
Figure 7. Methyl alkylzirconocene synthesis using 13 or 19	24
Figure 8. Molecular structure of 22	26
Table 1. Bond distances and angles from X-ray structure determination of 1	10
Table 2. Bond distances and angles from X-ray structure determination of 2	12
Table 3. Bond distances and angles from X-ray structure determination of 6	19
Table 4. Bond distances and angles from X-ray structure determination of 22	25

Chapter 2

Figure 1. Transition state model for alkene insertion	59
Figure 2. ¹ H and ¹⁹ F NMR spectra of 1	61
Figure 3. Product mixture obtained from 1 and 23 equiv propene (¹ H NMR)	64
Figure 4. Kinetics plot for the reaction of 2 and propene	65
Figure 5. Plot of observed rate constants for propene polymerization vs [Zr]	66
Figure 6. Eyring plot for the reaction of 2 with propene	67
Figure 7. 1 generated in the presence of one equiv 3 (¹ H, ¹⁹ F NMR)	70
Figure 8. Product mixture from 1 and 61 equiv propene with added 3 (¹ H NMR)	71
Figure 9. Plot of propene propagation rate constants vs [CH ₃ B(C ₆ F ₅) ₃]	73
Figure 10. Inner-sphere propagation step proposed for catalyst 2	82
Table 1. Propagation rate constants for 2 -catalyzed propene polymerization	67
Table 2. Propagation rate constants for 2 -catalyzed alkene polymerization	68
Table 3. Propene propagation rate constants for catalyst 2 with added 3	72
Table 4. Propene propagation rate constants for catalyst 2 in various solvents	75
Table 5. Dependence of observed rate constants on [1]	105
Table 6. Temperature dependence of propene propagation kinetics	105
Table 7. Propagation kinetics for various alkenes	106
Table 8. Propene propagation kinetics with added 3	106
Table 9. Propene propagation kinetics in toluene- <i>d</i> ₈ -chlorobenzene- <i>d</i> ₅ solvent	107

Chapter 3

Figure 1. Factors influencing the relative rates of initiation and propagation	112
Figure 2. Product mixture obtained from 1 and 12 equiv propene (¹ H NMR)	116
Figure 3. Product mixture obtained from 1 and two equiv propene (¹ H NMR)	117
Figure 4. Kinetics plot for the reaction of 1 and propene	119
Figure 5. Eyring plot for the reaction of 1 with propene	120
Figure 6. Product mixture obtained from 4 and 27 equiv propene (¹ H NMR)	122
Figure 7. Reaction of 5 with 93 equiv propene (¹ H NMR)	124
Figure 8. Initiation reaction of 1 with 11 equiv propene (¹ H NMR)	128

Chapter 3 (cont.)

Figure 9. Relating initiators 1 , 4 , and 5 to the propagating species	131
Table 1. Propene initiation and propagation rate constants for catalyst 1	119
Table 2. Propene initiation rate constants for initiators 1 , 4 , and 5	125
Table 3. Ion-pairing parameters for 1 , 4 , and 5 with added alkene (^1H , ^{19}F NMR)	127
Table 4. Temperature dependence of propene initiation kinetics with 1	153
Table 5. Propene initiation kinetics for various alkylzirconocene initiators	153

Appendix 1

Table 1. Crystal data and structure refinement for Compound 1	156
Table 2. Crystal data and structure refinement for Compound 2	158
Table 3. Crystal data and structure refinement for Compound 6	160
Table 4. Crystal data and structure refinement for Compound 22	162

Chapter 1

Dialkyl and Methyl alkylzirconocenes – Precursors to Propagating Species Models in Zirconocene-Catalyzed Alkene Polymerization

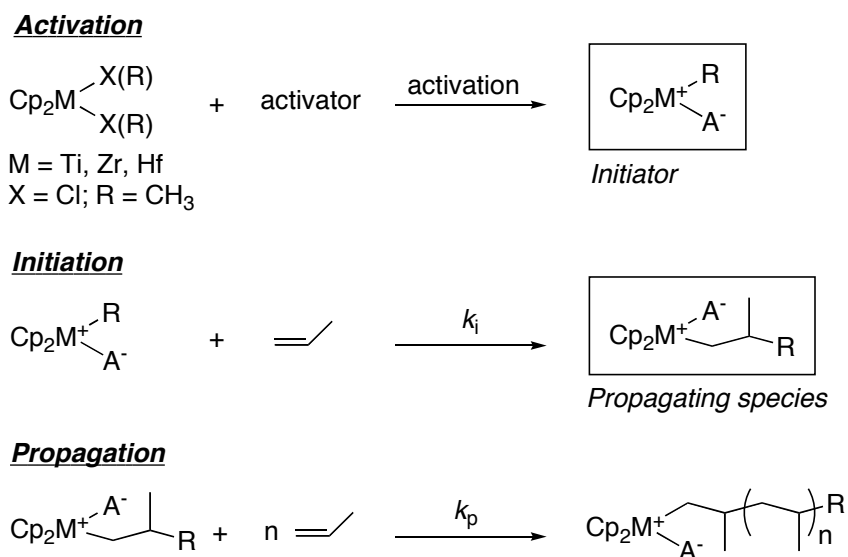
Abstract

Zirconocene precatalysts with sterically bulky alkyl groups were designed in order to obtain models for the propagating species in zirconocene-catalyzed alkene polymerization. Specialty alkyllithium reagents $\text{Li}(\text{CH}_2\text{CEt}_3)$ and $\text{Li}(\text{CH}_2\text{C}(\text{Me})_2\text{CH}_2\text{Ph})$ were prepared and utilized in methyl alkylzirconocene synthesis. Dialkyl and methyl alkylzirconocenes of the form $[(\eta^5\text{-C}_5\text{H}_5)(\eta^5\text{-C}_5\text{Me}_5)\text{Zr}(\text{R})_2]$, $[(\eta^5\text{-C}_5\text{H}_5)_2\text{Zr}(\text{R})(\text{CH}_3)]$, and $[(\eta^5\text{-C}_5\text{H}_5)(\eta^5\text{-C}_5\text{Me}_5)\text{Zr}(\text{R})(\text{CH}_3)]$ (where $\text{R} = \text{CH}_2\text{CMe}_3, \text{CH}_2\text{SiMe}_3, \text{CH}_2\text{CEt}_3, \text{CH}_2\text{C}(\text{Me})_2\text{CH}_2\text{Ph}$) were synthesized and fully characterized by NMR spectroscopy and in some cases X-ray diffraction. The molecular structures determined display the bent-sandwich coordination mode common for zirconocenes. The steric influence of the alkyl group on the observed structural parameters is reflected in slightly expanded carbon-Zr-carbon(chloride) angles in the equatorial plane and long zirconium-alkyl bond distance.

1 Introduction

The propagating catalyst species in metallocene-catalyzed alkene polymerization has been identified as a metallocenium-polymeryl ion having a weakly coordinating anion.¹ Traditionally, propagating species are generated in situ in a series of steps prior to propagation.² Starting from a neutral metallocene precatalyst (generally a dichloride or dimethyl species) the first step is reaction with an activator to generate a cationic, fourteen electron metal-alkyl initiator. This initiating species then reacts with alkene in the initiation step, to form the propagating species upon insertion of monomer into the metal-alkyl bond. (Scheme 1)

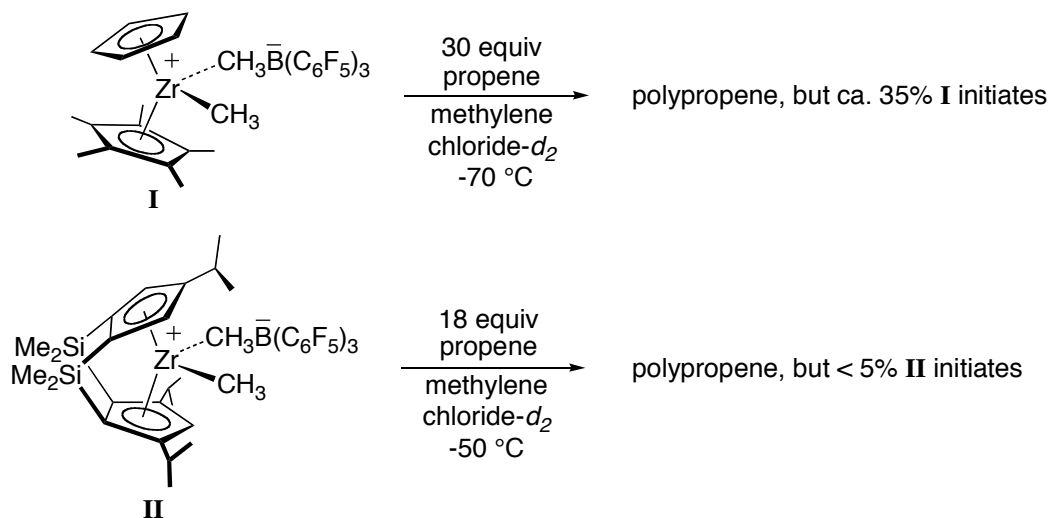
Scheme 1



The interest in developing models for the propagating species arose from a project examining fundamental aspects of zirconocene-catalyzed alkene polymerization using kinetic and mechanistic studies. Initial attempts towards these types of studies focused on propagation kinetics for propene polymerization and utilized anion-stabilized methyl-zirconocenium and hafnocenium catalysts of the type $[\text{Cp}^x_2\text{M}(\text{CH}_3)]^+[\text{CH}_3\text{B}(\text{C}_6\text{F}_5)_3]^-$ (Cp^x

$= \eta^5\text{-C}_5\text{R}_n\text{H}_{5-n}$). While this work suggested that propene propagation kinetics could be directly examined at low temperatures using direct ^1H NMR monitoring, limitations associated with the use of methyl-based initiators for these experiments were identified. In particular, these $[\text{M}]^+\text{-CH}_3$ cations displayed poor initiation behavior for propene polymerization, where only a small percentage of available catalyst was converted to the propagating species under the experimental conditions. When excess propene (18 - 30 equiv) was added to catalyst solutions at low temperatures, incomplete initiation occurred in all cases, as both $[\{\text{M}\}\text{-polymer}]^+[\text{CH}_3\text{B}(\text{C}_6\text{F}_5)_3]^-$ and unreacted $[\text{Cp}^x_2\text{M}(\text{CH}_3)]^+[\text{CH}_3\text{B}(\text{C}_6\text{F}_5)_3]^-$ were present after consumption of all monomer (Scheme 2).³

Scheme 2



For example, only 30-35% initiation was observed (^1H NMR, $-70\text{ }^\circ\text{C}$, CD_2Cl_2) for $[\text{CpCp}^*\text{Zr}(\text{CH}_3)]^+[\text{CH}_3\text{B}(\text{C}_6\text{F}_5)_3]^-$ ($\text{Cp} = \eta^5\text{-C}_5\text{H}_5$; $\text{Cp}^* = \eta^5\text{-C}_5\text{Me}_5$) (**I**) when treated with 30 equivalents of propene. Similarly, the *ansa*-zirconocene catalyst $[\text{iPrThpZr}(\text{CH}_3)]^+[\text{CH}_3\text{B}(\text{C}_6\text{F}_5)_3]^-$ ($\text{iPrThp} = [(1,2\text{-SiMe}_2)_2(4\text{-CHMe}_2\text{-}\eta^5\text{-C}_5\text{H}_2)(3,5\text{-}(\text{CHMe}_2)_2\text{-}\eta^5\text{-C}_5\text{H})]$) (**II**) showed less than 5% initiation after addition of 18 equivalents of

propene (^1H NMR, $-50\text{ }^\circ\text{C}$, CD_2Cl_2). These observations were attributed to $k_p \gg k_i$ (where k_p and k_i are the rate constants for propagation and initiation). Similar behavior has been reported for 1-hexene polymerization by other metallocene⁴ and nonmetallocene⁵ group 4 $[\text{M}]^+-\text{CH}_3$ initiators.

These findings prompted us to consider zirconocene initiators bearing polymeryl-like alkyl groups, where k_i may be on the same order as k_p . These compounds may model the propagating species formed in propene polymerization if the alkyl group, as compared to methyl, more closely resembles the polypropene polymeryl in both steric influence on ion pairing and Zr-C bond strength (Figure 1). Well-defined initiators suitable for use in kinetic studies may be produced directly from the activation step by reaction with an appropriate zirconocene precatalyst. Therefore, the synthesis of dialkyl- and methyl-alkyl-zirconocene precursors having polymeryl-like alkyl groups was targeted.

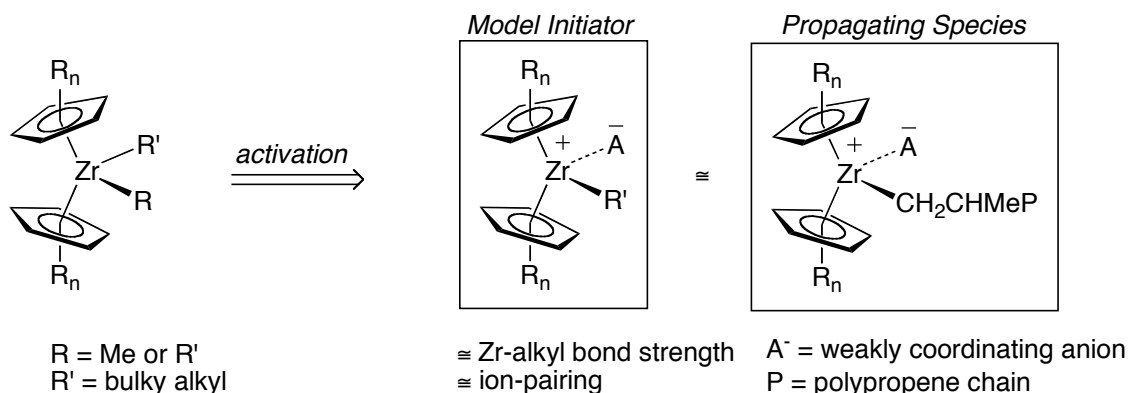


Figure 1. Well-defined initiators that may model the propagating species in zirconium-catalyzed propene polymerization.

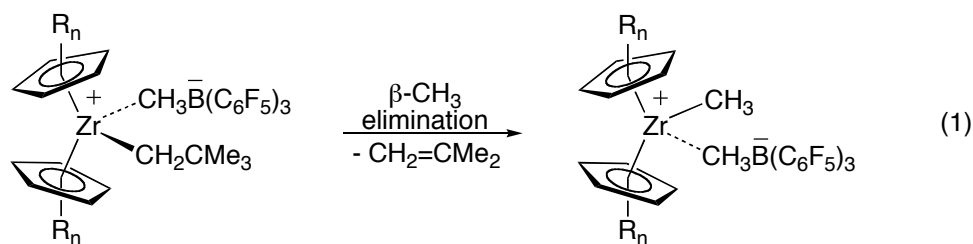
Considerable efforts in both academic and industrial laboratories have produced a rich body of literature precedence for the synthesis and activation of group 4 dimethyl metallocene precatalysts.⁶ These efforts offer great diversity with respect to choice of

ancillary ligands and activating reagents, but are more limited with respect to variations in alkyl groups. Examples using zirconium and hafnium precatalysts of the form $\text{Cp}^x_2\text{M}(\text{R})_2$ or $\text{Cp}^x_2\text{M}(\text{CH}_3)(\text{R})$ have generally been restricted to a small number of bulky alkyl groups ($\text{R} = \text{CH}_2\text{CMe}_3$ (Np), CH_2SiMe_3 (CH_2TMS), $\text{CH}(\text{SiMe}_3)_2$, or $\text{CH}_2(\text{C}_6\text{H}_5)$).^{1,2,7}

One difficulty associated with the synthesis and isolation of group 4 $\text{Cp}^x_2\text{M}(\text{R})_2$ or $\text{Cp}^x_2\text{M}(\text{CH}_3)(\text{R})$ compounds, where the R group is a polymeryl-like chain, is the propensity of these species to undergo decomposition via β -hydride elimination.⁸ Therefore, most compounds of the type $\text{Cp}^x_2\text{ZrR}_2$ containing β -hydrogens have been synthesized and examined in situ.⁹

For eventual use in kinetic studies, the stability of the dialkylzirconocene precatalysts as well as the generated zirconocene-alkyl cations towards decomposition via β -hydride elimination must also be considered. These reactions may be more facile for the cationic species given the increased electrophilicity of the metal center as compared to the neutral species. In fact, β -hydride elimination has been identified as a major chain termination pathway from propagating species in metallocene-catalyzed alkene polymerization.²

In order to avoid complications arising from this type of reactivity, we chose to investigate dialkyl- and methyl alkylzirconocenes with bulky alkyl groups having no β -hydrogens as precursors to models of the propagating species. Decomposition pathways involving other β -elimination reactions however, may occur for the cationic alkyl-initiators generated from these zirconocenes. Studies by Horton,¹⁰ Marks,⁷ and Bercaw¹¹ have demonstrated that $[\text{Cp}^x_2\text{Zr}(\text{CH}_2\text{CMe}_3)]^+[\text{CH}_3\text{B}(\text{C}_6\text{F}_5)_3]^-$ compounds decompose to zirconocene-methyl cations and isobutene via β -methyl elimination (eq 1).



For alkyl-zirconocenium ions, rate of β -methyl elimination¹⁰ and the relative rates of β -hydride elimination vs. β -methyl elimination appear to be sensitive to the steric influence of the cyclopentadienyl ancillary ligands.¹² β -H elimination is the primary chain termination pathway for the propagating catalyst produced in propene polymerization using $\text{Cp}_2\text{ZrCl}_2/\text{methylaluminoxane}$ (MAO) systems, while $\text{Cp}^*\text{ZrCl}_2/\text{MAO}$ derived catalyst chain terminates via β -methyl elimination. In the latter case, the increased rate of β -methyl compared to β -hydride elimination can be rationalized by considering steric interactions between the Cp^* ligand and the β -substituents on the polymeryl chain in the transition state structure.¹² These unfavorable steric interactions are minimized in the conformation leading to β -methyl elimination (Figure 2). These results suggested that the steric environment might be tuned using both the influence of the bulky alkyl group and the ancillary ligand framework to potentially inhibit β -methyl elimination for the proposed propagating species models containing β -methyl groups.

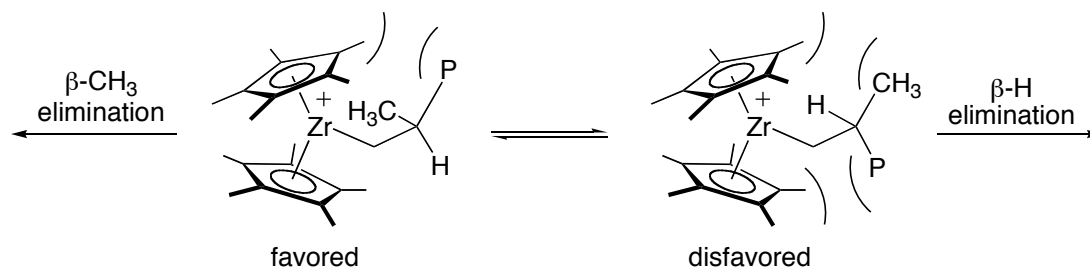


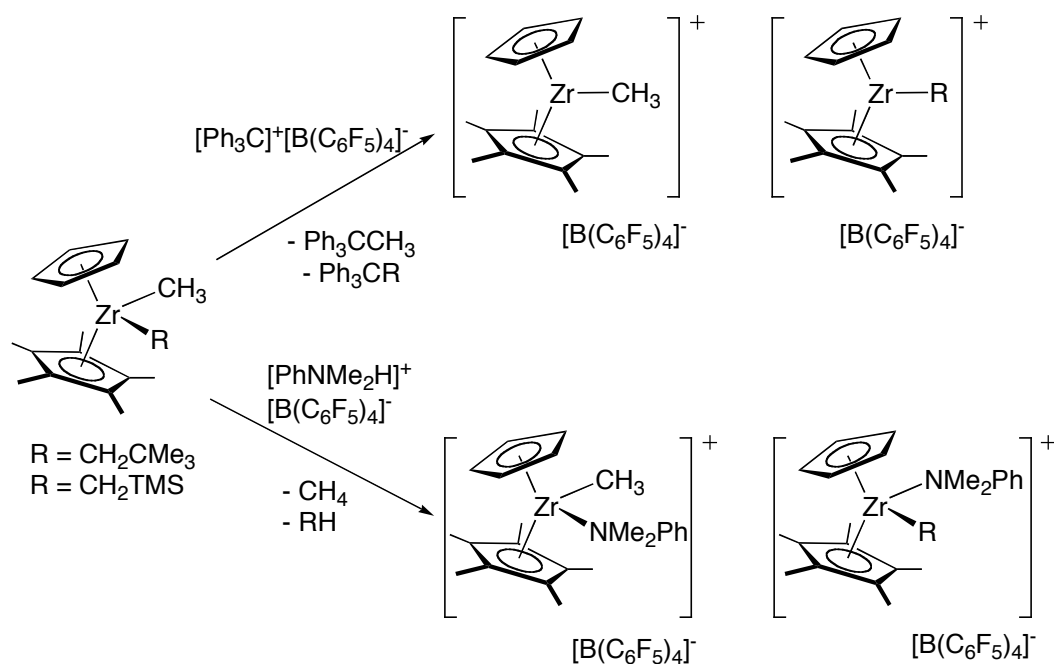
Figure 2. Proposed influence of sterically demanding ancillary ligation on β -H vs β -Me elimination.

2 Results and Discussion

2.1 Synthesis of mixed ring dialkylzirconocenes

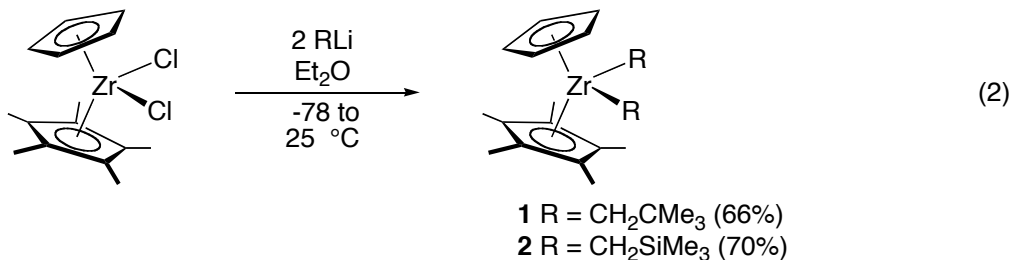
The mixed ring dialkylzirconocenes $\text{CpCp}^*\text{ZrNp}_2$ (**1**) and $\text{CpCp}^*\text{Zr}(\text{CH}_2\text{TMS})_2$ (**2**) are precursors to catalyst initiators of the form $[\text{CpCp}^*\text{ZrR}]^+[\text{B}(\text{C}_6\text{F}_5)_4]^-$ or $[\text{CpCp}^*\text{Zr}(\text{R})(\text{L})]^+[\text{B}(\text{C}_6\text{F}_5)_4]^-$ ($\text{R} = \text{Np}, \text{CH}_2\text{TMS}$; $\text{L} = \text{PhNMe}_2$), by activation of the precatalyst with $[\text{Ph}_3\text{C}]^+[\text{B}(\text{C}_6\text{F}_5)_4]^-$ or $[\text{PhNMe}_2\text{H}]^+[\text{B}(\text{C}_6\text{F}_5)_4]^-$ respectively.⁶ The dialkylzirconocenes were targeted for use with these activators rather than the methyl alkylzirconocenes as multiple cationic species, $[\text{Zr}]^+-\text{CH}_3$ and $[\text{Zr}]^+-\text{Np}$, may be generated upon activation (Scheme 3). Alkyl abstraction from non-metallocene zirconium and hafnium (IV) dialkyl compounds using $[\text{Ph}_3\text{C}]^+[\text{B}(\text{C}_6\text{F}_5)_4]^-$ has been reported for a number of alkyl groups, including neopentyl.¹³⁻¹⁵

Scheme 3



Horton has shown that the stability of zirconocene-neopentyl cations towards decomposition via β -methyl elimination is sensitive to the ancillary ligation.¹⁰ While $[\text{Cp}^*\text{ZrNp}]^+[\text{CH}_3\text{B}(\text{C}_6\text{F}_5)_3]^-$ undergoes rapid decomposition at temperatures as low as -80 °C, $[\text{Cp}_2\text{ZrNp}]^+[\text{CH}_3\text{B}(\text{C}_6\text{F}_5)_3]^-$ is stable up to 0 °C. Therefore, the mixed ring cyclopentadienyl ligation was chosen to provide an intermediate steric influence. Additionally, it was thought that the Si-substituted alkyl group may serve as neopentyl analogue stable towards β -methyl elimination, as silylene formation is unfavorable. Experimental support for this prediction comes from studies by Beswick and Marks.⁷

Compounds **1** and **2** are prepared according to the methodology reported by Lappert for the parent Cp_2ZrR_2 compounds.¹⁶ The reaction of two equivalents of the appropriate lithium reagent with $\text{CpCp}^*\text{ZrCl}_2$ proceeds cleanly in diethyl ether solvent to afford **1** or **2** as tan or off-white powders respectively in good yields (eq 2).



Cooling a saturated pentane solution of **1** to -35 °C resulted in the formation of pale yellow crystals that were suitable for X-ray diffraction. The molecular structure of **1** displays a bent-sandwich coordination mode common among zirconocenes (Figure 1). The Zr-Cp and Zr-Cp* centroid distances ($2.241(1)$, $2.260(1)$ Å) and Cp centroid-Zr-Cp* centroid angle ($129.1(1)$ °) are similar to those found for Cp_2ZrNp_2 (2.25 Å; 128.3 °) (Table 1).¹⁷ The structure is monoclinic and fits the $P2_1/c$ space group. All of the hydrogen atoms have been located in the difference map and have been refined. Details

of the data collection and solution and refinement of the structure can be found in Appendix 1.

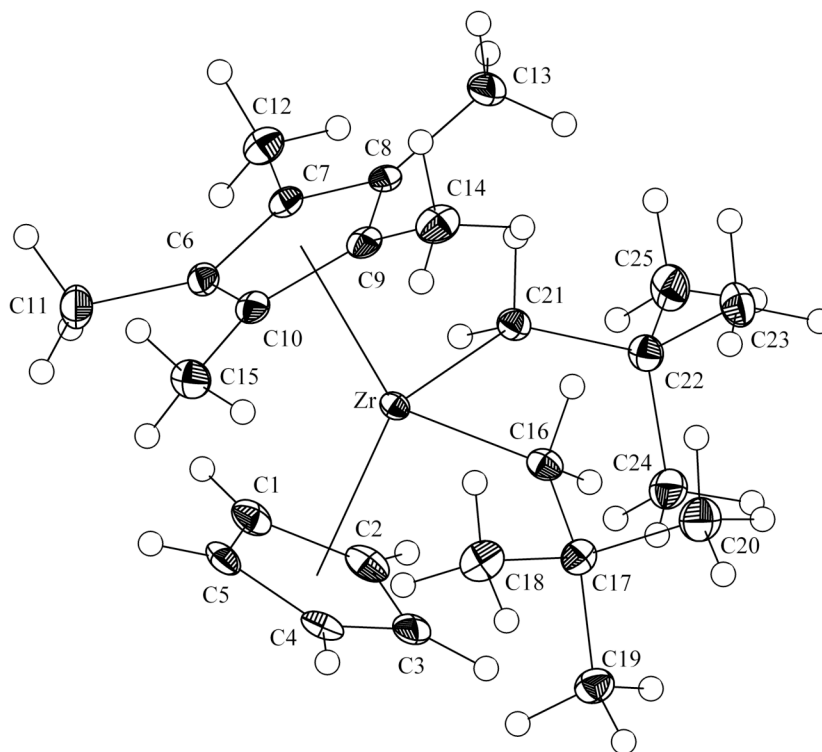


Figure 3. Molecular structure of **1** with 50% probability ellipsoids.

Table 1. Selected bond distances (Å) and bond angles (°) obtained from the X-ray structure determination of **1**

Feature	Distance (Å)	Feature	Angle (°)
Zr-Ct(1) ^a	2.241(1)	Ct(1)-Zr-Ct(2)	129.1(1)
Zr-Ct(2) ^b	2.260(1)	C(16)-Zr-C(21)	99.61(5)
Zr-C(16)	2.2651(14)		
Zr-C(21)	2.3524(14)		

^a Ct(1) is defined as the centroid of the ring made up of C(1)-C(5); ^b Ct(2) is defined as the centroid of the ring made up of C(6)-C(10).

The neopentyl groups are oriented to direct the bulky *tert*-butyl substituents towards the front, more open region of the zirconocene wedge and away from the Cp* group in the solid-state structure (Figure 3). Two unique bond lengths are found for Zr-C(σ)

bonding to the neopentyl groups (Zr-C(16) = 2.2651(14), Zr-C(21) = 2.3524(14) Å) however these short and long bond distances are within the range typically observed for Cp^x₂Zr-alkyl compounds (2.251-2.388 Å).^{18,19} The molecular structure of **1** does not indicate any ground state γ -agostic interactions since the closest zirconium- γ -hydrogen distance found is 3.821(1) Å. A close contact is found between zirconium and one α -hydrogen located on C(16) (Zr- α -H = 2.384 Å) and examination of the extended packing structure suggests a ground state α -agostic interaction. The ¹H and ¹³C spectra of **1** at ambient temperature in benzene-*d*₆ is not consistent with a static α -agostic structure in solution, where two doublets integrating to 2H are observed for the α -hydrogens and ¹J_{C- α H} = 109 Hz. These spectra also indicate that the asymmetric orientation of the neopentyl groups observed in the crystal structure is not maintained in solution.

Compound **2** has also been analyzed by X-ray crystallography. This compound crystallized as colorless blocks from pentane at -35 °C in the *P2*₁/*c* space group. The molecular structure of **2** - including orientation of the bulky alkyl groups - is isostructural to **1** (Figure 4). All hydrogens were located in the difference map and have been refined. The key structural parameters, including Zr-Cp centroid distances and angles and Zr-CH₂TMS bond lengths are close to those found for Cp₂Zr(CH₂TMS)₂ (2.24 Å; 128.3 °; 2.278(4), 2.281(4) Å) respectively (Table 2).¹⁷ While two unique bond distances are also found for Zr-CH₂TMS σ bonding in **2**, the difference in bond lengths (0.0375 Å) is much smaller than that observed for **1**. This may be due to the smaller steric bulk of this alkyl group, as compared to the neopentyl group. No ground state agostic interactions are observed since the closest zirconium- α -hydrogen and - γ -hydrogen found in **2** are

2.518(0) and 4.219(1) Å respectively. Details of the data collection and solution and refinement of the structure can be found in Appendix 1.

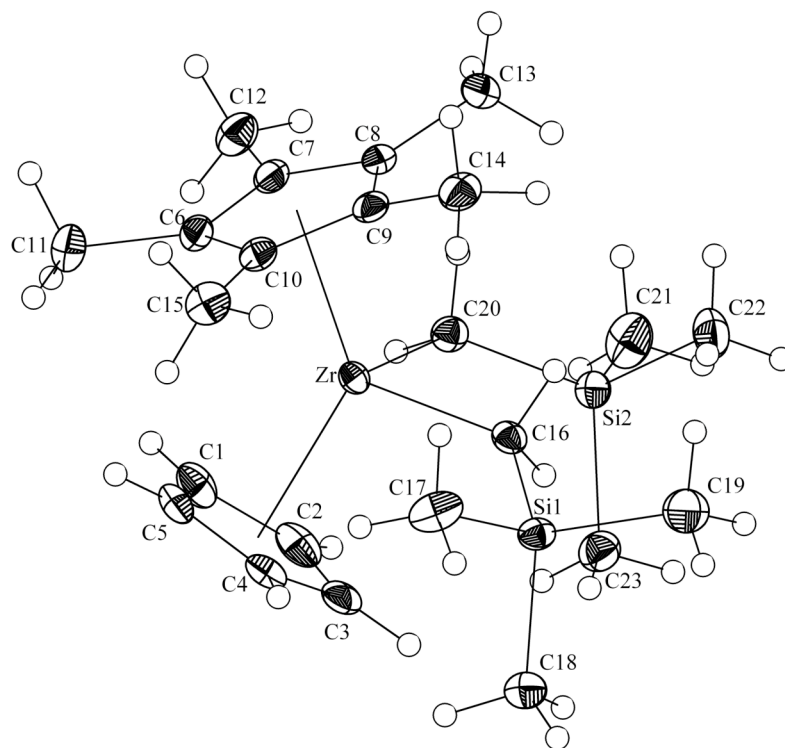


Figure 4. Molecular structure of **2** with 50% probability ellipsoids.

Table 2. Selected bond distances (Å) and bond Angles (°) obtained from the X-ray structure determination of **2**

Feature	Distance (Å)	Feature	Angle (°)
Zr-Ct(1) ^a	2.246(1)	Ct(1)-Zr-Ct(2)	131.1(1)
Zr-Ct(2) ^b	2.247(1)	C(16)-Zr-C(20)	98.09(6)
Zr-C(16)	2.2691(16)		
Zr-C(20)	2.3066(16)		

^a Ct(1) is defined as the centroid of the ring made up of C(1)-C(5); ^b Ct(2) is defined as the centroid of the ring made up of C(6)-C(10).

2.2 Precursors for methyl alkylzirconocene compounds

Methyl alkylzirconocene compounds of the form $\text{Cp}^x_2\text{Zr}(\text{CH}_3)\text{R}$ serve as precursors for $[\text{Cp}^x_2\text{Zr}(\text{R})]^+[\text{CH}_3\text{B}(\text{C}_6\text{F}_5)_3]^-$ type initiators formed via methide abstraction using the

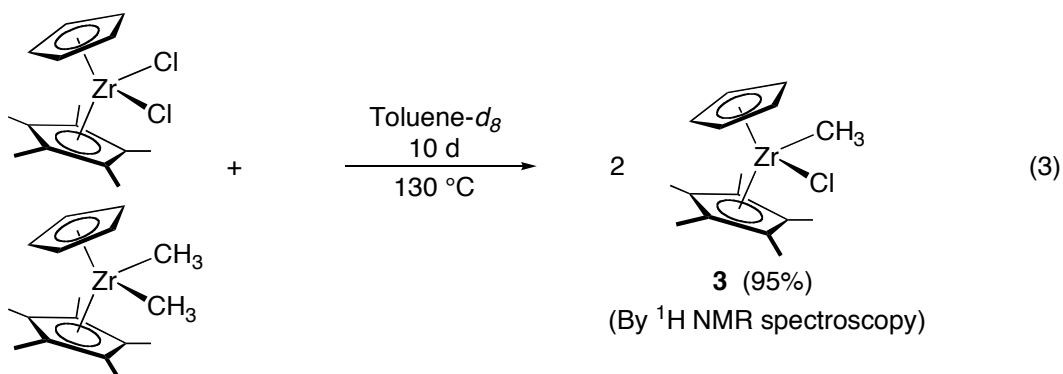
strongly Lewis acidic activator $B(C_6F_5)_3$.⁶ Again, the mixed ring ancillary ligation was targeted for its potential steric influence on initiator speciation. The steric demand of the Cp* group inhibits formation of bimetallic methyl-bridged monocations, such as $[\{Cp^x_2Zr(R)\}_2(\mu-CH_3)]^+[A]^-$ ($A = CH_3B(C_6F_5)_3, B(C_6F_5)_4$), which are often observed for zirconocene systems with open coordination environments.^{6,20}

The key starting material for the formation of methyl alkyl complexes in zirconocene systems is $Cp^x_2Zr(CH_3)Cl$. These compounds however, are not obtained from the reaction of $Cp^x_2ZrCl_2$ with one equivalent of methyllithium. Conventional routes to obtain $Cp^x_2Zr(CH_3)Cl$ compounds from $Cp^x_2Zr(CH_3)_2$ utilize HCl,¹¹ $[(CH_3)_3NH]^+[Cl]^-$,²¹ $[Pr_2NH_2]^+[Cl]^-$,²² and $PbCl_2$ ²³ as chlorinating reagents.

These routes were tested for the synthesis of $CpCp^*Zr(CH_3)Cl$ (**3**) from $CpCp^*Zr(CH_3)_2$. These reactions however, always resulted in **3** contaminated with at least 5% $CpCp^*ZrCl_2$ as well as starting material. Ultimately the purity **3** played an important role in the successful isolation of pure $CpCp^*Zr(CH_3)R$ compounds. Separation of mixtures of dialkyl- and chloro alkylzirconocenes was difficult due to their extreme solubility and similar physical properties as well as the limited number of compatible purification methods available.

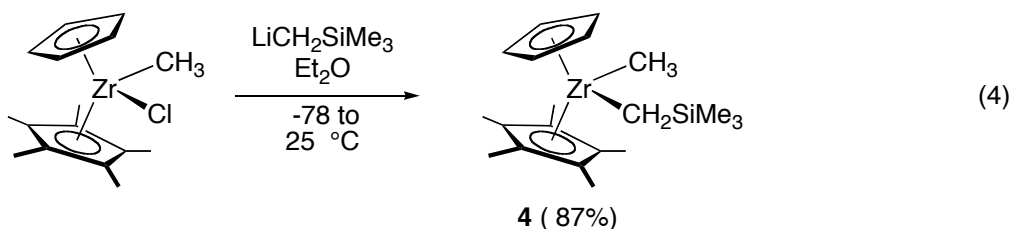
A method for the clean synthesis of **3** was developed based on the ligand redistribution chemistry reported by Jordan.²⁴ A 0.5 M solution of $CpCp^*ZrCl_2$ and $CpCp^*Zr(CH_3)_2$ in toluene- d_8 was heated at 130 °C in a J. Young NMR tube. After 10 days, 95% conversion to **3** was observed by 1H NMR spectroscopy (eq 3). These conditions were subsequently employed on preparative scale reactions and afforded **3**

contaminated with less than 3% CpCp*ZrCl₂ as a white powder or pale yellow needles in 87% yield after repeated purification from toluene-petroleum ether at -35 °C.



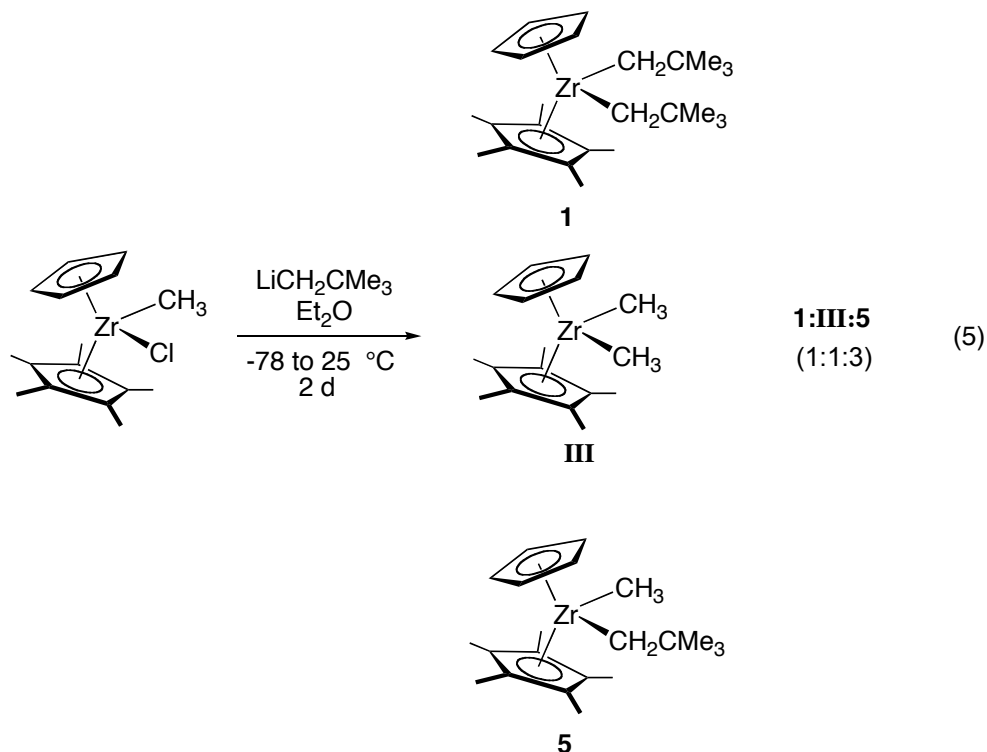
2.3 Synthesis of CpCp*Zr(CH₃)(CH₂TMS) and CpCp*Zr(CH₃)(Np)

The mixed ring zirconocene methyl alkyl compounds CpCp*Zr(CH₃)(CH₂TMS) (**4**) and CpCp*Zr(CH₃)(Np) (**5**) were prepared by the reaction of **3** with one equivalent of the appropriate lithium reagent. The synthesis of **4** proceeded smoothly by this route in diethyl ether and **4** was isolated as a pale yellow oil in good yields (eq 4). Lyophilization or trituration techniques as well as a variety of solvent systems failed in attempts to obtain **4** as a powder or crystalline material. This oil was judged to be > 95% pure by ¹H NMR spectroscopy however, and has been utilized successfully in subsequent reactions.



The reaction of **3** with neopentyl lithium was more sensitive to reaction conditions, including concentration, solvent, temperature, and reaction time. Reactions following the above methodology yielded **5** as a yellow oil (contaminated with other zirconocene compounds) that was resistant to purification by recrystallization or precipitation. These

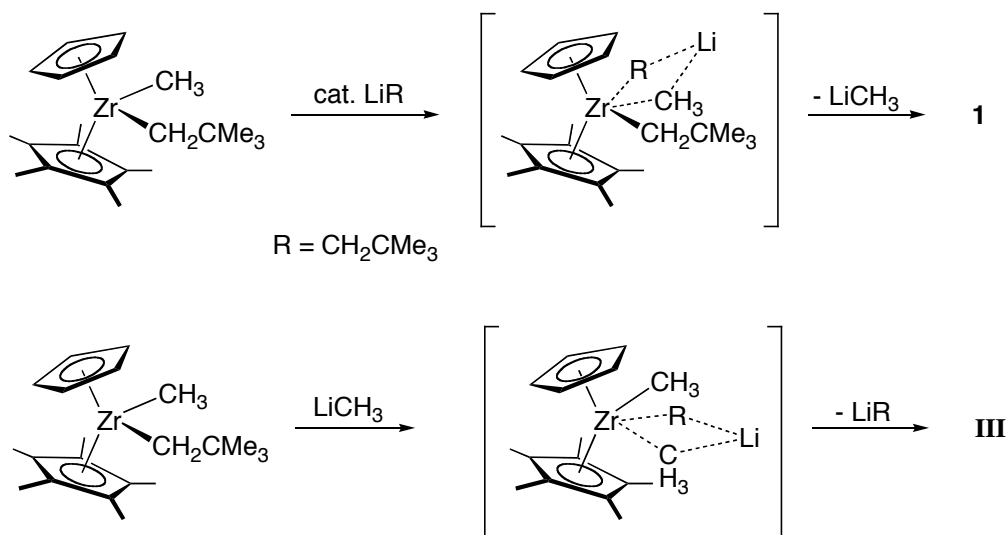
other zirconocenes include **1** and CpCp*Zr(CH₃)₂. Further experimental evidence supports the formation of **1** and CpCp*Zr(CH₃)₂ (**III**) in reactions of **5** with LiNp in diethyl ether (eq 5). Under these conditions the product mixture could be driven to **1**, **III**, and **5** in a 1:1:3 ratio respectively, as identified by comparison with the ¹H NMR spectra of independently synthesized compounds.



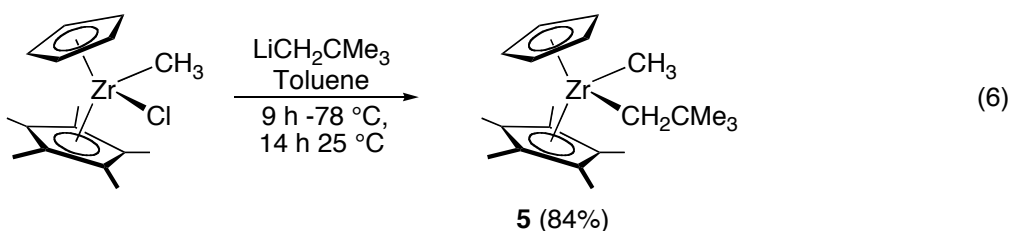
This observation suggests the alkylation of **3** may be reversible with alkyllithium reagents. Reversible alkylation catalyzed by trace neopentyl lithium would provide a pathway for alkyl exchange, potentially explaining the product mixture (Scheme 4). Alkyl exchange between group 4 centers via an intermolecular mechanism involving the formation of bridging alkyl groups has been documented for both metallocene²⁴ and non-metallocene compounds.²⁵ While this process is facile for methyl groups, which readily bridge metal centers, it is less likely to explain exchange of the bulky neopentyl group

between zirconocene centers having sterically demanding ancillary ligation such as that in **5**.

Scheme 4



Preparation in toluene along with careful control of reaction temperature afforded a clean and reproducible methodology for the synthesis of **5** (eq 6). This method allowed isolation of **5** as an analytically pure yellow powder after removal of lithium chloride by filtration.

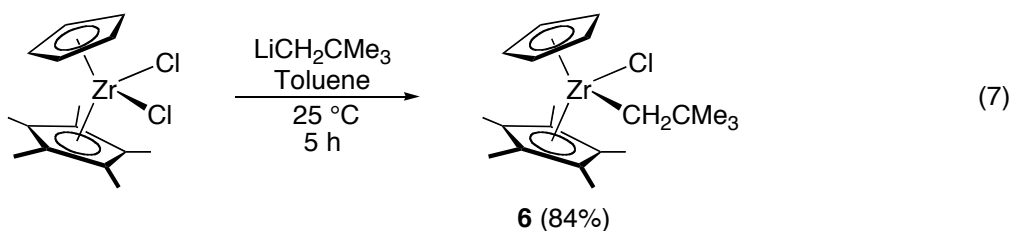


2.4 Alternate routes for the synthesis of CpCp*Zr(CH₃)(Np)

A methodology to synthesize **5** utilizing successive monoalkylation reactions starting from CpCp*ZrCl₂ is desirable as it would remove one step from the overall sequence and eliminate the long reaction time required to prepare **3**. Additionally, this type of strategy would also be useful in the preparation of isotopically labeled versions of

5, such as $\text{CpCp}^*\text{Zr}(\text{CD}_3)(\text{Np})$ or $\text{CpCp}^*\text{Zr}({}^{13}\text{CH}_3)(\text{Np})$, since a 15 mole% excess of $\text{CpCp}^*\text{Zr}(\text{CH}_3)_2$ is used in the preparative scale synthesis of **3**. As monomethylation of $\text{CpCp}^*\text{ZrCl}_2$ is not possible with the lithium reagent, this route can proceed via formation of the monoalkylated compound $\text{CpCp}^*\text{Zr}(\text{Np})(\text{Cl})$ (**6**).

Compound **6** is prepared by reaction of $\text{CpCp}^*\text{ZrCl}_2$ with one equivalent of neopentyl lithium in toluene (eq 7). Initially, **6** is a sticky, bright yellow solid but can be isolated as a yellow powder after precipitation from concentrated diethyl ether solutions followed by addition of petroleum ether and cooling to $-35\text{ }^\circ\text{C}$.



Yellow crystalline fragments of **6** were obtained by slow diffusion of petroleum ether into diethyl ether solutions at $-35\text{ }^\circ\text{C}$ and the molecular structure was determined by X-ray diffraction. This molecule crystallizes in the $P-1$ space group, with two unique molecules in the asymmetric unit (Figure 5). Overall, the structural parameters for **6**, including Zr-Cl bond lengths, are comparable to those in $\text{CpCp}^*\text{ZrCl}_2$ ($2.4421(9)\text{ \AA}$).²⁶ The observed zirconium-neopentyl bond distances ($2.3258(12)$, $2.3287(12)\text{ \AA}$) are on the long end of the range typically found in alkylzirconocenes, reflecting the steric bulk of this group (Table 3).^{18,19} Further evidence for crowding in the equatorial plane of **6** is suggested by the expanded C(16)-Zr-Cl angle ($100.18(13)$, $99.91(3)\text{ }^\circ$) as compared with the Cl-Zr-Cl angle ($97.78(5)\text{ }^\circ$) found in $\text{CpCp}^*\text{ZrCl}_2$. No special zirconium-hydrogen interactions are evident in **6** as the closest Zr-H contact is $2.748(1)\text{ \AA}$. Details of the data collection and solution and refinement of the structure can be found in Appendix 1.

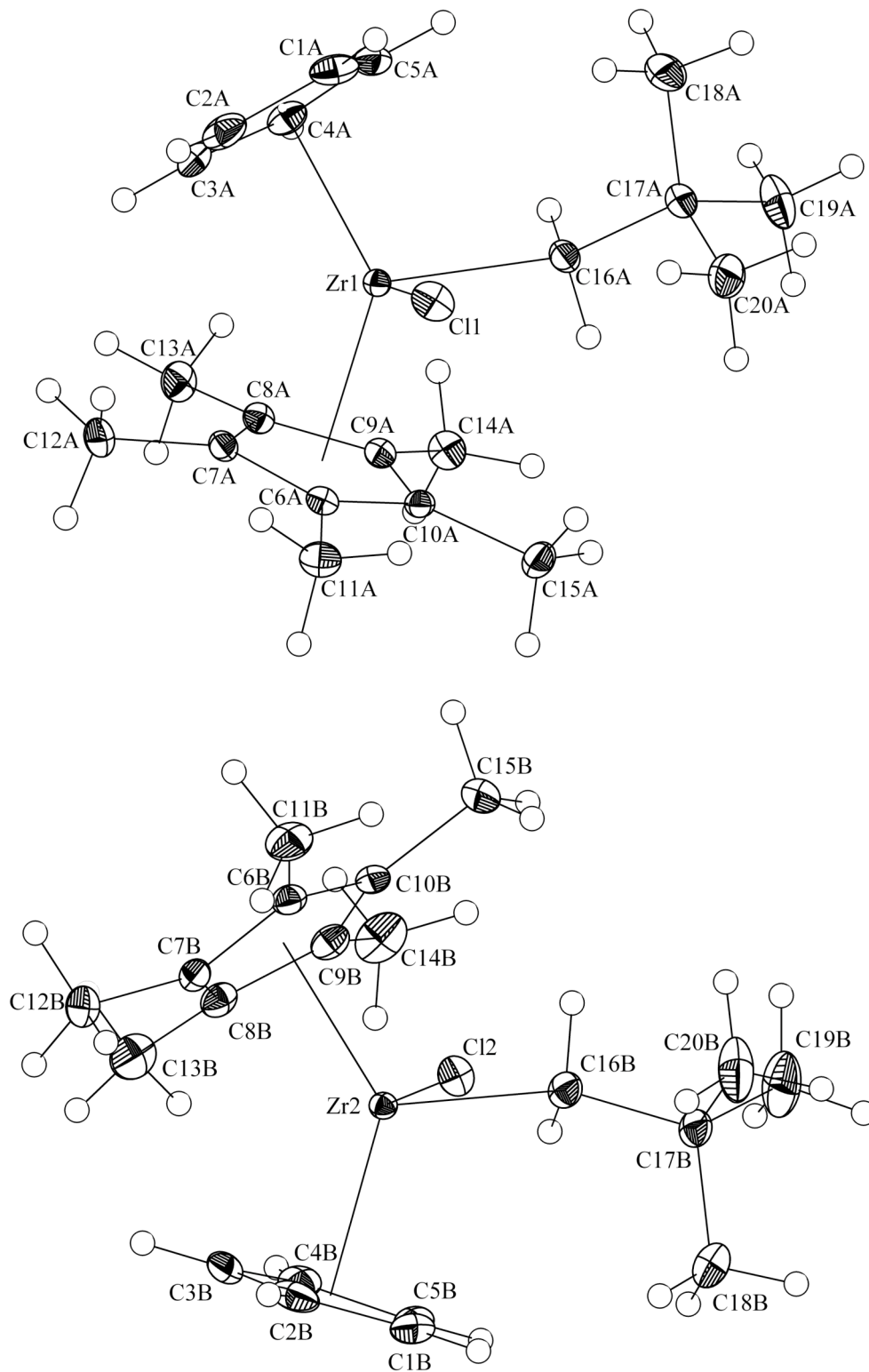


Figure 5. Molecular structure of **6** showing the unique molecules found in the asymmetric unit with 50% probability ellipsoids.

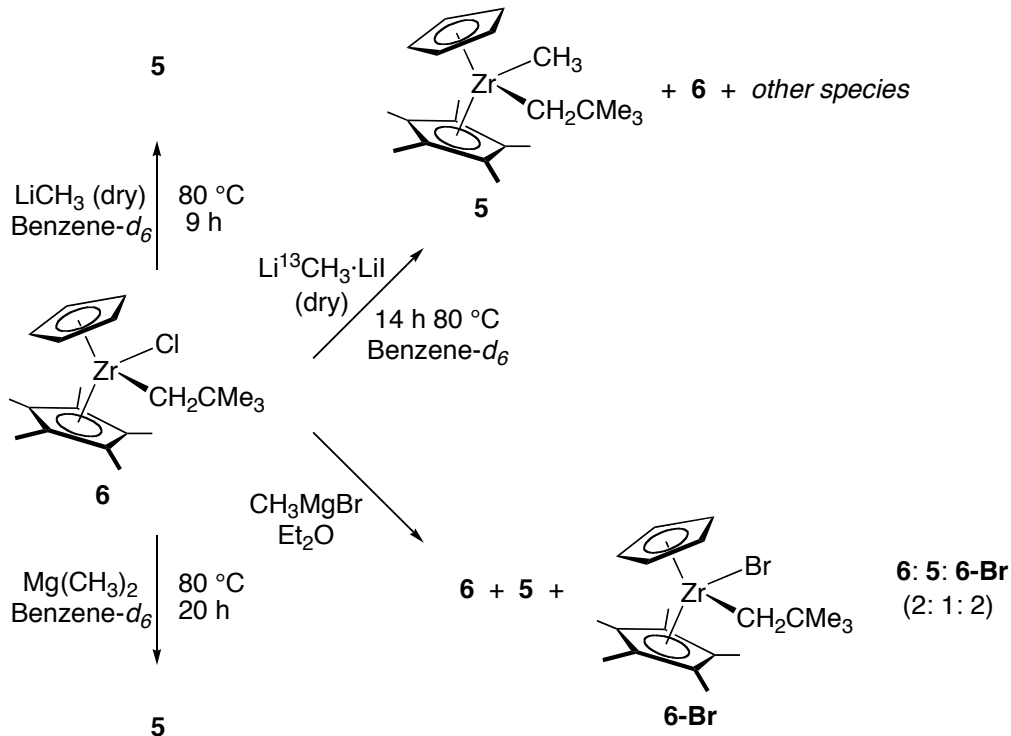
Table 3. Selected bond distances (Å) and bond angles (°) obtained from the X-ray structure determination of **6**

Feature	Distance (Å) or Angle (°)	Feature	Distance (Å) or Angle (°)
Zr(1)-Ct(1A) ^a	2.232	Zr(2)-Ct(1B) ^a	2.224
Zr(1)-Ct(2A) ^b	2.241	Zr(2)-Ct(2B) ^b	2.240
Zr(1)-C(16A)	2.3258(12)	Zr(2)-C(16B)	2.3287(12)
Zr(1)-Cl(1)	2.4503(3)	Zr(2)-Cl(2)	2.4432(3)
Ct(1A)-Zr(1)-Ct(2A)	129.5	Ct(1B)-Zr(2)-Ct(2B)	129.8
C(16A)-Zr(1)-Cl(1)	100.18(3)	C(16B)-Zr(2)-Cl(2)	99.91(3)

^a Ct(1A) is defined as the centroid of the ring made up of C(1A)-C(5A), Ct(1B) is defined as the centroid of the ring made up of C(1B)-C(5B); ^b Ct(2A) is defined as the centroid of the ring made up of C(6A)-C(10A), Ct(2B) is defined as the centroid of the ring made up of C(6B)-C(10B).

NMR scale reactions were used to explore methylation of **6** with several alkylating agents. Promising conditions were observed with pre-dried, ether-free methyllithium, as **5** formed cleanly in benzene-*d*₆ after heating for 9 hours at 80 °C (Scheme 5). These conditions were not suitable for the synthesis of isotopically labeled **5** by reaction with solid Li¹³CH₃·LiI complex however, as multiple zirconocene species, including **5** and **6**, were present after heating. Li¹³CH₃ or LiCD₃ are commonly prepared or purchased commercially as 1:1 complexes with lithium iodide and this additive appeared detrimental under these conditions.²⁷ One of the new species is likely CpCp*Zr(Np)(I) based on the chemical shift of a new Cp resonance in the ¹H NMR spectrum as compared with that in CpCp*ZrI₂.

Scheme 5



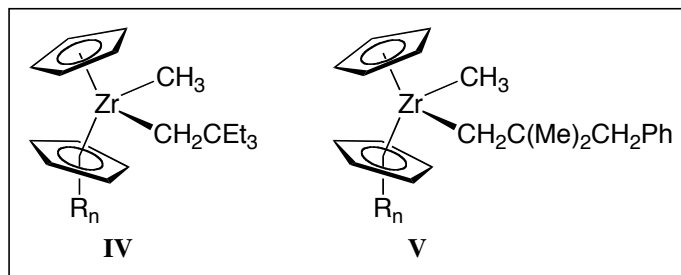
The reactivity of **6** with magnesium based methylating reagents was also examined. The reaction of **6** with CH_3MgBr resulted in the formation of **6**, **5**, and $\text{CpCp}^*\text{ZrNpBr}$ in a 2:1:2 ratio after 2 hours at room temperature in diethyl ether as determined by ^1H NMR spectroscopy. As the presence of added halide salts appears to be generally problematic, dimethyl magnesium was utilized and proved to be the best alternative methylating agent. Reaction of **6** with $(\text{CH}_3)_2\text{Mg}$ in benzene- d_6 at $80\text{ }^\circ\text{C}$ formed compound **5** cleanly in quantitative yield as assessed by ^1H NMR spectroscopy.

2.5 Design and synthesis of specialty alkyllithium reagents

One strategy to stabilize the alkylzirconocene cation formed upon activation towards decomposition via β -methyl elimination is to utilize a bulky alkyl group having no β -methyl groups. Another approach is to design a catalyst where unfavorable steric interactions between β -alkyl substituents and the cyclopentadienyl framework inhibit this

reaction. Therefore, synthesis of methyl alkylzirconocenes of the type shown in Chart 1 was targeted.

Chart 1



$R_n = (\text{Me})_5 \text{ or } (\text{H})_5$

Catalysts derived from zirconocenes of type **IV** may decompose via β -ethyl elimination. Generally this reaction has not been observed in related systems. Previously in our group, the decomposition of $\text{OpSc}(\text{CH}_2\text{CH}(\text{CH}_2\text{CH}_3)_2)$ [$\text{Op} = \{(\eta^5\text{-C}_5\text{Me}_4)_2\text{SiMe}_2\}$] was studied and no evidence for β -ethyl elimination was observed by ^1H NMR spectroscopy.²⁸ Resconi has also found that chain transfer by β -ethyl elimination did not occur during the polymerization of 1-butene by $\text{Cp}^*\text{ZrCl}_2/\text{MAO}$ ($\text{M} = \text{Zr, Hf}$) catalysts.¹²

Activated compounds based on type **V** zirconocenes can decompose via β -methyl elimination, however this reaction may be inhibited for catalysts with CpCp^* ancillary ligation. Unfavorable steric interactions between the alkyl benzyl substituent and the Cp^* ligand may destabilize the transition state for this reaction relative to that for $[\text{CpCp}^*\text{Zr}(\text{Np})]^+[\text{CH}_3\text{B}(\text{C}_6\text{F}_5)_3]^-$ (Figure 6).

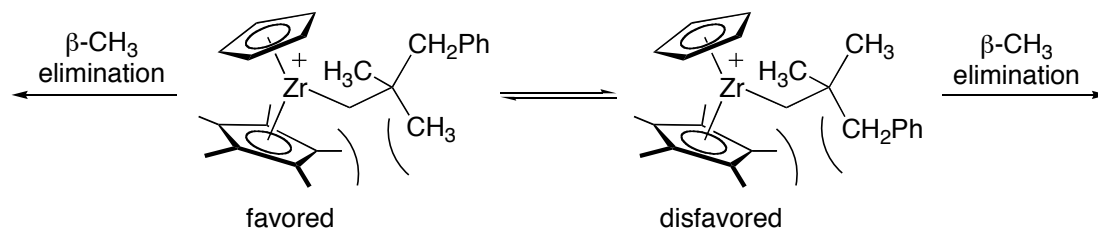
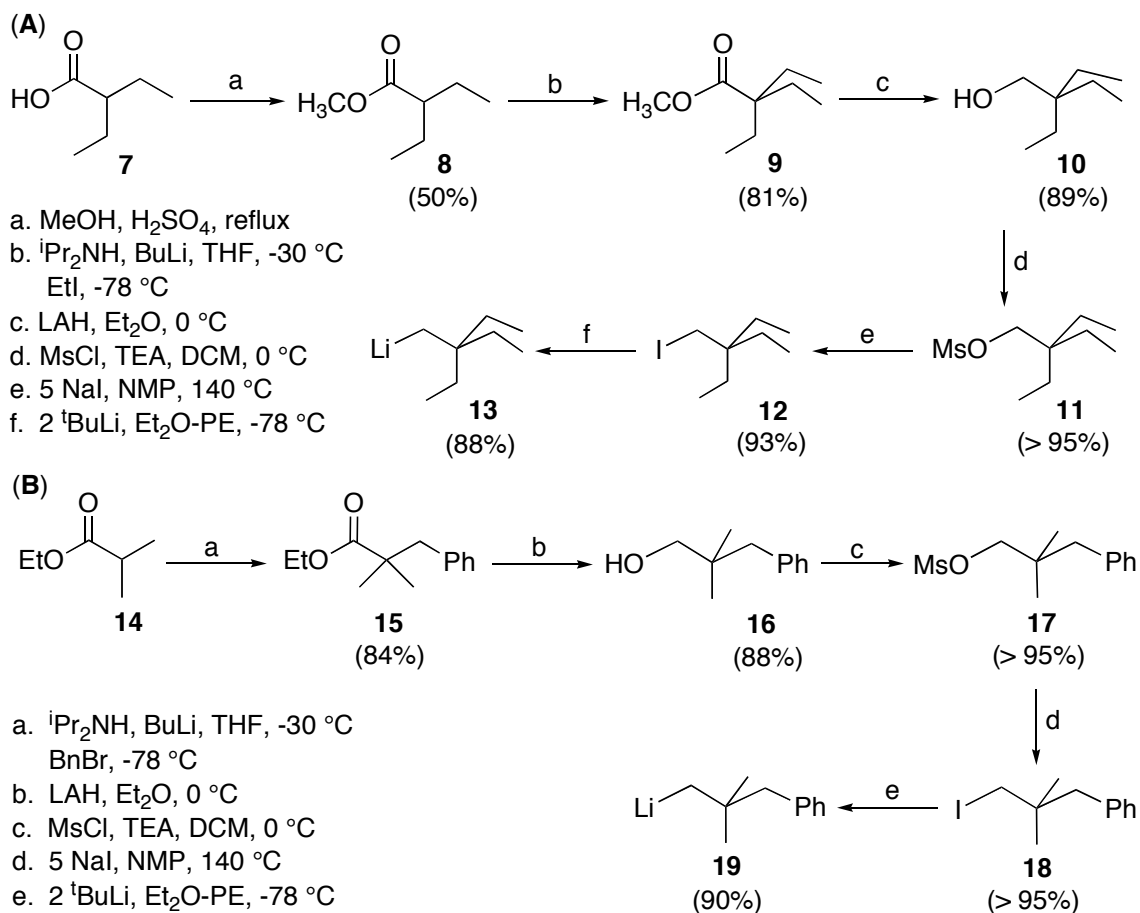


Figure 6. Destabilizing steric interactions between the Cp* ligand and alkyl β -CH₂Ph group in **V** may inhibit β -methyl elimination.

The synthetic methodology used to prepare 2,2-diethyl-butyl lithium ($\text{Li}(\text{CH}_2\text{CEt}_3)$) (**13**) and 2,2-dimethyl-3-phenyl-propyl lithium ($\text{Li}(\text{CH}_2\text{CMe}_2\text{CH}_2\text{Ph})$) (**19**) is shown in Scheme 6 along with optimized reaction conditions and product yields. 2,2-Diethylbutanol (**10**) was prepared conveniently in three steps from commercially available 2-ethylbutric acid (**7**) using standard procedures.²⁹ A similar sequence gave 2,2-dimethyl-3-phenylpropanol (**16**) from commercially available 2-methylpropionic acid ethylester (**14**).

Precedented reaction conditions for the conversion of neopentyl-type alcohols (PPh_3/Br_2 , CH_3CN , heat) to alkylbromides failed for **10** and **16**, low yields of products were recovered for both substrates, 30% and 10% respectively. The methane sulfonate esters, 2,2-diethyl-butyl mesylate (**11**) and 2,2-dimethyl-3-phenyl-propyl mesylate (**17**) were prepared after the methodology for hindered primary substrates of Servis.³⁰ Compounds **11** and **17** were converted to alkyl iodides **12** and **18** using conditions based on those reported by Stevens for the preparation of (-)-9-iodocamphor from (-)-9-bromocamphor.³¹ This transformation required forcing conditions, again reflecting the steric inhibition of $\text{S}_{\text{N}}2$ reactivity at the primary carbon center. The desired alkyllithium reagents, **13** and **19**, were synthesized from **12** and **18** respectively, using the lithium-halogen exchange procedure developed by Bailey³² and Negishi.³³

Scheme 6



2.6 Methyl alkylzirconocene synthesis using specialty alkyl lithium reagents

Synthesis of methyl alkylzirconocenes with the special alkyl groups, CpCp*Zr(CH₃)(CH₂CEt₃) (**20**), CpCp*Zr(CH₃)(CH₂C(Me)₂CH₂Ph) (**21**), Cp₂Zr(CH₃)(CH₂CEt₃) (**22**), and Cp₂Zr(CH₃)(CH₂C(Me)₂CH₂Ph) (**23**), was explored using the conditions shown in Figure 7. Reaction of **3** with one equivalent of either **13** or **19** resulted in formation of **20** and **21** respectively, along with additional zirconocene products as determined by analysis of the isolated material by ¹H NMR spectroscopy. These additional compounds are likely CpCp*Zr(CH₃)₂ and CpCp*ZrR'₂, possibly formed via the reversible-alkylation process postulated for alkyl exchange in **5**. Unfortunately, the oils containing **20** and **21** were resistant to purification by

crystallization or precipitation from pentane at temperatures below $-35\text{ }^{\circ}\text{C}$. This difficulty is attributed to the extreme solubility of these compounds.

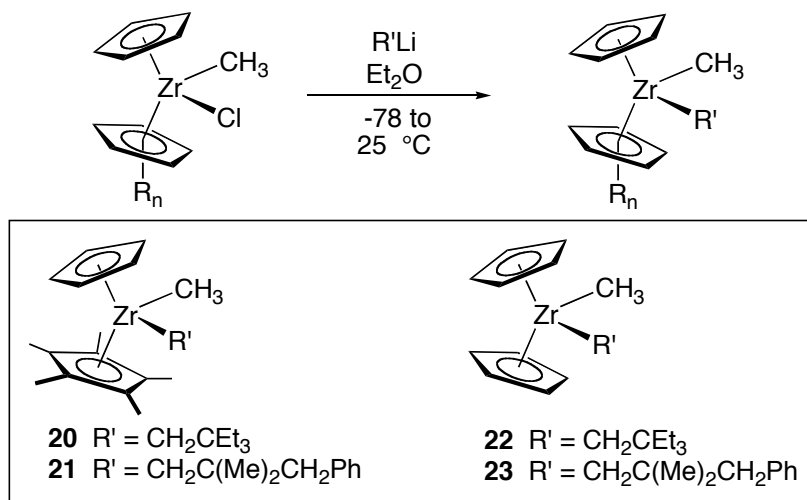


Figure 7. Conditions for methyl alkylzirconocene synthesis using **13** or **19**.

Compounds **22** and **23** are readily formed under these conditions and are isolated in modest yields after crystallization from pentane at $-35\text{ }^{\circ}\text{C}$. While pale yellow X-ray quality crystals of **22** were obtained, the brown pellets of **23** recovered always showed extremely poor diffraction. This zirconocene crystallizes as a radial cluster and maintains this preference under a variety of crystallization conditions.

The pale yellow blocks of **22** were determined to crystallize in the $P2/c$ space group. The asymmetric unit contained two unique molecules, differing in orientation of the bulky alkyl group (Figure 8). The zirconium-Cp centroid and zirconium-methyl distances as well as the Cp centroid-zirconium-Cp centroid and carbon-zirconium-carbon angles found for **22** are in line with those observed for $\text{Cp}_2\text{Zr}(\text{CH}_3)(\text{Np})$ (2.232, 2.2980(13) Å; 130.6, 94.99 °) (Table 4).¹¹ The Zr-C(12) bond lengths (2.248(3) and 2.252(3) Å) in **22** are short in comparison to the range typically seen for zirconocenes having bulky alkyl groups (2.251-2.388 Å).¹⁷⁻¹⁹ No close zirconium-hydrogen contacts

are located as the nearest zirconium-hydrogen distance found in **22** is 2.791(1) Å. Details of the data collection and solution and refinement of the structure can be found in Appendix 1.

Table 4. Selected bond distances (Å) and bond angles (°) obtained from the X-ray structure determination of **22**

Feature	Distance (Å) or Angle (°)	Feature	Distance (Å) or Angle (°)
Zr(1)-Ct(1A) ^a	2.23	Zr(2)-Ct(1B) ^a	2.25
Zr(1)-Ct(2A) ^b	2.24	Zr(2)-Ct(2B) ^b	2.24
Zr(1)-C(11A)	2.294(3)	Zr(2)-C(11B)	2.306(3)
Zr(1)-C(12A)	2.248(3)	Zr(2)-C(12B)	2.252(3)
Ct(1A)-Zr(1)-Ct(2A)	130.9	Ct(1B)-Zr(2)-Ct(2B)	130.9
C(11A)-Zr(1)-C(12A)	94.54(12)	C(11B)-Zr(2)-C(12B)	95.07(12)

^a Ct(1A) is defined as the centroid of the ring made up of C(1A)-C(5A), Ct(1B) is defined as the centroid of the ring made up of C(1B)-C(5B); ^b Ct(2A) is defined as the centroid of the ring made up of C(6A)-C(10A), Ct(2B) is defined as the centroid of the ring made up of C(6B)-C(10B).

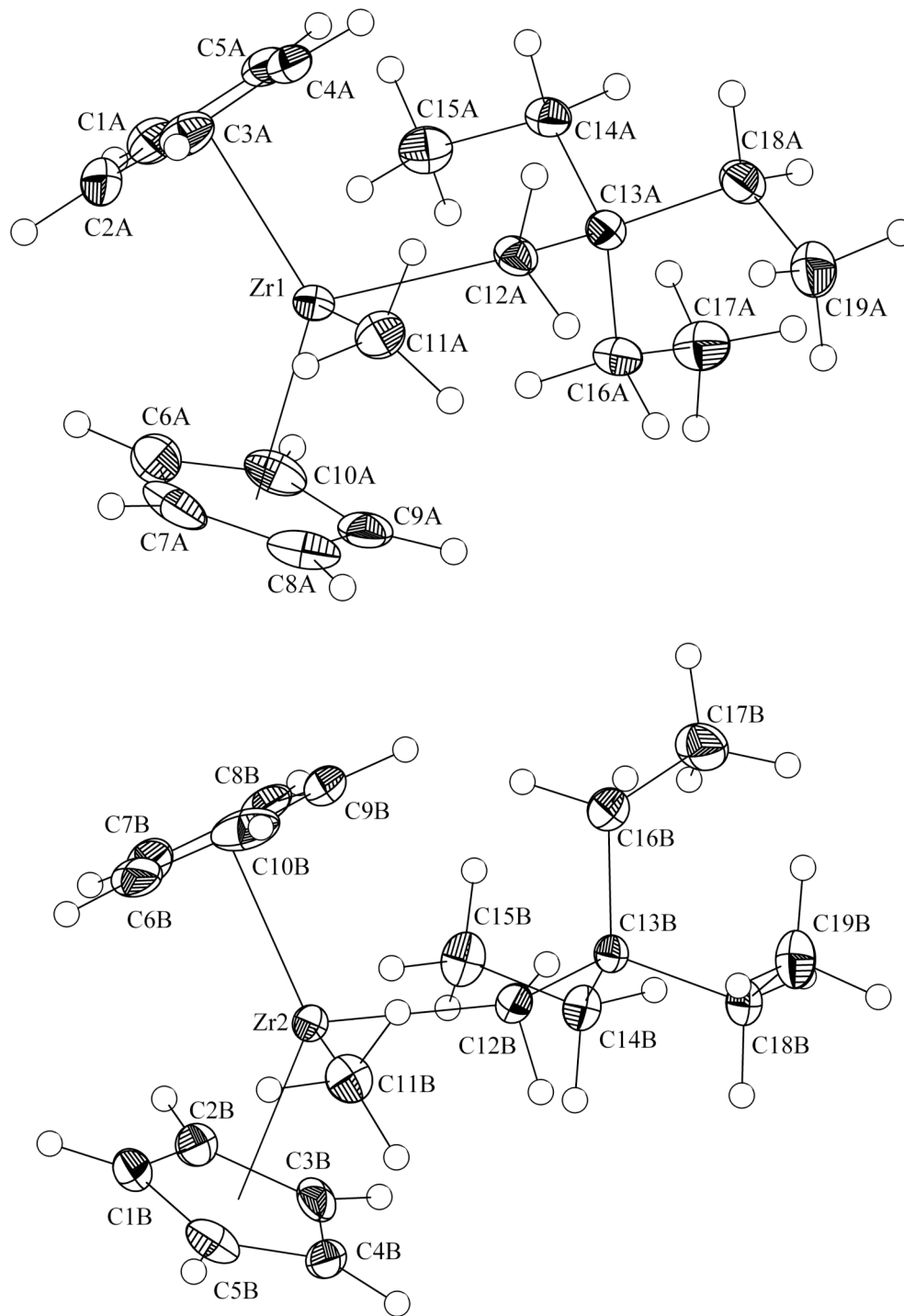


Figure 8. Molecular structure of **22** showing the unique molecules found in the asymmetric unit with 50% probability ellipsoids.

3 Conclusions

Synthesis and characterization of precatalysts leading to models for the propagating species in zirconocene-catalyzed alkene polymerization compatible with use in direct kinetic studies have been described. The intermediate steric demand of the mixed ring CpCp* ancillary ligation allows preparation of dialkylzirconocenes with two bulky alkyl groups and prevents the formation of methyl-bridged monocations when CpCp*Zr(CH₃)(R) are activated. A convenient general starting material for CpCp*Zr(CH₃)(R) synthesis is CpCp*Zr(CH₃)Cl. This compound is best prepared using ligand redistribution chemistry where the developed conditions minimize contamination by CpCp*ZrCl₂. Synthesis on the CpCp*{Zr} framework is often sensitive to the reaction conditions resulting in side-product formation via facile salt-mediated alkyl- or halide exchange processes. This reactivity can be minimized using optimized procedures. X-ray diffraction studies on CpCp*Zr(Np)₂, CpCp*Zr(CH₂TMS)₂, CpCp*Zr(Np)Cl, and Cp₂Zr(CH₂CEt₃)(CH₃) indicate minimal perturbation of the bent-sandwich coordination mode in the molecular structures. In some cases however, the steric bulk of the alkyl group is reflected in: slightly contracted Cp-Zr-Cp centroid angle, expanded carbon-Zr-carbon(chloride) angle, and zirconium-carbon bond lengths on the long end of the range commonly observed in Cp^x₂Zr(R)₂ and Cp^x₂Zr(CH₃)R type compounds. The structural design and synthetic procedures described here has afforded a variety of dialky- and methyl alkylzirconocene precatalysts that have been utilized successfully in further activation and kinetic studies.

4 Experimental Section

General Considerations

All air- and moisture-sensitive compounds were manipulated using standard high vacuum line, Schlenk, or cannula techniques, or in a drybox under a nitrogen atmosphere as described previously.³⁴ Argon gas was purified and dried by passage through columns of MnO on vermiculite and activated 4 Å molecular sieves. Solvents for air- and moisture-sensitive reactions were dried by the method of Grubbs³⁵ and were stored under vacuum over sodium benzophenone ketyl (diethyl ether, pentane, tetrahydrofuran), titanocene³⁶ (toluene, petroleum ether), calcium hydride (methylene chloride). Dioxane was vacuum distilled from calcium hydride and stored in a Schlenk flask under nitrogen. N-methylpyrrolidinone was purchased anhydrous from Aldrich in a Sure/Seal bottle. Benzene-*d*₆ and toluene-*d*₈ were purchased from Cambridge Isotopes and vacuum distilled from sodium benzophenone ketyl. Methylene chloride-*d*₂ was purchased from Cambridge Isotopes and vacuum distilled from calcium hydride. CDCl₃ was purchased from Cambridge Isotopes and stored over molecular sieves. The syntheses of CpCp*ZrCl₂, CpCp*Zr(CH₃)₂,³⁷ Cp₂Zr(CH₃)Cl,³⁸ LiNp,³⁹ and LiCH₂TMS⁴⁰ were carried out as previously reported. Li¹³CH₃·LiI²⁷ and (CH₃)₂Mg⁴¹ were prepared using standard procedures. NEt₃ and HN(ⁱPr)₂ were vacuum transferred from calcium hydride and stored in a Schlenk flask under argon. Butyllithium was purchased from Aldrich and stored under argon. Benzylbromide was purchased from Aldrich and distilled before use. NaI was dried under vacuum for 6 hours at 70 °C and stored under nitrogen in the drybox.

NMR spectra were recorded on Varian Mercury (300 MHz for ^1H) and Varian UNITY Inova (500.13 MHz for ^1H) spectrometers. Chemical shifts are given in ppm downfield from TMS using residual proton ($\text{C}_6\text{D}_5\text{H}$ 7.15; CHCl_3 7.26; $\text{C}_6\text{D}_5\text{CD}_2\text{H}$ 2.09; CDHCl_2 5.32) or carbon (C_6D_6 128.39; CDCl_3 77.23; CD_2Cl_2 54.00) signals of the deuterated solvents. X-ray crystallography was carried out using a Bruker SMART 1000 area detector. Elemental analyses were performed at Midwest MicroLab LLC.

Synthesis of $(\eta^5\text{-C}_5\text{H}_5)(\eta^5\text{-C}_5\text{Me}_5)\text{Zr}(\text{CH}_2\text{CMe}_3)_2$ (1). $(\text{CpCp}^*\text{Zr}(\text{Np})_2)$.

In an inert atmosphere glovebox, a 50 mL round bottom flask equipped with a stir bar was charged with $(\eta^5\text{-C}_5\text{H}_5)(\eta^5\text{-C}_5\text{Me}_5)\text{ZrCl}_2$ (0.502 g, 1.38 mmol) and $\text{LiCH}_2\text{CMe}_3$ (0.239 g, 3.06 mmol) and attached to a small swivel frit assembly. On the vacuum line, diethyl ether (25 mL) was vacuum transferred onto the solids at $-78\text{ }^\circ\text{C}$ and the apparatus was backfilled with Ar. The cooling bath was removed and the reaction mixture was allowed to warm to room temperature. Stirring for 36 h resulted in a yellow-brown solution and an off-white precipitate. The solvent was removed in vacuo leaving a tan solid. Petroleum ether (25 mL) was added to the solids by vacuum transfer. The resulting off-white precipitate was filtered away from the yellow-brown filtrate and washed once with recycled solvent. Removal of all volatiles and drying in vacuo yielded a tan powder. In the glovebox the solid was dissolved in pentane and the solution concentrated to 8 mL. The solution was cooled to $-35\text{ }^\circ\text{C}$ to recrystallize the desired product; pale yellow crystalline material suitable for X-ray diffraction was isolated and dried in vacuo. Yield: 0.398 g (66%). Anal. Calcd. for $\text{C}_{25}\text{H}_{42}\text{Zr}$: C, 69.21%, H, 9.76%. Found: C, 68.97, 69.24%, H, 9.64, 9.62%. ^1H NMR (500 MHz, C_6D_6): δ 5.94 (s, C_5H_5 ,

5H), 1.71 (s, $C_5(CH_3)_5$, 15H), 1.18 (s, $CH_2C(CH_3)_3$, 18H), 0.81 (d, $CH_2C(CH_3)_3$, 2H, $J = 11.6$ Hz), -0.47 (d, $CH_2C(CH_3)_3$, 2H, $J = 11.6$ Hz). $^{13}C\{^1H\}$ NMR (125 MHz, C_6D_6): δ 117.7 ($C_5(CH_3)_5$), 109.7 (C_5H_5), 78.4 (Zr- $CH_2C(CH_3)_3$), 37.1 ($CH_2C(CH_3)_3$), 35.6 ($CH_2C(CH_3)_3$), 12.5 ($C_5(CH_3)_5$). ^{13}C NMR (125 MHz, C_6D_6): δ 117.7 (s, $C_5(CH_3)_5$, 5C), 109.7 (d, C_5H_5 , 5C, $^1J_{CH} = 174.8$ Hz), 78.4 (t, Zr- $CH_2C(CH_3)_3$, 2C, $^1J_{CH} = 109.1$ Hz), 37.1 (s, $CH_2C(CH_3)_3$, 2C), 35.6 (q, $CH_2C(CH_3)_3$, 6C, $^1J_{CH} = 123.3$ Hz), 12.5 (q, $C_5(CH_3)_5$, 5C, $^1J_{CH} = 126.2$ Hz).

Synthesis of $(\eta^5-C_5H_5)(\eta^5-C_5Me_5)Zr(CH_2SiMe_3)_2$ (2). ($CpCp^*Zr(CH_2TMS)_2$).

In an inert atmosphere glovebox, a 50 mL round bottom flask equipped with a stir bar was charged with $(\eta^5-C_5H_5)(\eta^5-C_5Me_5)ZrCl_2$ (1.170 g, 3.23 mmol) and $LiCH_2SiMe_3$ (0.639 g, 6.78 mmol) and attached to a small swivel frit assembly. On the vacuum line, diethyl ether (30 mL) was vacuum transferred onto the solids at -78 °C and the apparatus was backfilled with Ar. The reaction mixture was allowed to warm to room temperature with stirring, and an off-white precipitate was observed. After stirring for 12 h, the solvent was removed in vacuo leaving a colorless oily paste. Pentane (35 mL) was added to the mixture by vacuum transfer. The resulting off-white precipitate was filtered away from the colorless filtrate and washed two times with recycled solvent. Removal of all volatiles and drying in vacuo yielded an off-white powder. In the glovebox the solid was dissolved in pentane and the solution concentrated to 8 mL. The solution was cooled to -35 °C to recrystallize the desired product; colorless crystalline material suitable for X-ray diffraction was isolated and dried in vacuo. Yield: 1.051 g (70%). Anal. Calcd. for $C_{23}H_{42}Si_2Zr$: C, 59.28%, H, 9.08%. Found: C, 59.45, 59.37%, H, 9.20, 8.95%. 1H NMR

(500 MHz, C_6D_6): δ 5.89 (s, C_5H_5 , 5H), 1.70 (s, $C_5(CH_3)_5$, 15H), 0.21 (s, $CH_2Si(CH_3)_3$, 18H), -0.25 (d, $CH_2Si(CH_3)_3$, 2H, $J = 10.7$ Hz), -0.54 (d, $CH_2Si(CH_3)_3$, 2H, $J = 10.9$ Hz).
 $^{13}C\{^1H\}$ NMR (125 MHz, C_6D_6): δ 118.2 ($C_5(CH_3)_5$), 110.8 (C_5H_5), 46.0 (Zr- $CH_2Si(CH_3)_3$), 12.4 ($C_5(CH_3)_5$), 4.10 ($CH_2Si(CH_3)_3$).

NMR scale synthesis of $(\eta^5-C_5H_5)(\eta^5-C_5Me_5)Zr(CH_3)Cl$ (3**). ($CpCp^*Zr(CH_3)Cl$).**

In an inert atmosphere glovebox $(\eta^5-C_5H_5)(\eta^5-C_5Me_5)ZrCl_2$ (45 mg, 0.12 mmol) was weighed into a small vial. To this was added 0.25 mL of a 0.5 M solution of $(\eta^5-C_5H_5)(\eta^5-C_5Me_5)Zr(CH_3)_2$ (40 mg, 0.12 mmol) in toluene- d_8 . The contents of the vial were transferred via pipet to a J. Young NMR tube and the vial was rinsed with an additional 0.45 mL of solvent. The reaction was heated in an oil bath regulated at 130 °C and the reaction progress was monitored by 1H NMR spectroscopy. The solution was pale yellow and a solid crystallized out upon cooling the sample to room temperature to acquire 1H NMR data. After 10 days of heating at this temperature, clean formation of **3** was observed in 95% yield (by 1H NMR).

Synthesis of $(\eta^5-C_5H_5)(\eta^5-C_5Me_5)Zr(CH_3)Cl$ (3**). ($CpCp^*Zr(CH_3)Cl$).**

In an inert atmosphere glovebox, a thick walled glass vessel equipped with a stir bar was charged with $(\eta^5-C_5H_5)(\eta^5-C_5Me_5)ZrCl_2$ (2.001 g, 5.52 mmol) and $(\eta^5-C_5H_5)(\eta^5-C_5Me_5)Zr(CH_3)_2$ (2.048 g, 6.37 mmol). Toluene (24 mL, vacuum transferred from titanocene) was added giving a mixture consisting of a yellow solution and remaining solid $(\eta^5-C_5H_5)(\eta^5-C_5Me_5)ZrCl_2$. The vessel was sealed with an 8 mm Kontes needle valve and the mixture was stirred in the box to break up the solid. In the hood, the

reaction was heated with stirring in an oil bath regulated at 130 °C for 11.64 d. At this temperature a homogeneous solution was observed. The reaction was removed from the oil bath and cooled to room temperature resulting in a green solution and an off-white precipitate. In the glovebox, a small heterogeneous sample was dried in vacuo for analysis by ^1H NMR spectroscopy and confirmed clean conversion to product ($< 5\%$ $(\eta^5\text{-C}_5\text{H}_5)(\eta^5\text{-C}_5\text{Me}_5)\text{ZrCl}_2$). At this point, toluene was added, and the reaction was transferred to a flask and was concentrated and dried in vacuo. The resulting solid was stirred in petroleum ether (100 mL) and filtered. The precipitate was isolated and was purified by precipitation from a concentrated toluene – petroleum ether solution at -35 °C. Removal of all volatiles gave 0.340 g of an off-white solid identical (by ^1H NMR spectroscopy) to that obtained using the literature procedure. An additional 2.953 g of product was obtained by concentration of the combined organic filtrates and several repetitions of the purification procedure. Yield: 3.293 g (87%). Anal. Calcd. for $\text{C}_{16}\text{H}_{23}\text{ClZr}$: C, 56.19%, H, 6.78%. Found: C, 55.31%, H, 6.51%. ^1H NMR (300 MHz, C_6D_6): δ 5.79 (s, C_5H_5 , 5H), 1.71 (s, $\text{C}_5(\text{CH}_3)_5$, 15H), 0.22 (s, CH_3 , 3H). $^{13}\text{C}\{^1\text{H}\}$ NMR (75 MHz, C_6D_6): δ 120.5 ($\text{C}_5(\text{CH}_3)_5$), 113.6 (C_5H_5), 35.3 (Zr-CH_3), 12.2 ($\text{C}_5(\text{CH}_3)_5$).

Synthesis of $(\eta^5\text{-C}_5\text{H}_5)(\eta^5\text{-C}_5\text{Me}_5)\text{Zr}(\text{CH}_2\text{SiMe}_3)(\text{CH}_3)$ (4). ($\text{CpCp}^*\text{Zr}(\text{CH}_2\text{TMS})\text{Me}$).

In an inert atmosphere glovebox, a 50 mL round bottom flask equipped with a stir bar was charged with $(\eta^5\text{-C}_5\text{H}_5)(\eta^5\text{-C}_5\text{Me}_5)\text{Zr}(\text{CH}_3)\text{Cl}$ (0.866 g, 2.53 mmol) and $\text{LiCH}_2\text{SiMe}_3$ (0.240 g, 2.54 mmol) and attached to a small swivel frit assembly. On the vacuum line, diethyl ether (25 mL) was vacuum transferred onto the solids at -78 °C and the apparatus was backfilled with Ar. The reaction mixture was allowed to warm to room temperature

over 12 h with stirring. At this time a colorless solution with a white precipitate was observed. The solvent was removed and resultant paste was dried in vacuo. Pentane (20 mL) was added to the mixture by vacuum transfer. The resulting white precipitate was filtered away from the colorless filtrate and washed twice with recycled solvent. Removal of all volatiles and drying in vacuo resulted in a pale yellow oil. Repeated attempts to solidify the product by trituration with pentane or lyophilization with benzene failed. Yield: 0.865 g (87%). ^1H NMR (300 MHz, C_6D_6): δ 5.79 (s, C_5H_5 , 5H), 1.68 (s, $\text{C}_5(\text{CH}_3)_5$, 15H), 0.21 (s, $\text{CH}_2\text{Si}(\text{CH}_3)_3$, 9H), -0.29 (s, CH_3 , 3H) -0.31 (d, $\text{CH}_2\text{Si}(\text{CH}_3)_3$, 1H, $J = 9.5$ Hz), -0.38 (d, $\text{CH}_2\text{Si}(\text{CH}_3)_3$, 1H, $J = 9.5$ Hz). $^{13}\text{C}\{^1\text{H}\}$ NMR (75 MHz, C_6D_6): δ 117.9 ($\text{C}_5(\text{CH}_3)_5$), 111.4 (C_5H_5), 44.9 (Zr- $\text{CH}_2\text{Si}(\text{CH}_3)_3$), 34.0 (Zr- CH_3), 12.4 ($\text{C}_5(\text{CH}_3)_5$), 4.3 ($\text{CH}_2\text{Si}(\text{CH}_3)_3$).

Reaction of $(\eta^5\text{-C}_5\text{H}_5)(\eta^5\text{-C}_5\text{Me}_5)\text{Zr}(\text{CH}_3)\text{Cl}$ and $\text{LiCH}_2\text{CMe}_3$ leading to multiple dialkylzirconocene products.

In an inert atmosphere glovebox, a 50 mL round bottom flask equipped with a stir bar was charged with $(\eta^5\text{-C}_5\text{H}_5)(\eta^5\text{-C}_5\text{Me}_5)\text{Zr}(\text{CH}_3)\text{Cl}$ (0.500 g, 1.46 mmol) and $\text{LiCH}_2\text{CMe}_3$ (0.126 g, 1.60 mmol) and attached to a small swivel frit assembly. On the vacuum line, diethyl ether (30 mL) was vacuum transferred onto the solids at -78 °C and the apparatus was backfilled with Ar. The cooling bath was removed and the reaction mixture was stirred for 48 h at room temperature. At this time a bright yellow solution with white precipitate was observed. The solvent was removed in vacuo leaving an oily residue. Pentane (15 mL) was added to the mixture by vacuum transfer. The resulting white precipitate was filtered away from the yellow filtrate and washed with recycled solvent.

Removal of all volatiles and drying in vacuo resulted in a yellow-brown oil. Characterization of the crude oil by ^1H NMR indicated three compounds in the product mixture. $(\eta^5\text{-C}_5\text{H}_5)(\eta^5\text{-C}_5\text{Me}_5)\text{Zr}(\text{CH}_3)_2$, $(\eta^5\text{-C}_5\text{H}_5)(\eta^5\text{-C}_5\text{Me}_5)\text{Zr}(\text{Np})(\text{CH}_3)$, and $(\eta^5\text{-C}_5\text{H}_5)(\eta^5\text{-C}_5\text{Me}_5)\text{Zr}(\text{Np})_2$ were present in a 16:66:18 ratio respectively.

Synthesis of $(\eta^5\text{-C}_5\text{H}_5)(\eta^5\text{-C}_5\text{Me}_5)\text{Zr}(\text{CH}_2\text{CMe}_3)(\text{CH}_3)$ (5). ($\text{CpCp}^*\text{Zr}(\text{Np})\text{Me}$).

In an inert atmosphere glovebox, a 100 mL round bottom flask equipped with a stir bar was charged with $(\eta^5\text{-C}_5\text{H}_5)(\eta^5\text{-C}_5\text{Me}_5)\text{Zr}(\text{CH}_3)\text{Cl}$ (0.592 g, 1.73 mmol) and $\text{LiCH}_2\text{CMe}_3$ (0.136 g, 1.74 mmol) and attached to a small swivel frit assembly. On the vacuum line, toluene (70 mL) was vacuum transferred onto the solids at $-78\text{ }^\circ\text{C}$ and the apparatus was backfilled with Ar. The reaction mixture was stirred for 9 h at $-78\text{ }^\circ\text{C}$, then allowed to warm to room temperature over 14 h with stirring. At this time a yellow-green solution was observed. The solvent was removed in vacuo leaving an oily paste. Pentane (25 mL) was added to the mixture by vacuum transfer. The resulting white precipitate was filtered away from the yellow filtrate and washed with recycled solvent. Removal of all volatiles and drying in vacuo resulted in a yellow oil. In the glovebox this oil was dissolved in petroleum ether (20 mL) and filtered via pipet through celite directly into a 50 mL Kjeldahl flask equipped with a stir bar. The flask was attached to a needle valve and on the vacuum line the volatiles were removed. Pentane (15 mL) was added by vacuum transfer to dissolve the oil, and was removed slowly in vacuo with rapid stirring. Further trituration with pentane (generally 3 cycles) gave a yellow powder that was dried in vacuo. Yield: 0.550 g (84%). Anal. Calcd. for $\text{C}_{21}\text{H}_{34}\text{Zr}$: C, 66.78%, H, 9.07%. Found: C, 66.52, 66.76%, H, 8.97, 9.01%. ^1H NMR (300 MHz, C_6D_6): δ 5.86 (s, C_5H_5 , 5H),

1.67 (s, $C_5(CH_3)_5$, 15H), 1.13 (s, $CH_2C(CH_3)_3$, 9H), 0.45 (d, $CH_2C(CH_3)_3$, 1H, $J = 12.6$ Hz), -0.18 (d, $CH_2C(CH_3)_3$, 1H, $J = 12.6$ Hz), -0.27 (s, CH_3 , 3H). $^{13}C\{^1H\}$ NMR (75 MHz, C_6D_6): δ 117.9 ($C_5(CH_3)_5$), 111.3 (C_5H_5), 70.9 (Zr- $CH_2C(CH_3)_3$), 36.5 (Zr- CH_3), 36.3 ($CH_2C(CH_3)_3$), 36.0 ($CH_2C(CH_3)_3$), 12.3 ($C_5(CH_3)_5$).

Synthesis of $(\eta^5-C_5H_5)(\eta^5-C_5Me_5)Zr(CH_2CMe_3)Cl$ (6). ($CpCp^*Zr(Np)(Cl)$).

In an inert atmosphere glovebox, a 50 mL round bottom flask equipped with a stir bar was charged with $(\eta^5-C_5H_5)(\eta^5-C_5Me_5)ZrCl_2$ (0.211 g, 0.58 mmol) and $LiCH_2CMe_3$ (0.046 g, 0.59 mmol) and attached to a small swivel frit assembly. On the vacuum line, toluene (25 mL) was vacuum transferred onto the solids at -78 °C and the apparatus was backfilled with Ar. The cooling bath was removed and the reaction mixture was allowed to warm to room temperature. Stirring for 5 h resulted in a bright yellow solution and a white precipitate. The reaction was filtered and the precipitate was washed twice with recycled solvent. The solvent was removed in vacuo leaving a bright yellow sticky solid. Petroleum ether (10 mL) was added to the isolated material by vacuum transfer followed by stirring at room temperature. Removal of all volatiles and drying in vacuo yielded a bright yellow powder. In the glovebox, the product was precipitated upon addition of petroleum ether to a concentrated diethyl ether solution (5 mL) and cooling to -35 °C. The resulting yellow precipitate was isolated and dried in vacuo. Alternatively, the product may be crystallized by slow diffusion of petroleum ether into a diethyl ether solution cooled to -35 °C; yellow crystalline fragments suitable for X-ray diffraction were obtained via this method. Yield: 0.195 g (84%). Anal. Calcd. for $C_{21}H_{31}ClZr$: C, 60.33%, H, 7.85%. Found: C, 60.10, 60.41%, H, 7.73, 7.87%. 1H NMR (300 MHz,

C_6D_6): δ 5.94 (s, C_5H_5 , 5H), 1.69 (s, $C_5(CH_3)_5$, 15H), 1.26 (s, $CH_2C(CH_3)_3$, 9H), 1.21 (d, $CH_2C(CH_3)_3$, 1H, $J = 13.2$ Hz), 0.16 (d, $CH_2C(CH_3)_3$, 1H, $J = 13.2$ Hz). $^{13}C\{^1H\}$ NMR (75 MHz, C_6D_6): δ 121.0 ($C_5(CH_3)_5$), 113.3 (C_5H_5), 68.9 (Zr- $CH_2C(CH_3)_3$), 36.5 ($CH_2C(CH_3)_3$), 35.5 ($CH_2C(CH_3)_3$), 12.4 ($C_5(CH_3)_5$).

Alternate methods for the synthesis of $(\eta^5-C_5H_5)(\eta^5-C_5Me_5)Zr(CH_2CMe_3)(CH_3)$ (5**):**

Reaction of $(\eta^5-C_5H_5)(\eta^5-C_5Me_5)Zr(CH_2CMe_3)Cl$ with $LiCH_3$.

In an inert atmosphere glovebox, a J. Young NMR tube was charged with $(\eta^5-C_5H_5)(\eta^5-C_5Me_5)Zr(CH_2CMe_3)Cl$ (12 mg, 0.03 mmol) and dry, ether-free solid $LiCH_3$ (1.5 mg, 0.07 mmol). Benzene- d_6 (0.78 mL) was added to give a yellow solution; $LiCH_3$ was not soluble in C_6D_6 at room temperature. The reaction was heated at 80 °C and monitored by 1H NMR spectroscopy. After 4 hr of heating, the 1H NMR spectrum indicated a 30:70 mixture of **6** and **5** respectively. The reaction was complete (by 1H NMR) after an additional 5 hr of heating at this temperature to yield **5** cleanly as the only product.

Alternate methods for the synthesis of $(\eta^5-C_5H_5)(\eta^5-C_5Me_5)Zr(CH_2CMe_3)(CH_3)$ (5**):**

Reaction of $(\eta^5-C_5H_5)(\eta^5-C_5Me_5)Zr(CH_2CMe_3)Cl$ with $Li^{13}CH_3 \cdot LiI$.

In an inert atmosphere glovebox, a J. Young NMR tube was charged with $(\eta^5-C_5H_5)(\eta^5-C_5Me_5)Zr(CH_2CMe_3)Cl$ (12.8 mg, 0.03 mmol) and dry, ether-free solid $Li^{13}CH_3 \cdot LiI$ (6.3 mg, 0.04 mmol). Benzene- d_6 (0.78 mL) was added to give a yellow solution; $Li^{13}CH_3 \cdot LiI$ was not soluble in C_6D_6 at room temperature. The reaction was heated in an oil bath regulated at 85 °C and allowed to proceed for 14 hr. At this time the sample was cooled to room temperature and a yellow-green solution with a white precipitate was observed.

Analysis by ^1H NMR spectroscopy indicated the formation of **5** as well as other zirconocene derived products.

Alternate methods for the synthesis of $(\eta^5\text{-C}_5\text{H}_5)(\eta^5\text{-C}_5\text{Me}_5)\text{Zr}(\text{CH}_2\text{CMe}_3)(\text{CH}_3)$ (5**):**

Reaction of $(\eta^5\text{-C}_5\text{H}_5)(\eta^5\text{-C}_5\text{Me}_5)\text{Zr}(\text{CH}_2\text{CMe}_3)\text{Cl}$ with CH_3MgBr .

In an inert atmosphere glovebox, $(\eta^5\text{-C}_5\text{H}_5)(\eta^5\text{-C}_5\text{Me}_5)\text{Zr}(\text{CH}_2\text{CMe}_3)\text{Cl}$ (31 mg, 0.08 mmol) was dissolved in diethyl ether (5 mL) and cooled to $-35\text{ }^\circ\text{C}$. A 3.17 M solution of CH_3MgBr (0.04 mL, 0.12 mmol) was diluted in diethyl ether (2 mL) and cooled to $-35\text{ }^\circ\text{C}$. The chilled solution of CH_3MgBr was added dropwise to the bright yellow solution of $(\eta^5\text{-C}_5\text{H}_5)(\eta^5\text{-C}_5\text{Me}_5)\text{Zr}(\text{CH}_2\text{CMe}_3)\text{Cl}$. The reaction was stirred for 2 hr over which time it became a darker yellow color. Dioxane (2 mL) was added and a white solid precipitated from the yellow solution. The reaction was filtered and removal of all volatiles followed by drying in vacuo yielded a yellow oily residue. Analysis of the isolated material by ^1H NMR spectroscopy revealed three compounds were present. Compounds **6**, $(\eta^5\text{-C}_5\text{H}_5)(\eta^5\text{-C}_5\text{Me}_5)\text{Zr}(\text{CH}_2\text{CMe}_3)\text{Br}$ (**6-Br**), and **5** were observed in roughly a 2:2:1 ratio respectively.

Alternate methods for the synthesis of $(\eta^5\text{-C}_5\text{H}_5)(\eta^5\text{-C}_5\text{Me}_5)\text{Zr}(\text{CH}_2\text{CMe}_3)(\text{CH}_3)$ (5**):**

Reaction of $(\eta^5\text{-C}_5\text{H}_5)(\eta^5\text{-C}_5\text{Me}_5)\text{Zr}(\text{CH}_2\text{CMe}_3)\text{Cl}$ with $\text{Mg}(\text{CH}_3)_2$.

In an inert atmosphere glovebox, a J. Young NMR tube was charged with $(\eta^5\text{-C}_5\text{H}_5)(\eta^5\text{-C}_5\text{Me}_5)\text{Zr}(\text{CH}_2\text{CMe}_3)\text{Cl}$ (15 mg, 0.04 mmol) and $\text{Mg}(\text{CH}_3)_2$ (1 mg, 0.02 mmol). Benzene- d_6 (0.78 mL) was added to give a yellow solution. The reaction was heated at $80\text{ }^\circ\text{C}$ and was allowed to proceed for 14 hr over which time the solution became more green in

color and a precipitate was observed. The ^1H NMR spectrum indicated a 40:60 mixture of **6** and **5** respectively. Additional $\text{Mg}(\text{CH}_3)_2$ (1 mg, 0.02 mmol) was added to the sample. The reaction was complete (by ^1H NMR) after an additional 4.5 hr of heating at this temperature to yield **5** cleanly as the only product.

2-Ethylbutyric acid methyl ester (8).

A 500 ml round bottom flask was charged with 2-ethylbutyric acid (**7**) (92.4 g, 795 mmol) and methanol (275 ml, 6760 mmol). Concentrated H_2SO_4 (23 ml) was added and a reflux condenser was attached. The mixture was heated to reflux for 24 h. Methanol was distilled off on a water bath. The residue was diluted with water (500 ml) and the layers were separated. Organics remaining in the aqueous layer were extracted with diethyl ether. The combined organic phases were washed with saturated NaHCO_3 , water, and dried over MgSO_4 . The solvent was removed under reduced pressure. The product was distilled (137 °C, 1 atm) to produce a clear liquid. Yield: 51.65 g (50%). ^1H NMR (300 MHz, CDCl_3) δ 3.67 (s, OCH_3 , 3H), 2.21 (m, $\text{CH}(\text{CH}_2\text{CH}_3)_2$, 1H), 1.56 (m, $\text{CH}(\text{CH}_2\text{CH}_3)_2$, 4H), 0.88 (t, $\text{CH}(\text{CH}_2\text{CH}_3)_2$, 6H, $J = 7.5$ Hz); ^{13}C NMR (75 MHz, CDCl_3) δ 176.89, 51.61, 49.19, 25.45, 12.24; DEPT (75 MHz, CDCl_3) δ 176.89 (quaternary C), 49.18 (CH), 25.43 (CH_2), 51.58, 12.23 (CH_3).

2,2-Diethylbutyric acid methylester (9).

A 1 L Schlenk flask with addition funnel was purged with argon and charged with $\text{HN}(\text{iPr})_2$ (47.4 ml, 338 mmol). THF (250 ml) was added via cannula and the solution cooled to 0 °C. Butyllithium (211 ml, 338 mmol) was transferred to the addition funnel

by cannula and was added to the reaction mixture over 40 min with stirring. The reaction was then cooled to $-30\text{ }^{\circ}\text{C}$ and **8** (40.0 g, 307 mmol) was added slowly by syringe. The yellow solution was stirred for 30 min at this temperature. Ethyliodide (27.3 ml, 338 mmol) was added at $-78\text{ }^{\circ}\text{C}$. The mixture stirred at this temperature for 5 h and then at room temperature overnight. The reaction was added to a separatory funnel with diethyl ether and water and the phases separated. The aqueous layer was extracted with additional diethyl ether. The combined organic layers were washed with saturated NaCl and dried over MgSO_4 . The solvent was removed under reduced pressure. The resulting yellow liquid was distilled under full vacuum ($30\text{-}31\text{ }^{\circ}\text{C}$, $\approx 1\text{ mm Hg}$) and a clear liquid was collected in two fractions. Yield: 39.3 g (81%). $^1\text{H NMR}$ (300 MHz, CDCl_3) δ 3.66 (s, OCH_3 , 3H), 1.57 (q, $\text{C}(\text{CH}_2\text{CH}_3)_3$, 6H, $J = 7.5\text{ Hz}$), 0.75 (t, $\text{C}(\text{CH}_2\text{CH}_3)_3$, 9H, $J = 7.3\text{ Hz}$); ^{13}C (75 MHz, CDCl_3) δ 177.90, 51.66, 50.32, 26.40, 8.71; DEPT (75 MHz, CDCl_3) δ 177.90, 50.32 (quaternary C), 26.40 (CH_2), 51.67, 8.71 (CH_3).

2,2-Diethylbutanol (10).

In the glovebox, a 3 L three neck flask was charged with LiAlH_4 (7.19 g, 190 mmol). Outside the glovebox, an addition funnel was attached under a flow of argon. All joints were sealed with Teflon tape and all adaptors secured with wire and rubber bands. The flask was cooled in an ice-NaCl bath and diethyl ether (750 ml) was added through the addition funnel by cannula. **9** (30.0 g, 190 mmol) was poured into the addition funnel and dissolved in diethyl ether against a strong flow of argon. This solution was added dropwise over 1 h and the temperature maintained at $0\text{ }^{\circ}\text{C}$. Stirring continued overnight. The reaction was quenched using Fieser conditions: water (8 ml), 15% NaOH (8 g of

solution), water (24 ml). The liquids were removed from the sludgy white precipitate with additional diethyl ether. The phases were separated and aqueous layer washed three times with diethyl ether. The combined organic layer was dried over MgSO_4 and the solvent removed under reduced pressure. The resulting cloudy liquid was distilled from CaSO_4 under reduced pressure (80-82 °C, 20 mm Hg) producing a white liquid. Yield: 22.0 g (89%). ^1H NMR (300 MHz, CDCl_3) δ 3.34 (d, $\text{CH}_2\text{C}(\text{CH}_2\text{CH}_3)_3$, 2H, $J = 3.9$ Hz), 1.30 (br, OH, 1H), 1.22 (q, $\text{CH}_2\text{C}(\text{CH}_2\text{CH}_3)_3$, 6H, $J = 7.5$ Hz), 0.77 (t, $\text{CH}_2\text{C}(\text{CH}_2\text{CH}_3)_3$, 9H, $J = 7.6$ Hz); ^{13}C (75 MHz, CDCl_3) δ 65.99, 39.79, 25.26, 7.73; DEPT (75 MHz, CDCl_3) δ 39.79 (quaternary C), 65.96, 25.25 (CH_2), 7.72 (CH_3).

(2,2-Diethyl)butyl mesylate (11).

A 250 ml round bottom flask was charged with **10** (7.07 g, 54.3 mmol) and purged with argon. CH_2Cl_2 (125 ml) was added via cannula. NEt_3 (11.4 ml, 81.7 mmol) was added by syringe and the mixture was cooled to 0 °C. $\text{CH}_3\text{SO}_2\text{Cl}$ (4.8 ml, 62.0 mmol) was added dropwise. The solution became pale yellow and a precipitate formed. Stirring continued at this temperature for 1 h. For workup, additional CH_2Cl_2 was added and organics were washed with ice water (250 ml), chilled 10% HCl (250 ml), saturated NaHCO_3 , and saturated NaCl. After drying over Na_2SO_4 the solvent was removed under reduced pressure to yield a thick yellow liquid that was > 95% pure by NMR. Yield: 11.3 g (quantitative). ^1H NMR (300 MHz, CDCl_3) δ 3.95 (s, $\text{CH}_2\text{C}(\text{CH}_2\text{CH}_3)_3$, 2H), 2.30 (s, CH_3 , 3H), 1.30 (q, $\text{CH}_2\text{C}(\text{CH}_2\text{CH}_3)_3$, 6H, $J = 7.5$ Hz), 0.81 (t, $\text{CH}_2\text{C}(\text{CH}_2\text{CH}_3)_3$, 9H, $J = 7.5$ Hz); ^{13}C (75 MHz, CDCl_3) δ 72.71, 39.13, 37.35, 25.34, 7.58; DEPT (75 MHz, CDCl_3) δ 39.13 (quaternary C), 72.69, 25.32 (CH_2), 37.35, 7.59 (CH_3).

2,2-Diethyl-1-iodobutane (12).

A 50 ml flask with condenser was charged with **11** (2.91 g, 13.9 mmol) and anhydrous NaI (10.45 g, 69.7 mmol) and was purged with argon. *N*-methylpyrrolidinone (30 ml) was added via syringe. The reaction was heated to 140 °C for 4 h under argon. The reaction was cooled and water and pentane were added. The phases were separated and the aqueous layer was extracted with pentane. The combined organic phases (400 ml) were washed with saturated Na₂S₂O₃, twice with saturated CuSO₄, and water. After drying over MgSO₄, the pentane was removed under reduced pressure. The yellow liquid was purified by column chromatography on silica with hexanes. The product was a clear liquid that was homogeneous by TLC. Yield: 3.13 g (93%). ¹H NMR (300 MHz, CDCl₃) δ 3.12 (s, CH₂C(CH₂CH₃)₃, 2H), 1.30 (q, CH₂C(CH₂CH₃)₃, 6H, J = 7.8 Hz), 0.76 (t, CH₂C(CH₂CH₃)₃, 9H, J = 7.35 Hz); ¹³C (75 MHz, CDCl₃) δ 38.04, 27.38, 20.25, 8.15; DEPT (75 MHz, CDCl₃) δ 38.04 (quaternary C), 27.38, 20.25 (CH₂), 8.14 (CH₃).

Synthesis of Li(CH₂C(CH₂CH₃)₃) (13). (LiCH₂CEt₃).

2,2-Diethyl-1-iodobutane (0.102 g, 0.43 mmol) was weighed into a 25 mL round bottom flask equipped with a 180 ° needle valve and was degassed with two freeze-pump-thaw cycles at 77 K on the high vacuum line. Pentane then diethyl ether were added by vacuum transfer at -78 °C in a 3:2 ratio respectively to give a total solvent volume of 12 mL. (Note: this reaction also worked effectively in 3:1 pentane-diethyl ether solvent). The apparatus was backfilled with Ar and stirred briefly at room temperature. The Kontes needle valve was replaced with a septum using a positive Ar counter-flow. The

solution was then cooled to $-78\text{ }^{\circ}\text{C}$ and a 1.7 M solution of *t*-butyllithium (0.56 mL, 0.95 mmol) was added dropwise using an Ar flushed syringe. During the addition, formation of a white precipitate was observed. The reaction was stirred at $-78\text{ }^{\circ}\text{C}$ for 40 min. The dry ice-acetone bath was removed and the reaction was allowed to warm to room temperature with stirring for 30 min during after which time a colorless solution was observed. The septum was replaced with a Kontes needle valve and the solvent was removed. Drying in vacuo yielded a white glassy solid. In the glovebox the reaction flask was attached to a small swivel frit assembly. On the vacuum line, pentane (12 mL) was vacuum transferred onto the glassy solid at $-78\text{ }^{\circ}\text{C}$. Warming to room temperature and stirring to break up the solids resulted in a colorless solution with a white precipitate. This solution was filtered and the precipitate washed one time with recycled solvent. The solvent was removed to yield a pale yellow - almost colorless - oil that was dried in vacuo. Yield: 0.045 g (88%). ^1H NMR (300 MHz, C_6D_6): δ 1.34 (br q, $\text{CH}_2\text{C}(\text{CH}_2\text{CH}_3)_3$, 6H, $J = 7.2$ Hz), 0.90 (t, $\text{CH}_2\text{C}(\text{CH}_2\text{CH}_3)_3$, 9H, $J = 7.5$ Hz), -0.71 (br s, $\text{CH}_2\text{C}(\text{CH}_2\text{CH}_3)_3$, 2H).

2,2-Dimethyl-3-phenylpropionic acid ethylester (15).

A 1 L Schlenk flask with addition funnel was purged with argon and charged with $\text{HN}(\text{iPr})_2$ (66.4 ml, 473 mmol). THF (300 ml) was added via cannula and the solution cooled to $0\text{ }^{\circ}\text{C}$. Butyllithium (296 ml, 474 mmol) was transferred to the addition funnel by cannula and was added to the reaction mixture over 40 min with stirring. The reaction was then cooled to $-30\text{ }^{\circ}\text{C}$ and 2-methylpropionic acid ethylester (**14**) (50.0 g, 430 mmol) was added slowly by syringe. The yellow solution was stirred for 30 min at this

temperature. Benzylbromide (56.3 ml, 473 mmol) was added at $-78\text{ }^{\circ}\text{C}$. The mixture stirred at this temperature for 5 h and then at room temperature overnight. The reaction was added to a separatory funnel with diethyl ether and water and the phases separated. The aqueous layer was extracted with additional diethyl ether. The combined organic layers were washed with saturated NaCl and dried over MgSO_4 . The solvent was removed under reduced pressure. The resulting yellow liquid was distilled under full vacuum ($55\text{-}57\text{ }^{\circ}\text{C}$, $\approx 1\text{ mm Hg}$) yielding a faintly yellow liquid. Yield: 74.8 g (84%). $^1\text{H NMR}$ (300 MHz, CDCl_3) δ 7.23 (m, *m* and *p*-PhH, 3H), 7.11 (dd, *o*-PhH, 2H, $J = 1.65$, 7.65 Hz), 4.11 (q, OCH_2CH_3 , 2H, $J = 7.2$ Hz), 2.85 (s, $\text{C}(\text{CH}_3)_2\text{CH}_2\text{Ph}$, 2H), 1.23 (t, OCH_2CH_3 , 3H, $J = 7.2$ Hz), 1.17 (s, $\text{C}(\text{CH}_3)_2\text{CH}_2\text{Ph}$, 6H); ^{13}C (75 MHz, CDCl_3) δ 177.54, 138.13, 130.33, 128.09, 126.54, 60.65, 46.59, 43.79, 25.30, 14.53; DEPT (75 MHz, CDCl_3) δ 177.54, 138.13, 43.79 (quaternary C), 130.32, 128.10, 126.56 (CH), 60.69, 46.58 (CH_2), 25.30, 14.57 (CH_3).

2,2-Dimethyl-3-phenylpropanol (16).

In the glovebox, a 3 L three neck flask was charged with LiAlH_4 (10.41 g, 274 mmol). Outside the glovebox, an addition funnel was attached under a flow of argon. All joints were sealed with Teflon tape and all adaptors secured with wire and rubber bands. The flask was cooled in an ice-NaCl bath and diethyl ether (850 ml) was added through the addition funnel by cannula. **15** (50.0 g, 242 mmol) was poured into the addition funnel and dissolved in diethyl ether against a strong flow of argon. This solution was added dropwise over 1 h and the temperature maintained at $0\text{ }^{\circ}\text{C}$. Stirring continued overnight. The reaction was quenched using Fieser conditions: water (11 ml), 15% NaOH (11 g of

solution), water (33 ml). The liquids were removed from the sludgy white precipitate with additional diethyl ether. The phases were separated and aqueous layer washed three times with diethyl ether. The combined organic layer was dried over MgSO_4 and the solvent removed under reduced pressure. The resulting cloudy liquid was distilled from CaSO_4 under full vacuum (68-72 °C, ≈ 0.2 mm Hg) producing a white liquid that later solidified to a hard white solid. Yield: 35.20 g (88%). ^1H NMR (300 MHz, CDCl_3) δ 7.26 (m, *m* and *p*-PhH, 3H), 7.17 (dd, *o*-PhH, 2H, $J = 1.5, 7.35$ Hz), 3.32 (d, $\text{CH}_2\text{C}(\text{CH}_3)_2\text{CH}_2\text{Ph}$, 2H, $J = 5.4$ Hz), 2.58 (s, $\text{CH}_2\text{C}(\text{CH}_3)_2\text{CH}_2\text{Ph}$, 2H), 1.54 (t, OH, 1H, $J = 5.4$ Hz), 0.89 (s, $\text{CH}_2\text{C}(\text{CH}_3)_2\text{CH}_2\text{Ph}$, 6H); ^{13}C (75 MHz, CDCl_3) δ 138.95, 130.68, 128.03, 126.13, 71.41, 44.97, 36.77, 24.35; DEPT (75 MHz, CDCl_3) δ 138.95, 36.77 (quaternary C), 130.68, 128.02, 126.12 (CH), 71.40, 44.98 (CH_2), 24.51 (CH_3).

(2,2-Dimethyl-3-phenyl)propyl mesylate (17).

A 250 ml round bottom flask was charged with **16** (5.82 g, 35.4 mmol) and purged with argon. CH_2Cl_2 (110 ml) was added via cannula. NEt_3 (7.6 ml, 54.5 mmol) was added by syringe and the mixture was cooled to 0 °C. $\text{CH}_3\text{SO}_2\text{Cl}$ (3.2 ml, 41.3 mmol) was added dropwise. The solution became pale yellow and a precipitate formed. The reaction stirred at this temperature for 1 h. For workup, additional CH_2Cl_2 was added and the organics were washed with ice water (250 ml), chilled 10% HCl (250 ml), saturated NaHCO_3 , and saturated NaCl. After drying over Na_2SO_4 the solvent was removed under reduced pressure to yield a yellow liquid that was > 95% pure by NMR. Yield: 8.50 g (quantitative). ^1H NMR (300 MHz, CDCl_3) δ 7.28 (m, *m* and *p*-PhH, 3H), 7.14 (dd, *o*-PhH, 2H, $J = 2.1, 7.35$ Hz), 3.87 (s, $\text{CH}_2\text{C}(\text{CH}_3)_2\text{CH}_2\text{Ph}$, 2H), 3.02 (s, CH_3 , 3H), 2.62 (s,

$\text{CH}_2\text{C}(\text{CH}_3)_2\text{CH}_2\text{Ph}$, 2H), 0.98 (s, $\text{CH}_2\text{C}(\text{CH}_3)_2\text{CH}_2\text{Ph}$, 6H); ^{13}C (75 MHz, CDCl_3) δ 137.47, 130.66, 128.26, 126.61, 77.05, 44.81, 37.47, 35.67, 24.39; DEPT (75 MHz, CDCl_3) δ 137.47, 35.67 (quaternary C), 130.65, 128.25, 126.60 (CH), 77.05, 44.79 (CH_2), 37.46, 24.39 (CH_3).

2-Methyl-2-benzyl-1-iodopropane (18).

A 50 ml flask with condenser was charged with **17** (3.42 g, 14.1 mmol) and anhydrous NaI (10.58 g, 70.6 mmol) and was purged with argon. *N*-methylpyrrolidinone (30 ml) was added via syringe. The reaction was heated to 140 °C for 7 h under argon. The reaction was cooled and water and pentane were added. The phases were separated and the aqueous layer was extracted with pentane. The combined organic phases (400 ml) were washed with saturated $\text{Na}_2\text{S}_2\text{O}_3$, twice with saturated CuSO_4 , and water. After drying over MgSO_4 , the pentane was removed under reduced pressure. The yellow liquid was purified by column chromatography on silica with hexanes and the product was a clear liquid that was homogeneous by TLC. Yield: 3.75 g (97%). ^1H NMR (300 MHz, CDCl_3) δ 7.25 (br m, *o,m* and *p*-PhH, 5H), 3.13 (s, $\text{CH}_2\text{C}(\text{CH}_3)_2\text{CH}_2\text{Ph}$, 2H), 2.65 (s, $\text{CH}_2\text{C}(\text{CH}_3)_2\text{CH}_2\text{Ph}$, 2H), 1.04 (s, $\text{CH}_2\text{C}(\text{CH}_3)_2\text{CH}_2\text{Ph}$, 6H); ^{13}C (75 MHz, CDCl_3) δ 138.36, 130.46, 128.15, 126.50, 46.63, 35.08, 27.44, 24.53; DEPT (75 MHz, CDCl_3) δ 138.46, 35.08 (quaternary C), 130.45, 128.14, 126.49 (CH), 46.62, 24.67 (CH_2), 27.44 (CH_3).

Synthesis of Li(CH₂C(CH₃)₂CH₂Ph) (19). (LiCH₂CMe₂CH₂Ph).

2-Methyl-2-benzyl-1-iodopropane (0.365 g, 1.33 mmol) was weighed into a 25 mL round bottom flask equipped with a 180 ° needle valve and was degassed with two freeze-pump-thaw cycles at 77 K on the high vacuum line. Pentane then diethyl ether were added by vacuum transfer at -78 °C in a 3:1 ratio respectively to give a total solvent volume of 12 mL. The apparatus was backfilled with Ar and stirred briefly at room temperature. The Kontes needle valve was replaced by a septum using a positive Ar counter-flow. The solution was then cooled to -78 °C and a 1.7 M solution of *t*-butyllithium (1.80 mL, 2.92 mmol) was added dropwise using an Ar flushed syringe. A white precipitate was observed immediately following the addition. The reaction was stirred at -78 °C for 35 min. The dry ice-acetone bath was removed and the reaction was allowed to warm to room temperature with stirring for 45 min during which time the solution turned yellow. The septum was replaced with a Kontes needle valve and the solvent was removed and the oily residue dried in vacuo. In the glovebox the reaction flask was attached to a small swivel frit assembly. On the vacuum line, pentane (12 mL) was vacuum transferred onto the oil at -78 °C. Warming to room temperature and stirring to break up the solids resulted in a yellow solution with a white precipitate. This solution was filtered and the precipitate washed three times with recycled solvent. The solvent was removed yielding a yellow oil that was dried in vacuo. (Note: this compound was generally isolated as a diethyl etherate). Yield: 0.185 g (90%). ¹H NMR (300 MHz, C₆D₆): δ 7.05-7.25 (m (partially obscured by C₆D₆), C₆H₅, 5H), 2.55 (s, CH₂C(CH₃)₂CH₂Ph, 2H), 1.07 (s, CH₂C(CH₃)₂CH₂Ph, 6H), -1.01 (br s, CH₂C(CH₃)₂CH₂Ph, 2H).

**Synthesis of $(\eta^5\text{-C}_5\text{H}_5)(\eta^5\text{-C}_5\text{Me}_5)\text{Zr}(\text{CH}_2\text{C}(\text{CH}_2\text{CH}_3)_3)(\text{CH}_3)$ (20).
(CpCp*Zr(CH₂CEt₃)Me).**

In an inert atmosphere glovebox, $(\eta^5\text{-C}_5\text{H}_5)(\eta^5\text{-C}_5\text{Me}_5)\text{Zr}(\text{CH}_3)\text{Cl}$ (0.129 g, 0.38 mmol) was added to the 25 mL round bottom flask equipped with a stir bar containing $\text{LiCH}_2\text{CEt}_3$ (0.045 g, 0.38 mmol) and attached to a small swivel frit assembly. On the vacuum line, diethyl ether (12 mL) was vacuum transferred onto the reaction at $-78\text{ }^\circ\text{C}$. The apparatus was backfilled with Ar and the yellow solution was allowed to warm to room temperature over 14 hr with stirring. A yellow solution with a white precipitate was observed. The solvent was removed and the oily residue was dried in vacuo. Pentane (10 mL) was added to the oil by vacuum transfer and the reaction was stirred briefly at room temperature to break up the solids. The resulting white precipitate was filtered away from the yellow filtrate and washed once with recycled solvent. Removal of all volatiles and drying in vacuo resulted in a yellow-brown oil. Repeated attempts to purify this material by crystallization or precipitation from concentrated pentane solutions at $-35\text{ }^\circ\text{C}$ have failed. Yield: 0.130 g (82%). ^1H NMR (500 MHz, C_6D_6): δ 5.89 (s, C_5H_5 , 5H), 1.69 (s, $\text{C}_5(\text{CH}_3)_5$, 15H), 1.43 (m, $\text{CH}_2\text{C}(\text{CH}_2\text{CH}_3)_3$, 3H, $J = 7.8\text{ Hz}$), 1.35 (m, $\text{CH}_2\text{C}(\text{CH}_2\text{CH}_3)_3$, 3H, $J = 7.8\text{ Hz}$), 0.83 (t, $\text{CH}_2\text{C}(\text{CH}_2\text{CH}_3)_3$, 9H, $J = 7.4\text{ Hz}$), -0.13 (d, $\text{CH}_2\text{C}(\text{CH}_2\text{CH}_3)_3$, 1H, $J = 13.4\text{ Hz}$), -0.16 (d, $\text{CH}_2\text{C}(\text{CH}_2\text{CH}_3)_3$, 1H, $J = 13.4\text{ Hz}$), -0.28 (s, CH_3 , 3H).

**Synthesis of $(\eta^5\text{-C}_5\text{H}_5)(\eta^5\text{-C}_5\text{Me}_5)\text{Zr}(\text{CH}_2\text{C}(\text{CH}_3)_2\text{CH}_2\text{Ph})(\text{CH}_3)$ (21).
 $(\text{CpCp}^*\text{Zr}(\text{CH}_2\text{CMe}_2\text{CH}_2\text{Ph})\text{Me})$.**

In an inert atmosphere glovebox, $(\eta^5\text{-C}_5\text{H}_5)(\eta^5\text{-C}_5\text{Me}_5)\text{Zr}(\text{CH}_3)\text{Cl}$ (0.410 g, 1.19 mmol) was added to the 25 mL round bottom flask equipped with a stir bar containing $\text{LiCH}_2\text{CMe}_2\text{CH}_2\text{Ph}$ (0.185 g, 1.19 mmol) and attached to a small swivel frit assembly. On the vacuum line, diethyl ether (18 mL) was vacuum transferred onto the reaction at $-78\text{ }^\circ\text{C}$. The apparatus was backfilled with Ar and the reaction mixture was allowed to warm to room temperature. After stirring for 36 hr a yellow-brown solution with an off-white precipitate was observed. The solvent was removed and the oily residue was dried for 1 hr in vacuo. Pentane (15 mL) was added to the oil by vacuum transfer and the reaction was stirred briefly at room temperature to break up the solids. The resulting white precipitate was filtered away from the dark brown filtrate and washed once with recycled solvent. Removal of all volatiles and drying in vacuo for 1.5 hr at $50\text{ }^\circ\text{C}$ resulted in a dark brown oil. Repeated attempts to purify this material by crystallization or precipitation from concentrated pentane solutions at $-35\text{ }^\circ\text{C}$ have failed. Yield: 0.396 g (73%). ^1H NMR (300 MHz, C_6D_6): δ 7.15-7.25 (m (partially obscured by C_6D_6), C_6H_5 , 5H), 5.82 (s, C_5H_5 , 5H), 2.58 (d, $\text{CH}_2\text{C}(\text{CH}_3)_2\text{CH}_2\text{Ph}$, 1H, $J = 12.6\text{ Hz}$), 2.54 (d, $\text{CH}_2\text{C}(\text{CH}_3)_2\text{CH}_2\text{Ph}$, 1H, $J = 12.1\text{ Hz}$), 1.64 (s, $\text{C}_5(\text{CH}_3)_5$, 15H), 1.15 (s, $\text{CH}_2\text{C}(\text{CH}_3)_2\text{CH}_2\text{Ph}$, 3H), 0.92 (s, $\text{CH}_2\text{C}(\text{CH}_3)_2\text{CH}_2\text{Ph}$, 3H), 0.44 (d, $\text{CH}_2\text{C}(\text{CH}_3)_2\text{CH}_2\text{Ph}$, 1H, $J = 12.0\text{ Hz}$), -0.27 (s, CH_3 , 3H), -0.33 (d, $\text{CH}_2\text{C}(\text{CH}_3)_2\text{CH}_2\text{Ph}$, 1H, $J = 12.7\text{ Hz}$).

Synthesis of $(\eta^5\text{-C}_5\text{H}_5)_2\text{Zr}(\text{CH}_2\text{C}(\text{CH}_2\text{CH}_3)_3)(\text{CH}_3)$ (22). $(\text{Cp}_2\text{Zr}(\text{CH}_2\text{CEt}_3)\text{Me})$.

2,2-Diethyl-1-iodobutane (0.274 g, 1.14 mmol) was weighed into a 25 mL round bottom flask equipped with a 180 ° needle valve and was degassed at 77 K on the high vacuum line. Pentane (8 to 10 mL) then diethyl ether (2 to 4 mL) were added by vacuum transfer at -78 °C. The apparatus was backfilled with Ar and stirred briefly at room temperature. The Kontes needle valve was replaced by a septum using a positive Ar counter-flow. The solution was then cooled to -78 °C and a 1.7 M solution of *t*-butyllithium (1.50 mL, 2.51 mmol) was added dropwise using an Ar flushed syringe. A white precipitate was observed in the colorless solution before the addition was completed. The reaction was stirred at -78 °C for 30 min. The dry ice-acetone bath was removed and the reaction stirred at room temperature for 30 min. The septum was replaced with a Kontes needle valve and the solvent was removed. Drying in vacuo yielded a white glassy solid. In an inert atmosphere glovebox, $(\eta^5\text{-C}_5\text{H}_5)_2\text{Zr}(\text{CH}_3)\text{Cl}$ (0.310 g, 1.14 mmol) was added to the flask containing this solid and it was attached to a small swivel frit assembly. On the vacuum line, diethyl ether (13 mL) was vacuum transferred onto the solids at -78 °C and the apparatus was backfilled with Ar. The reaction mixture was allowed to warm to room temperature over 20 h with stirring. At this time a brown-green solution with a white precipitate was observed. The solvent was removed and the resulting yellow-brown oil was dried at 30 °C in vacuo. Pentane (10 mL) was vacuum transferred onto the oil at -78 °C. Stirring at room temperature gave a yellow-brown solution with an off-white precipitate. Filtration followed by removal of solvent yielded a yellow-brown oil that was dried at 30 °C in vacuo. In the glovebox this oil was dissolved pentane giving a yellow solution that was filtered via pipet through celite and concentrated to less than 10

mL. The solution was cooled to $-35\text{ }^{\circ}\text{C}$ to recrystallize the desired product; pale yellow crystalline material suitable for X-ray diffraction was isolated and dried in vacuo. Yield: 0.128 g (32%). Anal. Calcd. for $\text{C}_{19}\text{H}_{30}\text{Zr}$: C, 65.26%, H, 8.65%. Found: C, 64.50, 64.39%, H, 8.65, 8.42%. ^1H NMR (500 MHz, C_6D_6): δ 5.78 (s, C_5H_5 , 10H), 1.29 (q, $\text{CH}_2\text{C}(\text{CH}_2\text{CH}_3)_3$, 6H, $J = 7.4$ Hz), 0.80 (t, $\text{CH}_2\text{C}(\text{CH}_2\text{CH}_3)_3$, 9H, $J = 7.4$ Hz), 0.15 (s, $\text{CH}_2\text{C}(\text{CH}_2\text{CH}_3)_3$, 2H), -0.015 (s, CH_3 , 3H). $^{13}\text{C}\{^1\text{H}\}$ NMR (125 MHz, C_6D_6): δ 110.3 (C_5H_5), 76.8 (Zr- $\text{CH}_2\text{C}(\text{CH}_2\text{CH}_3)_3$), 46.5 ($\text{CH}_2\text{C}(\text{CH}_2\text{CH}_3)_3$), 33.0 ($\text{CH}_2\text{C}(\text{CH}_2\text{CH}_3)_3$), 25.9 (Zr- CH_3), 9.3 ($\text{CH}_2\text{C}(\text{CH}_2\text{CH}_3)_3$).

**Synthesis of $(\eta^5\text{-C}_5\text{H}_5)_2\text{Zr}(\text{CH}_2\text{C}(\text{CH}_3)_2\text{CH}_2\text{Ph})(\text{CH}_3)$ (23).
($\text{Cp}_2\text{Zr}(\text{CH}_2\text{CMe}_2\text{CH}_2\text{Ph})\text{Me}$).**

2-Methyl-2-benzyl-1-iodopropane (0.4487 g, 1.63 mmol) was weighed into a 25 mL round bottom flask equipped with a 180 ° needle valve and was degassed at 77 K on the high vacuum line. Pentane (8 to 10 mL) then diethyl ether (2 to 4 mL) were added by vacuum transfer at $-78\text{ }^{\circ}\text{C}$. The apparatus was backfilled with Ar and stirred briefly at room temperature. The Kontes needle valve was replaced by a septum using a positive Ar counter-flow. The solution was then cooled to $-78\text{ }^{\circ}\text{C}$ and a 1.7 M solution of *t*-butyllithium (2.15 mL, 3.60 mmol) was added dropwise using an Ar flushed syringe. A white precipitate was observed in the colorless solution before the addition was completed. The reaction was stirred at $-78\text{ }^{\circ}\text{C}$ for 30 min. The dry ice-acetone bath was removed and the reaction stirred at room temperature for 30 min. The septum was replaced with a Kontes needle valve and the solvent was removed. Drying in vacuo yielded a bright yellow oily residue. In an inert atmosphere glovebox, $(\eta^5\text{-}$

$C_5H_5)_2Zr(CH_3)Cl$ (0.445 g, 1.14 mmol) was added to the flask containing this solid and it was attached to a small swivel frit assembly. On the vacuum line, diethyl ether (13 mL) was vacuum transferred onto the solids at $-78\text{ }^\circ\text{C}$ and the apparatus was backfilled with Ar. The reaction mixture was allowed to warm to room temperature over 19 h with stirring. At this time a yellow-brown solution with a white precipitate was observed. The solvent was removed and the resulting brown oil was dried at $45\text{ }^\circ\text{C}$ in vacuo. Pentane (10 mL) was vacuum transferred onto the oil at $-78\text{ }^\circ\text{C}$. Stirring at room temperature gave a yellow-brown solution with an off-white precipitate. Filtration followed by removal of solvent yielded a brown oil that was dried at $30\text{ }^\circ\text{C}$ in vacuo. In the glovebox this oil was dissolved pentane giving a yellow-brown solution that was filtered via pipet through celite and concentrated to less than 10 mL. The solution was cooled to $-35\text{ }^\circ\text{C}$ to recrystallize the desired product as brown pellets that were isolated and dried in vacuo. Yield: 0.208 g (33%). Anal. Calcd. for $C_{22}H_{28}Zr$: C, 68.87%, H, 7.35%. Found: C, 68.56, 68.62%, H, 7.26, 7.28%. ^1H NMR (300 MHz, C_6D_6): δ 7.16-7.25 (m (partially obscured by C_6D_6), C_6H_5 , 5H), 5.73 (s, C_5H_5 , 10H), 2.49 (s, $CH_2C(CH_3)_2CH_2Ph$, 2H), 0.98 (s, $CH_2C(CH_3)_2CH_2Ph$, 6H), 0.45 (s, $CH_2C(CH_3)_2CH_2Ph$, 2H), -0.043 (s, CH_3 , 3H). ^1H NMR (500 MHz, C_7D_8): δ 7.10-7.20 (m (partially obscured by C_7D_8), C_6H_5 , 5H), 5.73 (s, C_5H_5 , 10H), 2.43 (s, $CH_2C(CH_3)_2CH_2Ph$, 2H), 0.94 (s, $CH_2C(CH_3)_2CH_2Ph$, 6H), 0.41 (s, $CH_2C(CH_3)_2CH_2Ph$, 2H), -0.12 (s, CH_3 , 3H). ^1H NMR (500 MHz, C_7D_8 , 193K): δ 7.15-7.25 (m (partially obscured by C_7D_8), C_6H_5 , 5H), 5.63 (s, C_5H_5 , 10H), 2.49 (s, $CH_2C(CH_3)_2CH_2Ph$, 2H), 1.00 (s, $CH_2C(CH_3)_2CH_2Ph$, 6H), 0.40 (s, $CH_2C(CH_3)_2CH_2Ph$, 2H), 0.024 (s, CH_3 , 3H). ^1H NMR (500 MHz, CD_2Cl_2): δ 7.24 (t, *m*- C_6H_5 , 2H, $J = 7.0$ Hz), 7.17 (t, *p*- C_6H_5 , 1H, $J = 7.3$ Hz), 7.08 (d, *o*- C_6H_5 , 2H, $J = 7.25$ Hz), 6.08 (s, C_5H_5 ,

10H), 2.40 (s, $\text{CH}_2\text{C}(\text{CH}_3)_2\text{CH}_2\text{Ph}$, 2H), 0.89 (s, $\text{CH}_2\text{C}(\text{CH}_3)_2\text{CH}_2\text{Ph}$, 6H), 0.37 (s, $\text{CH}_2\text{C}(\text{CH}_3)_2\text{CH}_2\text{Ph}$, 2H), -0.31 (s, CH_3 , 3H). $^{13}\text{C}\{^1\text{H}\}$ NMR (125 MHz, CD_2Cl_2): δ 141.2 (*i*- C_6H_5), 131.2 (*m*- C_6H_5), 127.8 (*o*- C_6H_5), 126.0 (*p*- C_6H_5), 110.6 (C_5H_5), 75.6 (Zr- $\text{CH}_2\text{C}(\text{CH}_3)_2\text{CH}_2\text{Ph}$), 55.0 ($\text{CH}_2\text{C}(\text{CH}_3)_2\text{CH}_2\text{Ph}$), 41.4 ($\text{CH}_2\text{C}(\text{CH}_3)_2\text{CH}_2\text{Ph}$), 31.8 ($\text{CH}_2\text{C}(\text{CH}_3)_2\text{CH}_2\text{Ph}$), 27.6 (Zr- CH_3). DEPT (75 MHz, CD_2Cl_2): δ 141.2, 41.4 (quaternary C), 131.2, 127.8, 126.0, 110.6 (CH), 75.6, 55.0 (CH_2), 31.8, 27.6 (CH_3).

References

1. Jordan, R. F. *Adv. Organomet. Chem.* **1991**, *32*, 325-387.
2. Brintzinger, H. H.; Fischer, D.; Mulhaupt, R.; Rieger, B.; Waymouth, R. M. *Angew. Chem., Int. Ed. Engl.* **1995**, *34*, 1143-1170.
3. Wendt, O. F.; Bercaw, J. E., *unpublished results*.
4. Landis, C. R.; Rosaaen, K. A.; Sillars, D. R. *J. Am. Chem. Soc.* **2003**, *125*, 1710-1711.
5. Mehrkhodavandi, P.; Bonitatebus, P. J.; Schrock, R. R. *J. Am. Chem. Soc.* **2000**, *122*, 7841-7842.
6. Chen, E. Y. X.; Marks, T. J. *Chem. Rev.* **2000**, *100*, 1391-1434.
7. Beswick, C. L.; Marks, T. J. *J. Am. Chem. Soc.* **2000**, *122*, 10358-10370.
8. Wendt, O. F.; Bercaw, J. E. *Organometallics* **2001**, *20*, 3891-3895.
9. Negishi, E.; Nguyen, T.; Maye, J. P.; Choueiri, D.; Suzuki, N.; Takahashi, T. *Chem. Lett.* **1992**, 2367-2370.
10. Horton, A. D. *Organometallics* **1996**, *15*, 2675-2677.
11. Chirik, P. J.; Dalleska, N. F.; Henling, L. M.; Bercaw, J. E. *Organometallics* **2005**, *24*, 2789-2794.
12. Resconi, L.; Piemontesi, F.; Franciscano, G.; Abis, L.; Fiorani, T. *J. Am. Chem. Soc.* **1992**, *114*, 1025-1032.
13. Mehrkhodavandi, P.; Schrock, R. R. *J. Am. Chem. Soc.* **2001**, *123*, 10746-10747.
14. Mehrkhodavandi, P.; Schrock, R. R.; Pryor, L. L. *Organometallics* **2003**, *22*, 4569-4583.
15. Mehrkhodavandi, P. Ph.D. Thesis, Massachusetts Institute of Technology, 2002.
16. Collier, M. R.; Lappert, M. F.; Pearce, R. *J. Chem. Soc., Dalton Trans.* **1973**, 445-451.
17. Jeffery, J.; Lappert, M. F.; Luongthi, N. T.; Webb, M.; Atwood, J. L.; Hunter, W. E. *J. Chem. Soc., Dalton Trans.* **1981**, 1593-1605.
18. Atwood, J. L.; Hunter, W. E.; Hrcncir, D. C.; Samuel, E.; Alt, H.; Rausch, M. D. *Inorg. Chem.* **1975**, *14*, 1757-1762.

19. Jeffery, J.; Lappert, M. F.; Luongthi, N. T.; Atwood, J. L.; Hunter, W. E. *J. Chem. Soc., Chem. Commun.* **1978**, 1081-1083.
20. Bochmann, M.; Lancaster, S. J. *Angew. Chem., Int. Ed. Engl.* **1994**, *33*, 1634-1637.
21. Zuckerman, R. L.; Krska, S. W.; Bergman, R. G. *J. Am. Chem. Soc.* **2000**, *122*, 751-761.
22. Brandow, C. G.; Bercaw, J. E., *unpublished results*.
23. Wailes, P. C.; Weigold, H.; Bell, A. P. *J. Organomet. Chem.* **1972**, *34*, 155-164.
24. Jordan, R. F. *J. Organomet. Chem.* **1985**, *294*, 321-326.
25. Mehrkhodavandi, P.; Schrock, R. R.; Bonitatebus, P. J. *Organometallics* **2002**, *21*, 5785-5798.
26. Rogers, R. D.; Benning, M. M.; Kurihara, L. K.; Moriarty, K. J.; Rausch, M. D. *J. Organomet. Chem.* **1985**, *293*, 51-60.
27. Reynolds, K. A.; Ohagan, D.; Gani, D.; Robinson, J. A. *J. Chem. Soc., Perkin Trans. I* **1988**, 3195-3207.
28. Hajela, S. H.; Bercaw, J. E. *Organometallics* **1994**, *13*, 1147-1154.
29. Vogel, A. I. *Vogel's Textbook of Practical Organic Chemistry*; 5th ed.; Longman: New York, 1989.
30. Crossland, R. K.; Servis, K. L. *J. Org. Chem.* **1970**, *35*, 3195-3196.
31. Stevens, R. V.; Gaeta, F. C. A.; Lawrence, D. S. *J. Am. Chem. Soc.* **1983**, *105*, 7713-7719.
32. Bailey, W. F.; Punzalan, E. R. *J. Org. Chem.* **1990**, *55*, 5404-5406.
33. Negishi, E.; Swanson, D. R.; Rousset, C. J. *J. Org. Chem.* **1990**, *55*, 5406-5409.
34. Burger, B. J.; Bercaw, J. E. *New Developments in the Synthesis, Manipulation, and Characterization of Organometallic Compounds*; American Chemical Society: Washington, DC, 1987; Vol. 357.
35. Pangborn, A. B.; Giardello, M. A.; Grubbs, R. H.; Rosen, R. K.; Timmers, F. J. *Organometallics* **1996**, *15*, 1518-1520.
36. Marvich, R. H.; Brintzinger, H. H. *J. Am. Chem. Soc.* **1971**, *93*, 2046-2048.
37. Wolczanski, P. T.; Bercaw, J. E. *Organometallics* **1982**, *1*, 793-799.
38. Surtees, J. R. *Chem. Commun.* **1965**, 567.
39. Schrock, R. R.; Fellmann, J. D. *J. Am. Chem. Soc.* **1978**, *100*, 3359-3370.
40. Tessier-Youngs, C.; Beachley, O. T., Jr. *Inorg. Synth.* **1986**, *24*, 95-97.
41. Coates, G. E.; Heslop, J. A. *J. Chem. Soc. A* **1968**, 514-518.

Chapter 2

Direct Examination of Propagation Kinetics of Zirconocene-Catalyzed Alkene Polymerization

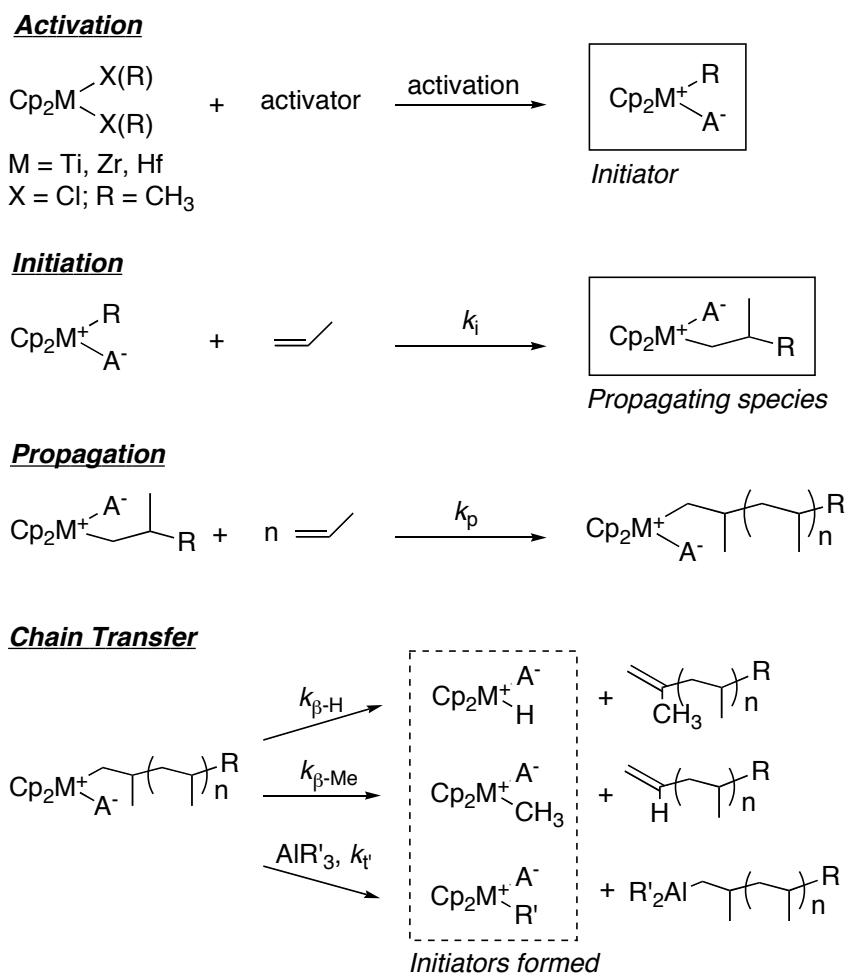
Abstract

A direct examination of propagation kinetics for alkene polymerization using the zirconocenium initiator, $[(\eta^5\text{-C}_5\text{H}_5)(\eta^5\text{-C}_5\text{Me}_5)\text{Zr}(\text{CH}_2\text{CMe}_3)]^+[\text{CH}_3\text{B}(\text{C}_6\text{F}_5)_3]^-$, is reported. Propagation rate constants (k_p) for the polymerization of propene and a series of 1-alkenes catalyzed by $[(\eta^5\text{-C}_5\text{H}_5)(\eta^5\text{-C}_5\text{Me}_5)\text{Zr}(\text{CH}_2\text{CHR})_n\text{CH}_2\text{CMe}_3]^+[\text{CH}_3\text{B}(\text{C}_6\text{F}_5)_3]^-$ were measured by ^1H NMR spectroscopy in toluene- d_8 at low temperature. The k_p obtained for propene and other alkenes decreases with increasing chain length and steric influence. These methods were used to investigate the temperature dependence and anion and solvent effects on propene propagation kinetics. The overall activation parameters for propagation determined from an Eyring analysis are $\Delta H^\ddagger = 8.5(3)$ kcal·mol $^{-1}$ and $\Delta S^\ddagger = -25(2)$ eu. The propagation rate was found to increase in the presence of $[\text{CH}_3\text{B}(\text{C}_6\text{F}_5)_3]^-$ counteranion and in a polar toluene- d_8 -chlorobenzene- d_5 solvent system. The experimental results are most consistent with propagation mechanism that does not involve the formation of outer-sphere ions for alkene polymerization by this catalyst system.

1 Introduction

The polymerization of propene and other alkenes by metallocene-derived catalysts is an area of considerable academic and industrial importance.^{1,2} Starting from the activated alkylmetallocene initiator this catalysis occurs in a series of distinct steps, initiation, propagation, and chain transfer (Scheme 1).² The relative rates of these steps determine polymer properties such as molecular weight and molecular weight distribution. Despite extensive investigation, fundamental aspects such as the rate laws of initiation, propagation, and chain transfer and the factors controlling their relative rates remain largely ill-defined.

Scheme 1

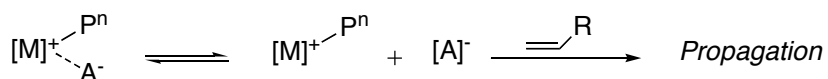


Examination of propagation kinetics can provide detailed information on this key chain growth step. Investigation of propagation kinetics for $\text{Cp}^x_2\text{MCl}_2/\text{MAO}$ ($\text{Cp}^x = \eta^5\text{-C}_5\text{R}_n\text{H}_{5-n}$; MAO = methylaluminoxane) catalysts has been complicated by uncertainty in determining active site concentration.³ In these systems a significant fraction of catalyst can remain dormant in the $[\text{Cp}^x_2\text{MCH}_3]^+[\text{CH}_3\text{MAO}]^-$ form during the polymerization. Recent methodology developed for active site counting⁴ has been utilized in kinetic studies of zirconocene-catalyzed 1-hexene polymerization using quenched-flow experiments.⁵

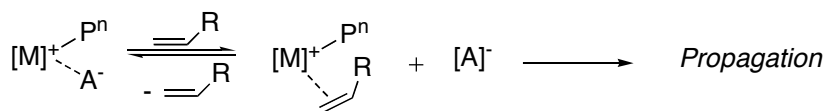
Direct examination of metallocene-catalyzed alkene polymerization would allow measurement of propagation kinetics and simultaneous monitoring of the species in solution for a suitably well-defined and well-behaved system. These types of studies may also address details of propagation, such as the mechanism for ion-pair separation and alkene binding, where alternative pathways have been previously proposed (Scheme 2).⁶⁻⁹

Scheme 2

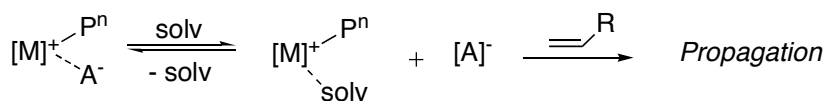
Dissociative



Associative



Solvent Assisted



$[\text{M}] = (\text{Cp}^x)_2\text{Ti, Zr, Hf}$; $\text{P}^n = \text{polymeryl chain of } n \text{ monomers}$; $\text{R} = \text{CH}_3, \text{ alkyl}$

The challenge of using a direct method is the design of an appropriate system. Most kinetic and mechanistic information obtained for $\text{Cp}^x_2\text{MCl}_2/\text{MAO}$ -catalyzed alkene

polymerization has come from indirect studies, e.g., where catalyst activity is examined as a function of ancillary ligation or polymerization conditions.^{1,10} These types of catalysts are generally not amenable to investigation using a direct method such as ¹H NMR spectroscopy. The large excess of MAO ([Al]/[M] > 500) required for polymerization produces an ill-defined and often heterogeneous system. Therefore the speciation of the active catalyst and mechanistic details of the propagation step remain elusive

While it is generally thought that ion-pair separation precedes alkene insertion and is required for high activities, the relevance of true 14 electron cations in the catalytic cycle has recently been questioned.^{9,11,12} Key studies by Brintzinger¹³ and Landis⁵ suggest the counteranion may not detectably leave the inner-sphere in some systems.

These findings are interesting in light of the transition state model developed for alkene insertion for these systems (Figure 1).¹⁴ Experiments by a number of researchers have identified three key interactions ($\{M\}^+$ -polymeryl, $\{M\}^+$ -alkene, and $\{M\}^+$ - α -agostic C-H) in the transition state for alkene insertion, with the alkene-substituent and polymeryl chain having a *trans* orientation.¹⁵⁻²¹ Notably a cation-anion interaction is not included in this model, suggesting an outer-sphere arrangement of ions. The nature of this interaction and influence of the counteranion on the regio- and stereochemical outcome of the alkene insertion step should be considered if propagation occurs through an inner-sphere ion-pair.⁶

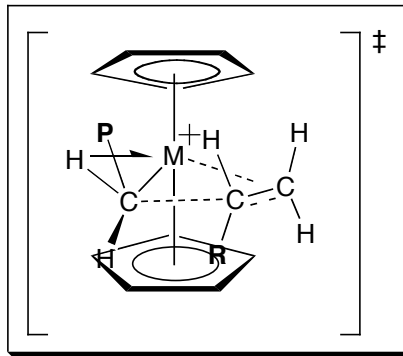


Figure 1. Proposed transition state model for alkene insertion in group 4 metallocene-catalyzed alkene polymerization.

The viability of using direct kinetic experiments to investigate well-defined group 4 metallocene catalysts has literature precedence. Studies of the solution behavior and dynamics – ion-pairing, anion and Lewis base exchange, and site epimerization – for a number of anion- and Lewis base-stabilized zirconocene and hafnocene cations have been undertaken, but almost all have been for methyl-metallocenium ions, and the conclusions generally have been extrapolated to a propagating species in alkene polymerization where polymeryl-metallocenium ion-pairs are involved.^{6,7,13,22,23}

There were few direct kinetic studies employing relevant models for the propagating species.^{22,24,25} Recently Landis and co-workers, using direct NMR methods have measured elementary rate constants for an *ansa*-zirconocene catalyst [*rac*-C₂H₄(1-indenyl)₂Zr(CH₃)]⁺[CH₃B(C₆F₅)₃]⁻, providing important kinetic and mechanistic information for this catalyst system.^{8,26}

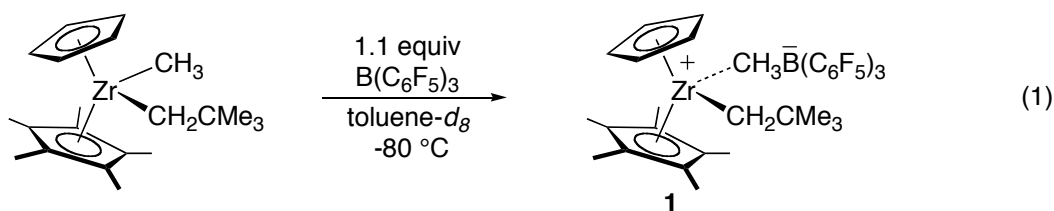
Chapter 2 reports a direct examination of propagation kinetics for alkene polymerization using a zirconocenium initiator, [CpCp*ZrNp]⁺[CH₃B(C₆F₅)₃]⁻ (Cp = η⁵-C₅H₅; Cp* = η⁵-C₅Me₅; Np = CH₂CMe₃), designed to model the propagating species, together with second-order rate constants for propagation in the polymerization of

propene and several other alkenes. These methods are used to examine the rate of propagation as a function of polymerization temperature, alkene substrate, counteranion concentration, or solvent. The results of these experiments are discussed in the context of alternative mechanistic pathways for the propagation step.

2 Results

2.1 Synthesis of $[\text{CpCp}^*\text{ZrNp}]^+[\text{CH}_3\text{B}(\text{C}_6\text{F}_5)_3]^-$ (**1**)

The catalyst $[\text{CpCp}^*\text{Zr}(\text{Np})]^+[\text{CH}_3\text{B}(\text{C}_6\text{F}_5)_3]^-$ (**1**), was generated cleanly in situ by selective methide abstraction from $\text{CpCp}^*\text{Zr}(\text{Np})(\text{CH}_3)$ using the strong Lewis acid $\text{B}(\text{C}_6\text{F}_5)_3$ at $-80\text{ }^\circ\text{C}$ in toluene- d_8 (eq 1).



Formation of **1** was indicated by the disappearance of the $\text{Zr}-\text{CH}_3$ resonance (-0.27 ppm) of $\text{CpCp}^*\text{Zr}(\text{Np})(\text{CH}_3)$ in the ^1H NMR spectrum and a Cp resonance shifted upfield (from 5.86 to 5.66 ppm in **1**) relative to that in $\text{CpCp}^*\text{Zr}(\text{Np})(\text{CH}_3)$. Compound **1** was fully characterized using low temperature ^1H , ^{19}F , and ^{13}C NMR spectroscopy. Characteristic ^1H NMR ($-57\text{ }^\circ\text{C}$, toluene- d_8) resonances of **1** included: Cp (5.66 ppm), Cp* (1.21 ppm), downfield shifted $\alpha\text{-CH}_2$ doublet (1.80 ppm, $J = 11$ Hz), and broad coincident signal for the other $\alpha\text{-CH}_2$ and $[\text{CH}_3\text{B}(\text{C}_6\text{F}_5)_3]^-$ (-0.11 ppm, $J = 11$ Hz) (Figure 2). The observed ^1H and ^{19}F NMR (where $\Delta\delta(m,p\text{-}F) = 5.2$ ppm) spectra of **1** are indicative of “tight ion-pairing” in solution.^{13,27} “Tight” ion-pairs – where the $[\text{CH}_3\text{B}(\text{C}_6\text{F}_5)_3]^-$ anion is coordinated to the zirconocenium center – have $\Delta\delta(m,p\text{-}F)$ values between 3-6 ppm. Values < 3 ppm are observed in noncoordinated systems. The $\text{Zr}-\text{CH}_2\text{CMe}_3$ resonance of

1 was located at 99.8 ppm in the ^{13}C NMR spectrum. The ^1H and ^{13}C spectra ($^1J_{\text{CH}} = 104$, 116 Hz; $^1J_{\text{CH}} = 125$ Hz) of **1** suggest the ground state solution structure does not have static α - or γ -agostic interactions.

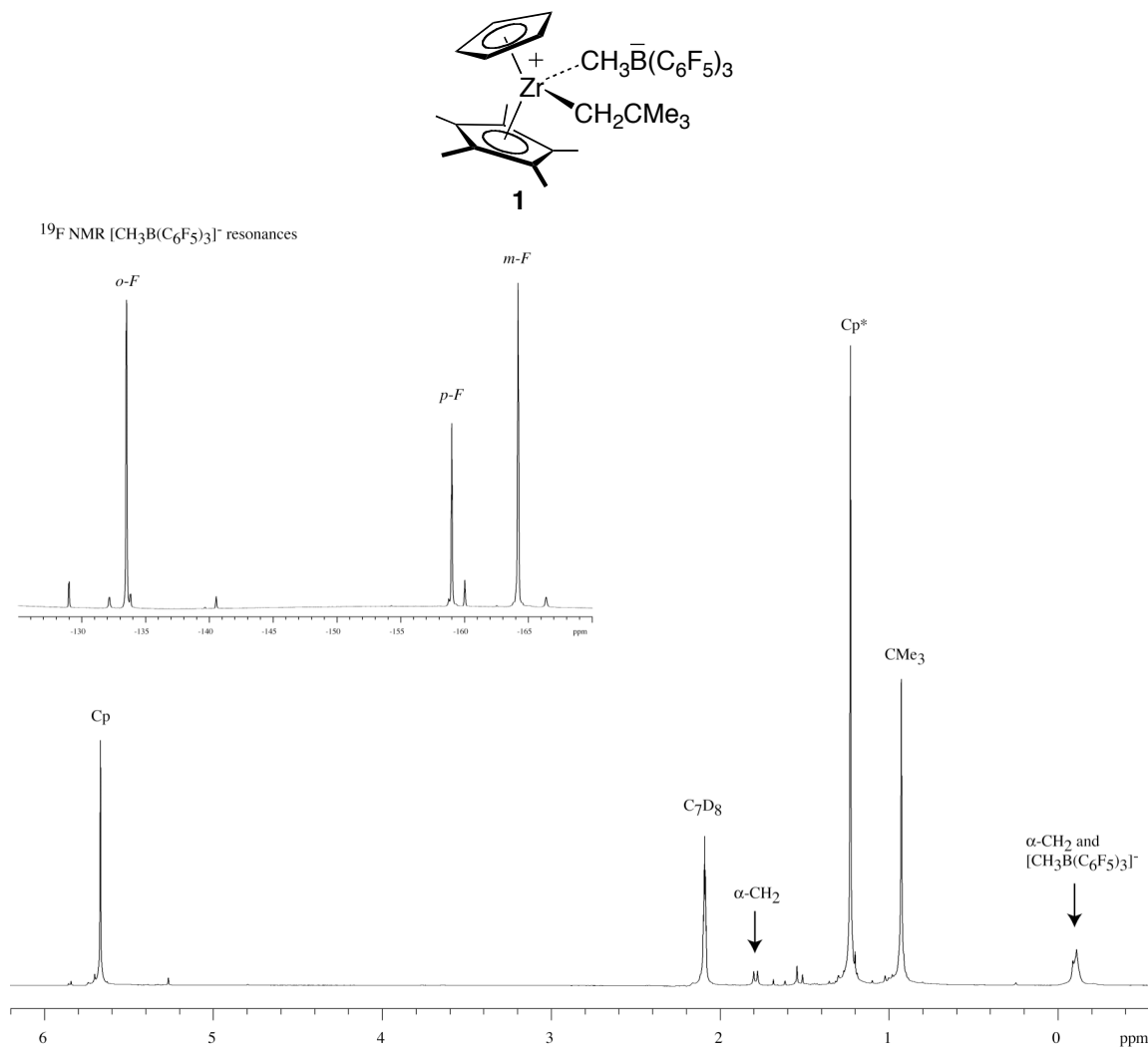
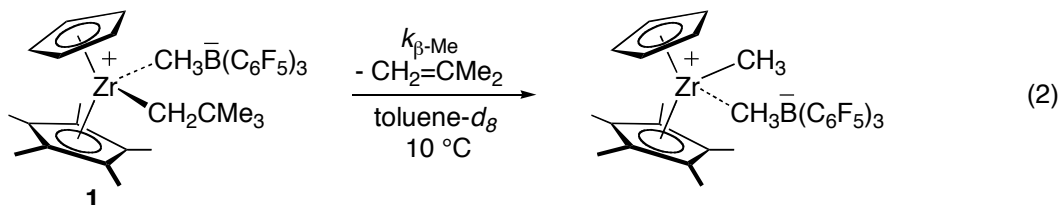


Figure 2. Partial ^1H NMR spectrum of **1** at -57°C in $\text{toluene-}d_8$. Inset shows ^{19}F NMR spectrum – unlabeled signals are for $\text{B}(\text{C}_6\text{F}_5)_3$.

2.2 Decomposition of $[\text{CpCp}^*\text{ZrNp}]^+[\text{CH}_3\text{B}(\text{C}_6\text{F}_5)_3]^-$ via β - CH_3 elimination

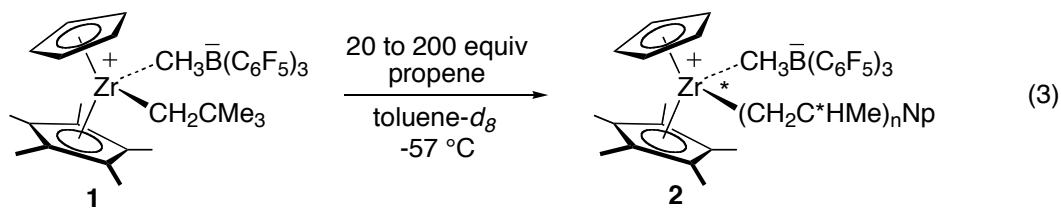
Solutions of **1** in toluene- d_8 were stable at -60 °C for > 24 h. Decomposition of **1** via irreversible β -methyl elimination occurred above -20 °C to generate the methyl-zirconocene catalyst, $[\text{CpCp}^*\text{Zr}(\text{CH}_3)]^+[\text{CH}_3\text{B}(\text{C}_6\text{F}_5)_3]^-$ and isobutene (eq 2).



The decomposition of **1** was monitored as a function of time by ^1H NMR spectroscopy at 10 °C in toluene- d_8 . A rate constant for β - CH_3 elimination, $k_{\beta\text{-Me}}(10$ °C) = $10.1(5) \times 10^{-4} \text{ s}^{-1}$, was obtained by curve fitting to the expression $I_t = I_f + (I_0 - I_f) \times \exp(-k_{\beta\text{-Me}}t)$, where I_t is the Cp peak height of **1**. The value reported is the average of four kinetic measurements.

2.3 Observation of propene polymerization catalyzed by $[\text{CpCp}^*\text{Zr}(\text{CH}_2\text{CHMe})_n\text{Np}]^+[\text{CH}_3\text{B}(\text{C}_6\text{F}_5)_3]^-$

The propagation step in catalysis is observed directly upon reaction of **1** with excess propene. Propene (20-200 equiv) was condensed onto samples of **1** in toluene- d_8 at -196 °C and mixed into the catalyst solution without significant sample warming (eq 3). Sample preparation and mixing is described in the experimental section. The ^1H NMR spectrum (-57 °C) indicated complete conversion of initiating species **1** to new zirconocenium species. Therefore, initiation of **1** occurred within minutes on warming to above -80 °C. The new compound detected was assigned to the propagating zirconium-polymeryl species $[\text{CpCp}^*\text{Zr}(\text{CH}_2\text{CHMe})_n\text{Np}]^+[\text{CH}_3\text{B}(\text{C}_6\text{F}_5)_3]^-$ (2)



The propagating species **2** was observed as sets of diastereomers (zirconium and β -carbon of the polymeryl chain are stereogenic) having polymeryl chains of various lengths in a roughly 60:40 mixture. Consistent with this assignment were the appearance of two new sets of broad resonances (unresolved) for the Cp (5.60, 5.56 ppm), Cp* (1.26, 1.20 ppm), and $[\text{CH}_3\text{B}(\text{C}_6\text{F}_5)_3]^-$ (-0.10, -0.18 ppm) groups of **2** in the ^1H NMR spectrum (Figure 3).

The reaction of **2** with propene was followed over time by ^1H NMR spectroscopy at -57 $^\circ\text{C}$. Polymerization was indicated by the disappearance of free propene resonances and the growth of broad polypropene signals [1.80 ppm (CH), 1.31, 1.06 (CH_2), 0.98 (CH_3)]. No significant change was detected in the resonances of **2** over the course of the reaction. Therefore, in the presence of propene, there was no evidence (^1H NMR) for catalyst deactivation or chain transfer reactions ($[\text{propene}]: [\text{Zr}] > 3$ equiv, -57 $^\circ\text{C}$, toluene- d_8).

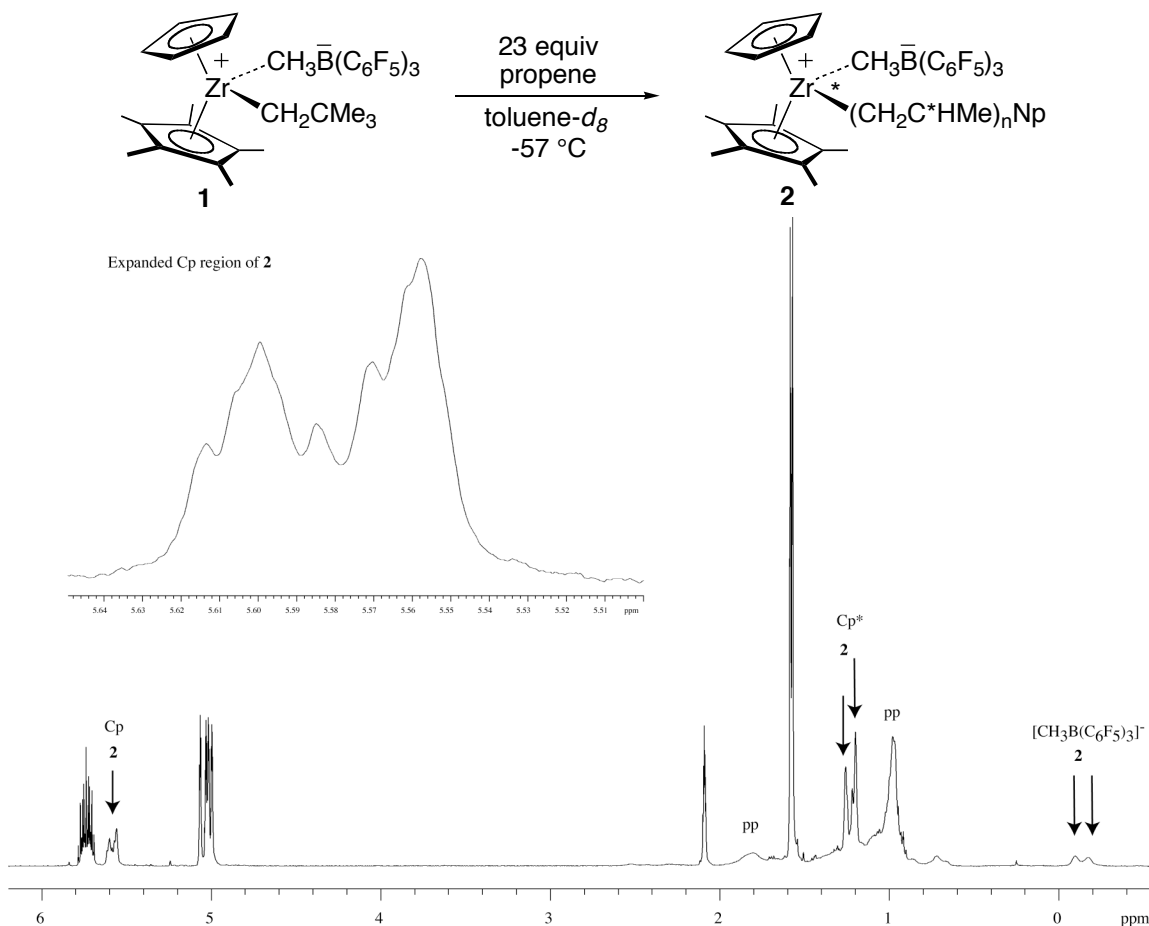


Figure 3. Partial ^1H NMR spectrum of the product mixture obtained from **1** and 23 equivalents of propene in toluene- d_8 at $-57\text{ }^\circ\text{C}$. “pp” denotes signals for polypropene and unlabeled signals are for unreacted propene and $\text{C}_6\text{D}_5\text{CD}_2\text{H}$ (2.09 ppm). The inset shows the expanded Cp resonances of **2**.

2.4 Measurement of propagation kinetics of propene polymerization by $[\text{CpCp}^*\text{Zr}(\text{CH}_2\text{CHMe})_n\text{Np}]^+[\text{CH}_3\text{B}(\text{C}_6\text{F}_5)_3]^-$

Propagation kinetic measurements were carried out at $-57\text{ }^\circ\text{C}$ using 2.5-16.4 mM of zirconocene catalyst and 0.3-0.61 M of propene in toluene- d_8 . The decrease of [propene] with time was followed by ^1H NMR spectroscopy ($-57\text{ }^\circ\text{C}$, toluene- d_8). Spectra were recorded at regular intervals until the reaction was $> 88\%$ complete. The integral of alkene $\text{CH}_2\text{CH}(\text{Me})$ resonance (relative to $\text{C}_6\text{D}_5\text{CD}_2\text{H}$ as an internal standard) was

calculated as a function of time. Since the **[2]** remains constant, the data can be treated as for pseudo-first-order kinetics. A representative plot of the kinetics ($\ln([\text{propene}]_t)$ vs time) for propene polymerization by **2** is shown in Figure 4. From the slope an observed rate constant, k_{obs} , was obtained.

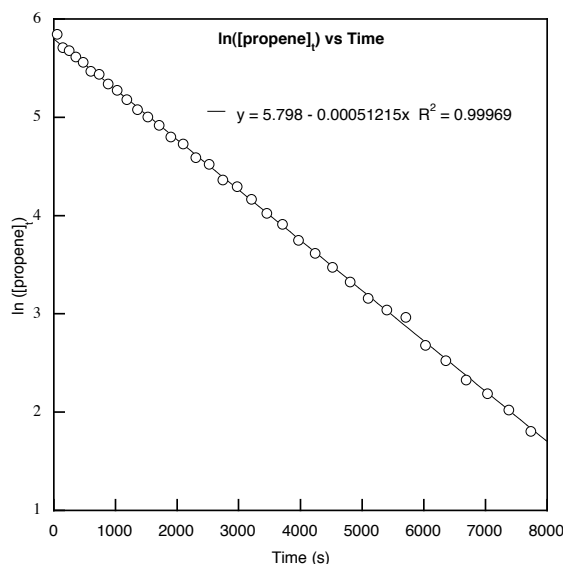


Figure 4. Representative kinetics plot for the reaction of **2** and propene at $-57\text{ }^{\circ}\text{C}$ in toluene- d_8 ($[\text{Zr}] = 0.0131\text{ M}$, $[\text{propene}]_0 = 0.305\text{ M}$).

Propene propagation kinetics was measured as a function of $[\text{Zr}]$ over a 2.5-16.4 mM range. Experiments at higher catalyst concentrations resulted in solubility problems. Well-behaved kinetics was observed in all reactions and the resulting plots of $\ln([\text{propene}]_t)$ vs time were linear over at least three half-lives. The observed rate constants varied linearly with $[\text{Zr}]$ over the range examined. This allowed determination of the propagation rate constant k_p from the slope of the plot of k_{obs} vs $[\text{Zr}]$ (Figure 5). The rate law that best describes these data was found to be: $\text{rate} = k_p[\text{Zr}][\text{propene}]$, where $k_p(-57^{\circ}\text{C}) = 0.042(4)\text{ M}^{-1}\text{s}^{-1}$.

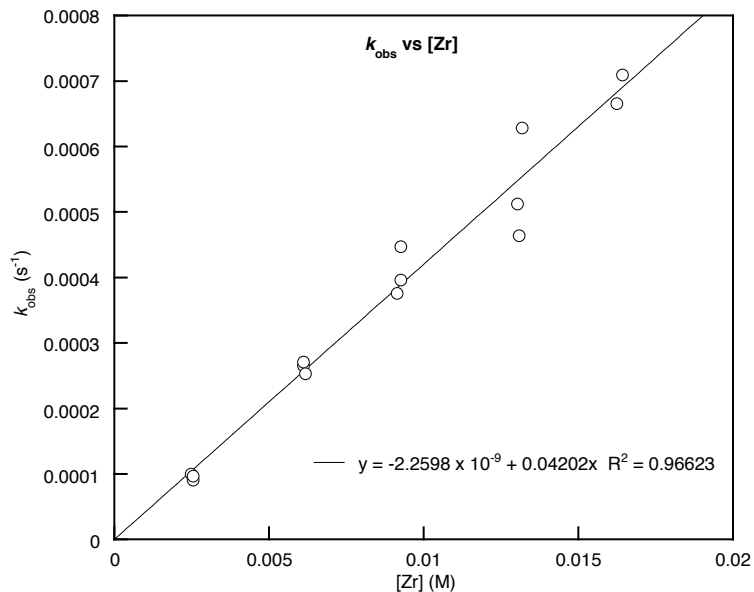


Figure 5. Plot of observed rate constants for propene polymerization vs [Zr] ($-57\text{ }^{\circ}\text{C}$, toluene- d_8). The slope of the fit gives $k_p = 0.042(4)\text{ M}^{-1}\text{s}^{-1}$.

The temperature dependence on propene propagation kinetics was also examined for this system between -45 and $-80\text{ }^{\circ}\text{C}$ in toluene- d_8 . Kinetic measurements were conducted using 6.0 mM of zirconocene catalyst and 0.63 M of propene (228 K) or 16.3 mM of zirconocene catalyst and 0.34 M of propene ($203, 192\text{ K}$). Observed rate constants were obtained using the method described above. Second-order k_p for these temperatures were calculated using the expression $k_p = k_{\text{obs}}/[\text{Zr}]$ (Table 1). The values reported are the average of three kinetic measurements. The overall activation parameters for propagation were calculated from an Eyring plot to give $\Delta H^{\ddagger} = 8.5(3)\text{ kcal}\cdot\text{mol}^{-1}$ and $\Delta S^{\ddagger} = -25(2)\text{ eu}$ (Figure 6).

Table 1. Second-order propagation rate constants for **2**- catalyzed propene polymerization in toluene- d_8

T (K)	$k_p \times 10^3$ ($M^{-1}s^{-1}$)
192	2.5(2)
203	9.2(9)
216	42(4)
228	105(10)

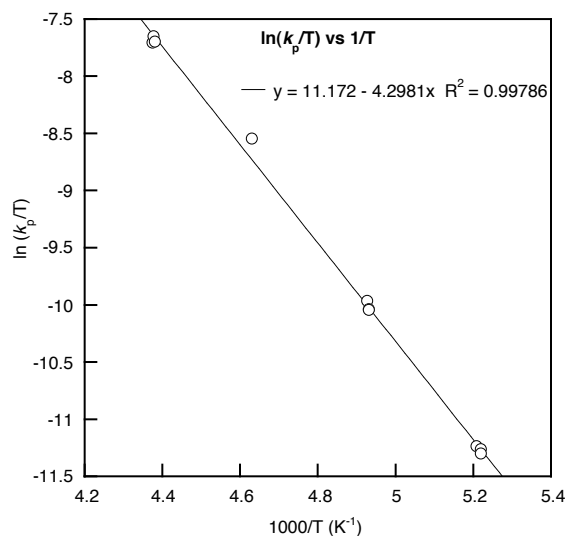


Figure 6. Eyring plot for the reaction of **2** with propene in toluene- d_8 . The fit gives activation parameters: $\Delta H^\ddagger = 8.5(3)$ kcal·mol⁻¹ and $\Delta S^\ddagger = -25(2)$ eu.

2.5 Measurement of propagation kinetics of alkene polymerization by [CpCp*Zr(CH₂CHMe)_nNp]⁺[CH₃B(C₆F₅)₃]⁻

Propagation kinetics for the polymerization of a series of linear 1-alkenes (CH₂=CH(R)) of increasing chain length and of 4-methyl-1-pentene by **2** was monitored by ¹H NMR spectroscopy as described above. Kinetic measurements were carried out using ca. 10-16 mM of zirconocene catalyst and 0.59-1 M of alkene in toluene- d_8 at -45 °C. The ethene propagation rate was too fast to measure using these techniques; the monomer was rapidly polymerized at temperatures as low as -100 °C. For all other

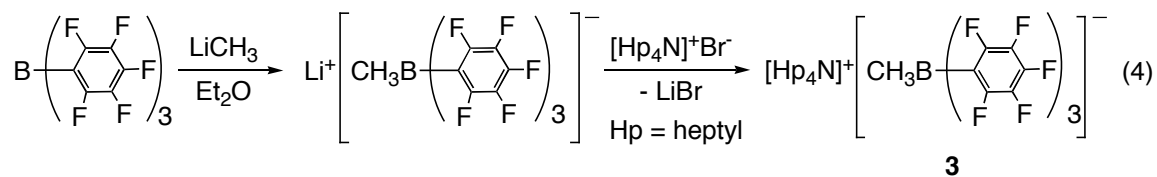
alkenes, the integral of alkene $CH_2CH(R)$ resonance (relative to Ph_2CH_2 as an internal standard) was determined as a function of time and the kinetic data were treated using the method described above. Observed rate constants were obtained from plots of $\ln([\text{alkene}]_t)$ vs time that were linear over several half-lives. Propagation rate constants were calculated using the expression $k_p = k_{\text{obs}}/[\text{Zr}]$ (Table 2). The values reported are the average of at least three kinetic measurements.

Table 2. Second-order propagation rate constants for **2**- catalyzed alkene polymerization (-45 °C, toluene- d_8)

Alkene	$k_p \times 10^3$ ($M^{-1}s^{-1}$)	Alkene	$k_p \times 10^3$ ($M^{-1}s^{-1}$)
propene	105(10)	1-hexene	15(1)
1-butene	27(5)	1-undecene	7.8(7)
1-pentene	18(1)	4-methyl-1-pentene	4.3(5)

2.6 Synthesis of $[\text{CpCp}^*\text{ZrNp}]^+[\text{CH}_3\text{B}(\text{C}_6\text{F}_5)_3]^-$ in the presence of $[\text{Hp}_4\text{N}]^+[\text{CH}_3\text{B}(\text{C}_6\text{F}_5)_3]^-$

The salt $[\text{Hp}_4\text{N}]^+[\text{CH}_3\text{B}(\text{C}_6\text{F}_5)_3]^-$ (**3**) (Hp = $(\text{CH}_2)_6\text{CH}_3$) was prepared as a source of “free” counteranion for use in kinetic studies.^{13,27} Compound **3** was synthesized using a methylation-cation exchange procedure starting from $\text{B}(\text{C}_6\text{F}_5)_3$ (eq 4). The intermediate $[\text{Li}]^+[\text{CH}_3\text{B}(\text{C}_6\text{F}_5)_3]^-$ was generated in situ and reacted directly with $[\text{Hp}_4\text{N}]^+[\text{Br}]^-$ to yield **3** as a colorless oil. Characteristic ^1H and ^{19}F NMR spectroscopic features of **3** include: broad Hp α - CH_2 resonance located at 2.25 ppm and $\Delta\delta(m,p\text{-F}) = 2.6$ ppm (benzene- d_6 , 25°C).



The initiator **1** was generated in the presence of the salt **3** (up to 3 equiv) using the procedure shown in eq 1. Experiments at higher [**3**] resulted in solubility problems. The ^1H and ^{19}F NMR spectra of these samples in toluene- d_8 at $-45\text{ }^\circ\text{C}$ indicated **1** and **3** were the major species present in solution (Figure 7). The characteristic ^1H NMR resonances of **1** were identified at: Cp (5.66 ppm), Cp* (1.22 ppm), downfield shifted $\alpha\text{-CH}_2$ doublet (1.78 ppm, $J = 11.5\text{ Hz}$), and broad coincident signal for the other $\alpha\text{-CH}_2$ and $[\text{CH}_3\text{B}(\text{C}_6\text{F}_5)_3]^-$ (-0.10 ppm). Broad signals for the heptyl group of **3** were observed at 2.21 ppm ($\alpha\text{-CH}_2$) and between 0.9-1.5 ppm. The ^{19}F NMR spectra showed sets of resonances for $\{\text{Zr}\}^+$ -coordinated $[\text{CH}_3\text{B}(\text{C}_6\text{F}_5)_3]^-$ group (-131.7, -156.3, -161.5 ppm) and “free” $[\text{CH}_3\text{B}(\text{C}_6\text{F}_5)_3]^-$ (-129.7, -161.5, -164.1 ppm). No significant change in the ^1H and ^{19}F NMR features of **1** was observed over the range of **3** added (0.1 to 3 equiv).

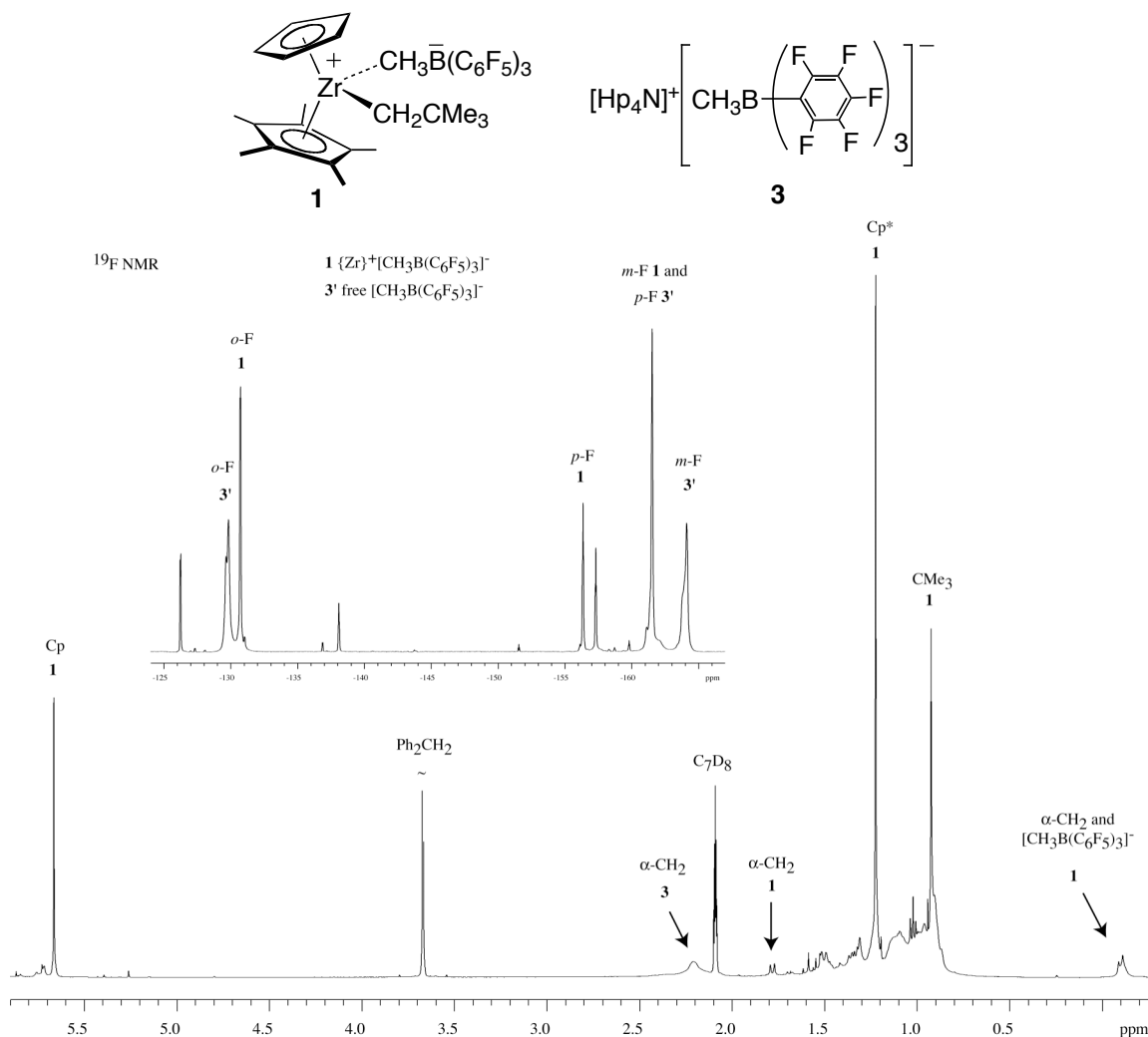


Figure 7. Partial ^1H NMR spectrum of **1** generated in the presence of 1 equivalent **3** in toluene- d_8 at -45°C . Heptyl resonances (0.9-1.5 ppm) of **3** are not labeled. Inset shows ^{19}F NMR spectrum. Unlabeled signals are due to excess $\text{B}(\text{C}_6\text{F}_5)_3$ (-126.2, -138.1, -157.3 ppm).

2.7 Observation and measurement of propagation kinetics of propene polymerization by $[\text{CpCp}^*\text{Zr}(\text{CH}_2\text{CHMe})_n\text{Np}]^+[\text{CH}_3\text{B}(\text{C}_6\text{F}_5)_3]^-$ in the presence of added $[\text{Hp}_4\text{N}]^+ [\text{CH}_3\text{B}(\text{C}_6\text{F}_5)_3]^-$

The propagating species **2** rapidly formed upon addition of propene (40-90 equiv) to solutions of **1** in the presence of added salt **3** (up to approximately 3 equiv). The species detected in solution by ^1H NMR spectroscopy at -45°C were **2**, **3**, and free propene

(Figure 8). Consistent with this assignment were the sets of broad resonances (unresolved) of **2** located at: Cp (5.62, 5.57 ppm), Cp*(1.23, 1.22 ppm), and $[\text{CH}_3\text{B}(\text{C}_6\text{F}_5)_3]^-$ (-0.10, -0.17 ppm) in the ^1H NMR spectrum. The broad Hp $\alpha\text{-CH}_2$ resonance of **3** was observed at 2.27 ppm. Broad signals due to polypropylene were also present and increased over time as **2**-catalyzed polymerization occurred.

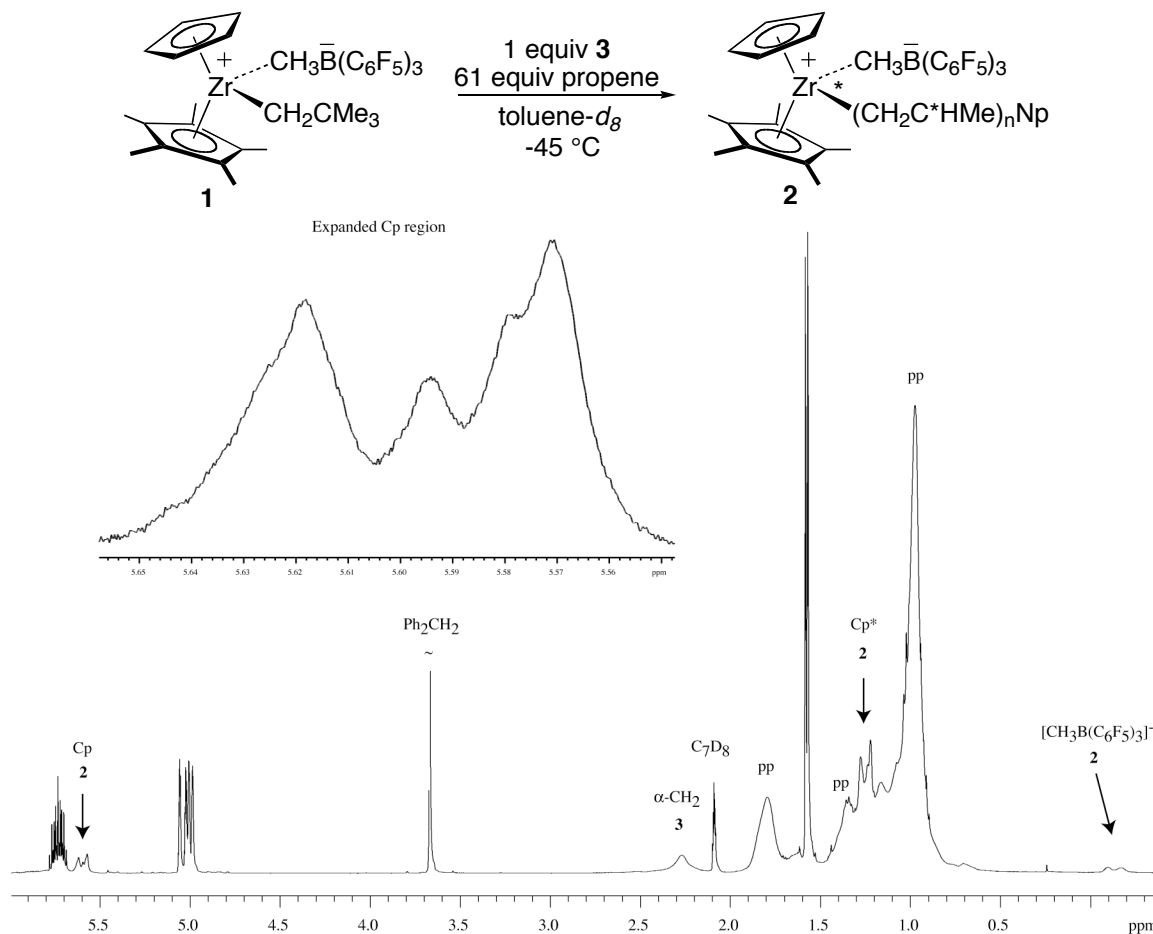


Figure 8. Partial ^1H NMR spectrum of the product mixture obtained from **1** and 61 equivalents of propene with 1 equivalent added **3** in toluene- d_8 at $-45\text{ }^\circ\text{C}$. “pp” denotes signals for polypropylene and unlabeled signals are for unreacted propene. The inset shows the expanded Cp resonances of **2**.

Propagation kinetics for propene polymerization by **2** in the presence of **3** was monitored by ^1H NMR as described above. Kinetic measurements were carried out using

ca. 5-11 mM of zirconocene catalyst, 1-10 mM of “free” counteranion, and 0.42-0.46 M of alkene in toluene- d_8 at -45 °C. Observed rate constants were obtained using the method described above. Second-order k_p for these reactions were calculated using the expression $k_p = k_{\text{obs}}/[\text{Zr}]$ (Table 3). “Free” counteranion is defined as all noncoordinated $[\text{CH}_3\text{B}(\text{C}_6\text{F}_5)_3]^-$. The concentration of “free” $[\text{CH}_3\text{B}(\text{C}_6\text{F}_5)_3]^-$ is calculated using the relative integrals of coordinated and noncoordinated anion in the ^{19}F NMR spectra and the mass-balance of $[\text{CH}_3\text{B}(\text{C}_6\text{F}_5)_3]^-$ determined from the ^1H NMR spectra (by integration of **1** and **3** versus the Ph_2CH_2 internal standard). The value obtained is always greater than that determined from the concentration of **3** (by 3-57%). The reason for this difference is currently under investigation. The ionic strength of the solution, μ , is calculated for all solvent-separated ions, i , in solution (based on the “free” $[\text{CH}_3\text{B}(\text{C}_6\text{F}_5)_3]^-$ concentration) using the definition: $\mu = 1/2\sum[i]z_i^2$ where z_i is the charge of ion i .

The propagation rate was observed to increase with “free” $[\text{CH}_3\text{B}(\text{C}_6\text{F}_5)_3]^-$ as shown in a plot of k_p vs “free” $[\text{CH}_3\text{B}(\text{C}_6\text{F}_5)_3]^-$ (Figure 9). Since $\mu =$ “free” $[\text{CH}_3\text{B}(\text{C}_6\text{F}_5)_3]^-$ in this case, k_p also increases with increasing ionic strength of the solution.

Table 3. Second-order rate constants for **2**-catalyzed propene polymerization with added $[\text{CH}_3\text{B}(\text{C}_6\text{F}_5)_3]^-$ counteranion (-45 °C, toluene- d_8)

free $[\text{CH}_3\text{B}(\text{C}_6\text{F}_5)_3]^-$ (mM)	$k_p \times 10^3$ ($\text{M}^{-1}\text{s}^{-1}$)	μ (M) ^a	free $[\text{CH}_3\text{B}(\text{C}_6\text{F}_5)_3]^-$ (mM)	$k_p \times 10^3$ ($\text{M}^{-1}\text{s}^{-1}$)	μ (M) ^a
1.0	137(2)	0.0010	8.5	216(4)	0.0085
1.3	136(2)	0.0013	10.0	230(9)	0.0100
3.8	165(9)	0.0038	10.2	233(6)	0.0102
7.9	212(4)	0.0079	10.4	239(9)	0.0104

^a Ionic strength of the solution determined from free $[\text{CH}_3\text{B}(\text{C}_6\text{F}_5)_3]^-$

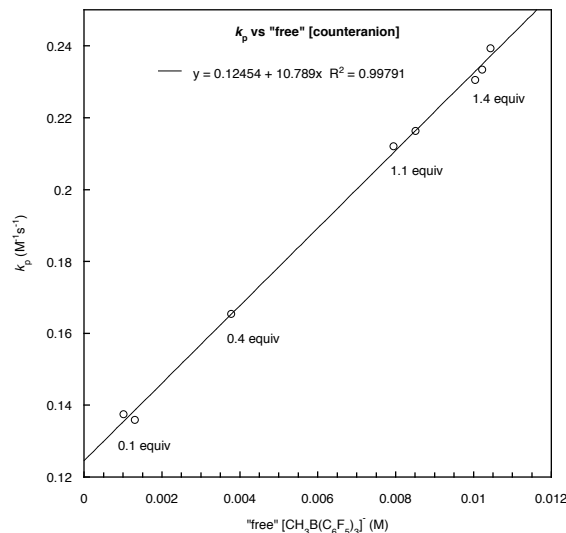


Figure 9. Propagation kinetics for **2**-catalyzed propene polymerization in the presence of “free” [CH₃B(C₆F₅)₃]⁻ counteranion.

2.8 Synthesis of [CpCp*ZrNp]⁺[CH₃B(C₆F₅)₃]⁻ and decomposition via β-CH₃ elimination in toluene-*d*₈-chlorobenzene-*d*₅ solvent

The catalyst **1** was also generated cleanly in situ by reaction of CpCp*Zr(Np)(CH₃) with B(C₆F₅)₃ at -60 °C in 1:1 (w/w) toluene-*d*₈-chlorobenzene-*d*₅ solvent. Compound **1** was characterized using low temperature ¹H and ¹⁹F NMR spectroscopy in this solvent system. This data showed features analogous to those observed in pure toluene-*d*₈ solvent upon formation of **1** (vide supra). Characteristic ¹H NMR (-60 °C, toluene-*d*₈-chlorobenzene-*d*₅) resonances of **1** included: Cp (5.75 ppm), Cp* (1.32 ppm), downfield shifted α-CH₂ doublet (1.83 ppm, J = 10.4 Hz), and broad coincident signal for the other α-CH₂ and [CH₃B(C₆F₅)₃]⁻ (-0.11 ppm). The observed ¹H and ¹⁹F NMR (where Δδ(*m,p-F*) = 5.1 ppm) spectra of **1** are indicative of contact ion-pairing in solution as was observed in toluene-*d*₈ solvent. Therefore, the speciation of **1** is best described as an inner-sphere

ion-pair rather than solvent separated ions (i.e., $[\text{CpCp}^*\text{Zr}(\text{Np})(\text{C}_6\text{D}_5\text{Cl})]^+[\text{CH}_3\text{B}(\text{C}_6\text{F}_5)_3]^-$) under these conditions.

Solutions of **1** in toluene- d_8 -chlorobenzene- d_5 were stable at low temperatures but decomposition was detected (^1H NMR) at temperatures above -25 °C. A β -methyl elimination decomposition pathway operated as confirmed by the formation of the methyl-zirconocene catalyst, $[\text{CpCp}^*\text{Zr}(\text{CH}_3)]^+[\text{CH}_3\text{B}(\text{C}_6\text{F}_5)_3]^-$ and isobutene according to eq 2.

The decomposition of **1** was monitored as a function of time by ^1H NMR spectroscopy at -7 °C and 10 °C in toluene- d_8 -chlorobenzene- d_5 . Rate constants for β - CH_3 elimination at these temperatures were obtained by curve fitting to the expression $I_t = I_f + (I_0 - I_f) \times \exp(-k_{\beta\text{-Me}}t)$, where I_t is the Cp peak height of **1**. These measurements gave $k_{\beta\text{-Me}}(-7$ °C) = $3(1) \times 10^{-4} \text{ s}^{-1}$ and $k_{\beta\text{-Me}}(10$ °C) = $21(2) \times 10^{-4} \text{ s}^{-1}$ in 1:1 (w/w) toluene- d_8 -chlorobenzene- d_5 . The values reported are the average of three kinetic measurements.

2.9 Observation and measurement of propagation kinetics of propene polymerization by $[\text{CpCp}^*\text{Zr}(\text{CH}_2\text{CHMe})_n\text{Np}]^+[\text{CH}_3\text{B}(\text{C}_6\text{F}_5)_3]^-$ in toluene- d_8 -chlorobenzene- d_5 solvent

The propagating species **2** rapidly formed upon addition of propene (roughly 58 equiv) to solutions of **1** in 1:1 (w/w) toluene- d_8 -chlorobenzene- d_5 as described above. Therefore, initiation of **1** occurred within minutes on warming to above -70 °C. A product mixture consistent with eq 3 was observed, where free propene and **2** are detected in solution by ^1H NMR spectroscopy at -60 °C. The two new sets of broad resonances (unresolved) characteristic of **2** were located at: Cp (5.71, 5.65 ppm), Cp*(1.35, 1.31 ppm), and $[\text{CH}_3\text{B}(\text{C}_6\text{F}_5)_3]^-$ (-0.12, -0.20 ppm) groups of **2** in the ^1H NMR

spectrum. The sets of diastereomers of **2** appeared to form in the same roughly 60:40 ratio as was observed in toluene- d_8 .

Monitoring these reactions over time confirmed reaction of **2** with propene. Broad signals due to polypropene (located at 1.77 (CH), 1.25, 1.05 (CH₂), and 0.94 (CH₃) ppm) grow in along with concomitant decrease in those for free propene (¹H NMR, -60 °C).

Propagation kinetic measurements were carried out at -45 °C and -60 °C using ca. 10.8 mM of zirconocene catalyst and 0.62 M of propene in toluene- d_8 - chlorobenzene- d_5 . Observed rate constants were obtained using the method described above for propene propagation kinetics in toluene- d_8 . Second-order k_p for these temperatures were calculated using the expression $k_p = k_{\text{obs}}/[\text{Zr}]$ (Table 4).

Table 4. Second-order propagation rate constants for **2**- catalyzed propene polymerization in toluene- d_8 and toluene- d_8 - chlorobenzene- d_5 solvent

T (K)	Solvent	$k_p \times 10^3$ (M ⁻¹ s ⁻¹)
213	C ₇ D ₈ -C ₆ D ₅ Cl ^a	59(5)
213	C ₇ D ₈	26(3) ^b
228	C ₇ D ₈ -C ₆ D ₅ Cl ^a	280(30)
228	C ₇ D ₈	105(10) ^c

^a 1:1 (w/w) mixture; ^b calculated from Eyring plot; ^c measured experimentally.

3 Discussion

The neopentyl-zirconocenium initiator **1** is cleanly and reproducibly synthesized in situ under rigorously anhydrous conditions at low temperatures in inert solvents (toluene- d_8 or toluene- d_8 -chlorobenzene- d_5) using the methide abstraction approach developed by Marks.²⁸ The observed ¹H and ¹⁹F NMR spectra are indicative of a {Zr}⁺-[CH₃B(C₆F₅)₃]⁻ interaction over the range of conditions examined.^{13,27} Consistent with counteranion coordination are the upfield [CH₃B(C₆F₅)₃]⁻ resonance (-0.11 ppm) and the $\Delta\delta(m,p-F)$

value of 5.2 ppm found for **1**. These values can be compared with the phosphine-stabilized $[(\text{Me}_2\text{SiCp}_2)\text{Zr}(\text{CH}_3)(\text{PPh}_3)]^+[\text{CH}_3\text{B}(\text{C}_6\text{F}_5)_3]^-$ compound having a noncoordinated anion, where $\delta[\text{CH}_3\text{B}(\text{C}_6\text{F}_5)_3]^- = 1.39$ ppm and $\Delta\delta(m,p-F) = 2.3$ ppm (benzene- d_6 , 25 °C).²⁹ Therefore, the solution structure of **1** is best described as a contact ion-pair.

Catalyst **1** is stable at low temperatures but decomposes upon warming via the β -methyl elimination pathway common among group 4 $[\text{Cp}^x_2\text{MNp}]^+[\text{CH}_3\text{B}(\text{C}_6\text{F}_5)_3]^-$.^{19,22,27} The stability of **1** appears intermediate between that reported for $[\text{Cp}^*_2\text{ZrNp}]^+[\text{CH}_3\text{B}(\text{C}_6\text{F}_5)_3]^-$ and $[\text{Cp}_2\text{ZrNp}]^+[\text{CH}_3\text{B}(\text{C}_6\text{F}_5)_3]^-$.²⁷ As β -methyl elimination is proposed to involve ion-pair separation,²⁷ this observed reactivity could reflect the steric influence of the ancillary ligation on the extent of ion-pairing. An increased cation-anion interaction is expected for **1** relative to the more sterically congested $[\text{Cp}^*_2\text{ZrNp}]^+[\text{CH}_3\text{B}(\text{C}_6\text{F}_5)_3]^-$.

While the decomposition of **1** occurs at roughly the same temperature in either toluene- d_8 or toluene- d_8 -chlorobenzene- d_5 , the $k_{\beta\text{-Me}}$ measured in the mixed solvent system is twice that measured in toluene- d_8 . The increased rate of decomposition can again be related to the relative ease of ion-pair separation, where weakening of ion-pairing is facilitated in the more polar solvent.²²

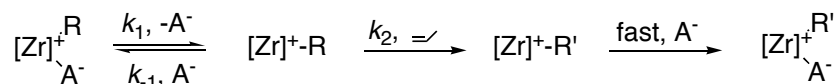
The catalyst **1** serves as a well-defined initiator for use in studies investigating alkene propagation kinetics. In all conditions examined, the reaction of **1** with excess propene results in complete catalyst initiation as observed by ¹H NMR spectroscopy. Qualitatively, this is interpreted as a fast initiation step and suggests that $k_i \cong k_p$ for this system. The propagating species **2** formed during polymerization appeared stable

towards chain transfer reactions under the reaction conditions in the presence of greater than three equivalents propene, which indicates that the catalyst does not decompose or pool in an inactive form. These features overcome the limitations associated with studies of alkene propagation kinetics using $\text{Cp}^x_2\text{MCl}_2/\text{MAO}$ catalysts.³ This allows direct monitoring of the propagation step by ^1H NMR spectroscopy and determination of propagation rate constants.

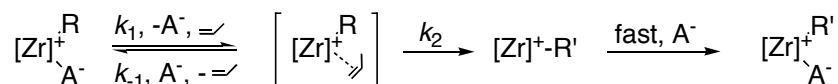
This well-behaved system has also been used to examine factors influencing propagation kinetics, including temperature dependence and monomer, common counteranion, and solvent effects. These experiments provide information useful in distinguishing between limiting mechanisms for the propagation step (Scheme 3).

Scheme 3

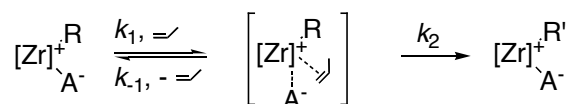
Dissociative



Associative 1



Associative 2



These limiting cases for the propagation step differ in the mechanism of alkene binding, ion-pair separation, and whether outer-sphere ions are formed. A rate-limiting insertion step is presumed based on literature precedence.^{20,30} In the dissociative limit, separated ions are formed by initial counteranion dissociation followed by alkene binding to a formally 14 electron zirconium-polymeryl cation.^{12,31} Both associative limits involve

alkene binding to a contact $\{\text{Zr}\}^+[\text{A}]^-$ propagating species to produce an intermediate or transition state of higher coordination.²⁰ In associative 1 counteranion is lost from this intermediate or transition state and insertion then occurs from the resulting ion-separated $\{\text{Zr}\}^+(\text{alkene})$ adduct.^{9,11} This differs from associative 2 where the formation of formally outer-sphere ions is not invoked.¹³

Overall entropy of activation and counteranion dependence predictions may perhaps distinguish between the limiting cases of outer-sphere and inner-sphere speciation of the propagating species. For dissociative and associative 1, an overall $\Delta S^\ddagger \approx 0$ is predicted. These limits should show an inverse counteranion dependence and the rate of propagation should decrease with added counteranion. For associative 2, a overall $\Delta S^\ddagger < 0$ is predicted, along with no counteranion dependence. Additional information may be provided by the examination of propagation rates over a series of alkenes with varying steric influence. Increasing the alkene steric bulk should disfavor binding and lead to a greater steric barrier in the insertion step for both associative limits, resulting in a slower propagation rate.³² In the dissociative limit, ion-pair separation should be favored (larger k_1/k_{-1}) for increased steric bulk at the β -position of the polymeryl chain.²² This contribution could partially offset a decreased k_2 for sterically demanding alkenes in the binding and insertion step; i.e., a smaller relative decrease in propagation rate may be observed with increasing monomer steric bulk.

A propagation rate constant is directly measured for zirconocene-catalyzed propene polymerization and a rate law developed for this step. The propagation rate law determined from the kinetic data is first order in $[\text{Zr}]$ and first-order in $[\text{propene}]$. This is consistent with the propagation rate law, $\text{rate} = k_p[\text{Zr}][\text{propene}]$, found for the *rac*-

$\text{C}_2\text{H}_4(1\text{-indenyl})_2\text{Zr}(\text{polyhexenyl})^+[\text{CH}_3\text{B}(\text{C}_6\text{F}_5)_3]^-$ catalyst in complementary experiments using direct NMR methods.²⁶ The first-order dependence on [propene] indicates that rate-limiting $[\text{CH}_3\text{B}(\text{C}_6\text{F}_5)_3]$ dissociation prior to propene binding does not occur under these conditions. Eyring analysis of the propagation step for **2**-catalyzed propene polymerization yields a modest ΔH^\ddagger , consistent with a transition-state involving both bond breaking and formation. The significantly negative ΔS^\ddagger term determined for propagation best fits the associative **2** limiting mechanism for propene binding and insertion; however, contributions from solvent and ion-pair reorganization must also be considered.

These methods are applied to the measurement of k_p for a series of alkenes. These rate constants ($\text{M}^{-1}\text{s}^{-1}$, $-45\text{ }^\circ\text{C}$, toluene- d_8) establish the following order of reactivity for alkenes in metallocene-catalyzed polymerization: propene ($105(10) \times 10^{-3}$) > 1-butene ($27(5) \times 10^{-3}$) > 1-pentene ($18(1) \times 10^{-3}$) > 1-hexene ($15(1) \times 10^{-3}$) > 1-undecene ($7.8(7) \times 10^{-3}$) > 4-methyl-1-pentene ($4.3(5) \times 10^{-3}$). Rapid consumption of ethene at temperatures as low as $-100\text{ }^\circ\text{C}$ precluded measurement of its rate constant. The kinetic data for propene vs 1-hexene are comparable to results obtained by Landis and coworkers, who found that propene propagates three times faster than 1-hexene.²⁶

The different propagation rates found for the series of linear alkenes has mechanistic implications. The observed variations in k_p indicate that increasing the steric bulk at the monomer allylic position (and likewise the β -position of the migrating polymeryl chain) effects a decrease in propagation rate. The steric deceleration of polymerization rate with increasing size of the (single) allylic substituent is similar to the deceleration in insertion rate of linear alkenes into $\text{Cp}^*_2\text{Y-CH}_2\text{CH}_2\text{CHMe}_2$ reported by Casey.³² In their case,

however, propene reacted faster than 1-butene and 1-hexene by only a factor of 1.6 and 2.3 respectively, leading to the conclusion that the alkene chain length had only a modest effect on the rate of insertion (where the rate of insertion measured is a composite of alkene binding to yttrium and migratory insertion). Group 3 Cp*₂M-alkyl compounds are models for group 4 [Cp^x₂M-polymeryl]⁺ species.³³ Therefore, a similar effect may be considered in the context of linear alkene binding to [CpCp*Zr-polymeryl]⁺ - formed in the dissociative limit – and insertion. Extrapolation to the present system – where a small difference in relative *n*-alkene binding and migratory insertion rate could be offset by contribution of the anion-dissociation step – may result in similar propagation rates for the linear alkenes. Here however, the propagation rate is sensitive to the alkene chain length: propene reacts 3.8 times faster than 1-butene and 7 times faster than 1-hexene. Therefore, the results obtained for alkene propagation kinetics are most consistent with an associative mechanism for the propagation step.

The counteranion dependence on propagation kinetics for **2**-catalyzed propene polymerization has been examined. An effect of added common counteranion was detected, where the measured k_p increased in the presence of “free” [CH₃B(C₆F₅)₃]⁻. These findings contrast the results of counteranion dependence studies for [*rac*-C₂H₄(1-indenyl)₂Zr(polyhexenyl)]⁺[CH₃B(C₆F₅)₃]⁻-catalyzed 1-hexene polymerization using quenched-flow methods.⁵ Here no change in propagation rate was observed in the presence of free [CH₃B(C₆F₅)₃]⁻.

The effect of common counteranion on the observed propagation kinetics opposes that predicted for propagation via the dissociative or associative 1 limit. More specifically, the increase in polymerization rate found is not compatible with limiting

mechanisms where formation of outer-sphere ions is invoked. Notably, associative 2 does not involve the formation of outer-sphere ions, but should also show no counteranion dependence.

While this data appears at odds with all mechanisms, the observed effect may be best described as an ionic-strength effect on propagation kinetics rather than a formal $[\text{CH}_3\text{B}(\text{C}_6\text{F}_5)_3]^-$ dependence.³⁴ The addition of common counteranion source **3** to polymerization reactions increases the ionic-strength of the solutions. Additionally, specific ion-pairing interactions are reduced at higher ionic-strengths. In the context of the catalyst system examined here, $[\text{CpCp}^*\text{Zr-polymeryl}]^+ - [\text{CH}_3\text{B}(\text{C}_6\text{F}_5)_3]^-$ ion-pairing may be lessened at higher ionic strength, increasing the electrophilicity of the zirconocenium center and the propensity to bind alkene. Any ion-pair separation or reorganization (within the inner-sphere) required upon going to the transition state for alkene insertion would be facilitated in solutions with higher ionic-strength, again leading to an increased rate of propagation (Figure 10). If this explanation is occurring then the same effect should be observed by using other inert electrolytes or more polar solvents.

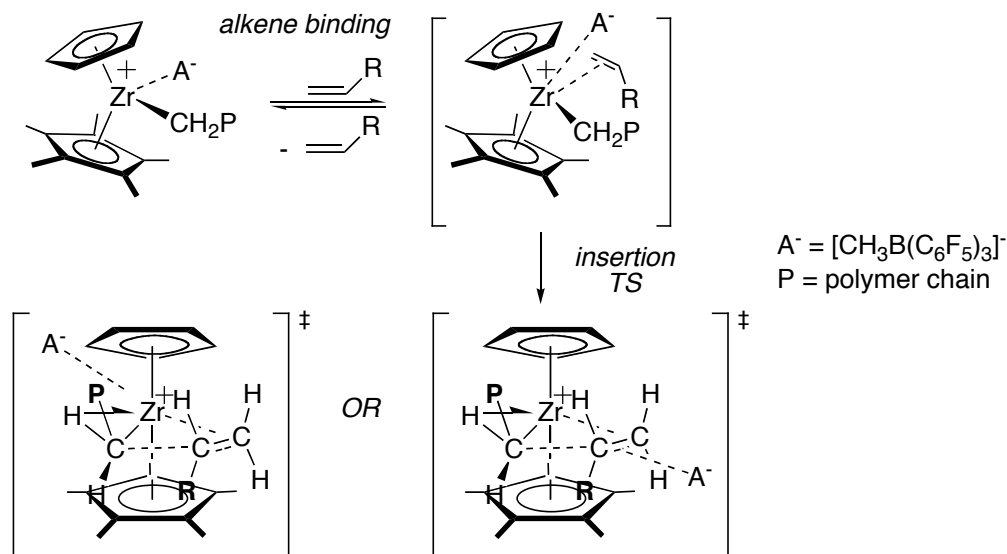


Figure 10. Plausible ion-pair separation and reorganization of [CH₃B(C₆F₅)₃]⁻ counteranion within the inner-sphere during the propagation step.

Solvent effects on propene propagation kinetics with catalyst **2** have been briefly explored. Comparison of kinetic measurements in toluene-*d*₈-chlorobenzene-*d*₅ vs pure toluene-*d*₈ solvent reveals a modest solvent effect on the propagation step. The propagation rate constant increases in the more polar solvent, where propagation occurs roughly two times faster than in toluene-*d*₈ at a given temperature. The magnitude of this effect is comparable with that seen for the β-methyl elimination in **1**. This is not surprising given that these processes should share very similar transition states.¹⁹

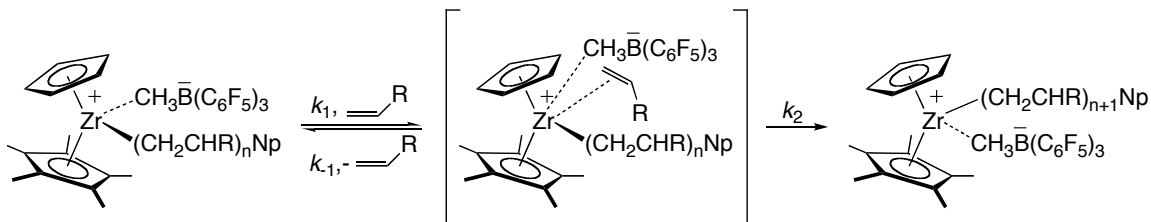
Propagation studies in the polar solvent system provided no strong evidence for the formation of a ground-state [CpCp*Zr-polymeryl]⁺-solvento species with an outer-sphere [CH₃B(C₆F₅)₃]⁻ anion.^{13,27} The solvent effect can be interpreted analogously to the anion effect. Specific ion-pairing is weakened in the more polar toluene-*d*₈-chlorobenzene-*d*₅ relative to in toluene-*d*₈.²² The polar solvent facilitates ion-pair separation and reorganization (within the inner-sphere) resulting in a faster propagation rate.

4 Conclusions

The neopentyl-zirconocene initiator **1** is well-defined and shows favorable relative rates of initiation and propagation when reacted with propene and other alkenes. These properties are utilized in investigating propagation kinetics for zirconocene-catalyzed alkene polymerization using ^1H NMR spectroscopic methods. Second-order propagation rate constants are measured directly for propene and a series of alkenes and a propagation rate-law determined.

Details of propagation kinetics, including temperature dependence and counteranion and solvent effects have been examined with this catalyst system. The results of these studies together with the trend in k_p observed over the series of alkenes are most consistent with propagation via the associative 2 mechanism for this system (Scheme 4).

Scheme 4



Catalyst 2 propagates via an inner-sphere ion-pair. The alkene binds to a contact ion-pair propagating species and the $[\text{CH}_3\text{B}(\text{C}_6\text{F}_5)_3]^-$ anion remains within the inner-sphere during the migratory insertion step. While the observed anion and solvent effects support some separation and reorganization of ions from the ground state to the insertion transition state, formally outer-sphere ions are not relevant intermediates in the propagation step. This finding suggests that the formation of solvent separated $[\text{Cp}^x_2\text{M-polymeryl}]^+$ ions are not required for catalytic alkene polymerization in group 4 metallocene systems.

5 Experimental Section

General Considerations

All air- and moisture-sensitive compounds were manipulated using standard high vacuum line, Schlenk, or cannula techniques, or in a glovebox under a nitrogen atmosphere as described previously.³⁵ Argon gas was purified and dried by passage through columns of MnO on vermiculite and activated 4 Å molecular sieves. Solvents for air- and moisture-sensitive reactions were dried by the method of Grubbs³⁶ and were stored under vacuum over sodium benzophenone ketyl (diethyl ether, pentane) or titanocene³⁷ (toluene, petroleum ether). Benzene-*d*₆ and toluene-*d*₈ were purchased from Cambridge Isotopes and vacuum distilled from sodium benzophenone ketyl. Chlorobenzene-*d*₅ was purchased from Cambridge Isotopes and vacuum distilled from calcium hydride. The synthesis of $(\eta^5\text{-C}_5\text{H}_5)(\eta^5\text{-C}_5\text{Me}_5)\text{Zr}(\text{CH}_2\text{CMe}_3)(\text{CH}_3)$ was carried out as described in Chapter 1. $\text{B}(\text{C}_6\text{F}_5)_3$ was prepared according to literature procedure³⁸ or was purchased (Strem) and sublimed before use. Diphenylmethane (Aldrich) was dried by passage through a plug of activated alumina and stored over activated 4 Å molecular sieves under N_2 . Ethene (CP grade, Air Liquide) and propene (Polymer grade, Matheson) were purified and dried by passage through columns of MnO on vermiculite and activated 4 Å molecular sieves and were subjected to a freeze-pump-thaw cycle prior to use. 1-Butene, 1-pentene, 4-methyl-1-pentene (Aldrich) were stored under vacuum over LiAlH_4 and distilled immediately before use.³⁹ 1-Hexene (Aldrich) was distilled from LiAlH_4 and stored over activated 4 Å molecular sieves under N_2 . 1-Undecene was dried with LiAlH_4 , isolated from the drying agent by filtration, and stored over activated 4 Å molecular sieves under N_2 . Methyl lithium was purchased as a solution in diethyl ether (Aldrich),

filtered through celite, and dried to a white solid in vacuo. (*n*-Heptyl)₄NBr (Aldrich) was dried in vacuo at room temperature for 12 h. Other materials were used as received.

Glassware used for vacuum transfer and storage of toluene-*d*₈ and chlorobenzene-*d*₅ was flame-evacuated prior to use. Glassware and J. Young NMR tubes used for kinetics experiments were pre-treated by washing with a 15% (w/w) solution of trimethylchlorosilane in methylene chloride, then rinsed with methylene chloride then acetone. J. Young NMR tubes were *gently* heated and evacuated on the high vacuum line before use in kinetics experiments.

NMR spectra were recorded on a Varian Mercury 300 (¹H, 299.868 MHz, ¹³C, 75.409 MHz) or a Varian INOVA 500 (¹H, 499.851 MHz, ¹⁹F, 470.261 MHz, ¹³C, 125.697 MHz). Chemical shifts in ¹H and ¹³C NMR spectra are reported in ppm downfield from TMS using residual proton (C₆D₅H, δ 7.16; C₆D₅CD₂H, δ 2.09) or carbon (C₆D₆, δ 128.39; C₆D₅CD₃, δ 20.4) signals of the deuterated solvents. Chemical shifts in ¹⁹F NMR spectra are given in ppm downfield from CFC₃ used as an external reference. NMR spectra are reported at ambient temperature, unless otherwise indicated. Temperatures were measured using a pure methanol standard.

Synthesis of $[(\eta^5\text{-C}_5\text{H}_5)(\eta^5\text{-C}_5\text{Me}_5)\text{Zr}(\text{CH}_2\text{CMe}_3)]^+[\text{CH}_3\text{B}(\text{C}_6\text{F}_5)_3]^-$ (1).
 $([\text{CpCp}^*\text{Zr}(\text{Np})]^+[\text{MeBAr}_3\text{F}])^-$.

Due to its temperature instability, compound **1** was prepared in situ. In an inert atmosphere glovebox, the following were added to a J. Young NMR tube via gas-tight

microsyringe at ambient temperature: 100 μL stock solution ($\eta^5\text{-C}_5\text{H}_5$)($\eta^5\text{-C}_5\text{Me}_5$)Zr(CH₂CMe₃)(CH₃) (3.5 mg, 0.009 mmol) in toluene-*d*₈ and 50 μL stock solution Ph₂CH₂ (5.1 mg, 0.03 mmol) in toluene-*d*₈ as an internal standard. The walls of the NMR tube were rinsed with 250 μL toluene-*d*₈. The NMR tube was inserted into a glass sample holder located in the glovebox cold well, which was cooled externally with liquid nitrogen. The pale yellow solution was allowed to freeze. An additional 200 μL toluene-*d*₈ was added on top of the frozen layer, and was allowed to freeze. Then 100 μL of a stock solution of B(C₆F₅)₃ (5.3 mg, 0.010 mmol) in toluene-*d*₈ was added on top of the frozen layer, and was allowed to freeze. The NMR tube was sealed with a Teflon needle valve. The chilled sample holder was removed from the glovebox, and the NMR tube was *immediately* transferred to a -196 °C bath. The frozen sample was evacuated on the vacuum line. The sample was thawed at -78 °C in a dry ice-acetone bath and carefully mixed without warming the contents. Upon mixing a bright yellow solution was observed. The sample was then characterized using NMR spectroscopy. ¹H NMR (500 MHz, C₇D₈, 216 K): δ 5.66 (s, C₅H₅, 5H), 1.80 (d, CH₂C(CH₃)₃, 1H, J = 11 Hz), 1.21 (s, C₅(CH₃)₅, 15H), 0.93 (s, CH₂C(CH₃)₃, 9H), -0.11 (br d, CH₂C(CH₃)₃ and [CH₃B(C₆F₅)₃]⁻, 4H, J = 11.5 Hz); δ 7.15 to 6.97 (aryl resonances, Ph₂CH₂), 3.66 (s, Ph₂CH₂, 2H). ¹⁹F NMR (470 MHz, C₇D₈, 216 K): δ -130.5 (d, *o*-F [CH₃B(C₆F₅)₃]⁻, 6F, ³J_{FF} = 20.7 Hz), -156.0 (t, *p*-F [CH₃B(C₆F₅)₃]⁻, 3F, ³J_{FF} = 20.2 Hz), -161.2 (t, *m*-F [CH₃B(C₆F₅)₃]⁻, 6F, ³J_{FF} = 18.1 Hz); δ -126.0 (d, *o*-F B(C₆F₅)₃, 6F, ³J_{FF} = 21.6 Hz), -137.6 (t, *p*-F B(C₆F₅)₃, 3F, ³J_{FF} = 16.0 Hz), -157.1 (t, *m*-F B(C₆F₅)₃, 6F, ³J_{FF} = 18.8 Hz). ¹³C{¹H} NMR (125 MHz, C₇D₈, 216 K): δ 148.4 (d, [CH₃B(C₆F₅)₃]⁻, 6C, ¹J_{CF} = 237.2 Hz), 139.2 (d, [CH₃B(C₆F₅)₃]⁻, 3C, ¹J_{CF} = 246 Hz), 137.3 (d, [CH₃B(C₆F₅)₃]⁻, 6C, ¹J_{CF} = 243 Hz), 123.7 (C₅(CH₃)₅), 123.0 (br,

[CH₃B(C₆F₅)₃]⁻, 3C), 113.7 (C₅H₅), 99.8 (Zr-CH₂C(CH₃)₃), 39.3 (CH₂C(CH₃)₃), 34.2 (CH₂C(CH₃)₃), 13.9 ([CH₃B(C₆F₅)₃]⁻), 11.9 (C₅(CH₃)₅). ¹³C NMR (125 MHz, C₇D₈, 216 K): δ 148.4 (d, [CH₃B(C₆F₅)₃]⁻, 6C, ¹J_{CF} = 237.2 Hz), 139.2 (d, [CH₃B(C₆F₅)₃]⁻, 3C, ¹J_{CF} = 246 Hz), 137.3 (d, [CH₃B(C₆F₅)₃]⁻, 6C, ¹J_{CF} = 243 Hz), 123.7 (s, C₅(CH₃)₅, 5C), 123.0 (br, [CH₃B(C₆F₅)₃]⁻, 3C), 113.7 (d, C₅H₅, 5C, ¹J_{CH} = 174.3 Hz), 99.8 (dd, Zr-CH₂C(CH₃)₃, 1C, ¹J_{CH} = 103.6, 115.6 Hz), 39.3 (s, CH₂C(CH₃)₃, 1C), 34.2 (q, CH₂C(CH₃)₃, 3C, ¹J_{CH} = 125.0 Hz), 13.9 ([CH₃B(C₆F₅)₃]⁻), 11.9 (q, C₅(CH₃)₅, 5C, ¹J_{CH} = 127.6 Hz).

Variable-temperature NMR experiments with **1**.

A sample of **1** was prepared according to the above procedure. The NMR probe was cooled and the probe temperature calculated using a pure methanol standard. The sample was inserted into the pre-thermostatted probe and allowed to equilibrate for 10 minutes prior to data acquisition. ¹H NMR (500 MHz, C₇D₈, 192 K): δ 5.65 (s, C₅H₅, 5H), 1.84 (d, CH₂C(CH₃)₃, 1H, J = 10 Hz), 1.18 (s, C₅(CH₃)₅, 15H), 0.96 (s, CH₂C(CH₃)₃, 9H), -0.11 (br d, CH₂C(CH₃)₃ and [CH₃B(C₆F₅)₃]⁻, 4H, J = 9.5 Hz). ¹⁹F NMR (470 MHz, C₇D₈, 192 K): δ -130.4 (br, *o*-F [CH₃B(C₆F₅)₃]⁻, 6F), -155.6 (br, *p*-F [CH₃B(C₆F₅)₃]⁻, 3F), -160.9 (br, *m*-F [CH₃B(C₆F₅)₃]⁻, 6F); δ -125.8 (d, *o*-F B(C₆F₅)₃, 6F, ³J_{FF} = 18.8 Hz), -136.8 (br, *p*-F B(C₆F₅)₃, 3F), -156.8 (t, *m*-F B(C₆F₅)₃, 6F, ³J_{FF} = 17.4 Hz). ¹H NMR (500 MHz, C₇D₈, 203 K): δ 5.65 (s, C₅H₅, 5H), 1.82 (d, CH₂C(CH₃)₃, 1H, J = 11.5 Hz), 1.19 (s, C₅(CH₃)₅, 15H), 0.95 (s, CH₂C(CH₃)₃, 9H), -0.11 (br d, CH₂C(CH₃)₃ and [CH₃B(C₆F₅)₃]⁻, 4H, J = 11 Hz). ¹⁹F NMR (470 MHz, C₇D₈, 203 K): δ -130.6 (d, *o*-F [CH₃B(C₆F₅)₃]⁻, 6F, ³J_{FF} = 16 Hz), -155.9 (br, *p*-F [CH₃B(C₆F₅)₃]⁻, 3F), -161.1 (br, *m*-F [CH₃B(C₆F₅)₃]⁻, 6F); δ -126.0 (d, *o*-F B(C₆F₅)₃, 6F, ³J_{FF} = 20.2 Hz), -137.2 (br, *p*-F B(C₆F₅)₃, 3F), -157.0 (t, *m*-F

$B(C_6F_5)_3$, 6F, $^3J_{FF} = 16.9$ Hz). 1H NMR (500 MHz, C_7D_8 , 228 K): δ 5.66 (s, C_5H_5 , 5H), 1.78 (d, $CH_2C(CH_3)_3$, 1H, $J = 11$ Hz), 1.22 (s, $C_5(CH_3)_5$, 15H), 0.92 (s, $CH_2C(CH_3)_3$, 9H), -0.10 (br d, $CH_2C(CH_3)_3$ and $[CH_3B(C_6F_5)_3]^-$, 4H, $J = 11$ Hz). ^{19}F NMR (470 MHz, C_7D_8 , 228 K): δ -130.5 (d, *o-F* $[CH_3B(C_6F_5)_3]^-$, 6F, $^3J_{FF} = 20.7$ Hz), -156.2 (t, *p-F* $[CH_3B(C_6F_5)_3]^-$, 3F, $^3J_{FF} = 20$ Hz), -161.3 (t, *m-F* $[CH_3B(C_6F_5)_3]^-$, 6F, $^3J_{FF} = 18.3$ Hz); δ -126.1 (d, *o-F* $B(C_6F_5)_3$, 6F, $^3J_{FF} = 21.6$ Hz), -137.9 (br, *p-F* $B(C_6F_5)_3$, 3F), -157.1 (t, *m-F* $B(C_6F_5)_3$, 6F, $^3J_{FF} = 18.1$ Hz).

Decomposition of **1** via β -methyl elimination.

Solutions of **1** as prepared above were stable at temperatures below -25 °C. Above this temperature, decomposition via β -methyl elimination occurred producing $[(\eta^5-C_5H_5)(\eta^5-C_5Me_5)Zr(CH_3)]^+[CH_3B(C_6F_5)_3]^-$ (**4**) and isobutene. This reaction was monitored by variable-temperature NMR spectroscopy. Probe temperatures were calculated using a pure methanol standard. 1H NMR (500 MHz, C_7D_8 , 248 K): **1**: δ 5.69 (s, C_5H_5 , 5H), 1.78 (d, $CH_2C(CH_3)_3$, 1H, $J = 11$ Hz), 1.27 (s, $C_5(CH_3)_5$, 15H), 0.92 (s, $CH_2C(CH_3)_3$, 9H), -0.085 (br, $CH_2C(CH_3)_3$ and $[CH_3B(C_6F_5)_3]^-$, 4H); **4**: δ 5.32 (s, C_5H_5 , 5H), 1.23 (s, $C_5(CH_3)_5$, 15H), 0.25 (s, CH_3 , 3H), -0.19 (br, $[CH_3B(C_6F_5)_3]^-$, 3H); isobutene: δ 4.77 (m, $CH_2C(CH_3)_2$, 2H), 1.61 (m, $CH_2C(CH_3)_2$, 6H). ^{19}F NMR (470 MHz, C_7D_8 , 248 K): **1**: δ -133.5 (br, *o-F* $[CH_3B(C_6F_5)_3]^-$, 6F), -159.4 (br, *p-F* $[CH_3B(C_6F_5)_3]^-$, 3F), -164.5 (br, *m-F* $[CH_3B(C_6F_5)_3]^-$, 6F); **4**: δ -133.8 (d, *o-F* $[CH_3B(C_6F_5)_3]^-$, 6F, $^3J_{FF} = 21.6$ Hz), -159.2 (t, *p-F* $[CH_3B(C_6F_5)_3]^-$, 3F, $^3J_{FF} = 20.4$ Hz), -164.4 (t, *m-F* $[CH_3B(C_6F_5)_3]^-$, 6F). 1H NMR (500 MHz, C_7D_8 , 260 K): **1**: δ 5.71 (s, C_5H_5 , 5H), 1.77 (br, $CH_2C(CH_3)_3$, 1H), 1.29 (s, $C_5(CH_3)_5$, 15H), 0.91 (s, $CH_2C(CH_3)_3$, 9H), -0.074 (br, $CH_2C(CH_3)_3$ and $[CH_3B(C_6F_5)_3]^-$,

4H); **4**: δ 5.35 (s, C_5H_5 , 5H), 1.25 (s, $C_5(CH_3)_5$, 15H), 0.25 (s, CH_3 , 3H), -0.18 (br, $[CH_3B(C_6F_5)_3]^-$, 3H); isobutene: δ 4.76 (m, $CH_2C(CH_3)_2$, 2H), 1.61 (m, $CH_2C(CH_3)_2$, 6H). ^{19}F NMR (470 MHz, C_7D_8 , 260 K): **1**: δ -133.4 (br, *o-F* $[CH_3B(C_6F_5)_3]^-$, 6F), -159.5 (br, *p-F* $[CH_3B(C_6F_5)_3]^-$, 3F), -164.6 (br, *m-F* $[CH_3B(C_6F_5)_3]^-$, 6F); **4**: δ -133.8 (d, *o-F* $[CH_3B(C_6F_5)_3]^-$, 6F, $^3J_{FF} = 21.6$ Hz), -159.3 (t, *p-F* $[CH_3B(C_6F_5)_3]^-$, 3F, $^3J_{FF} = 20.7$ Hz), -164.4 (t, *m-F* $[CH_3B(C_6F_5)_3]^-$, 6F). 1H NMR (500 MHz, C_7D_8 , 271 K): **1**: δ 5.72 (s, C_5H_5 , 5H), 1.78 (br, $CH_2C(CH_3)_3$, 1H), 1.31 (s, $C_5(CH_3)_5$, 15H), 0.91 (s, $CH_2C(CH_3)_3$, 9H), -0.043 (br, $CH_2C(CH_3)_3$ and $[CH_3B(C_6F_5)_3]^-$, 4H); **4**: δ 5.38 (s, C_5H_5 , 5H), 1.27 (s, $C_5(CH_3)_5$, 15H), 0.25 (s, CH_3 , 3H), -0.17 (br, $[CH_3B(C_6F_5)_3]^-$, 3H); isobutene: δ 4.74 (m, $CH_2C(CH_3)_2$, 2H), 1.61 (m, $CH_2C(CH_3)_2$, 6H). ^{19}F NMR (470 MHz, C_7D_8 , 271 K): **1**: δ -133.4 (br, *o-F* $[CH_3B(C_6F_5)_3]^-$, 6F), -159.7 (br, *p-F* $[CH_3B(C_6F_5)_3]^-$, 3F), -164.7 (br, *m-F* $[CH_3B(C_6F_5)_3]^-$, 6F); **4**: δ -133.8 (d, *o-F* $[CH_3B(C_6F_5)_3]^-$, 6F, $^3J_{FF} = 21.6$ Hz), -159.4 (t, *p-F* $[CH_3B(C_6F_5)_3]^-$, 3F, $^3J_{FF} = 20.7$ Hz), -164.5 (t, *m-F* $[CH_3B(C_6F_5)_3]^-$, 6F, $^3J_{FF} = 19.0$ Hz). 1H NMR (500 MHz, C_7D_8 , 282 K): **1**: δ 5.74 (s, C_5H_5 , 5H), 1.33 (s, $C_5(CH_3)_5$, 15H), 0.91 (s, $CH_2C(CH_3)_3$, 9H), -0.043 (br, $CH_2C(CH_3)_3$ and $[CH_3B(C_6F_5)_3]^-$, 4H), not located at this temperature: ($CH_2C(CH_3)_3$, 2H) and ($[CH_3B(C_6F_5)_3]^-$, 3H); **4**: δ 5.40 (s, C_5H_5 , 5H), 1.29 (s, $C_5(CH_3)_5$, 15H), 0.25 (s, CH_3 , 3H), -0.16 (br, $[CH_3B(C_6F_5)_3]^-$, 3H); isobutene: δ 4.73 (m, $CH_2C(CH_3)_2$, 2H), 1.60 (m, $CH_2C(CH_3)_2$, 6H). ^{19}F NMR (470 MHz, C_7D_8 , 282 K): **1**: δ -133.3 (br, *o-F* $[CH_3B(C_6F_5)_3]^-$, 6F), -159.9 (br, *p-F* $[CH_3B(C_6F_5)_3]^-$, 3F), -165.0 (br, *m-F* $[CH_3B(C_6F_5)_3]^-$, 6F); **4**: δ -133.8 (d, *o-F* $[CH_3B(C_6F_5)_3]^-$, 6F, $^3J_{FF} = 21.6$ Hz), -159.6 (t, *p-F* $[CH_3B(C_6F_5)_3]^-$, 3F, $^3J_{FF} = 20.4$ Hz), -164.6 (t, *m-F* $[CH_3B(C_6F_5)_3]^-$, 6F, $^3J_{FF} = 19.3$ Hz). The reaction products were characterized as follows: 1H NMR (500 MHz, C_7D_8 , 216 K): **4**: δ 5.24 (s, C_5H_5 , 5H), 1.19 (s, $C_5(CH_3)_5$, 15H), 0.26 (s, CH_3 , 3H), -0.22 (br,

[CH₃B(C₆F₅)₃]⁻, 3H); isobutene: δ 4.81 (m, CH₂C(CH₃)₂, 2H), 1.62 (m, CH₂C(CH₃)₂, 6H).
¹⁹F NMR (470 MHz, C₇D₈, 216 K): **4**: δ -133.6 (d, *o*-F [CH₃B(C₆F₅)₃]⁻, 6F, ³J_{FF} = 21.2 Hz), -158.6 (t, *p*-F [CH₃B(C₆F₅)₃]⁻, 3F, ³J_{FF} = 20.4 Hz), -163.8 (t, *m*-F [CH₃B(C₆F₅)₃]⁻, 6F, ³J_{FF} = 18.8 Hz). ¹H NMR (500 MHz, C₇D₈): **4**: δ 5.45 (s, C₅H₅, 5H), 1.33 (s, C₅(CH₃)₅, 15H), 0.26 (s, CH₃, 3H), -0.14 (br, [CH₃B(C₆F₅)₃]⁻, 3H); isobutene: δ 4.72 (m, CH₂C(CH₃)₂, 2H), 1.60 (m, CH₂C(CH₃)₂, 6H). ¹⁹F NMR (470 MHz, C₇D₈): **4**: δ -133.8 (d, *o*-F [CH₃B(C₆F₅)₃]⁻, 6F, ³J_{FF} = 18.8 Hz), -159.9 (t, *p*-F [CH₃B(C₆F₅)₃]⁻, 3F, ³J_{FF} = 20.2 Hz), -164.9 (br, *m*-F [CH₃B(C₆F₅)₃]⁻, 6F).

Measurement of kinetics for β-methyl elimination in **1**.

A solution of **1** (approximately 12 mM) in toluene-*d*₈ was prepared in a 5mm thin-walled NMR tube with a J. Young valve as described above. The sample was evacuated on the vacuum line at -196 °C, then was thawed at -78 °C in a dry ice-acetone bath. Careful mixing of the sample - without warming the contents - generated a bright yellow solution. The NMR probe was pre-equilibrated at 10 °C. The probe temperature was calibrated with a methanol thermometer before and after each kinetic experiment and was maintained at ± 0.2 °C throughout data acquisition. The sample was removed from the cooling bath, positioned in the spinner, and *immediately* inserted into the NMR spectrometer. Following equilibration (5 to 10 minutes) to the preset probe temperature, disappearance of **1** (and appearance of **4** and isobutene) was monitored by ¹H NMR spectroscopy. Spectra were recorded at regular intervals until the reaction was > 88% complete. The peak height of the (η⁵-C₅H₅) resonance of **1** was obtained as a function of time. The rate constant was calculated by curve fitting to the expression $I_t = I_f + (I_0 - I_f) \times$

$\exp(-k_{\beta\text{-Me}}t)$, where I_t is the peak height. The value reported is the average of four kinetic measurements.

Measurement of propagation kinetics for alkene polymerization.

Sample preparation for ethene, propene, 1-butene, and 1-pentene substrates

A solution of **1** (0.002-0.013 mmol, 2-17 mM, 1 equiv) in toluene- d_8 was prepared in a 5mm thin-walled NMR tube with a J. Young valve as described above. The sample was evacuated on the vacuum line at $-196\text{ }^\circ\text{C}$, then was thawed at $-78\text{ }^\circ\text{C}$ in a dry ice-acetone bath. Careful mixing of the sample - without warming the contents - generated a bright yellow solution. The ^1H and ^{19}F NMR spectra of the sample were obtained at the experimental temperature. On the vacuum line the sample was frozen, degassed, and a measured gas volume of the alkene (0.23-0.52 mmol, 0.3-0.6 M, 20-250 equiv) was condensed into the tube at $-196\text{ }^\circ\text{C}$.⁴⁰

Sample preparation for 1-hexene, 1-undecene, and 4-methyl-1-pentene substrates

A 5mm thin-walled NMR tube with a J. Young valve was charged with solutions of $(\eta^5\text{-C}_5\text{H}_5)(\eta^5\text{-C}_5\text{Me}_5)\text{Zr}(\text{CH}_2\text{CMe}_3)(\text{CH}_3)$ (0.0115 mmol, 1 equiv) and $\text{B}(\text{C}_6\text{F}_5)_3$ (0.013 mmol, 1.15 equiv) as described above. A predetermined amount of alkene (0.48-0.79 mmol, 0.6-1.0 M, 40-60 equiv) was then added to frozen sample via gas-tight microsyringe. The NMR tube was sealed with a Teflon needle valve. The chilled sample holder was removed from the glovebox, and the NMR tube was *immediately* transferred to a $-196\text{ }^\circ\text{C}$ bath. The frozen sample was evacuated on the vacuum line.

General procedure for all alkene substrates

The NMR probe was pre-equilibrated at the experimental temperature. The probe temperature was calibrated with a methanol thermometer before and after each kinetic experiment and was maintained at ± 0.2 °C throughout data acquisition. The NMR samples were mixed using the following procedures.⁴¹ (1) The frozen sample was removed from the -196 °C bath, positioned in the spinner, and *immediately* inserted into the NMR spectrometer. After thawing at the preset temperature of the probe, the sample was ejected, *quickly* mixed, and reinserted into the spectrometer without substantial warming. Alternatively, (2) the frozen sample was removed from the -196 °C bath, thawed and *rapidly* mixed at -78 °C in a dry ice-acetone bath, and positioned in the spinner. The sample was *immediately* frozen at -196 °C, was inserted into the NMR spectrometer, and was thawed at the preset temperature of the probe. Following equilibration (5 to 10 minutes) to the probe temperature, disappearance of alkene was monitored by ^1H NMR spectroscopy. Spectra were recorded at regular intervals until the reaction was $> 88\%$ complete. The integral of alkene $\text{CH}_2\text{CH}(\text{R})$ resonance (relative to Ph_2CH_2 or $\text{C}_6\text{D}_5\text{CD}_2\text{H}$ as an internal standard) was calculated as a function of time. The observed rate constants, k_{obs} , were obtained from the slope of plots of $\ln[\text{alkene}]_t$ versus time. The volume of the reaction mixture was determined as V (mL) = $0.01384H - 0.006754$, where H is the solution height in millimeters. For propene, the propagation rate constant, k_p , at 216 K was obtained from the slope of a plot of k_{obs} versus $[\text{Zr}]$. For all other experiments, k_p was calculated from the expression $k_p = k_{\text{obs}} \div [\text{Zr}]$, where $[\text{Zr}]$ was determined by integration using an internal standard. The values reported are the average of at least three kinetic measurements.

Characterization of species observed upon addition of alkene to solutions of **1** (*note*: some resonances could not be reported with certainty due to overlap with alkene or poly(alkene) resonances):

propene: ^1H NMR (500 MHz, C_7D_8 , 193 K): **2**: δ 5.58, 5.56 (br, C_5H_5 , 5H), 1.24, 1.17 (br, $\text{C}_5(\text{CH}_3)_5$, 15H), -0.10, -0.17 (br, $[\text{CH}_3\text{B}(\text{C}_6\text{F}_5)_3]^-$, 3H); *propene*: δ 5.75 (m, $\text{CH}_2\text{CH}(\text{CH}_3)$, 1H), 5.06 (m, $\text{CH}_2\text{CH}(\text{CH}_3)$, 2H), 1.58 (m, $\text{CH}_2\text{CH}(\text{CH}_3)$, 3H); *poly(propene)*: 1.84 (br, *CH*, 1H), 1.36 (br, CH_2 , 2H), 0.99 (br, CH_3 , 3H). ^1H NMR (500 MHz, C_7D_8 , 203 K): **2**: δ 5.58, 5.56 (br, C_5H_5 , 5H), 1.24, 1.17 (br, $\text{C}_5(\text{CH}_3)_5$, 15H), -0.09, -0.17 (br, $[\text{CH}_3\text{B}(\text{C}_6\text{F}_5)_3]^-$, 3H); *propene*: δ 5.74 (m, $\text{CH}_2\text{CH}(\text{CH}_3)$, 1H), 5.05 (m, $\text{CH}_2\text{CH}(\text{CH}_3)$, 2H), 1.58 (m, $\text{CH}_2\text{CH}(\text{CH}_3)$, 3H); *poly(propene)*: 1.83 (br, *CH*, 1H), 1.36 (br, CH_2 , 2H), 0.99 (br, CH_3 , 3H). ^1H NMR (500 MHz, C_7D_8 , 216 K): **2**: δ 5.60, 5.56 (br, C_5H_5 , 5H), 1.26, 1.20 (br, $\text{C}_5(\text{CH}_3)_5$, 15H), -0.10, -0.18 (br, $[\text{CH}_3\text{B}(\text{C}_6\text{F}_5)_3]^-$, 3H); *propene*: δ 5.74 (m, $\text{CH}_2\text{CH}(\text{CH}_3)$, 1H), 5.05 (m, $\text{CH}_2\text{CH}(\text{CH}_3)$, 2H), 1.58 (m, $\text{CH}_2\text{CH}(\text{CH}_3)$, 3H); *poly(propene)*: 1.80 (br, *CH*, 1H), 1.31, 1.06 (br, CH_2 , 2H), 0.98 (br, CH_3 , 3H). ^1H NMR (500 MHz, C_7D_8 , 228 K): **2**: δ 5.61, 5.56 (br, C_5H_5 , 5H), 1.26, 1.21 (br, $\text{C}_5(\text{CH}_3)_5$, 15H), -0.10, -0.17 (br, $[\text{CH}_3\text{B}(\text{C}_6\text{F}_5)_3]^-$, 3H); *propene*: δ 5.73 (m, $\text{CH}_2\text{CH}(\text{CH}_3)$, 1H), 5.02 (m, $\text{CH}_2\text{CH}(\text{CH}_3)$, 2H), 1.58 (m, $\text{CH}_2\text{CH}(\text{CH}_3)$, 3H); *poly(propene)*: 1.80 (br, *CH*, 1H), 1.32, 1.08 (br, CH_2 , 2H), 0.97 (br, CH_3 , 3H).

1-butene: ^1H NMR (500 MHz, C_7D_8 , 228 K): $[\text{Zr}]$ -polymeryl: δ 5.66, 5.60 (br, C_5H_5 , 5H), -0.07, -0.17 (br, $[\text{CH}_3\text{B}(\text{C}_6\text{F}_5)_3]^-$, 3H); *1-butene*: δ 5.81 (m, $\text{CH}_2\text{CH}(\text{CH}_2\text{CH}_3)$, 1H), 5.01 (m, $\text{CH}_2\text{CH}(\text{CH}_2\text{CH}_3)$, 2H), 1.94 (m, $\text{CH}_2\text{CH}(\text{CH}_2\text{CH}_3)$, 2H), 0.91 (t, $\text{CH}_2\text{CH}(\text{CH}_2\text{CH}_3)$, 3H); *poly(1-butene)*: 1.61, 1.48, 1.41 (br, *CH* and CH_2 , 3H), 1.28 (br, CH_2 , 2H), 1.03 (br, CH_3 , 3H).

1-pentene: ^1H NMR (500 MHz, C_7D_8 , 228 K): [Zr]-polymeryl: δ 5.70, 5.66 (br, C_5H_5 , 5H), -0.10, -0.14 (br, $[\text{CH}_3\text{B}(\text{C}_6\text{F}_5)_3]^-$, 3H); 1-pentene: δ 5.73 (m, $\text{CH}_2\text{CH}(\text{CH}_2\text{CH}_2\text{CH}_3)$, 1H), 5.03 (m, $\text{CH}_2\text{CH}(\text{CH}_2\text{CH}_2\text{CH}_3)$, 2H), 1.91 (m, $\text{CH}_2\text{CH}(\text{CH}_2\text{CH}_2\text{CH}_3)$, 2H), 1.30 (m, $\text{CH}_2\text{CH}(\text{CH}_2\text{CH}_2\text{CH}_3)$, 2H), 0.85 (t, $\text{CH}_2\text{CH}(\text{CH}_2\text{CH}_2\text{CH}_3)$, 3H); poly(1-pentene): 1.69 (br, CH , 1H), 1.49, 1.36 (br, CH_2 , 6H), 1.08 (br, CH_3 , 3H).

1-hexene: ^1H NMR (500 MHz, C_7D_8 , 228 K): [Zr]-polymeryl: δ 5.70, 5.67 (br, C_5H_5 , 5H), -0.09, -0.17 (br, $[\text{CH}_3\text{B}(\text{C}_6\text{F}_5)_3]^-$, 3H); 1-hexene: δ 5.75 (m, $\text{CH}_2\text{CH}(\text{H}_2\text{CH}_2\text{CH}_2\text{CH}_3)$, 1H), 5.03 (m, $\text{CH}_2\text{CH}(\text{CH}_2\text{CH}_2\text{CH}_2\text{CH}_3)$, 2H), 1.94 (m, $\text{CH}_2\text{CH}(\text{CH}_2\text{CH}_2\text{CH}_2\text{CH}_3)$, 2H), 1.23 (m, $\text{CH}_2\text{CH}(\text{CH}_2\text{CH}_2\text{CH}_2\text{CH}_3)$, 4H), 0.87 (t, $\text{CH}_2\text{CH}(\text{CH}_2\text{CH}_2\text{CH}_2\text{CH}_3)$, 3H); poly(1-hexene): 1.74 (br, CH , 1H), 1.48 (br, CH_2 , 8H), 1.06 (br, CH_3 , 3H).

1-undecene: ^1H NMR (500 MHz, C_7D_8 , 228 K): [Zr]-polymeryl: δ 5.72, 5.71 (br, C_5H_5 , 5H), -0.08, -0.12 (br, $[\text{CH}_3\text{B}(\text{C}_6\text{F}_5)_3]^-$, 3H); 1-undecene: δ 5.80 (m, $\text{CH}_2\text{CH}(\text{H}_2(\text{CH}_2)_7\text{CH}_3)$, 1H), 5.06 (m, $\text{CH}_2\text{CH}(\text{CH}_2(\text{CH}_2)_7\text{CH}_3)$, 2H), 1.99 (m, $\text{CH}_2\text{CH}(\text{H}_2(\text{CH}_2)_7\text{CH}_3)$, 2H), 1.31, 1.22 (br, $\text{CH}_2\text{CH}(\text{CH}_2(\text{CH}_2)_7\text{CH}_3)$, 14H), 0.96 (t, $\text{CH}_2\text{CH}(\text{H}_2(\text{CH}_2)_7\text{CH}_3)$, 3H); poly(1-undecene): 1.79 (br, CH , 1H), 1.39 (br, CH_2 , 18H), 1.02 (br, CH_3 , 3H).

4-methyl-1-pentene: ^1H NMR (500 MHz, C_7D_8 , 228 K): [Zr]-polymeryl: δ -0.14 (br, $[\text{CH}_3\text{B}(\text{C}_6\text{F}_5)_3]^-$, 3H); 4-methyl-1-pentene: δ 5.70 (m, $\text{CH}_2\text{CH}(\text{CH}_2\text{CH}(\text{CH}_3)_2)$, 1H), 5.04, 5.01 (br, $\text{CH}_2\text{CH}(\text{CH}_2\text{CH}(\text{CH}_3)_2)$, 2H), 1.83 (t, $\text{CH}_2\text{CH}(\text{CH}_2\text{CH}(\text{CH}_3)_2)$, 2H), 1.49 (m, $\text{CH}_2\text{CH}(\text{CH}_2\text{CH}(\text{CH}_3)_2)$, 1H), 0.86 (d, $\text{CH}_2\text{CH}(\text{CH}_2\text{CH}(\text{CH}_3)_2)$, 6H); poly(4-methyl-1-pentene): 1.85, 1.66 (br, CH , 2H), 1.35 (br, CH_2 , 4H), 1.07 (br, CH_3 , 6H).

Synthesis of $[(\text{CH}_3(\text{CH}_2)_5\text{CH}_2)_4\text{N}]^+[\text{CH}_3\text{B}(\text{C}_6\text{F}_5)_3]^-$ (3**). ($[(\text{Hp})_4\text{N}]^+[\text{CH}_3\text{B}(\text{C}_6\text{F}_5)_3]^-$).**

In the glovebox a 100 mL roundbottom flask was charged with $\text{B}(\text{C}_6\text{F}_5)_3$ (0.510 g, 0.996 mmol) dissolved in diethyl ether (30 mL) and cooled to $-35\text{ }^\circ\text{C}$. A 20 mL vial was charged with dry MeLi (0.024 g, 1.11 mmol), diethyl ether was added (10 mL), and the slurry was cooled to $-35\text{ }^\circ\text{C}$. The cooled MeLi slurry was added dropwise to the cooled stirring solution of $\text{B}(\text{C}_6\text{F}_5)_3$. The reaction was diluted with additional diethyl ether to bring the total volume to 40 mL and sealed with a septum. The reaction stirred for 12 h over which time it became homogeneous. The $[(\text{CH}_3(\text{CH}_2)_5\text{CH}_2)_4\text{N}]^+[\text{Br}]^-$ (0.540 g, 1.11 mmol) was added to the reaction as a solid. The flask was sealed with a ground-glass stopper and allowed to stir for > 72 h. The solvent was removed in vacuo yielding an opaque oil. This oil was dissolved in toluene and the white precipitate was removed by filtration through celite. The product was isolated as a colorless oil after removal of solvent in vacuo. For further purification from bromide salts the oil was extracted into minimal toluene, cooled to $-35\text{ }^\circ\text{C}$, then filtered cold through celite using a pipet filter. This procedure was repeated two times. The solution was then transferred to a tared flask (using additional diethyl ether to dissolve the product) and sealed with a 180 ° needle valve. On the vacuum line, the solvent was removed and the product oil was dried in vacuo at $35\text{ }^\circ\text{C}$ for 3 h. Yield: 0.519 g (56%). ^1H NMR (300 MHz, C_6D_6): δ 2.46 (br, $[(\text{CH}_3\text{CH}_2(\text{CH}_2)_3\text{CH}_2\text{CH}_2)_4\text{N}]^+$, 8H), 1.31 (br m, $[(\text{CH}_3\text{CH}_2(\text{CH}_2)_3\text{CH}_2\text{CH}_2)_4\text{N}]^+$, 8H), 1.21 (br, $[(\text{CH}_3\text{CH}_2(\text{CH}_2)_3\text{CH}_2\text{CH}_2)_4\text{N}]^+$, 24H), 1.07 (br, $[(\text{CH}_3\text{CH}_2(\text{CH}_2)_3\text{CH}_2\text{CH}_2)_4\text{N}]^+$ and $[\text{CH}_3\text{B}(\text{C}_6\text{F}_5)_3]^-$, 11H), 0.97 (t, $[(\text{CH}_3\text{CH}_2(\text{CH}_2)_3\text{CH}_2\text{CH}_2)_4\text{N}]^+$, 12H, $J = 7.0$ Hz). ^{19}F NMR (282 MHz, C_6D_6): δ -134.5 (d, *o*-F $[\text{CH}_3\text{B}(\text{C}_6\text{F}_5)_3]^-$, 6F, $^3J_{\text{FF}} = 18.9$ Hz), -166.8 (t, *p*-F $[\text{CH}_3\text{B}(\text{C}_6\text{F}_5)_3]^-$, 3F, $^3J_{\text{FF}} = 20.7$ Hz), -169.3 (t, *m*-F $[\text{CH}_3\text{B}(\text{C}_6\text{F}_5)_3]^-$, 6F, $^3J_{\text{FF}} = 22.0$ Hz). ^1H

NMR (500 MHz, C₇D₈): δ 2.56 (br, [(CH₃CH₂(CH₂)₃CH₂CH₂)₄N]⁺, 8H), 1.32 (m, [(CH₃CH₂(CH₂)₃CH₂CH₂)₄N]⁺, 8H, J = 7.0 Hz), 1.23 (br, [(CH₃CH₂(CH₂)₃CH₂CH₂)₄N]⁺, 24H), 1.11 (br, [(CH₃CH₂(CH₂)₃CH₂CH₂)₄N]⁺ and [CH₃B(C₆F₅)₃]⁻, 11H), 0.96 (t, [(CH₃CH₂(CH₂)₃CH₂CH₂)₄N]⁺, 12H, J = 7.2 Hz). ¹⁹F NMR (470 MHz, C₇D₈): δ -129.5 (d, *o*-F [CH₃B(C₆F₅)₃]⁻, 6F, ³J_{FF} = 21.6 Hz), -161.7 (t, *p*-F [CH₃B(C₆F₅)₃]⁻, 3F, ³J_{FF} = 20.4 Hz), -164.3 (t, *m*-F [CH₃B(C₆F₅)₃]⁻, 6F, ³J_{FF} = 19.3 Hz). ¹³C{¹H} NMR (125 MHz, C₆D₆-C₇D₈): δ 149.6 (d, [CH₃B(C₆F₅)₃]⁻, 6C, ¹J_{CF} = 233 Hz), 138.6 (d, [CH₃B(C₆F₅)₃]⁻, 3C, ¹J_{CF} = 235 Hz), 137.5 (d, [CH₃B(C₆F₅)₃]⁻, 6C, ¹J_{CF} = 237 Hz), 59.1 ([[(CH₃(CH₂)₅CH₂)₄N]⁺), 32.1, 29.3, 26.6, 23.2, 22.1 ([[(CH₃(CH₂)₅CH₂)₄N]⁺), 14.5 ([[(CH₃(CH₂)₅CH₂)₄N]⁺), not located: *i*-C [CH₃B(C₆F₅)₃]⁻ and [CH₃B(C₆F₅)₃]⁻.

Synthesis of **1** in the presence of **3**.

In an inert atmosphere glovebox a J. Young NMR tube was charged with toluene-*d*₈ stock solutions of: (η⁵-C₅H₅)(η⁵-C₅Me₅)Zr(CH₂CMe₃)(CH₃) (0.006 mmol, 1 equiv), B(C₆F₅)₃ (0.007 mmol, 1.15 equiv), and Ph₂CH₂ (0.030 mmol, 5 equiv, internal standard) and additional toluene-*d*₈ using the glovebox cold-well procedure described above. The sample was charged with a predetermined amount of a stock solution of **3** in toluene-*d*₈ (0.005 mmol, 0.95 equiv). The J. Young NMR tube containing the frozen sample was sealed with a Teflon needle valve. The chilled sample holder was removed from the glovebox, and the NMR tube was *immediately* transferred to a -196 °C bath. The frozen sample was evacuated on the vacuum line. The sample was thawed at -78 °C in a dry ice-acetone bath and carefully mixed without warming the contents. Upon mixing a bright yellow solution was observed. The sample was then characterized using NMR

spectroscopy. ^1H NMR (500 MHz, C_7D_8 , 228 K): **1**: δ 5.66 (s, C_5H_5 , 5H), 1.78 (d, $\text{CH}_2\text{C}(\text{CH}_3)_3$, 1H, $J = 11.5$ Hz), 1.22 (s, $\text{C}_5(\text{CH}_3)_5$, 15H), 0.92 (s, $\text{CH}_2\text{C}(\text{CH}_3)_3$, 9H), -0.10 (br d, $\text{CH}_2\text{C}(\text{CH}_3)_3$ and $[\text{CH}_3\text{B}(\text{C}_6\text{F}_5)_3]^-$, 4H, $J = 11.5$ Hz); **3**: δ 2.21 (br, $[(\text{CH}_3\text{CH}_2(\text{CH}_2)_3\text{CH}_2\text{CH}_2)_4\text{N}]^+$, 8H), 1.51 (br, $[(\text{CH}_3\text{CH}_2(\text{CH}_2)_3\text{CH}_2\text{CH}_2)_4\text{N}]^+$, 8H), 1.34 (br, $[(\text{CH}_3\text{CH}_2(\text{CH}_2)_3\text{CH}_2\text{CH}_2)_4\text{N}]^+$, 24H), 1.09 (br, $[(\text{CH}_3\text{CH}_2(\text{CH}_2)_3\text{CH}_2\text{CH}_2)_4\text{N}]^+$, 8H), and, 1.02 (t, $[(\text{CH}_3\text{CH}_2(\text{CH}_2)_3\text{CH}_2\text{CH}_2)_4\text{N}]^+$, 12H, $J = 7.5$ Hz), not located ($[\text{CH}_3\text{B}(\text{C}_6\text{F}_5)_3]^-$, 3H); Ph_2CH_2 : δ 7.14 to 6.98 (aryl resonances, Ph_2CH_2), 3.67 (s, Ph_2CH_2 , 2H). ^{19}F NMR (470 MHz, C_7D_8 , 228 K): **1**: δ -130.7 (d, *o*-F $[\text{CH}_3\text{B}(\text{C}_6\text{F}_5)_3]^-$, 6F, $^3J_{\text{FF}} = 17.9$ Hz), -156.3 (br, *p*-F $[\text{CH}_3\text{B}(\text{C}_6\text{F}_5)_3]^-$, 3F), -161.5 (br, *m*-F $[\text{CH}_3\text{B}(\text{C}_6\text{F}_5)_3]^-$, 6F); **3**: δ -129.7 (br, *o*-F $[\text{CH}_3\text{B}(\text{C}_6\text{F}_5)_3]^-$, 6F), -161.5 (br, *p*-F $[\text{CH}_3\text{B}(\text{C}_6\text{F}_5)_3]^-$, 3F), -164.1 (br, *m*-F $[\text{CH}_3\text{B}(\text{C}_6\text{F}_5)_3]^-$, 6F); $\text{B}(\text{C}_6\text{F}_5)_3$: δ -126.2 (d, *o*-F $\text{B}(\text{C}_6\text{F}_5)_3$, 6F, $^3J_{\text{FF}} = 21.6$ Hz), -138.1 (br, *p*-F $\text{B}(\text{C}_6\text{F}_5)_3$, 3F), -157.3 (br, *m*-F $\text{B}(\text{C}_6\text{F}_5)_3$, 6F).

Measurement of propagation kinetics for propene polymerization with added **3**.

A sample of **1** (0.004-0.009 mmol, 5-11 mM, 1 equiv) and **3** (0.001-0.007 mmol, 1-9 mM, 0.8-2 equiv) in toluene- d_8 was prepared in a 5mm thin-walled NMR tube with a J. Young valve as described above. The sample was evacuated on the vacuum line at -196 $^\circ\text{C}$, then was thawed at -78 $^\circ\text{C}$ in a dry ice-acetone bath. Careful mixing of the sample - without warming the contents - generated a bright yellow solution. The ^1H and ^{19}F NMR spectra of the sample were obtained at -45 $^\circ\text{C}$. On the vacuum line the sample was frozen, degassed, and a measured gas volume of propene (0.33-0.36 mmol, 0.42-0.46 M, 39-91 equiv) was condensed into the tube at -196 $^\circ\text{C}$. The NMR probe was pre-equilibrated at -45 $^\circ\text{C}$. The probe temperature was calibrated with a methanol

thermometer before and after each kinetic experiment and was maintained at ± 0.2 °C throughout data acquisition. The NMR samples were mixed using the following procedure. The frozen sample was removed from the -196 °C bath, thawed and *rapidly* mixed at -78 °C in a dry ice-acetone bath, and positioned in the spinner. The sample was *immediately* frozen at -196 °C, was inserted into the NMR spectrometer, and was thawed at the preset temperature of the probe. Following equilibration (5 to 10 minutes) to the probe temperature, disappearance of propene was monitored by ^1H NMR spectroscopy. Spectra were recorded at regular intervals until the reaction was $> 88\%$ complete. The integral of propene $\text{CH}_2\text{CH}(\text{CH}_3)$ resonance (relative to Ph_2CH_2 as an internal standard) was calculated as a function of time. The observed rate constants, k_{obs} , were obtained from the slope of plots of $\ln[\text{propene}]_t$ versus time. The volume of the reaction mixture was determined as V (mL) = $0.01384H - 0.006754$, where H is the solution height in millimeters. The propagation rate constant, k_p was calculated from the expression $k_p = k_{\text{obs}} \div [\text{Zr}]$, where $[\text{Zr}]$ was determined by integration using an internal standard.

Characterization of species observed upon addition of propene to solutions of **1** with added **3** (*note*: some resonances could not be reported with certainty due to overlap with propene or poly(propene) resonances): ^1H NMR (500 MHz, C_7D_8 , 228 K): **2**: δ 5.62, 5.58 (br, C_5H_5 , 5H), 1.28, 1.22 (br, $\text{C}_5(\text{CH}_3)_5$, 15H), -0.10, -0.17 (br, $[\text{CH}_3\text{B}(\text{C}_6\text{F}_5)_3]^+$, 3H); **3**: δ 2.23 (br, $[(\text{CH}_3\text{CH}_2(\text{CH}_2)_3\text{CH}_2\text{CH}_2)_4\text{N}]^+$, 8H); propene: δ 5.73 (m, $\text{CH}_2\text{CH}(\text{CH}_3)$, 1H), 5.02 (m, $\text{CH}_2\text{CH}(\text{CH}_3)$, 2H), 1.57 (m, $\text{CH}_2\text{CH}(\text{CH}_3)$, 3H); poly(propene): 1.79 (br, CH, 1H), 1.34, 1.08 (br, CH_2 , 2H), 0.97 (br, CH_3 , 3H).

Synthesis of **1** in toluene-*d*₈-chlorobenzene-*d*₅ solvent.

Compound **1** was prepared in 1:1 (w/w) toluene-*d*₈-chlorobenzene-*d*₅ using: 80 μL stock solution (η⁵-C₅H₅)(η⁵-C₅Me₅)Zr(CH₂CMe₃)(CH₃) (3.4 mg, 0.009 mmol), 150 μL stock solution Ph₂CH₂ (3.9 mg, 0.02 mmol) as an internal standard, and 80 μL stock solution B(C₆F₅)₃ (5.1 mg, 0.01 mmol) in 1:1 (w/w) toluene-*d*₈-chlorobenzene-*d*₅ and an additional 460 μL of the solvent mixture according to the procedure described above. The J. Young NMR tube containing the frozen sample was sealed with a Teflon needle valve. The chilled sample holder was removed from the glovebox, and the NMR tube was *immediately* transferred to a -196 °C bath. The frozen sample was evacuated on the vacuum line. The sample was thawed at -60 °C in a dry ice-acetone (or a dry ice-chloroform) bath and carefully mixed without warming the contents. Upon mixing a bright yellow solution was observed. The sample was then characterized using NMR spectroscopy. ¹H NMR (500 MHz, C₇D₈-C₆D₅Cl, 213 K): δ 5.75 (s, C₅H₅, 5H), 1.83 (d, CH₂C(CH₃)₃, 1H, J = 10 Hz), 1.32 (s, C₅(CH₃)₅, 15H), 0.92 (s, CH₂C(CH₃)₃, 9H), -0.12 (br, CH₂C(CH₃)₃ and [CH₃B(C₆F₅)₃]⁻, 4H); δ 7.15 to 6.97 (aryl resonances, Ph₂CH₂), 3.67 (s, Ph₂CH₂, 2H). ¹⁹F NMR (470 MHz, C₇D₈-C₆D₅Cl, 213 K): δ -130.3 (d, *o*-F [CH₃B(C₆F₅)₃]⁻, 6F, ³J_{FF} = 15.5 Hz), -155.9 (br, *p*-F [CH₃B(C₆F₅)₃]⁻, 3F), -161.0 (br, *m*-F [CH₃B(C₆F₅)₃]⁻, 6F); δ -125.0 (d, *o*-F B(C₆F₅)₃, 6F, ³J_{FF} = 18.8 Hz), -138.2 (br, *p*-F B(C₆F₅)₃, 3F), -156.9 (br, *m*-F B(C₆F₅)₃, 6F). ¹H NMR (500 MHz, C₇D₈-C₆D₅Cl, 228 K): δ 5.76 (s, C₅H₅, 5H), 1.83 (br, CH₂C(CH₃)₃, 1H), 1.34 (s, C₅(CH₃)₅, 15H), 0.91 (s, CH₂C(CH₃)₃, 9H), -0.11 (br, CH₂C(CH₃)₃ and [CH₃B(C₆F₅)₃]⁻, 4H); δ 7.14 to 6.98 (aryl resonances, Ph₂CH₂), 3.69 (s, Ph₂CH₂, 2H). ¹⁹F NMR (470 MHz, C₇D₈-C₆D₅Cl, 228 K): δ -130.4 (br, *o*-F [CH₃B(C₆F₅)₃]⁻, 6F), -156.2 (br, *p*-F [CH₃B(C₆F₅)₃]⁻, 3F), -161.3 (br, *m*-F

$[\text{CH}_3\text{B}(\text{C}_6\text{F}_5)_3]^-$, 6F); δ -125.3 (d, *o*-F $\text{B}(\text{C}_6\text{F}_5)_3$, 6F, $^3J_{\text{FF}} = 19.3$ Hz), -138.5 (br, *p*-F $\text{B}(\text{C}_6\text{F}_5)_3$, 3F), -157.0 (br, *m*-F $\text{B}(\text{C}_6\text{F}_5)_3$, 6F).

Variable-temperature NMR experiments with 1 in toluene- d_8 -chlorobenzene- d_5 solvent.

A sample of **1** was prepared according to the above procedure. The NMR probe was cooled and the probe temperature calculated using a pure methanol standard. The sample was inserted into the pre-thermostatted probe and allowed to equilibrate for 10 minutes prior to data acquisition. ^1H NMR (500 MHz, C_7D_8 - $\text{C}_6\text{D}_5\text{Cl}$, 215 K): δ 5.75 (s, C_5H_5 , 5H), 1.83 (d, $\text{CH}_2\text{C}(\text{CH}_3)_3$, 1H, $J = 10.3$ Hz), 1.32 (s, $\text{C}_5(\text{CH}_3)_5$, 15H), 0.92 (s, $\text{CH}_2\text{C}(\text{CH}_3)_3$, 9H), -0.11 (br, $\text{CH}_2\text{C}(\text{CH}_3)_3$ and $[\text{CH}_3\text{B}(\text{C}_6\text{F}_5)_3]^-$, 4H). ^{19}F NMR (470 MHz, C_7D_8 - $\text{C}_6\text{D}_5\text{Cl}$, 215 K): δ -130.3 (d, *o*-F $[\text{CH}_3\text{B}(\text{C}_6\text{F}_5)_3]^-$, 6F, $^3J_{\text{FF}} = 15.5$ Hz), -155.9 (br, *p*-F $[\text{CH}_3\text{B}(\text{C}_6\text{F}_5)_3]^-$, 3F), -161.0 (br, *m*-F $[\text{CH}_3\text{B}(\text{C}_6\text{F}_5)_3]^-$, 6F); δ -125.0 (d, *o*-F $\text{B}(\text{C}_6\text{F}_5)_3$, 6F, $^3J_{\text{FF}} = 17.9$ Hz), -138.2 (br, *p*-F $\text{B}(\text{C}_6\text{F}_5)_3$, 3F), -156.8 (t, *m*-F $\text{B}(\text{C}_6\text{F}_5)_3$, 6F, $^3J_{\text{FF}} = 19.3$ Hz). ^1H NMR (500 MHz, C_7D_8 - $\text{C}_6\text{D}_5\text{Cl}$, 226 K): δ 5.76 (s, C_5H_5 , 5H), 1.83 (br, $\text{CH}_2\text{C}(\text{CH}_3)_3$, 1H), 1.33 (s, $\text{C}_5(\text{CH}_3)_5$, 15H), 0.91 (s, $\text{CH}_2\text{C}(\text{CH}_3)_3$, 9H), -0.12 (br, $\text{CH}_2\text{C}(\text{CH}_3)_3$ and $[\text{CH}_3\text{B}(\text{C}_6\text{F}_5)_3]^-$, 4H). ^{19}F NMR (470 MHz, C_7D_8 - $\text{C}_6\text{D}_5\text{Cl}$, 226 K): δ -130.3 (br, *o*-F $[\text{CH}_3\text{B}(\text{C}_6\text{F}_5)_3]^-$, 6F), -156.0 (br, *p*-F $[\text{CH}_3\text{B}(\text{C}_6\text{F}_5)_3]^-$, 3F), -161.1 (br, *m*-F $[\text{CH}_3\text{B}(\text{C}_6\text{F}_5)_3]^-$, 6F); δ -125.1 (d, *o*-F $\text{B}(\text{C}_6\text{F}_5)_3$, 6F, $^3J_{\text{FF}} = 19.3$ Hz), -138.3 (br, *p*-F $\text{B}(\text{C}_6\text{F}_5)_3$, 3F), -156.8 (t, *m*-F $\text{B}(\text{C}_6\text{F}_5)_3$, 6F, $^3J_{\text{FF}} = 19.7$ Hz). ^1H NMR (500 MHz, C_7D_8 - $\text{C}_6\text{D}_5\text{Cl}$, 238 K): δ 5.77 (s, C_5H_5 , 5H), 1.84 (br, $\text{CH}_2\text{C}(\text{CH}_3)_3$, 1H), 1.35 (s, $\text{C}_5(\text{CH}_3)_5$, 15H), 0.91 (s, $\text{CH}_2\text{C}(\text{CH}_3)_3$, 9H), -0.11 (br, $\text{CH}_2\text{C}(\text{CH}_3)_3$ and $[\text{CH}_3\text{B}(\text{C}_6\text{F}_5)_3]^-$, 4H). ^{19}F NMR (470 MHz, C_7D_8 - $\text{C}_6\text{D}_5\text{Cl}$, 238 K): δ -130.3 (br, *o*-F $[\text{CH}_3\text{B}(\text{C}_6\text{F}_5)_3]^-$, 6F), -156.2 (br, *p*-F $[\text{CH}_3\text{B}(\text{C}_6\text{F}_5)_3]^-$, 3F), -

161.2 (br, *m-F* [$\text{CH}_3\text{B}(\text{C}_6\text{F}_5)_3$] $^-$, 6F); δ -125.2 (d, *o-F* $\text{B}(\text{C}_6\text{F}_5)_3$, 6F, $^3J_{\text{FF}} = 19.7$ Hz), -138.5 (br, *p-F* $\text{B}(\text{C}_6\text{F}_5)_3$, 3F), -156.9 (t, *m-F* $\text{B}(\text{C}_6\text{F}_5)_3$, 6F, $^3J_{\text{FF}} = 19.3$ Hz).

Decomposition of 1 via β -methyl elimination in toluene- d_8 -chlorobenzene- d_5 solvent.

Solutions of **1** as prepared above were stable at temperatures below -25 °C. Above this temperature, decomposition via β -methyl elimination occurred producing $[(\eta^5\text{-C}_5\text{H}_5)(\eta^5\text{-C}_5\text{Me}_5)\text{Zr}(\text{CH}_3)]^+[\text{CH}_3\text{B}(\text{C}_6\text{F}_5)_3]^-$ (**4**) and isobutene. This reaction was monitored by variable-temperature NMR spectroscopy. Probe temperatures were calculated using a pure methanol standard. ^1H NMR (500 MHz, $\text{C}_7\text{D}_8\text{-C}_6\text{D}_5\text{Cl}$, 248 K): **1**: δ 5.78 (s, C_5H_5 , 5H), 1.83 (br, $\text{CH}_2\text{C}(\text{CH}_3)_3$, 1H), 1.37 (s, $\text{C}_5(\text{CH}_3)_5$, 15H), 0.90 (s, $\text{CH}_2\text{C}(\text{CH}_3)_3$, 9H), -0.02 (br, $\text{CH}_2\text{C}(\text{CH}_3)_3$ and $[\text{CH}_3\text{B}(\text{C}_6\text{F}_5)_3]^-$, 4H); **4**: δ 5.45 (s, C_5H_5 , 5H), 1.33 (s, $\text{C}_5(\text{CH}_3)_5$, 15H), 0.27 (s, CH_3 , 3H), -0.21 (br, $[\text{CH}_3\text{B}(\text{C}_6\text{F}_5)_3]^-$, 3H); isobutene: δ 4.71 (m, $\text{CH}_2\text{C}(\text{CH}_3)_2$, 2H), 1.59 (m, $\text{CH}_2\text{C}(\text{CH}_3)_2$, 6H). ^{19}F NMR (470 MHz, $\text{C}_7\text{D}_8\text{-C}_6\text{D}_5\text{Cl}$, 248 K): **1**: δ -130.2 (d, *o-F* $[\text{CH}_3\text{B}(\text{C}_6\text{F}_5)_3]^-$, 6F, $^3J_{\text{FF}} = 18.8$ Hz), -156.5 (br, *p-F* $[\text{CH}_3\text{B}(\text{C}_6\text{F}_5)_3]^-$, 3F), -161.4 (br, *m-F* $[\text{CH}_3\text{B}(\text{C}_6\text{F}_5)_3]^-$, 6F); **4**: δ -130.6 (d, *o-F* $[\text{CH}_3\text{B}(\text{C}_6\text{F}_5)_3]^-$, 6F, $^3J_{\text{FF}} = 22.1$ Hz), -156.1 (t, *p-F* $[\text{CH}_3\text{B}(\text{C}_6\text{F}_5)_3]^-$, 3F, $^3J_{\text{FF}} = 19.7$ Hz), -161.1 (t, *m-F* $[\text{CH}_3\text{B}(\text{C}_6\text{F}_5)_3]^-$, 6F, $^3J_{\text{FF}} = 20.7$ Hz). ^1H NMR (500 MHz, $\text{C}_7\text{D}_8\text{-C}_6\text{D}_5\text{Cl}$, 260 K): **1**: δ 5.79 (s, C_5H_5 , 5H), 1.39 (s, $\text{C}_5(\text{CH}_3)_5$, 15H), 0.90 (s, $\text{CH}_2\text{C}(\text{CH}_3)_3$, 9H), -0.004 (br, $[\text{CH}_3\text{B}(\text{C}_6\text{F}_5)_3]^-$, 3H), (not located at this temperature $\text{CH}_2\text{C}(\text{CH}_3)_3$, 2H); **4**: δ 5.47 (s, C_5H_5 , 5H), 1.35 (s, $\text{C}_5(\text{CH}_3)_5$, 15H), 0.27 (s, CH_3 , 3H), -0.20 (br, $[\text{CH}_3\text{B}(\text{C}_6\text{F}_5)_3]^-$, 3H); isobutene: δ 4.71 (m, $\text{CH}_2\text{C}(\text{CH}_3)_2$, 2H), 1.59 (m, $\text{CH}_2\text{C}(\text{CH}_3)_2$, 6H). ^{19}F NMR (470 MHz, $\text{C}_7\text{D}_8\text{-C}_6\text{D}_5\text{Cl}$, 260 K): **1**: δ -130.2 (d, *o-F* $[\text{CH}_3\text{B}(\text{C}_6\text{F}_5)_3]^-$, 6F, $^3J_{\text{FF}} = 20.7$ Hz), -156.7 (br, *p-F* $[\text{CH}_3\text{B}(\text{C}_6\text{F}_5)_3]^-$, 3F), -161.5 (br, *m-F* $[\text{CH}_3\text{B}(\text{C}_6\text{F}_5)_3]^-$, 6F); **4**: δ -130.6 (d, *o-F*

$[\text{CH}_3\text{B}(\text{C}_6\text{F}_5)_3]^-$, 6F, $^3J_{\text{FF}} = 21.1$ Hz), -156.2 (t, *p-F* $[\text{CH}_3\text{B}(\text{C}_6\text{F}_5)_3]^-$, 3F, $^3J_{\text{FF}} = 19.3$ Hz), -161.2 (t, *m-F* $[\text{CH}_3\text{B}(\text{C}_6\text{F}_5)_3]^-$, 6F, $^3J_{\text{FF}} = 15.5$ Hz). ^1H NMR (500 MHz, $\text{C}_7\text{D}_8\text{-C}_6\text{D}_5\text{Cl}$, 266 K): **1**: δ 5.80 (s, C_5H_5 , 5H), 1.40 (s, $\text{C}_5(\text{CH}_3)_5$, 15H), 0.90 (s, $\text{CH}_2\text{C}(\text{CH}_3)_3$, 9H), 0.014 (br, $[\text{CH}_3\text{B}(\text{C}_6\text{F}_5)_3]^-$, 3H), (not located at this temperature $\text{CH}_2\text{C}(\text{CH}_3)_3$, 2H); **4**: δ 5.49 (s, C_5H_5 , 5H), 1.36 (s, $\text{C}_5(\text{CH}_3)_5$, 15H), 0.27 (s, CH_3 , 3H), -0.19 (br, $[\text{CH}_3\text{B}(\text{C}_6\text{F}_5)_3]^-$, 3H); isobutene: δ 4.71 (m, $\text{CH}_2\text{C}(\text{CH}_3)_2$, 2H), 1.59 (m, $\text{CH}_2\text{C}(\text{CH}_3)_2$, 6H). ^1H NMR (500 MHz, $\text{C}_7\text{D}_8\text{-C}_6\text{D}_5\text{Cl}$, 283 K): **1**: δ 5.81 (s, C_5H_5 , 5H), 1.42 (s, $\text{C}_5(\text{CH}_3)_5$, 15H), 0.90 (s, $\text{CH}_2\text{C}(\text{CH}_3)_3$, 9H), (not located at this temperature: $\text{CH}_2\text{C}(\text{CH}_3)_3$, 2H; $[\text{CH}_3\text{B}(\text{C}_6\text{F}_5)_3]^-$, 3H); **4**: δ 5.51 (s, C_5H_5 , 5H), 1.38 (s, $\text{C}_5(\text{CH}_3)_5$, 15H), 0.27 (s, CH_3 , 3H), -0.17 (br, $[\text{CH}_3\text{B}(\text{C}_6\text{F}_5)_3]^-$, 3H); isobutene: δ 4.69 (m, $\text{CH}_2\text{C}(\text{CH}_3)_2$, 2H), 1.59 (m, $\text{CH}_2\text{C}(\text{CH}_3)_2$, 6H).

Measurement of β -methyl elimination kinetics for **1 in toluene- d_8 -chlorobenzene- d_5 solvent.**

A solution of **1** (approximately 11 mM) in 1:1 (w/w) toluene- d_8 -chlorobenzene- d_5 was prepared in a 5mm thin-walled NMR tube with a J. Young valve as described above. The sample was evacuated on the vacuum line at -196 °C, then was thawed at -60 °C in a dry ice-acetone (or a dry ice-chloroform) bath. Careful mixing of the sample - without warming the contents - generated a bright yellow solution. The NMR probe was pre-equilibrated at -7 °C or 10 °C. The probe temperature was calibrated with a methanol thermometer before and after each kinetic experiment and was maintained at ± 0.2 °C throughout data acquisition. The sample was removed from the cooling bath, positioned in the spinner, and *immediately* inserted into the NMR spectrometer. Following equilibration (5 to 10 minutes) to the preset probe temperature, disappearance of **1** (and

appearance of **4** and isobutene) was monitored by ^1H NMR spectroscopy. Spectra were recorded at regular intervals until the reaction was > 88% complete. The peak height of the ($\eta^5\text{-C}_5\text{H}_5$) resonance of **1** was obtained as a function of time. The rate constant was calculated by curve fitting to the expression $I_t = I_f + (I_0 - I_f) \times \exp(-k_{\beta\text{-Me}}t)$, where I_t is the peak height. The values reported are the average of three kinetic measurements.

Measurement of propagation kinetics for propene polymerization in toluene- d_8 -chlorobenzene- d_5 solvent.

A solution of **1** (0.009 mmol, 10-11 mM, 1 equiv) in 1:1 (w/w) toluene- d_8 -chlorobenzene- d_5 was prepared in a 5mm thin-walled NMR tube with a J. Young valve as described above. The sample was evacuated on the vacuum line at $-196\text{ }^\circ\text{C}$, then was thawed at $-60\text{ }^\circ\text{C}$ in a dry ice-acetone (or a dry ice-chloroform) bath. Careful mixing of the sample - without warming the contents - generated a bright yellow solution. The ^1H and ^{19}F NMR spectra of the sample were obtained at the experimental temperature. On the vacuum line the sample was frozen, degassed, and a measured gas volume of propene (0.46-0.51 mmol, 0.58-0.64 M, 55-58 equiv) was condensed into the tube at $-196\text{ }^\circ\text{C}$. The NMR probe was pre-equilibrated at the experimental temperature. The probe temperature was calibrated with a methanol thermometer before and after each kinetic experiment and was maintained at $\pm 0.2\text{ }^\circ\text{C}$ throughout data acquisition. The NMR samples were mixed using the following procedure. The frozen sample was removed from the $-196\text{ }^\circ\text{C}$ bath, thawed and *rapidly* mixed in a $-60\text{ }^\circ\text{C}$ bath, and positioned in the spinner. The sample was *immediately* frozen at $-196\text{ }^\circ\text{C}$, was inserted into the NMR spectrometer, and was thawed at the preset temperature of the probe. Following

equilibration (5 to 10 minutes) to the probe temperature, disappearance of propene was monitored by ^1H NMR spectroscopy. Spectra were recorded at regular intervals until the reaction was $> 88\%$ complete. The integral of propene $\text{CH}_2\text{CH}(\text{CH}_3)$ resonance (relative to Ph_2CH_2 as an internal standard) was calculated as a function of time. The observed rate constants, k_{obs} , were obtained from the slope of plots of $\ln[\text{propene}]_t$ versus time. The volume of the reaction mixture was determined as $V \text{ (mL)} = 0.01384H - 0.006754$, where H is the solution height in millimeters. The propagation rate constant, k_p was calculated from the expression $k_p = k_{\text{obs}} \div [\text{Zr}]$.

Characterization of species observed upon addition of propene to solutions of **1** (*note*: some resonances could not be reported with certainty due to overlap with propene or poly(propene) resonances): ^1H NMR (500 MHz, $\text{C}_7\text{D}_8\text{-C}_6\text{D}_5\text{Cl}$, 213 K): **2**: δ 5.71, 5.65 (br, C_5H_5 , 5H), 1.35, 1.31 (br, $\text{C}_5(\text{CH}_3)_5$, 15H), -0.12, -0.20 (br, $[\text{CH}_3\text{B}(\text{C}_6\text{F}_5)_3]^-$, 3H); propene: δ 5.72 (m, $\text{CH}_2\text{CH}(\text{CH}_3)$, 1H), 5.00 (m, $\text{CH}_2\text{CH}(\text{CH}_3)$, 2H), 1.56 (m, $\text{CH}_2\text{CH}(\text{CH}_3)$, 3H); poly(propene): 1.77 (br, CH , 1H), 1.27, 1.05 (br, CH_2 , 2H), 0.94 (br, CH_3 , 3H). ^1H NMR (500 MHz, $\text{C}_7\text{D}_8\text{-C}_6\text{D}_5\text{Cl}$, 228 K): **2**: δ 5.71, 5.66 (br, C_5H_5 , 5H), 1.37, 1.33 (br, $\text{C}_5(\text{CH}_3)_5$, 15H), -0.13, -0.20 (br, $[\text{CH}_3\text{B}(\text{C}_6\text{F}_5)_3]^-$, 3H); propene: δ 5.72 (m, $\text{CH}_2\text{CH}(\text{CH}_3)$, 1H), 4.98 (m, $\text{CH}_2\text{CH}(\text{CH}_3)$, 2H), 1.56 (m, $\text{CH}_2\text{CH}(\text{CH}_3)$, 3H); poly(propene): 1.76 (br, CH , 1H), 1.28, 1.04 (br, CH_2 , 2H), 0.94 (br, CH_3 , 3H).

Summary of Propagation Kinetics Data

Table 5. Dependence of k_{obs} on **1** concentration (216 K, toluene- d_8)

[1] (M) ^a	[propene] ₀ (M)	$k_{\text{obs}} \times 10^5$ (s ⁻¹)
0.0025	0.615	10.0(5)
0.0025	0.605	9.1(5)
0.0025	0.599	9.7(5)
0.0061	0.300	26(1)
0.0061	0.312	27(1)
0.0062	0.296	25(1)
0.0091	0.600	38(4)
0.0093	0.608	45(4)
0.0093	0.614	40(4)
0.0131	0.305	51(9)
0.0131	0.309	46(9)
0.0132	0.296	63(9)
0.0162	0.314	67(2)
0.0164	0.305	71(2)

^a [**1**] reported after correction for decomposition.

Table 6. Temperature dependence of propene propagation kinetics (toluene- d_8).

T (K)	[1] (M)	[propene] ₀ (M)	$k_{\text{obs}} \times 10^5$ (s ⁻¹)	$k_p \times 10^3$ (M ⁻¹ s ⁻¹)
191.6	0.0164	0.347	4.1(2)	2.5(2)
191.6	0.0162	0.353	3.9(2)	2.4(2)
192.0	0.0162	0.353	4.1(2)	2.5(2)
202.8	0.0164	0.338	14.6(8)	8.9(5)
202.8	0.0164	0.332	14.5(8)	8.8(5)
203.0	0.0164	0.326	15.7(8)	9.6(5)
216.0	^a	^b	^c	42(4)
228.3	0.0060	0.620	62(2)	104(10)
228.5	0.0060	0.644	65(2)	109(10)
228.6	0.0061	0.622	63(2)	103(10)

^a [**1**] = 2.5 to 16.4 mM (Table 5).

^b [propene] = 0.3 to 0.6 M (Table 5).

^c For the range of k_{obs} see Table 5.

Table 7. Propagation kinetics for various alkenes (228 K, toluene-*d*₈)

Alkene	[1] (M)	[alkene] ₀ (M)	$k_{\text{obs}} \times 10^5$ (s ⁻¹)	$k_p \times 10^3$ (M ⁻¹ s ⁻¹)
ethene	0.0119	0.638	- ^a	- ^a
ethene	0.0119	0.644	- ^a	- ^a
ethene	0.0119	0.684	- ^a	- ^a
propene	0.0060	0.620	62(2)	104(10)
propene	0.0060	0.644	65(2)	109(10)
propene	0.0061	0.622	63(2)	103(10)
1-butene	0.0105	0.603	34(5)	32(5)
1-butene	0.0113	0.633	30(5)	27(5)
1-butene	0.0113	0.667	25(5)	22(5)
1-pentene	0.0112	0.590	20.5(6)	18(1)
1-pentene	0.0112	0.585	19.8(6)	18(1)
1-pentene	0.0113	0.596	19.4(6)	17(1)
1-hexene	0.0149	0.624	23.4(8)	16(1)
1-hexene	0.0149	0.624	21.8(8)	15(1)
1-hexene	0.0149	0.624	23.0(8)	16(1)
1-hexene	0.0150	0.630	22.3(8)	15(1)
1-undecene	0.0151	0.638	11.3(5)	7.5(7)
1-undecene	0.0152	0.644	12.2(5)	8.0(7)
1-undecene	0.0152	0.644	11.8(5)	7.8(7)
4-Me-1-pentene	0.0156	1.08	6(1)	3.7(5)
4-Me-1-pentene	0.0156	1.08	6(1)	3.9(5)
4-Me-1-pentene	0.0158	0.604	8(1)	4.8(5)
4-Me-1-pentene	0.0162	0.616	8(1)	4.6(5)

^a Rapid polymerization at temperatures as low as 173 K precluded experimental determination of k_{obs} and k_p .

Table 8. Propene propagation kinetics with added **3** (228 K, toluene-*d*₈)

[1] (M)	[3] (M)	[CH ₃ B(C ₆ F ₅) ₃] (M)	[propene] ₀ (M)	$k_{\text{obs}} \times 10^5$ (s ⁻¹)	$k_p \times 10^3$ (M ⁻¹ s ⁻¹)
0.0106	0.0098	0.0010	0.458	146(1)	137(2)
0.0108	0.0010	0.0013	0.424	147(1)	136(2)
0.0095	0.0024	0.0038	0.435	157(1)	165(9)
0.0071	0.0060	0.0079	0.434	150(1)	212(4)
0.0072	0.0068	0.0085	0.442	156(4)	216(4)
0.0078	0.0073	0.0100	0.422	180(1)	230(9)
0.0046	0.0087	0.0102	0.417	107(2)	233(6)
0.0073	0.0084	0.0104	0.435	175(1)	239(9)

Table 9. Propene propagation kinetics in 1:1 (w/w) toluene- d_8 -chlorobenzene- d_5

T (K)	[1] (M)	[propene] ₀ (M)	$k_{\text{obs}} \times 10^5$ (s ⁻¹)	$k_p \times 10^3$ (M ⁻¹ s ⁻¹)
213	0.0112	0.618	67.6(5)	60(5)
213	0.0107	0.638	62.2(1)	58(5)
213	0.0108	0.623	69.8(1)	64(5)
213	0.0108	0.641	61.7(2)	57(5)
213	0.0108	0.611	62.2(1)	57(5)
228	0.0106	0.580	300(4)	280(30)

References

1. Resconi, L.; Cavallo, L.; Fait, A.; Piemontesi, F. *Chem. Rev.* **2000**, *100*, 1253-1345.
2. Brintzinger, H. H.; Fischer, D.; Mulhaupt, R.; Rieger, B.; Waymouth, R. M. *Angew. Chem., Int. Ed. Engl.* **1995**, *34*, 1143-1170.
3. Herfert, N.; Fink, G. *Makromol. Chem., Macromol. Symp.* **1993**, *66*, 157-178.
4. Liu, Z. X.; Somsook, E.; Landis, C. R. *J. Am. Chem. Soc.* **2001**, *123*, 2915-2916.
5. Liu, Z. X.; Somsook, E.; White, C. B.; Rosaaen, K. A.; Landis, C. R. *J. Am. Chem. Soc.* **2001**, *123*, 11193-11207.
6. Chen, M. C.; Roberts, J. A. S.; Marks, T. J. *J. Am. Chem. Soc.* **2004**, *126*, 4605-4625.
7. Schaper, F.; Geyer, A.; Brintzinger, H. H. *Organometallics* **2002**, *21*, 473-483.
8. Landis, C. R.; Rosaaen, K. A.; Sillars, D. R. *J. Am. Chem. Soc.* **2003**, *125*, 1710-1711.
9. Bochmann, M. *J. Chem. Soc., Dalton Trans.* **1996**, 255-270.
10. Alt, H. G.; Koppl, A. *Chem. Rev.* **2000**, *100*, 1205-1221.
11. Richardson, D. E.; Alameddin, N. G.; Ryan, M. F.; Hayes, T.; Eyster, J. R.; Siedle, A. R. *J. Am. Chem. Soc.* **1996**, *118*, 11244-11253.
12. Jordan, R. F. *Adv. Organomet. Chem.* **1991**, *32*, 325-387.
13. Beck, S.; Lieber, S.; Schaper, F.; Geyer, A.; Brintzinger, H. H. *J. Am. Chem. Soc.* **2001**, *123*, 1483-1489.
14. Coates, G. W. *Chem. Rev.* **2000**, *100*, 1223-1252.
15. Piers, W. E.; Bercaw, J. E. *J. Am. Chem. Soc.* **1990**, *112*, 9406-9407.
16. Burger, B. J.; Cotter, W. D.; Coughlin, E. B.; Chacon, S. T.; Hajela, S.; Herzog, T.; Köhn, R.; Mitchell, J.; Piers, W. E.; Shapiro, P. J.; Bercaw, J. E. In *Ziegler-Catalysts*; Fink, G., Mülhaupt, R., Brintzinger, H. H., Eds.; Springer-Verlag: Berlin, 1995, p 317-331.
17. Krauledat, H.; Brintzinger, H. H. *Angew. Chem., Int. Ed. Engl.* **1990**, *29*, 1412-1413.
18. Leclerc, M. K.; Brintzinger, H. H. *J. Am. Chem. Soc.* **1995**, *117*, 1651-1652.
19. Chirik, P. J.; Dalleska, N. F.; Henling, L. F.; Bercaw, J. E. *Organometallics* **2005**, *24*, 2789-2794.
20. Landis, C. R.; Rosaaen, K. A.; Uddin, J. *J. Am. Chem. Soc.* **2002**, *124*, 12062-12063.
21. Clawson, L.; Soto, J.; Buchwald, S. L.; Steigerwald, M. L.; Grubbs, R. H. *J. Am. Chem. Soc.* **1985**, *107*, 3377-3378.

22. Beswick, C. L.; Marks, T. J. *J. Am. Chem. Soc.* **2000**, *122*, 10358-10370.
23. Wendt, O. F.; Bercaw, J. E. *manuscript in preparation*.
24. Brandow, C. G.; Mendiratta, A.; Bercaw, J. E. *Organometallics* **2001**, *20*, 4253-4261.
25. Casey, C. P.; Carpenetti, D. W.; Sakurai, H. *Organometallics* **2001**, *20*, 4262-4265.
26. Sillars, D. R.; Landis, C. R. *J. Am. Chem. Soc.* **2003**, *125*, 9894-9895.
27. Horton, A. D. *Organometallics* **1996**, *15*, 2675-2677.
28. Yang, X. M.; Stern, C. L.; Marks, T. J. *J. Am. Chem. Soc.* **1994**, *116*, 10015-10031.
29. Zuccaccia, C.; Stahl, N. G.; Macchioni, A.; Chen, M. C.; Roberts, J. A.; Marks, T. J. *J. Am. Chem. Soc.* **2004**, *126*, 1448-1464.
30. Grubbs, R. H.; Coates, G. W. *Acc. Chem. Res.* **1996**, *29*, 85-93.
31. Chen, E. Y. X.; Marks, T. J. *Chem. Rev.* **2000**, *100*, 1391-1434.
32. Casey, C. P.; Tunge, J. A.; Lee, T. Y.; Fagan, M. A. *J. Am. Chem. Soc.* **2003**, *125*, 2641-2651.
33. Burger, B. J.; Thompson, M. E.; Cotter, W. D.; Bercaw, J. E. *J. Am. Chem. Soc.* **1990**, *112*, 1566-1577.
34. Espenson, J. H. *Chemical Kinetics and Reaction Mechanisms*; McGraw-Hill: New York, 1981.
35. Burger, B. J.; Bercaw, J. E. *New Developments in the Synthesis, Manipulation, and Characterization of Organometallic Compounds*; American Chemical Society: Washington, DC, 1987; Vol. 357.
36. Pangborn, A. B.; Giardello, M. A.; Grubbs, R. H.; Rosen, R. K.; Timmers, F. J. *Organometallics* **1996**, *15*, 1518-1520.
37. Marvich, R. H.; Brintzinger, H. H. *J. Am. Chem. Soc.* **1971**, *93*, 2046-2048.
38. Massey, A. G.; Park, A. J. *J. Organomet. Chem.* **1964**, *2*, 245-250.
39. Alternatively, 4-methyl-1-pentene was distilled from LiAlH_4 and stored over activated 4 Å molecular sieves under N_2 .
40. 4-methyl-1-pentene was also added to the samples by this method. The same k_p (within experimental error) was obtained by either method.
41. The same k_p (within experimental error) were obtained by either mixing method.

Chapter 3

Direct Examination of Propene Initiation Kinetics Using Mixed-Ring Zirconocene Initiators

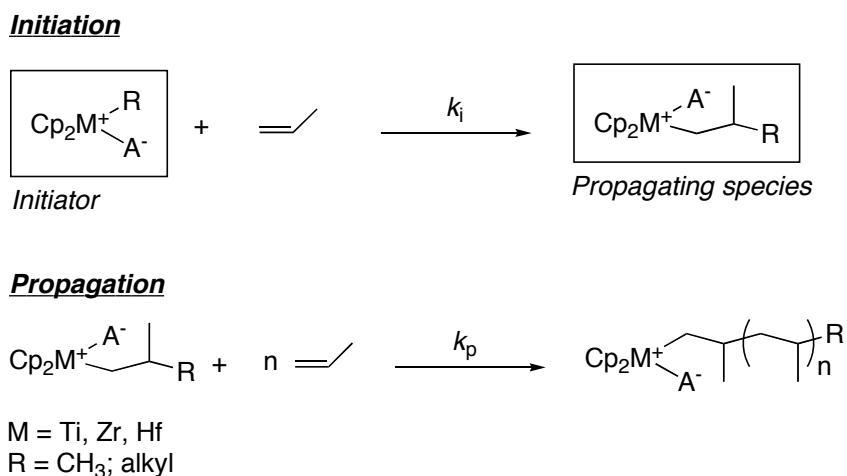
Abstract

Propene initiation kinetics have been examined for a series of alkylzirconocene initiators, $[(\eta^5\text{-C}_5\text{H}_5)(\eta^5\text{-C}_5\text{Me}_5)\text{Zr}(\text{R})]^+[\text{CH}_3\text{B}(\text{C}_6\text{F}_5)_3]^-$ ($\text{R} = \text{CH}_3$ (**5**), CH_2CMe_3 (**1**), CH_2SiMe_3 (**4**)). Measurement of k_i for the neopentyl initiator reveals that the rate of initiation is on the order of propagation for this catalyst. This initiator – with a polymeryl like alkyl group – serves as a model of the propagating species in propene polymerization. The catalyst initiation behavior has been investigated and the observed relative rates of propene initiation are not always predicted by ground-state (zirconium-carbon bond strength or extent of ion-pairing) considerations. The catalysts **4** and **5** are both poor initiators with $k_i \ll k_p$ and show less than 50% initiation in the presence of excess propene at $-60\text{ }^\circ\text{C}$ in toluene- d_8 .

1 Introduction

The initiation step in metallocene-catalyzed alkene polymerization is defined as the first insertion of alkene into the metal-carbon bond of the alkyl initiator (Scheme 1).¹ For group 4 metallocene catalysts this initiator is an alkylmetallocene cation paired with a weakly coordinating counteranion.² The reaction of initiator with alkene occurs with rate constant of initiation, k_i , generating the propagating species. Initiation is followed by polymer chain growth in the propagation step. Here further insertion of alkene into the metal-carbon bond of the propagating species occurs with rate constant for propagation, k_p .

Scheme 1



The relative rates of initiation and propagation have important consequences on the properties of these catalytic systems.³ For a given number of metal centers, systems with $k_i \ll k_p$ produce polymer with higher molecular weights and broader molecular weight distributions compared to systems where $k_i \approx k_p$. The former situation often results in a large fraction (> 50%) of the total catalyst remaining in an inactive form, reducing overall catalyst efficiency.⁴

Therefore, although initiation and propagation are conceptually similar steps, these processes can occur with dramatically different rates. This disparity between k_i and k_p is related to the nature of the metal-alkyl initiator and has been named the alkyl initiator effect. This effect has been explored in detail in 1-hexene polymerization studies using a series of group 4 nonmetallocene alkyl initiators.⁵

For group 4 metallocene systems, the alkyl initiator effect has been discussed in terms of $\{M\}^+-CH_3$ initiators and the resulting $\{M\}^+$ -polymeryl species.^{4,6,7} For these initiators, the first insertion of alkene occurs at a substantially slower rate than subsequent insertions of alkene into the metal-alkyl bond of the propagating species. A $k_p/k_i \approx 120$ has been estimated by Herfert and Fink for insertion into $[Cp_2Ti]^+$ -poly(ethenyl) vs. $[Cp_2Ti]^+-CH_3$ [$Cp = (\eta^5-C_5H_5)$].⁴ Landis and coworkers have determined $k_p/k_i = 70$ (0 °C, toluene) for 1-hexene polymerization catalyzed by $[rac-(C_2H_4(1-indenyl)_2)ZrCH_3]^+[CH_3B(C_6F_5)_3]^-$.⁶

The slow insertion of alkenes into $\{M\}^+-CH_3$ relative to $\{M\}^+$ -polymeryl has been attributed to two factors: (1) the relative difference in metal-alkyl bond strengths and (2) the steric influence of the alkyl group on ion-pairing (Figure 1).⁶

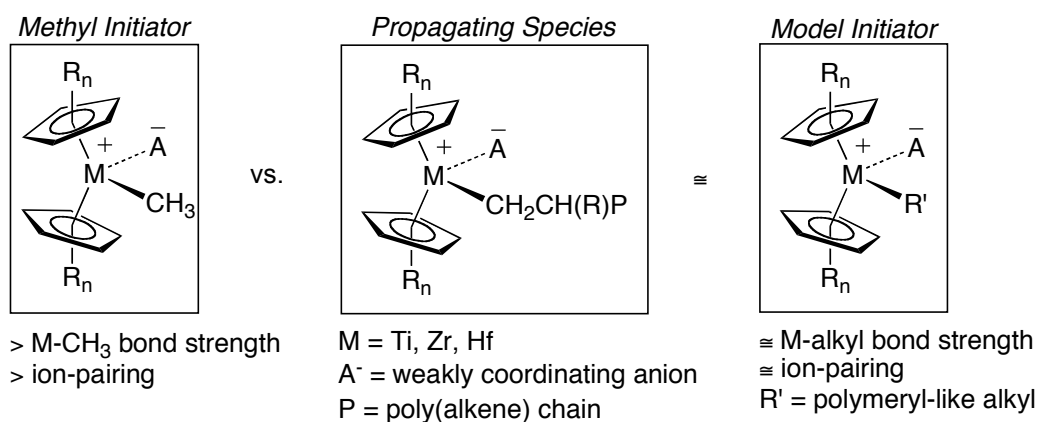
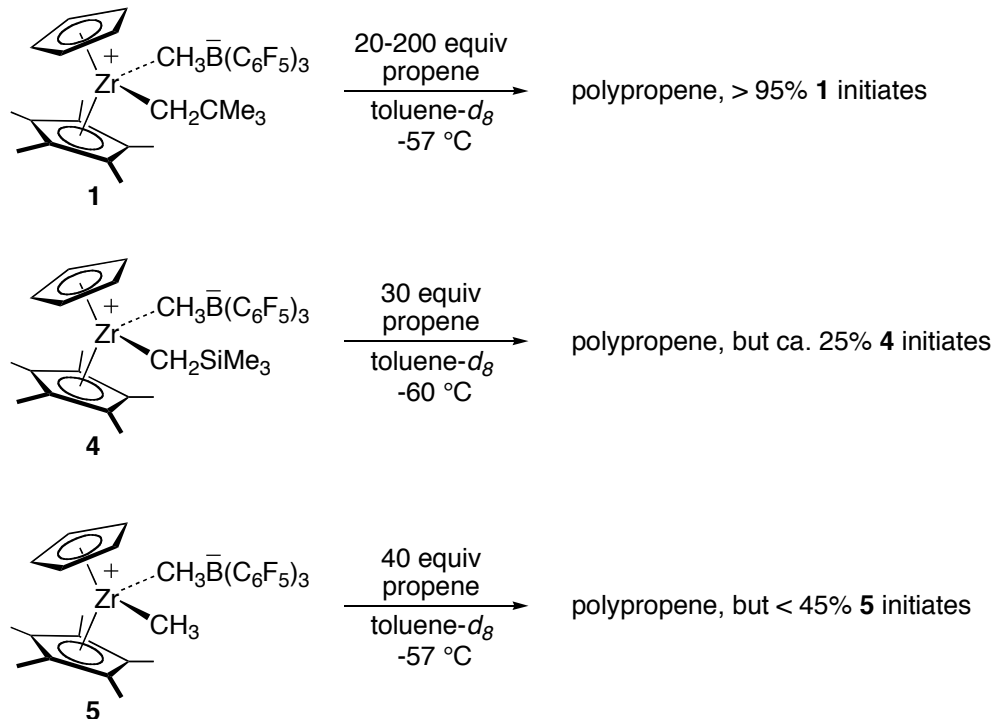


Figure 1. Relative rates of initiation and propagation may be related to differences in M-alkyl bond strengths and extent of ion-pairing.

Initiation of a methylmetallocene catalyst requires breaking a stronger M-C bond as compared to that broken in the propagation step, leading to higher ΔH_i^\ddagger than ΔH_p^\ddagger . Examples of such an effect have been observed with metallocene catalysts. Higher activities are observed for Cp^xZrCl_2 systems activated with MMAO (modified methylaluminoxane, containing ${}^i\text{Bu}_3\text{Al}$) instead of MAO.⁸ If these polymerizations proceed via $\{\text{Zr}\}^+ - {}^i\text{Bu}$ initiators, where $\Delta H_i^\ddagger \approx \Delta H_p^\ddagger$, a greater fraction of catalyst may be initiated in these systems. Additionally, the steric-influence of the polymeryl chain is proposed to reduce the extent of ion-pairing in the propagating species relative to that in the methyl initiator.⁶ This idea is supported by Marks et al. who found that site epimerization rates increased with the steric bulk of R for $[(\text{Me}_2\text{Cp})_2\text{Zr}(\text{R})]^+[\text{CH}_3\text{B}(\text{C}_6\text{F}_5)_3]^-$.⁹

A family of alkylzirconocene initiators based on the catalyst framework $[\text{CpCp}^*\text{Zr}(\text{R})]^+[\text{CH}_3\text{B}(\text{C}_6\text{F}_5)_3]^-$ [$\text{Cp}^* = (\eta^5\text{-C}_5\text{Me}_5)$] were evaluated for use in the studies examining zirconocene-catalyzed alkene propagation kinetics described in Chapter 2. A significant alkyl initiator effect was observed for propene polymerization within the series: R = CH_2CMe_3 (Np) (**1**); CH_2SiMe_3 (CH_2TMS) (**4**); CH_3 (**5**) (Scheme 2). Catalyst **1** was a superior initiator for propene polymerization as greater than 95% initiation was observed by ${}^1\text{H}$ NMR spectroscopy (20-200 equiv propene, -57°C , toluene- d_8). This contrasts the initiation behavior observed for **4** and **5** where only partial initiation occurred for both catalysts, approximately 25% and 45% respectively, under comparable polymerization conditions.

Scheme 2



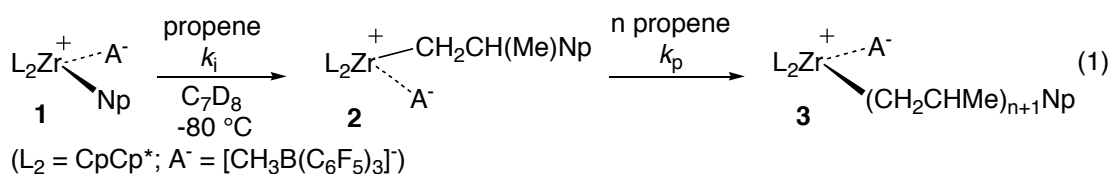
This chapter describes the examination of initiation kinetics for propene polymerization by catalysts **1**, **4**, and **5** by ^1H NMR spectroscopy. Direct measurement of k_i allows a rare example of a quantification of the alkyl initiator effect for this series of catalysts. The initiation behavior observed is discussed in the context of relative differences in zirconium-alkyl bond strength and ion-pairing among these initiators.

2 Results

2.1 Direct observation of the initiation step in $[\text{CpCp}^*\text{Zr}(\text{Np})]^+[\text{CH}_3\text{B}(\text{C}_6\text{F}_5)_3]^-$ -catalyzed propene polymerization

The experiments examining propene propagation kinetics catalyzed by $[\text{CpCp}^*\text{Zr}(\text{Np})]^+[\text{CH}_3\text{B}(\text{C}_6\text{F}_5)_3]^-$ (**1**) described in Chapter 2 did not allow direct monitoring of the initiation step. Complete initiation of **1** occurred upon sample mixing at temperatures as low as -80°C ($[\mathbf{1}]_0 = 16 \text{ mM}$, $[\text{propene}]_0 = 0.35 \text{ M}$, 22 equiv, toluene- d_8).

Addition of 12 equivalents of propene to samples of **1** in toluene- d_8 at $-196\text{ }^\circ\text{C}$ followed by mixing at $-78\text{ }^\circ\text{C}$ allowed observation of the initiation step by ^1H NMR spectroscopy at $-80\text{ }^\circ\text{C}$. Under these conditions ($[\mathbf{1}]_0 = 11\text{ mM}$, $[\text{propene}]_0 = 0.12\text{ M}$, 12 equiv) three catalyst species were detected in solution (eq 1).



These compounds were assigned as **1**, the initiation product $[\text{CpCp}^*\text{ZrCH}_2\text{CH}(\text{Me})\text{Np}]^+[\text{CH}_3\text{B}(\text{C}_6\text{F}_5)_3]^-$ (**2**), and propagating species (**3**) using characteristic ^1H NMR resonances of the Cp, Cp*, and $[\text{CH}_3\text{B}(\text{C}_6\text{F}_5)_3]^-$ groups (Figure 2). All resonances of initiator **1** (including diastereotopic α -methylene protons) were located and were consistent with independently prepared samples at $-80\text{ }^\circ\text{C}$. The Cp, Cp*, and $[\text{CH}_3\text{B}(\text{C}_6\text{F}_5)_3]^-$ groups of **1** are found at 5.63, 1.17, and -0.11 ppm respectively ^1H NMR spectrum. The propagating species **3** was identified by characteristic broad sets of Cp (centered around 5.59 and 5.55 ppm) and $[\text{CH}_3\text{B}(\text{C}_6\text{F}_5)_3]^-$ (-0.09 and -0.17 ppm) resonances as observed during the propagation kinetics studies in Chapter 2. The new set of resonances was attributed to **2**. The signals observed for the Cp (5.56 and 5.59 ppm) and Cp* (1.18 and 1.19 ppm) were consistent with the diastereomeric first insertion product **2** (due to the chirality at zirconium and at the alkyl group β -carbon).

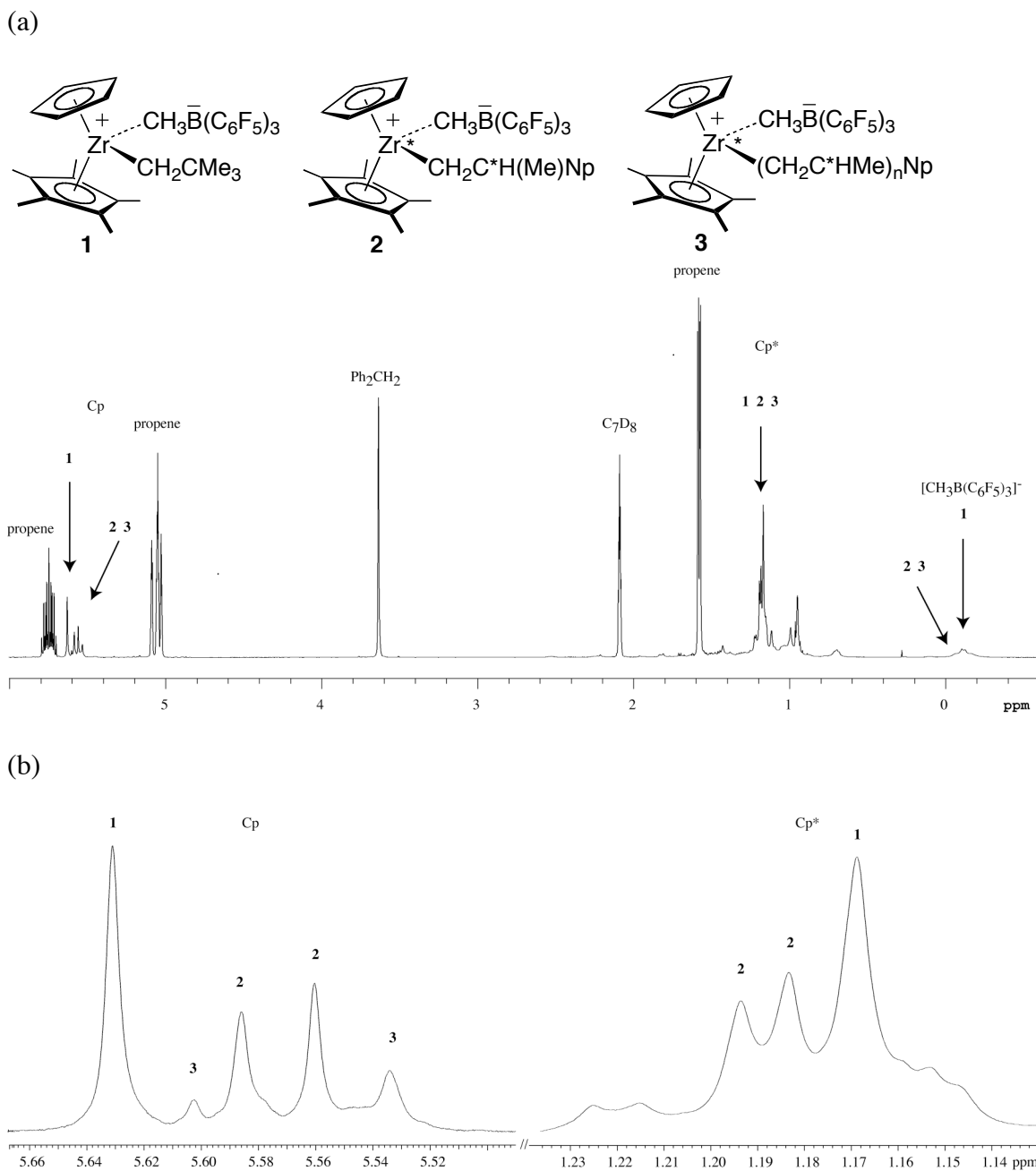


Figure 2. (a) Partial ^1H NMR spectrum of product mixture obtained from **1** and 12 equivalents propene (toluene- d_8 , $-80\text{ }^\circ\text{C}$); (b) Expanded regions showing Cp and Cp* resonances.

Further support for the species **2** comes from addition of ca. two equivalents propene to samples of **1** as described above. Under these conditions ($[\mathbf{1}]_0 = 11.4\text{ mM}$, $[\text{propene}]_0 = 25\text{ mM}$, 2 equiv) the discrete Cp and Cp* resonances of **2** are clearly observed by ^1H

NMR spectroscopy at $-80\text{ }^{\circ}\text{C}$ (Figure 3). Here these regions in the ^1H NMR spectrum were not obstructed by the broad resonances due to **3**. Compound **2** formed as a roughly 45:55 ratio of diastereomers.

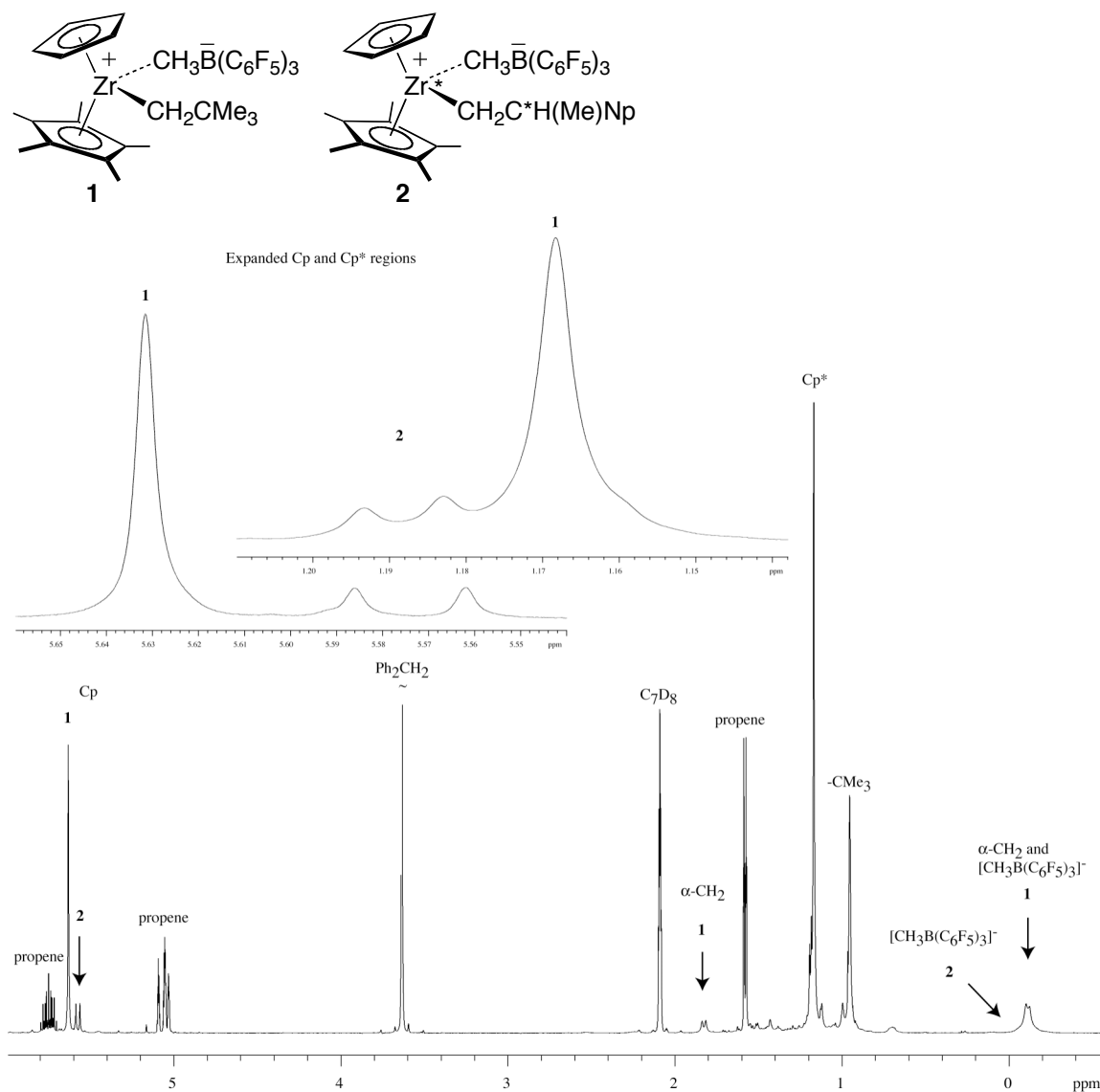


Figure 3. ^1H NMR spectrum of product mixture obtained from **1** and two equivalents of propene ($\text{toluene-}d_8$, $-80\text{ }^{\circ}\text{C}$). The inset shows expanded Cp (left) and Cp* regions.

2.2 Measurement of initiation kinetics for the reaction of $[\text{CpCp}^*\text{Zr}(\text{Np})]^+[\text{CH}_3\text{B}(\text{C}_6\text{F}_5)_3]^-$ with propene

Initiation kinetics for the reaction of **1** with propene were examined using the following conditions: $[\mathbf{1}]_0 = 10\text{-}12$ mM and $[\text{propene}]_0 = 0.08\text{-}0.25$ M in toluene- d_8 over the temperature range -70 to -90 °C. Typical $[\text{propene}]/[\mathbf{1}]_0$ ratios were between 8 and 22, with the lower ratios utilized at higher temperatures. The disappearance of **1** and propene were monitored by ^1H NMR spectroscopy, and the concentrations of **1** and propene were determined as a function of time by integration relative to the internal standard Ph_2CH_2 . Since propene reacts with **1** and **3**, its concentration changes over the duration of the kinetic experiment and standard techniques (under pseudo-first-order conditions) for obtaining second-order rate constants do not directly apply.¹⁰ A correction factor $[\text{propene}]_t/[\text{propene}]_0$ was applied to each data point (to account for the continuous disappearance of propene) and the data were then plotted as for pseudo-first-order kinetics.¹¹ A representative plot of $\ln([\mathbf{1}]_t[\text{propene}]_t/[\text{propene}]_0)$ vs time for kinetics measurements at -80 °C is shown in Figure 4. The observed rate constants, k_{obs} , were obtained from the slope of these plots. Second-order rate constants for initiation, k_i , were calculated using the expression $k_i = k_{\text{obs}} \div [\text{propene}]_0$, where $[\text{propene}]_0$ is the initial propene concentration. The k_i reported are the average of two to four kinetic measurements (Table 1).

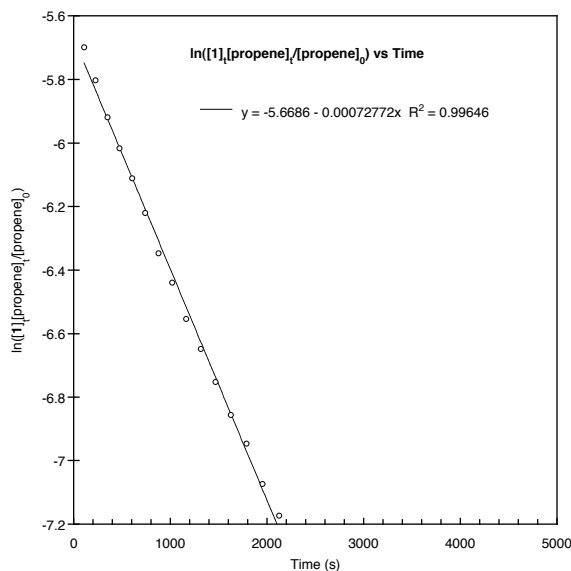


Figure 4. Representative kinetics plot for the reaction of **1** and propene ($[1]_0 = 11.3$ mM, $[\text{propene}] = 0.126$ M) in toluene- d_8 at -80 °C. From the fit $k_i = 6(1) \text{ M}^{-1}\text{s}^{-1}$.

Table 1. Summary of initiation and propagation rate constants for propene polymerization catalyzed by **1** in toluene- d_8

T (K)	$k_i \times 10^3$ ($\text{M}^{-1}\text{s}^{-1}$)	$k_p \times 10^3$ ^a ($\text{M}^{-1}\text{s}^{-1}$)	k_p/k_i
203	13(1)	9.2(9)	0.7
193	7(1)	3(1)	0.4
183	2.4(6)	0.9(1)	0.36

^a Obtained from Eyring analysis in Chapter 2.

An Eyring plot was constructed using the second-order k_i obtained over the temperature range 183-203 K for the reaction of **1** and propene (Table 1; Figure 5). Calculation of the overall activation parameters for initiation from this analysis gave $\Delta H^\ddagger = 6(1) \text{ kcal}\cdot\text{mol}^{-1}$ and $\Delta S^\ddagger = -36(6) \text{ eu}$.

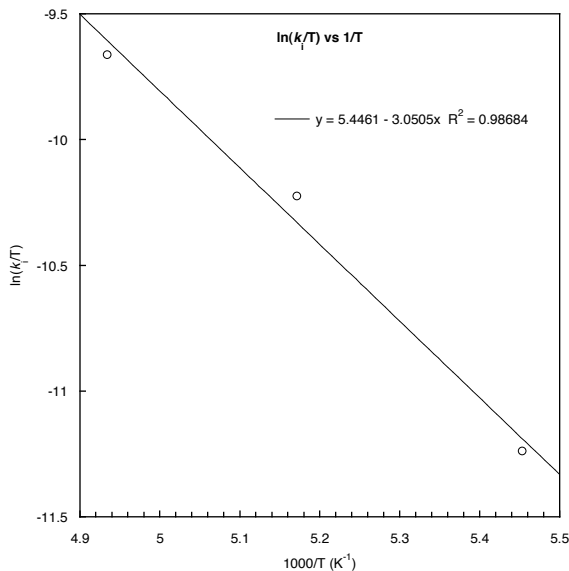
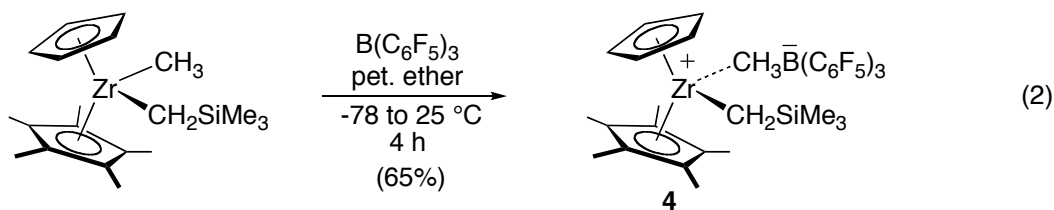


Figure 5. Eyring plot for the reaction of **1** with propene (toluene-*d*₈). The fit gives overall activation parameters for initiation of: $\Delta H^\ddagger = 6(1)$ kcal·mol⁻¹; $\Delta S^\ddagger = -36(6)$ eu.

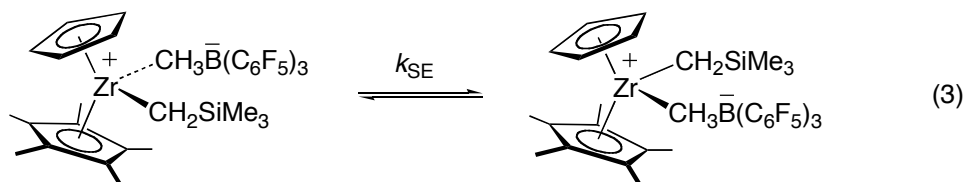
2.3 Synthesis and characterization of [CpCp*Zr(CH₂TMS)]⁺[CH₃B(C₆F₅)₃]⁻

The alkylzirconocene initiator [CpCp*Zr(CH₂TMS)]⁺[CH₃B(C₆F₅)₃]⁻ (**4**) was synthesized by selective methide abstraction from CpCp*Zr(CH₂TMS)(CH₃) using the strong Lewis acid B(C₆F₅)₃ (eq 2).¹² Compound **4** was isolated as a pale yellow powder on a preparative scale. This initiator appeared stable in the solid-state (indefinitely at -35 °C under N₂) as well as in solution (in benzene-*d*₆ or toluene-*d*₈) at temperatures as high as 50 °C.



Compound **4** has been characterized by ¹H, ¹³C, and ¹⁹F NMR spectroscopy, including variable temperature studies. The ¹H NMR spectroscopic data obtained for **4** suggested dynamic behavior in solution (benzene-*d*₆ or toluene-*d*₈). At ambient

temperature resonances for the α -protons of the alkyl group - {Zr}-CH₂TMS – were not located in the ¹H NMR spectrum of **4**. Upon cooling samples (in toluene-*d*₈) below -20 °C two doublets (1.41 and 0.44 ppm, *J* = 9.2 Hz) assigned to these resonances were resolved from the baseline. Above this temperature these resonances broadened and began to coalesce. The observed data was consistent with site epimerization (or racemization at zirconium) (eq 3).



Simulation of the methylene proton resonance located at 0.44 ppm in the ¹H NMR spectra of **4** using the program gNMR allowed estimation of rate constants for site epimerization, *k*_{SE}, over a 223-253 K temperature range.¹³ The value determined at the coalescence temperature (253 K) was *k*_{SE} = 33(3) s⁻¹ ($\Delta G^\ddagger = 12.9(1)$ kcal·mol⁻¹).

2.4 Observation of propene polymerization catalyzed by [CpCp*Zr(CH₂TMS)]⁺[CH₃B(C₆F₅)₃]⁻ or [CpCp*Zr(CH₃)]⁺[CH₃B(C₆F₅)₃]⁻

Reactions of **4** or [CpCp*Zr(CH₃)]⁺[CH₃B(C₆F₅)₃]⁻ (**5**) with propene were examined at -60 °C using 10-12 mM of catalyst initiator and 0.33-0.44 M of propene (roughly 30 to 40 equiv) in toluene-*d*₈. Poor initiation was observed for **4**, where only about 25% of catalyst initiated as judged by ¹H NMR spectroscopy (Figure 6). The major alkylzirconocene species detected in solution during the reaction was **4**, identified by characteristic Cp (5.65 ppm), Cp* (1.28 ppm), α -CH₂ (d, 0.31, *J* = 9.5 Hz), SiMe₃ (0.014 ppm), and [CH₃B(C₆F₅)₃]⁻ (-0.51 ppm) signals. Evidence for the formation of the propagating species [CpCp*Zr(CH₂CHMe)_{*n*}CH₂TMS]⁺[CH₃B(C₆F₅)₃]⁻ (**6**) included broad

sets of resonances for the Cp, Cp*, and $[\text{CH}_3\text{B}(\text{C}_6\text{F}_5)_3]^-$ groups located at (5.60, 5.56), (1.21, 1.28), and (-0.1, -0.15 ppm) respectively, along with a signal for the SiMe_3 groups on the $\{\text{Zr}\}^+$ -poly(propenyl) terminus located at 0.11 ppm. As the reaction progressed, broad polypropene resonances were observed [1.80 ppm (*CH*), 1.32 and 1.08 (*CH*₂), 0.98 (*CH*₃). However, catalyst **4** was never fully initiated.

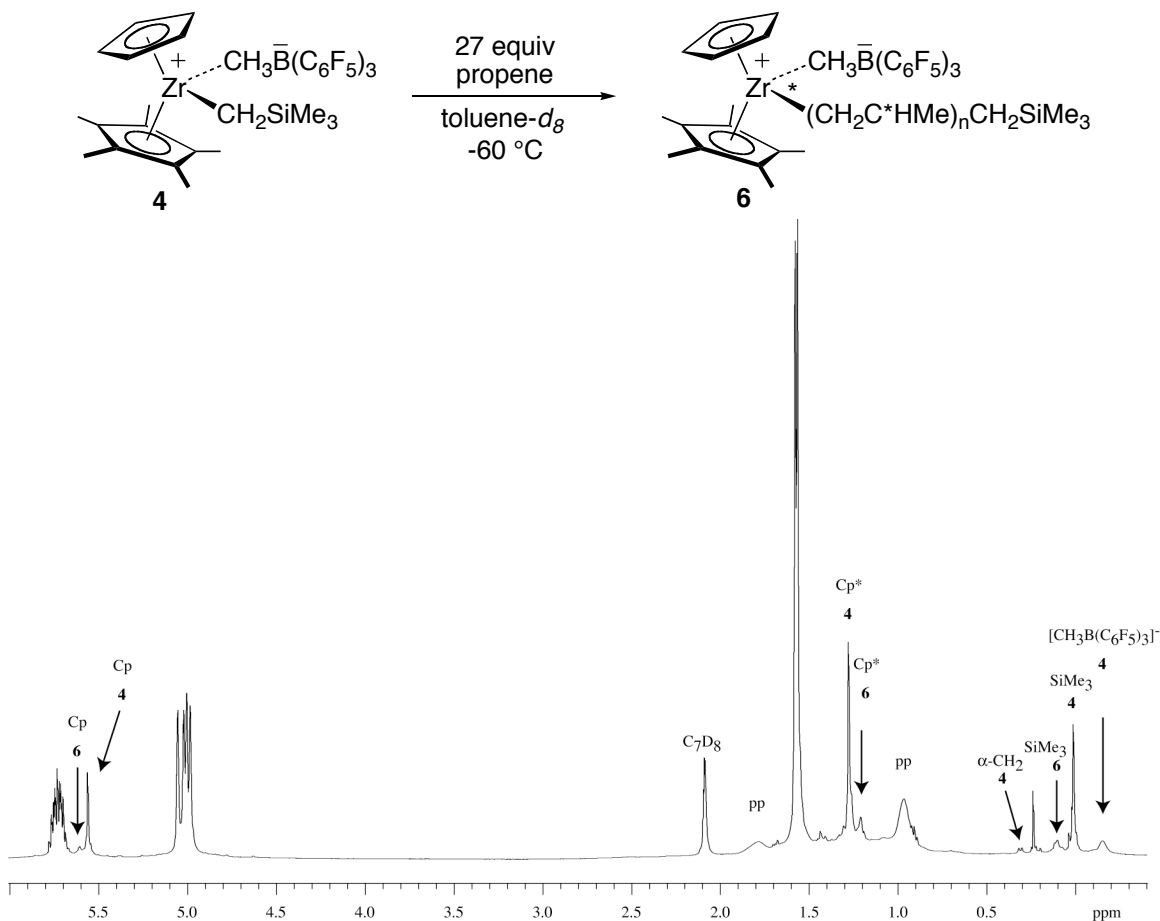


Figure 6. Partial ^1H NMR spectrum of product mixture obtained from **4** and 27 equivalents of propene in toluene- d_8 at $-60\text{ }^\circ\text{C}$. “pp” denotes signals for polypropene and unlabeled signals are for unreacted propene.

Similar initiation behavior was observed for catalyst **5**. Addition of 44 equivalents of propene to the catalyst solution in toluene- d_8 resulted in initiation of only 40-45% **5** upon mixing (^1H NMR spectroscopy, $-57\text{ }^\circ\text{C}$). Again the major species detected in

solution were **5** and free propene. Unreacted catalyst **5** was identified by signals for: Cp (5.22 ppm), Cp* (1.17 ppm), Zr-CH₃ (0.24 ppm), and [CH₃B(C₆F₅)₃]⁻ (-0.23 ppm) groups. Formation of the propagating species [CpCp*Zr(CH₂CHMe)_nCH₃]⁺[CH₃B(C₆F₅)₃]⁻ (**7**) was confirmed by the observation of characteristic broad sets of resonances for the Cp (5.59, 5.55 ppm), Cp* (1.25, 1.19 ppm), and [CH₃B(C₆F₅)₃]⁻ (-0.1, -0.18 ppm) groups. The sets of diastereomers of **7** formed in roughly the same 60:40 ratio as observed with neopentyl initiator **1**. As the reaction progressed, propene was polymerized by **7** while the bulk of initiator **5** remained inactive in the propagation step.

2.5 Measurement of initiation kinetics for the reaction of [CpCp*Zr(CH₂SiMe₃)⁺][CH₃B(C₆F₅)₃]⁻ or [CpCp*Zr(CH₃)⁺][CH₃B(C₆F₅)₃]⁻ with propene

Initiation kinetics for the reaction of **5** with propene was carried out at -70 °C using 16 mM of zirconium complex and 1.4 M of propene (approximately 85 equiv) in toluene-*d*₈. Upon mixing at -78 °C the major species observed in solution were due to **5** – with characteristic Cp (5.20 ppm), Cp* (1.17 ppm), Zr-CH₃ (0.23 ppm), and [CH₃B(C₆F₅)₃]⁻ (-0.26 ppm) resonances – along with free propene (Figure 7). The initiation reaction was monitored over time by ¹H NMR spectroscopy and the signals for **5** decreased with a concomitant formation of broad resonances due to the propagating species **7** located at: Cp (5.59, 5.55 ppm), Cp* (1.24, 1.19 ppm), and [CH₃B(C₆F₅)₃]⁻ (-0.12, -0.19 ppm) and polypropene.

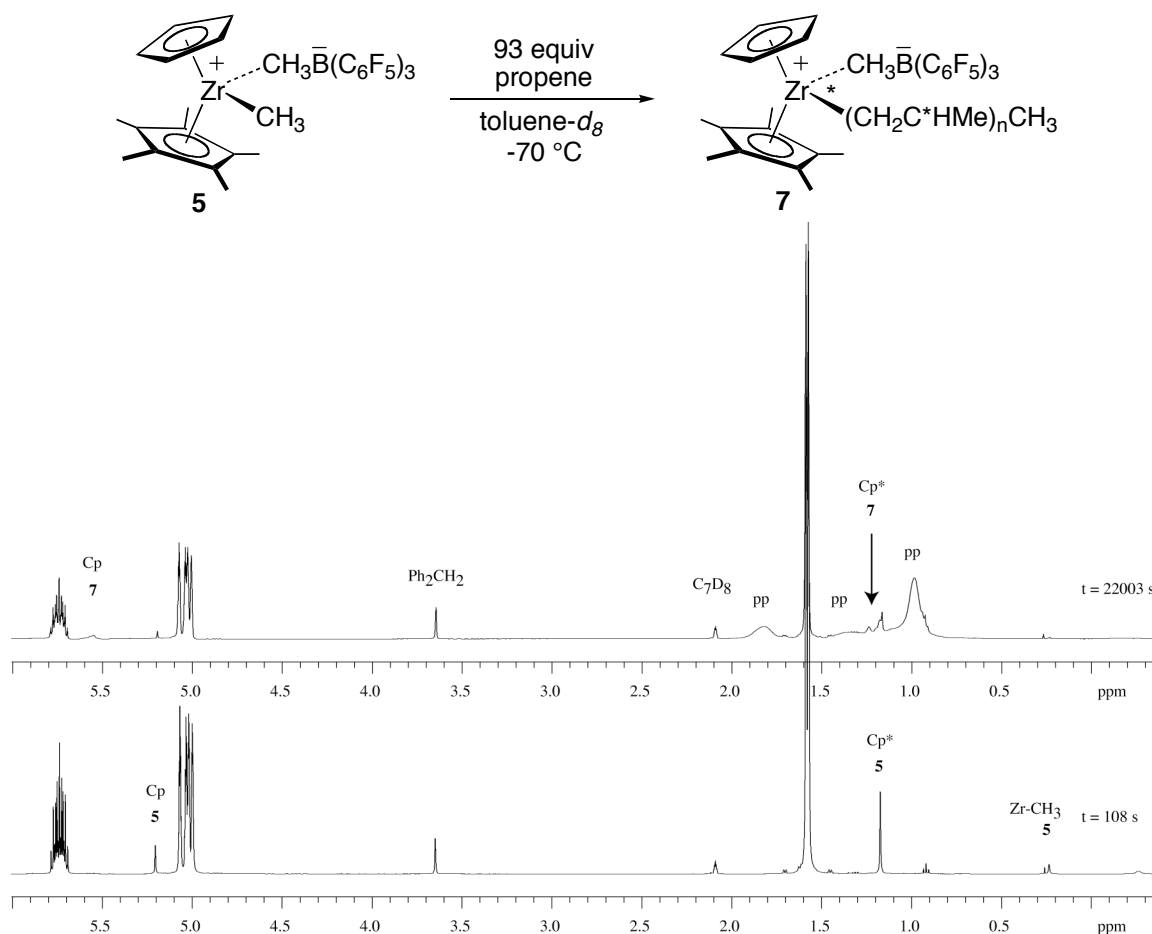


Figure 7. Partial ^1H NMR spectra showing the reaction of **5** with 93 equivalents propene in toluene- d_8 at $-70\text{ }^\circ\text{C}$ at $t = 108\text{ s}$ and $t = 22003\text{ s}$. “pp” denotes signals for polypropene and unlabeled signals are for unreacted propene.

Initiation kinetics for the reaction of **4** with propene was monitored using analogous conditions: $[\mathbf{4}]_0 = 13\text{ mM}$; $[\text{propene}]_0 = 1.22\text{ M}$ (100 equiv); in toluene- d_8 at $-70\text{ }^\circ\text{C}$. The reaction mixture first observed upon mixing at $-78\text{ }^\circ\text{C}$ was as found for initiator **5**; the major species observed in solution were due to **4** – with characteristic Cp (5.55 ppm), Cp* (1.26 ppm), SiMe_3 (0.023 ppm), and $[\text{CH}_3\text{B}(\text{C}_6\text{F}_5)_3]^-$ (-0.18 ppm) resonances – and free propene. The initiation reaction was monitored over time by ^1H NMR spectroscopy and the signals for **4** decreased with a concomitant formation of broad resonances due to

the propagating species **6** located at: Cp (5.59, 5.55 ppm), Cp* (1.24, 1.19 ppm), polymeryl-SiMe₃ (0.13 ppm), and [CH₃B(C₆F₅)₃]⁻ (-0.12, -0.17 ppm) and polypropene.

Initiation kinetics were measured at -70 °C in toluene-*d*₈ for both initiators and the disappearance of starting catalyst and propene were monitored as a function of time by ¹H NMR spectroscopy. This data was analyzed and treated as described above, with *k*_{obs} obtained from the slope of ln([initiator]_t[propene]_t/[propene]₀) vs time plots. Second-order rate constants for initiation, *k*_i, were calculated using the expression *k*_i = *k*_{obs} ÷ [propene]₀, where [propene]₀ is the initial propene concentration. The *k*_i reported are the average of two to three kinetic measurements (Table 2).

Table 2. Initiation rate constants for the reaction of propene with [CpCp*Zr(R)]⁺[CH₃B(C₆F₅)₃]⁻ in toluene-*d*₈ at -70 °C

R	<i>k</i> _i × 10 ³ (M ⁻¹ s ⁻¹)	<i>k</i> _p / <i>k</i> _i ^a
CH ₂ CMe ₃	13(1)	0.7
CH ₂ SiMe ₃	0.043(3)	214
CH ₃	0.061(5)	151

^a At -70 °C *k*_p × 10³ = 9.2(9) M⁻¹s⁻¹.

2.6 Addition of 2,3,3-trimethyl-1-butene to [CpCp*Zr(Np)]⁺[CH₃B(C₆F₅)₃]⁻, [CpCp*Zr(CH₂TMS)]⁺[CH₃B(C₆F₅)₃]⁻, and [CpCp*Zr(CH₃)]⁺[CH₃B(C₆F₅)₃]⁻ initiators

¹H and ¹⁹F NMR spectroscopic parameters are used to describe the cation-anion interaction in group 4 [Cp₂M(R)]⁺[CH₃B(C₆F₅)₃]⁻ (M = Ti, Zr, Hf; R = alkyl) compounds. These parameters are the chemical shift of the [CH₃B(C₆F₅)₃]⁻ resonance in the ¹H NMR spectrum and the chemical shift separation of the *p*-F and *m*-F resonances of the [CH₃B(C₆F₅)₃]⁻ group [Δδ(*m,p*-F)] in the ¹⁹F NMR spectrum.^{14,15} Contact or “tight” ion-pairs have [CH₃B(C₆F₅)₃]⁻ resonances located < 0.5 ppm and [Δδ(*m,p*-F)] values between

3-6 ppm. Weak or solvent-separated ion-pairs have downfield shifted $[CH_3B(C_6F_5)_3]^-$ resonances (found > 1 ppm) and $[\Delta\delta(m,p-F)] < 3$ ppm.

In toluene- d_8 at -70°C the initiators **1**, **4**, and **5** showed $[CH_3B(C_6F_5)_3]^-$ chemical shift and $\Delta\delta(m,p-F)$ values consistent with contact ion-pairing (Table 3).^{14,15} A predetermined amount of 2,3,3-trimethyl-1-butene $H_2C=C(Me)(^tBu)$ was injected into catalyst solutions and NMR spectra (1H , ^{19}F) were acquired. Up to 123 equivalents $H_2C=C(Me)(^tBu)$ was sequentially added to each initiator.

In all cases the species detected in solution were **1**, **4**, or **5** and free $H_2C=C(Me)(^tBu)$. No evidence for alkene adducts was observed (by 1H or ^{19}F NMR spectroscopy) over the range of conditions examined: **1** (0.008 mmol), alkene (0.03-0.7 mmol, 4-82 equiv); **4** (0.008 mmol), alkene (0.01-0.9 mmol, 1-104 equiv); **5** (0.01 mmol), alkene (0.03-0.8 mmol, 3-83 equiv). Likewise, there was no substantial change in the $[CH_3B(C_6F_5)_3]^-$ chemical shift and $\Delta\delta(m,p-F)$ values at moderate concentrations of $H_2C=C(Me)(^tBu)$ (< 30 equiv).

At greater concentrations of $H_2C=C(Me)(^tBu)$ an upfield shift of the $[CH_3B(C_6F_5)_3]^-$ resonance was observed for all initiators. This shift is most likely due to a change in solvent dielectric constant. The solvent volume was between 10-16% $H_2C=C(Me)(^tBu)$ at the highest alkene concentrations examined.

Table 3. NMR spectroscopic ion-pairing parameters for alkyl initiators in the presence of $\text{H}_2\text{C}=\text{C}(\text{Me})(^t\text{Bu})^{\text{a}}$

Initiator ^b	$\text{H}_2\text{C}=\text{C}(\text{Me})(^t\text{Bu})$ (equiv)	δ [$\text{CH}_3\text{B}(\text{C}_6\text{F}_5)_3$] ⁻ (ppm)	$\Delta\delta(m,p\text{-F})$ (ppm)
1	0	-0.113	5.27
	4	-0.115	5.24
	28	-0.123	5.25
	82	-0.136	5.18
4	0	-0.144	5.20
	1	-0.144	5.21
	31	-0.162	5.18
	104	-0.205	5.13
5	0	-0.224	5.40
	3	-0.230	5.36
	27	-0.245	5.33
	83	-0.284	5.30

^a Toluene- d_8 , -70 °C; ^b Initiator (mmol): **1** (0.008); **4** (0.008); **5** (0.01).

3 Discussion

The initiation step in zirconocene-catalyzed propene polymerization can be examined directly using NMR spectroscopy for $[\text{CpCp}^*\text{Zr}(\text{R})]^+[\text{CH}_3\text{B}(\text{C}_6\text{F}_5)_3]^-$ catalysts. The initiation of neopentylzirconocenium catalyst **1** is observed at low temperatures using low propene concentrations ($[\text{propene}]/[\mathbf{1}] < 10$). Under these conditions, spectroscopic evidence for the first-insertion product of initiation is the appearance of two discrete sets of resonances for the diastereomers of **2** (Figure 8). Qualitatively, detection of **2** implies that k_i is on the order of k_p . If k_p is much greater than k_i the major species in solution would be due to starting catalyst **1** and the propagating species **3**. Experimentally, this is consistent with relative rates of initiation and propagation predicted based on the propagation studies in Chapter 2.

These experiments also confirm that the two broad sets of resonances – first detected in propagation studies and assigned to propagating species **3** – do originate from zirconium-polymeryl species having polypropene chains of various lengths. As the

initiation reaction is followed over time, the discrete signals assigned to **2** decrease and broaden into those associated with **3**. The appearance of two sets of signals is attributed to the influence of the stereogenic centers at zirconium and the β -carbon of the polymeryl chains of **3**. The broadness of the resonances reflects the distribution of propagating species in solution, formally the different $\{\text{Zr}\}^+$ -polymeryl chain lengths.

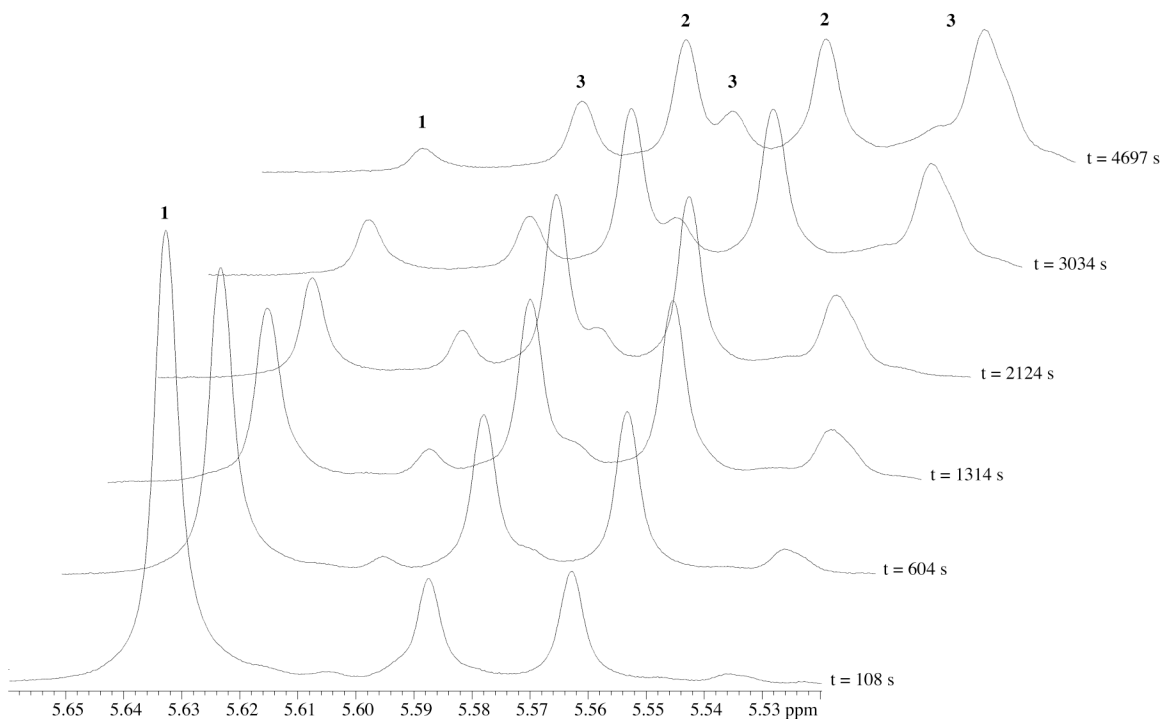


Figure 8. Partial ^1H NMR spectra showing expanded Cp region following the initiation reaction of **1** with 11 equivalents propene in toluene- d_8 at $-80\text{ }^\circ\text{C}$.

Measurement of propene initiation kinetics for catalyst **1** confirms that $k_i \cong k_p$. This special property may be related to the similarity of this initiator to the propagating species.⁷ The neopentyl group should closely resemble the polymeryl in propene propagation, in both Zr-C bond strength and steric influence on extent of ion-pairing. Therefore, initiation of **1** and propagation via **3** require breaking Zr-C bonds of comparable BDE. This leads to similar rates of initiation and propagation, since the

magnitude of the activation barrier is related to the Zr-C bond strength.¹¹ Consistent with this are the close ΔH^\ddagger ($\Delta H_i^\ddagger = 6(1)$ kcal·mol⁻¹; $\Delta H_p^\ddagger = 8.5(3)$ kcal·mol⁻¹) values for propene initiation and propagation kinetics determined from temperature dependence studies.

A comparison of the relative extent of cation-anion ion-pairing in neopentyl initiator and the propagating species also supports the assessment of catalyst **1** as a propagating species model. The nearly coincident location of $[\text{CH}_3\text{B}(\text{C}_6\text{F}_5)_3]^-$ resonances in the ¹H NMR spectra of **1** and **3** is qualitatively interpreted as a similar degree of cation-anion interaction.¹⁴ Thus the neopentyl and poly(propenyl) groups appear to exert similar steric influence on the ion-pairing interaction in the ground state structure.

Entirely different initiation behavior is observed for the reaction of catalysts **4** or **5** with propene. In both cases, less than 50% catalyst initiation occurs in the presence of > 20 equivalents propene suggesting k_i is much smaller than k_p for these systems. Measurement of k_i (-70 °C, toluene-*d*₈) for the methyl initiator **5** reveals that insertion of propene into $\{\text{Zr}\}^+-\text{CH}_3$ is slower than subsequent insertions into $\{\text{Zr}\}^+-\text{poly}(\text{propenyl})$ by a factor of ca. 150. This is in line with the k_p/k_i (-40 °C) = 400 found for insertion of 1-hexene into $[\text{rac}-(\text{C}_2\text{H}_4(1\text{-indenyl})_2)\text{Zr}-\text{CH}_3]^+[\text{CH}_3\text{B}(\text{C}_6\text{F}_5)_3]^-$ vs the propagating $[\{\text{Zr}\}-\text{poly}(\text{hexenyl})]^+ [\text{CH}_3\text{B}(\text{C}_6\text{F}_5)_3]^-$.⁷ Both studies lead to the conclusion that methyl initiators are poor models for the propagating species in polymerization.

Somewhat surprising is the poor initiation behavior of the $[\{\text{Zr}\}-\text{CH}_2\text{TMS}]^+ [\text{CH}_3\text{B}(\text{C}_6\text{F}_5)_3]^-$ catalyst **4** as it was expected to serve as a propagating species analogue. This catalyst appears to behave similarly to methyl initiator **5** with k_p/k_i (-70 °C) \approx 200 for propene polymerization.

The initiation behavior observed for the $[\text{CpCp}^*\text{Zr}(\text{R})]^+[\text{CH}_3\text{B}(\text{C}_6\text{F}_5)_3]^-$ series can be considered in the context of relative differences in Zr-alkyl bond dissociation energies (BDE) and in extent of $[\{\text{Zr}\}-\text{R}]^+[\text{CH}_3\text{B}(\text{C}_6\text{F}_5)_3]^-$ ion-pairing interaction. The relative Zr-C BDEs can be predicted using the hydrocarbon R-H BDEs as a metric.¹⁶ The chemical shift of the $[\text{CH}_3\text{B}(\text{C}_6\text{F}_5)_3]^-$ group in the ^1H NMR spectra is used to indicate the degree of ion-pairing.¹⁴

Both of these factors predict that methyl initiator **5** should be a poor initiator relative to neopentyl initiator **1**, as is observed experimentally (Figure 9). The BDE of $\{\text{Zr}\}^+-\text{CH}_2\text{CMe}_3$ is estimated to be less than the BDE of $\{\text{Zr}\}^+-\text{CH}_3$ by at least $5 \text{ kcal}\cdot\text{mol}^{-1}$.^{16,17} For catalysts **1** and **5** the relative rates of initiation in propene polymerization parallel the predicated ordering of Zr-C bond strengths. This finding is consistent with the trend observed previously for ethylene insertion into $\text{Cp}^*_2\text{Sc}-\text{CH}_3$ vs $\text{Cp}^*_2\text{Sc}-\text{CH}_2\text{CH}_2\text{CH}_3$.¹¹ That propene insertion into **1** is only favored by a factor of 213 suggests that $\Delta(\Delta H^\ddagger) < \Delta(\text{BDE})$ and may result in part from an increased steric contribution to the insertion barrier for the bulky neopentyl alkyl.

The cation-anion interaction in **1** is relatively weaker than that in **5** as assessed by ^1H NMR spectroscopy.¹⁴ The downfield shift of $[\text{CH}_3\text{B}(\text{C}_6\text{F}_5)_3]^-$ in **1** (-0.11 ppm) relative to **5** (-0.23 ppm) is consistent with a diminished ion-pair interaction, as expected for the more congested **1**. Therefore, separation of ions is more difficult with **5** and being less electrophilic it should have reduced propene binding affinity. These factors also contribute to the slow rate of initiation.

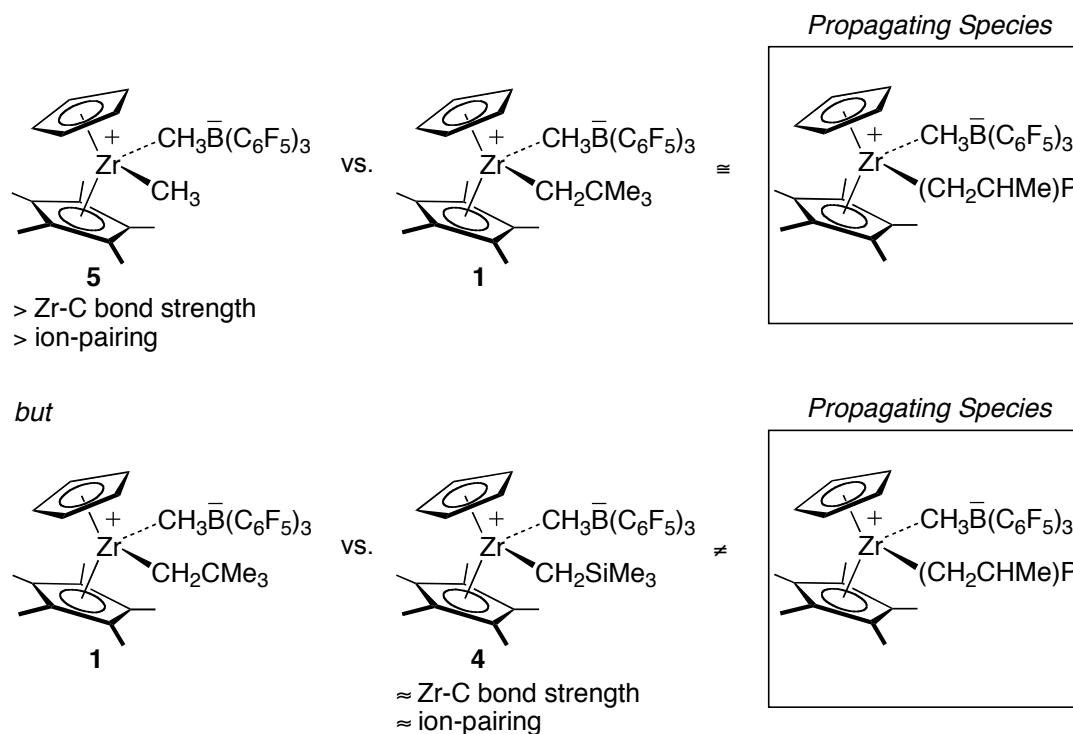


Figure 9. Using predicted difference in Zr-C bond strengths and extent of ion-pairing to relate initiators **1**, **4**, and **5** to the propagating species.

These Zr-C bond strength and ion-pairing metrics predict similar initiation behavior for the $[\{\text{Zr}\}\text{-CH}_2\text{CMe}_3]^+[\text{CH}_3\text{B}(\text{C}_6\text{F}_5)_3]^-$ and $[\{\text{Zr}\}\text{-CH}_2\text{TMS}]^+[\text{CH}_3\text{B}(\text{C}_6\text{F}_5)_3]^-$ catalysts. The relative difference in H-CH₂CMe₃ (99 kcal/mol) and H-CH₂TMS (99 kcal/mol) BDEs suggest $\Delta(\text{BDE}) \approx 0 \text{ kcal}\cdot\text{mol}^{-1}$ for these catalysts.¹⁷ Similar degrees of ion-pairing are observed with $\delta[\text{CH}_3\text{B}(\text{C}_6\text{F}_5)_3]^- = -0.11$ and -0.14 ppm for **1** and **4** respectively. This prediction is not borne out experimentally as **4** is a poor initiator relative to **1** with propene insertion into $[\{\text{Zr}\}\text{-CH}_2\text{CMe}_3]^+[\text{CH}_3\text{B}(\text{C}_6\text{F}_5)_3]^-$ favored by a factor of 300.

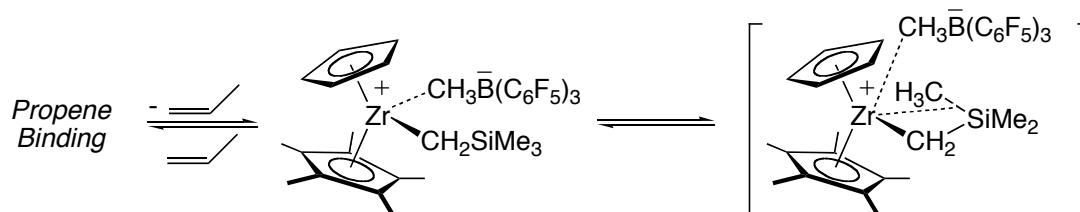
The disparity in initiation behavior observed for catalysts **1** and **4** may be due to the β -silyl group and therefore electronic in origin. Recent DFT studies by Eisenstein et al. on $\text{La}\{\text{CH}(\text{SiMe}_3)_2\}_3$ find highly polarized La-C bonding where negative charge build-up on the α -carbon is delocalized into the β -SiMe₃ group.¹⁸ This negative hyperconjugation

results in negative charge build-up on a Si-CH₃ group and in an elongated Si-C bond. The electropositive La³⁺ interacts with this Si-CH₃ group leading to a contraction of the La-C-Si angle and a formally β-agostic La-(CH₃)-Si interaction. The authors suggest this type of interaction is generally important for electropositive metal centers with an available β-SiMe₃ group.

This bridging M-(CH₃)-Si interaction has been observed in the solid-state for group 3 metallocene compounds in X-ray diffraction studies^{19,20} and in solution for [(Me)₂Cp₂Zr CH(SiMe₃)₂]⁺[CH₃B(C₆F₅)₃]⁻.⁹ In the later case a static interaction was identified at -126 °C.

A bridging Zr-(CH₃)-Si interaction may stabilize the ground state of **4** relative to **1** and explain the slow rate of propene insertion into the {Zr}⁺-CH₂TMS bond (Scheme 3). Interaction with the β-Si-CH₃ group would reduce the electrophilicity of the Zr center. Additionally, propene would compete with this intramolecular interaction for binding to the metal center. Current experimental studies have not identified this interaction in initiator **4** as the ¹H and ¹³C spectroscopic data do not support a static β agostic Si-C ground state structure at the lowest accessible temperature (-80 °C). However, much lower temperatures should be required to observe a static interaction based on literature precedence (vide supra).⁹

Scheme 3



Alternatively, the relative initiation behavior observed for **1** and **4** may be due to transition state differences. Based on the DFT studies, these alkyl groups are likely quite different both electronically and in geometrical arrangement.¹⁸ If the $\{\text{Zr}\}^+\text{-CH}_2\text{TMS}$ group facilitates a $\beta\text{-Si-CH}_3$ interaction rather than an $\alpha\text{-C-H}$ agostic interaction, the transition state for propene insertion may be destabilized for **4** relative to **1**. Along these lines a contracted Zr-C-Si angle would make this alkyl appear more sterically bulky leading to a larger steric barrier for insertion.

4 Conclusions

Propene initiation kinetics have been investigated for a series of $[\text{CpCp}^*\text{Zr(R)}]^+[\text{CH}_3\text{B}(\text{C}_6\text{F}_5)_3]^-$ initiators using direct NMR methods. Measurement of the propene initiation rate constant for the neopentylzirconocene catalyst confirms that $k_i \cong k_p$ for this system. This initiation behavior along with spectral properties (^1H , ^{19}F NMR) suggests that it models the propagating zirconium-polymeryl catalyst species in propene polymerization.

The relative rates of initiation observed for $[\text{CpCp}^*\text{Zr(R)}]^+[\text{CH}_3\text{B}(\text{C}_6\text{F}_5)_3]^-$ methyl vs neopentyl initiators follows the trend predicted by ordering of Zr-C bond strength and extent of ion-pairing. Propene insertion into a $\{\text{Zr}\}^+\text{-polymeryl}$ is favored over into the methyl initiator by at least a factor of 150. That $k_i \ll k_p$ for the methyl initiator confirms this catalyst is a poor model for the propagating species in propene polymerization. The slow initiation rate of the $[\text{CpCp}^*\text{Zr}(\text{CH}_2\text{TMS})]^+[\text{CH}_3\text{B}(\text{C}_6\text{F}_5)_3]^-$ catalyst is not explained by these ground-state considerations. The observed difference is most likely electronic in origin – either due to a ground-state stabilizing negative hyperconjugative interaction or a destabilization of the insertion transition state. The disparity in initiation rate between the

$[\text{CpCp}^*\text{Zr}(\text{CH}_2\text{CMe}_3)]^+[\text{CH}_3\text{B}(\text{C}_6\text{F}_5)_3]^-$ and $[\text{CpCp}^*\text{Zr}(\text{CH}_2\text{TMS})]^+[\text{CH}_3\text{B}(\text{C}_6\text{F}_5)_3]^-$ catalysts highlights the delicate interplay of factors – M-C bond strength, alkyl and ligand steric influence, and appropriate electronics – required to achieve the special property of $k_i \cong k_p$.

5 Experimental Section

General Considerations

All air- and moisture-sensitive compounds were manipulated using standard high vacuum line, Schlenk, or cannula techniques, or in a drybox under a nitrogen atmosphere as described previously.²¹ Argon gas was purified and dried by passage through columns of MnO on vermiculite and activated 4 Å molecular sieves. Solvents for air- and moisture-sensitive reactions were dried by the method of Grubbs²² and were stored under vacuum over sodium benzophenone ketyl (pentane) or titanocene²³ (toluene, petroleum ether). Benzene-*d*₆ and toluene-*d*₈ were purchased from Cambridge Isotopes and vacuum distilled from sodium benzophenone ketyl. The syntheses of $(\eta^5\text{-C}_5\text{H}_5)(\eta^5\text{-C}_5\text{Me}_5)\text{Zr}(\text{CH}_2\text{CMe}_3)(\text{CH}_3)$ and $(\eta^5\text{-C}_5\text{H}_5)(\eta^5\text{-C}_5\text{Me}_5)\text{Zr}(\text{CH}_2\text{SiMe}_3)(\text{CH}_3)$ were carried out as described in Chapter 1. $[(\eta^5\text{-C}_5\text{H}_5)(\eta^5\text{-C}_5\text{Me}_5)\text{Zr}(\text{CH}_3)]^+[\text{CH}_3\text{B}(\text{C}_6\text{F}_5)_3]^-$ was prepared using standard methodology.²⁴ $\text{B}(\text{C}_6\text{F}_5)_3$ was prepared according to literature procedure²⁵ or was purchased (Strem) and sublimed before use. Diphenylmethane (Aldrich) was dried by passage through a plug of activated alumina and stored over activated 4 Å molecular sieves under N₂. Propene (Polymer grade, Matheson) was purified and dried by passage through columns of MnO on vermiculite and activated 4 Å molecular sieves and was subjected to a freeze-pump-thaw cycle prior to use. 2,3,3-Trimethyl-1-butene was

vacuum distilled from LiAlH_4 and stored over activated 4 Å molecular sieves under N_2 . Other materials were used as received.

Glassware used for vacuum transfer and storage of toluene- d_8 was flame-evacuated prior to use. Glassware and J. Young NMR tubes used for kinetics experiments and screw-capped NMR tubes were pre-treated by washing with a 15% (w/w) solution of trimethylchlorosilane in methylene chloride, then rinsed with methylene chloride then acetone. J. Young NMR tubes were *gently* heated and evacuated on the high vacuum line before use in kinetics experiments.

NMR spectra were recorded on a Varian Mercury 300 (^1H , 299.868 MHz, ^{13}C , 75.409 MHz) or a Varian INOVA 500 (^1H , 499.851 MHz, ^{19}F , 470.261 MHz, ^{13}C , 125.697 MHz). Chemical shifts in ^1H and ^{13}C NMR spectra are reported in ppm downfield from TMS using residual proton ($\text{C}_6\text{D}_5\text{H}$, δ 7.16; $\text{C}_6\text{D}_5\text{CD}_2\text{H}$, δ 2.09) or carbon (C_6D_6 , δ 128.39; $\text{C}_6\text{D}_5\text{CD}_3$, δ 20.4) signals of the deuterated solvents. Chemical shifts in ^{19}F NMR spectra are given in ppm downfield from CFCl_3 used as an external reference. NMR spectra are reported at ambient temperature, unless otherwise indicated. Temperatures were measured using a pure methanol standard.

**Synthesis of $[(\eta^5\text{-C}_5\text{H}_5)(\eta^5\text{-C}_5\text{Me}_5)\text{Zr}(\text{CH}_2\text{CMe}_3)]^+[\text{CH}_3\text{B}(\text{C}_6\text{F}_5)_3]^-$ (1).
 $([\text{CpCp}^*\text{Zr}(\text{Np})]^+[\text{MeBAr}_3\text{F}])^-$.**

Due to its temperature instability, compound **1** was prepared in situ. In an inert atmosphere glovebox, the following were added to a J. Young NMR tube via gas-tight

microsyringe at ambient temperature: 100 μL stock solution ($\eta^5\text{-C}_5\text{H}_5$)($\eta^5\text{-C}_5\text{Me}_5$)Zr(CH₂CMe₃)(CH₃) (3.5 mg, 0.009 mmol) in toluene-*d*₈ and 50 μL stock solution Ph₂CH₂ (5.1 mg, 0.03 mmol) in toluene-*d*₈ as an internal standard. The walls of the NMR tube were rinsed with 250 μL toluene-*d*₈. The NMR tube was inserted into a glass sample holder located in the glovebox cold well, which was cooled externally with liquid nitrogen. The pale yellow solution was allowed to freeze. An additional 200 μL toluene-*d*₈ was added on top of the frozen layer, and was allowed to freeze. Then 100 μL of a stock solution of B(C₆F₅)₃ (5.3 mg, 0.010 mmol) in toluene-*d*₈ was added on top of the frozen layer, and was allowed to freeze. The NMR tube was sealed with a Teflon needle valve. The chilled sample holder was removed from the glovebox, and the NMR tube was *immediately* transferred to a $-196\text{ }^\circ\text{C}$ bath. The frozen sample was evacuated on the vacuum line. The sample was thawed at $-78\text{ }^\circ\text{C}$ in a dry ice-acetone bath and carefully mixed without warming the contents. Upon mixing a bright yellow solution was observed. The sample was then characterized using NMR spectroscopy. ¹H NMR (500 MHz, C₇D₈, 183 K): δ 5.63 (s, C₅H₅, 5H), 1.85 (br d, CH₂C(CH₃)₃, 1H), 1.16 (s, C₅(CH₃)₅, 15H), 0.97 (s, CH₂C(CH₃)₃, 9H), -0.10 (br, CH₂C(CH₃)₃ and [CH₃B(C₆F₅)₃]⁻, 4H); δ 7.20 to 6.90 (aryl resonances, Ph₂CH₂), 3.62 (s, Ph₂CH₂, 2H). ¹⁹F NMR (470 MHz, C₇D₈, 183 K): δ -130.5 (br, *o*-F [CH₃B(C₆F₅)₃]⁻, 6F), -155.6 (br, *p*-F [CH₃B(C₆F₅)₃]⁻, 3F), -160.9 (br, *m*-F [CH₃B(C₆F₅)₃]⁻, 6F); δ -126.0 (br, *o*-F B(C₆F₅)₃, 6F), -136.7 (br, *p*-F B(C₆F₅)₃, 3F), -158.0 (br, *m*-F B(C₆F₅)₃, 6F).

Measurement of initiation kinetics for propene polymerization with $[(\eta^5\text{-C}_5\text{H}_5)(\eta^5\text{-C}_5\text{Me}_5)\text{Zr}(\text{CH}_2\text{CMe}_3)]^+[\text{CH}_3\text{B}(\text{C}_6\text{F}_5)_3]^-$ (1**).**

A solution of **1** (0.007-0.009 mmol, 10-11.5 mM, 1 equiv) in toluene- d_8 was prepared in a 5mm thin-walled NMR tube with a J. Young valve as described above. The sample was evacuated on the vacuum line at $-196\text{ }^\circ\text{C}$, then was thawed at $-78\text{ }^\circ\text{C}$ in a dry ice-acetone bath. Careful mixing of the sample - without warming the contents - generated a bright yellow solution. The ^1H and ^{19}F NMR spectra of the sample were obtained at the experimental temperature. On the vacuum line the sample was frozen, degassed, and a measured gas volume of the propene (0.065-0.19 mmol, 0.08-0.25 M, 8-22 equiv) was condensed into the tube at $-196\text{ }^\circ\text{C}$.

The NMR probe was pre-equilibrated at the experimental temperature. The probe temperature was calibrated with a methanol thermometer before and after each kinetic experiment and was maintained at $\pm 0.2\text{ }^\circ\text{C}$ throughout data acquisition. The NMR samples were mixed using the following procedure: the frozen sample was removed from the $-196\text{ }^\circ\text{C}$ bath, thawed and *rapidly* mixed at $-78\text{ }^\circ\text{C}$ in a dry ice-acetone bath, and positioned in the spinner. The sample was *immediately* frozen at $-196\text{ }^\circ\text{C}$, was inserted into the NMR spectrometer, and was thawed at the preset temperature of the probe. Following equilibration (5 to 10 minutes) to the probe temperature, disappearance of **1** and propene were monitored by ^1H NMR spectroscopy. Spectra were recorded at regular intervals until the reaction was $> 88\%$ complete. The integral of **1** ($\eta^5\text{-C}_5\text{H}_5$) resonance and propene $\text{CH}_2\text{CH}(\text{CH}_3)$ resonance (relative to Ph_2CH_2 as an internal standard) was calculated as a function of time. The volume of the reaction mixture was determined as V (mL) = $0.01384H - 0.006754$, where H is the solution height in millimeters. The

observed rate constants, k_{obs} , were obtained from the slope of plots of $\ln([\mathbf{1}]_t[\text{propene}]_t/[\text{propene}]_0)$ versus time. The correction factor applied to each data point is $[\text{propene}]_t/[\text{propene}]_0$ which accounts for the continuous disappearance of propene. The initiation rate constant, k_i , at various temperatures was then calculated from the expression $k_i = k_{\text{obs}} \div [\text{propene}]_0$, where $[\text{propene}]_0$ represents the initial propene concentration. The values reported are the average of two to four kinetic measurements. Characterization of species observed upon addition of propene to solutions of **1** (note: some resonances cannot be assigned with certainty):

^1H NMR (500 MHz, C_7D_8 , 183 K): **1**: δ 5.63 (s, C_5H_5 , 5H), 1.84 (br, $\text{CH}_2\text{C}(\text{CH}_3)_3$, 1H), 1.16 (s, $\text{C}_5(\text{CH}_3)_5$, 15H), 0.96 (s, $\text{CH}_2\text{C}(\text{CH}_3)_3$, 9H), -0.10 (br, $\text{CH}_2\text{C}(\text{CH}_3)_3$ and $[\text{CH}_3\text{B}(\text{C}_6\text{F}_5)_3]^-$, 4H); **2**: δ 5.58, 5.56 (s, C_5H_5 , 5H), 1.17, 1.80 (s, $\text{C}_5(\text{CH}_3)_5$, 15H), -0.11 (br, $[\text{CH}_3\text{B}(\text{C}_6\text{F}_5)_3]^-$, 3H); **3**: δ 5.61, 5.53 (br, C_5H_5 , 5H), 1.21, 1.14 (br, $\text{C}_5(\text{CH}_3)_5$, 15H), -0.07, -0.16 (br, $[\text{CH}_3\text{B}(\text{C}_6\text{F}_5)_3]^-$, 3H); propene: δ 5.75 (m, $\text{CH}_2\text{CH}(\text{CH}_3)$, 1H), 5.07 (m, $\text{CH}_2\text{CH}(\text{CH}_3)$, 2H), 1.58 (m, $\text{CH}_2\text{CH}(\text{CH}_3)$, 3H). ^1H NMR (500 MHz, C_7D_8 , 193 K): **1**: δ 5.63 (s, C_5H_5 , 5H), 1.82 (d, $\text{CH}_2\text{C}(\text{CH}_3)_3$, 1H, $J = 11$ Hz), 1.17 (s, $\text{C}_5(\text{CH}_3)_5$, 15H), 0.95 (s, $\text{CH}_2\text{C}(\text{CH}_3)_3$, 9H), -0.11 (br d, $\text{CH}_2\text{C}(\text{CH}_3)_3$ and $[\text{CH}_3\text{B}(\text{C}_6\text{F}_5)_3]^-$, 4H, $J = 11$ Hz); **2**: δ 5.59, 5.56 (s, C_5H_5 , 5H), 1.19, 1.83 (s, $\text{C}_5(\text{CH}_3)_5$, 15H), -0.11 (br, $[\text{CH}_3\text{B}(\text{C}_6\text{F}_5)_3]^-$, 3H); **3**: δ 5.59, 5.55 (br, C_5H_5 , 5H), 1.22, 1.15 (br, $\text{C}_5(\text{CH}_3)_5$, 15H), -0.09, -0.17 (br, $[\text{CH}_3\text{B}(\text{C}_6\text{F}_5)_3]^-$, 3H); propene: δ 5.75 (m, $\text{CH}_2\text{CH}(\text{CH}_3)$, 1H), 5.06 (m, $\text{CH}_2\text{CH}(\text{CH}_3)$, 2H), 1.58 (m, $\text{CH}_2\text{CH}(\text{CH}_3)$, 3H). ^1H NMR (500 MHz, C_7D_8 , 203 K): **1**: δ 5.64 (s, C_5H_5 , 5H), 1.81 (d, $\text{CH}_2\text{C}(\text{CH}_3)_3$, 1H, $J = 11.5$ Hz), 1.18 (s, $\text{C}_5(\text{CH}_3)_5$, 15H), 0.94 (s, $\text{CH}_2\text{C}(\text{CH}_3)_3$, 9H), -0.11 (br d, $\text{CH}_2\text{C}(\text{CH}_3)_3$ and $[\text{CH}_3\text{B}(\text{C}_6\text{F}_5)_3]^-$, 4H, $J = 11.5$ Hz); **2**: δ 5.59, 5.56 (s, C_5H_5 , 5H), 1.21, 1.94 (s, $\text{C}_5(\text{CH}_3)_5$, 15H), -0.08, -0.16 (br, $[\text{CH}_3\text{B}(\text{C}_6\text{F}_5)_3]^-$, 3H); **3**: δ 5.59, 5.55 (br,

C_5H_5 , 5H), 1.23, 1.18 (br, $C_5(CH_3)_5$, 15H), -0.09, -0.17 (br, $[CH_3B(C_6F_5)_3]^-$, 3H); propene: δ 5.75 (m, $CH_2CH(CH_3)$, 1H), 5.05 (m, $CH_2CH(CH_3)$, 2H), 1.58 (m, $CH_2CH(CH_3)$, 3H).

Synthesis of $[(\eta^5-C_5H_5)(\eta^5-C_5Me_5)Zr(CH_2SiMe_3)]^+[CH_3B(C_6F_5)_3]^-$ (4). $[CpCp^*Zr(CH_2SiMe_3)]^+[CH_3B(C_6F_5)_3]^-$.

In the drybox a round bottom flask containing the oil $CpCp^*Zr(CH_2SiMe_3)(CH_3)$ (0.853 g, 2.16 mmol) was attached to a medium swivel frit assembly and $B(C_6F_5)_3$ (1.110 g, 2.16 mmol) was added on the frit, separated in space from $CpCp^*Zr(CH_2SiMe_3)(CH_3)$. On the vacuum line, the apparatus was evacuated and petroleum ether (100 ml) was transferred onto the oil at -78 °C. Vigorous stirring dissolved the oil and then solvent was transferred to the upper portion of the swivel frit to dissolve $B(C_6F_5)_3$. This solution filtered slowly into the reaction and immediately a pale yellow precipitate formed. This addition process was repeated four times. The reaction stirred at room temperature for 4 h. The precipitate was collected by filtration at -78 °C and washed one time with recycled solvent. The pale yellow solid was dried in vacuo. In the drybox, this solid transferred to a 25 mL round bottom flask equipped with a small swivel frit assembly. On the vacuum line petroleum ether (10 mL) was transferred onto the solid at -78 °C. The resulting slurry was stirred briefly at room temperature. The product was isolated by filtration at -78 °C and was dried in vacuo. Yield: 1.28 g (65%). 1H NMR (500 MHz, C_7D_8): δ 5.69 (s, C_5H_5 , 5H), 1.42 (s, $C_5(CH_3)_5$, 15H), 0.008 (s, $CH_2Si(CH_3)_3$, 9H), not located at this temperature: ($[CH_3B(C_6F_5)_3]^-$, 3H), ($CH_2Si(CH_3)_3$, 2H). ^{19}F NMR (470 MHz, C_7D_8): δ -133.6 (*o-F* $[CH_3B(C_6F_5)_3]^-$, 6F), -160.4 (*p-F* $[CH_3B(C_6F_5)_3]^-$, 3F), -165.2 (*m-F* $[CH_3B(C_6F_5)_3]^-$, 6F). $^{13}C\{^1H\}$ NMR (125 MHz, C_7D_8): δ 149.1 (d, $[CH_3B(C_6F_5)_3]^-$,

6C, $^1J_{CF} = 238.9$ Hz), 139.8 (d, $[\text{CH}_3\text{B}(\text{C}_6\text{F}_5)_3]^-$, 3C, $^1J_{CF} = 238.9$ Hz), 137.9 (d, $[\text{CH}_3\text{B}(\text{C}_6\text{F}_5)_3]^-$, 6C, $^1J_{CF} = 245.8$ Hz), 125.1 ($\text{C}_5(\text{CH}_3)_5$), 124.3 (br, $[\text{CH}_3\text{B}(\text{C}_6\text{F}_5)_3]^-$, 3C), 114.4 (C_5H_5), 72.9 ($\text{Zr-CH}_2\text{Si}(\text{CH}_3)_3$), 13.5 (br, $[\text{CH}_3\text{B}(\text{C}_6\text{F}_5)_3]^-$, 1C), 12.1 ($\text{C}_5(\text{CH}_3)_5$), 3.9 ($\text{CH}_2\text{Si}(\text{CH}_3)_3$).

Variable temperature NMR spectroscopic characterization of $[(\eta^5\text{-C}_5\text{H}_5)(\eta^5\text{-C}_5\text{Me}_5)\text{Zr}(\text{CH}_2\text{Si}(\text{CH}_3)_3)]^+[\text{CH}_3\text{B}(\text{C}_6\text{F}_5)_3]^-$ (4).

A J. Young NMR tube was charged with a sample of **4** and toluene- d_8 giving a yellow solution. The NMR probe was cooled and the probe temperature calculated using a pure methanol standard. The sample was inserted into the pre-thermostatted probe and allowed to equilibrate for 10 minutes prior to data acquisition. ^1H NMR (500 MHz, C_7D_8 , 193 K): δ 5.54 (s, C_5H_5 , 5H), 1.40 (d, $\text{CH}_2\text{Si}(\text{CH}_3)_3$, 1H, $J = 7.4$ Hz), 1.24 (s, $\text{C}_5(\text{CH}_3)_5$, 15H), 0.47 (d, $\text{CH}_2\text{Si}(\text{CH}_3)_3$, 1H, $J = 5.9$ Hz), 0.04 (s, $\text{CH}_2\text{Si}(\text{CH}_3)_3$, 9H), -0.144 (br s, $[\text{CH}_3\text{B}(\text{C}_6\text{F}_5)_3]^-$, 3H). ^{19}F NMR (470 MHz, C_7D_8 , 193 K): δ -133.4 (d, *o-F* $[\text{CH}_3\text{B}(\text{C}_6\text{F}_5)_3]^-$, 6F), -158.3 (br, *p-F* $[\text{CH}_3\text{B}(\text{C}_6\text{F}_5)_3]^-$, 3F), -163.5 (br, *m-F* $[\text{CH}_3\text{B}(\text{C}_6\text{F}_5)_3]^-$, 6F). $^{13}\text{C}\{^1\text{H}\}$ NMR (125 MHz, C_7D_8 , 195 K): δ 148.9 (d, $[\text{CH}_3\text{B}(\text{C}_6\text{F}_5)_3]^-$, 6C, $^1J_{CF} = 241.2$ Hz), 139.6 (d, $[\text{CH}_3\text{B}(\text{C}_6\text{F}_5)_3]^-$, 3C, $^1J_{CF} = 261.0$ Hz), 137.7 (d, $[\text{CH}_3\text{B}(\text{C}_6\text{F}_5)_3]^-$, 6C, $^1J_{CF} = 231.2$ Hz), 124.4 ($\text{C}_5(\text{CH}_3)_5$), 113.8 (C_5H_5), 70.1 ($\text{Zr-CH}_2\text{Si}(\text{CH}_3)_3$), 13.5 (br, $[\text{CH}_3\text{B}(\text{C}_6\text{F}_5)_3]^-$, 3C), 11.9 ($\text{C}_5(\text{CH}_3)_5$), 3.9 ($\text{CH}_2\text{Si}(\text{CH}_3)_3$), not located: ($[\text{CH}_3\text{B}(\text{C}_6\text{F}_5)_3]^-$, 3C), ($[\text{CH}_3\text{B}(\text{C}_6\text{F}_5)_3]^-$, 1C). ^{13}C NMR (125 MHz, 195 K): δ 148.9 (d, $[\text{CH}_3\text{B}(\text{C}_6\text{F}_5)_3]^-$, 6C, $^1J_{CF} = 241.2$ Hz), 139.6 (d, $[\text{CH}_3\text{B}(\text{C}_6\text{F}_5)_3]^-$, 3C, $^1J_{CF} = 261.0$ Hz), 137.7 (d, $[\text{CH}_3\text{B}(\text{C}_6\text{F}_5)_3]^-$, 6C, $^1J_{CF} = 231.2$ Hz), 124.3 (s, $\text{C}_5(\text{CH}_3)_5$, 5C), 113.8 (d, C_5H_5 , 5C, $^1J_{CH} = 171.6$ Hz), 11.9 (q, $\text{C}_5(\text{CH}_3)_5$, 5C, $^1J_{CH} = 127.5$ Hz), 3.9 ($\text{CH}_2\text{Si}(\text{CH}_3)_3$, 3C, $^1J_{CH} = 119.0$ Hz), not located: ($[\text{CH}_3\text{B}(\text{C}_6\text{F}_5)_3]^-$,

3C), (Zr-CH₂Si(CH₃)₃, 1C), ([CH₃B(C₆F₅)₃]⁻, 1C). ¹H NMR (500 MHz, C₇D₈, 203 K): δ 5.55 (s, C₅H₅, 5H), 1.41 (d, CH₂Si(CH₃)₃, 1H, J = 8.4 Hz), 1.25 (s, C₅(CH₃)₅, 15H), 0.42 (d, CH₂Si(CH₃)₃, 1H, J = 8.7 Hz), 0.033 (s, CH₂Si(CH₃)₃, 9H), -0.145 (br s, [CH₃B(C₆F₅)₃]⁻, 3H). ¹⁹F NMR (470 MHz, C₇D₈, 203 K): δ -133.8 (d, *o*-F [CH₃B(C₆F₅)₃]⁻, 6F), -158.7 (br, *p*-F [CH₃B(C₆F₅)₃]⁻, 3F), -164.0 (br, *m*-F [CH₃B(C₆F₅)₃]⁻, 6F). ¹H NMR (500 MHz, C₇D₈, 213 K): δ 5.56 (s, C₅H₅, 5H), 1.42 (d, CH₂Si(CH₃)₃, 1H, J = 8.5 Hz), 1.28 (s, C₅(CH₃)₅, 15H), 0.30 (d, CH₂Si(CH₃)₃, 1H, J = 8.5 Hz), 0.007 (s, CH₂Si(CH₃)₃, 9H), -0.146 (br s, [CH₃B(C₆F₅)₃]⁻, 3H). ¹⁹F NMR (470 MHz, C₇D₈, 213 K): δ -133.7 (d, *o*-F [CH₃B(C₆F₅)₃]⁻, 6F, ³J_{FF} = 19.4 Hz), -159.0 (t, *p*-F [CH₃B(C₆F₅)₃]⁻, 3F, ³J_{FF} = 19.4 Hz), -164.2 (br, *m*-F [CH₃B(C₆F₅)₃]⁻, 6F).

NMR observation of propene polymerization catalyzed by [(η⁵-C₅H₅)(η⁵-C₅Me₅)Zr(CH₂Si(CH₃)₃)]⁺[CH₃B(C₆F₅)₃]⁻ (4**).**

A solution of **4** (0.009 mmol, 12 mM, 1 equiv) in toluene-*d*₈ was prepared in a 5mm thin-walled NMR tube with a J. Young valve. Dissolution of the sample generated a yellow solution. The sample was evacuated on the vacuum line at -196 °C, then was thawed at ambient temperature. The NMR probe was pre-equilibrated at -60 °C. The probe temperature was calibrated with a methanol thermometer before and after the polymerization experiment and was maintained at ± 0.2 °C throughout data acquisition. The ¹H and ¹⁹F NMR spectra of the sample were obtained at -60 °C. On the vacuum line the sample was frozen, degassed, and a measured gas volume of propene (0.23 mmol, 0.33 M, 27 equiv) was condensed into the tube at -196 °C. The frozen sample was removed from the -196 °C bath, positioned in the spinner, and *immediately* inserted into

the NMR spectrometer. After thawing at the preset temperature of the probe, the sample was ejected, *quickly* mixed, and reinserted into the spectrometer without substantial warming. Following equilibration (5 to 10 minutes) to the probe temperature, disappearance of propene was monitored by ^1H NMR spectroscopy. Spectra were recorded at regular intervals until the reaction was $> 88\%$ complete. The volume of the reaction mixture was determined as $V \text{ (mL)} = 0.01384H - 0.006754$, where H is the solution height in millimeters.

Characterization of species observed upon addition of propene to solutions of **4**:

^1H NMR (500 MHz, C_7D_8 , 216 K): **6**: δ 5.60, 5.56 (br, C_5H_5 , 5H), 1.25, 1.19 (br, $\text{C}_5(\text{CH}_3)_5$, 15H), 0.11 (br, $\text{CH}_2\text{Si}(\text{CH}_3)_3$, 9H), -0.096 (br, $[\text{CH}_3\text{B}(\text{C}_6\text{F}_5)_3]^-$, 3H); **4**: δ 5.56 (s, C_5H_5 , 5H), 1.28 (s, $\text{C}_5(\text{CH}_3)_5$, 15H), 0.007 (s, $\text{CH}_2\text{Si}(\text{CH}_3)_3$, 9H), -0.15 (br s, $[\text{CH}_3\text{B}(\text{C}_6\text{F}_5)_3]^-$, 3H); propene: δ 5.74 (m, $\text{CH}_2\text{CH}(\text{CH}_3)$, 1H), 5.02 (m, $\text{CH}_2\text{CH}(\text{CH}_3)$, 2H), 1.57 (m, $\text{CH}_2\text{CH}(\text{CH}_3)$, 3H); poly(propene): δ 1.80 (br, CH , 1H), 1.33, 1.06 (br, CH_2 , 2H), 0.98 (br, CH_3 , 3H). ^{19}F NMR (470 MHz, C_7D_8 , 216 K): **6**: δ -133.2, 133.6 (br, *o-F* $[\text{CH}_3\text{B}(\text{C}_6\text{F}_5)_3]^-$, 6F), -159.0 (br, *p-F* $[\text{CH}_3\text{B}(\text{C}_6\text{F}_5)_3]^-$, 3F), -164.1 (br, *m-F* $[\text{CH}_3\text{B}(\text{C}_6\text{F}_5)_3]^-$, 6F); **4**: δ -133.7 (d, *o-F* $[\text{CH}_3\text{B}(\text{C}_6\text{F}_5)_3]^-$, 6F, $^3J_{\text{FF}} = 19.3$ Hz), -159.0 (br, *p-F* $[\text{CH}_3\text{B}(\text{C}_6\text{F}_5)_3]^-$, 3F), -164.1 (br, *m-F* $[\text{CH}_3\text{B}(\text{C}_6\text{F}_5)_3]^-$, 6F).

Variable temperature NMR spectroscopic characterization of $[(\eta^5\text{-C}_5\text{H}_5)(\eta^5\text{-C}_5\text{Me}_5)\text{Zr}(\text{CH}_3)]^+[\text{CH}_3\text{B}(\text{C}_6\text{F}_5)_3]^-$ (5**).**

A J. Young NMR tube was charged with a sample of **5** and toluene- d_8 giving a yellow solution. The NMR probe was cooled and the probe temperature calculated using a pure methanol standard. The sample was inserted into the pre-thermostatted probe and

allowed to equilibrate for 10 minutes prior to data acquisition. ^1H NMR (500 MHz, C_7D_8 , 193 K): δ 5.17 (s, C_5H_5 , 5H), 1.16 (s, $\text{C}_5(\text{CH}_3)_5$, 15H), 0.264 (s, CH_3 , 3H), -0.226 (br s, $[\text{CH}_3\text{B}(\text{C}_6\text{F}_5)_3]^-$, 3H). ^{19}F NMR (470 MHz, C_7D_8 , 193 K): δ -133.5 (br, *o-F* $[\text{CH}_3\text{B}(\text{C}_6\text{F}_5)_3]^-$, 6F), -158.2 (br, *p-F* $[\text{CH}_3\text{B}(\text{C}_6\text{F}_5)_3]^-$, 3F), -163.6 (br, *m-F* $[\text{CH}_3\text{B}(\text{C}_6\text{F}_5)_3]^-$, 6F). ^1H NMR (500 MHz, C_7D_8 , 203 K): δ 5.20 (s, C_5H_5 , 5H), 1.17 (s, $\text{C}_5(\text{CH}_3)_5$, 15H), 0.258 (s, CH_3 , 3H), -0.224 (br s, $[\text{CH}_3\text{B}(\text{C}_6\text{F}_5)_3]^-$, 3H). ^{19}F NMR (470 MHz, C_7D_8 , 203 K): δ -133.7 (br, *o-F* $[\text{CH}_3\text{B}(\text{C}_6\text{F}_5)_3]^-$, 6F), -158.6 (br, *p-F* $[\text{CH}_3\text{B}(\text{C}_6\text{F}_5)_3]^-$, 3F), -164.0 (br, *m-F* $[\text{CH}_3\text{B}(\text{C}_6\text{F}_5)_3]^-$, 6F). ^1H NMR (500 MHz, C_7D_8 , 216 K): δ 5.22 (s, C_5H_5 , 5H), 1.17 (s, $\text{C}_5(\text{CH}_3)_5$, 15H), 0.245 (s, CH_3 , 3H), -0.227 (br s, $[\text{CH}_3\text{B}(\text{C}_6\text{F}_5)_3]^-$, 3H). ^{19}F NMR (470 MHz, C_7D_8 , 216 K): δ -133.8 (d, *o-F* $[\text{CH}_3\text{B}(\text{C}_6\text{F}_5)_3]^-$, 6F, $^3J_{\text{FF}} = 21.5$ Hz), -158.7 (br, *p-F* $[\text{CH}_3\text{B}(\text{C}_6\text{F}_5)_3]^-$, 3F), -164.0 (br, *m-F* $[\text{CH}_3\text{B}(\text{C}_6\text{F}_5)_3]^-$, 6F). ^1H NMR (500 MHz, C_7D_8): δ 5.43 (s, C_5H_5 , 5H), 1.31 (s, $\text{C}_5(\text{CH}_3)_5$, 15H), 0.246 (s, CH_3 , 3H), -0.139 (br s, $[\text{CH}_3\text{B}(\text{C}_6\text{F}_5)_3]^-$, 3H). ^{19}F NMR (470 MHz, C_7D_8): δ -133.6 (d, *o-F* $[\text{CH}_3\text{B}(\text{C}_6\text{F}_5)_3]^-$, 6F, $^3J_{\text{FF}} = 22.2$ Hz), -159.5 (t, *p-F* $[\text{CH}_3\text{B}(\text{C}_6\text{F}_5)_3]^-$, 3F, $^3J_{\text{FF}} = 20.4$ Hz), -164.6 (br t, *m-F* $[\text{CH}_3\text{B}(\text{C}_6\text{F}_5)_3]^-$, 6F, $^3J_{\text{FF}} = 19.0$ Hz).

NMR observation of propene polymerization catalyzed by $[(\eta^5\text{-C}_5\text{H}_5)(\eta^5\text{-C}_5\text{Me}_5)\text{Zr}(\text{CH}_3)]^+[\text{CH}_3\text{B}(\text{C}_6\text{F}_5)_3]^-$ (5**).**

A solution of **5** (0.008 mmol, 10 mM, 1 equiv) in toluene- d_8 was prepared in a 5mm thin-walled NMR tube with a J. Young valve. Dissolution of the sample generated a yellow solution. The sample was evacuated on the vacuum line at -196 °C, then was thawed at ambient temperature. The NMR probe was pre-equilibrated at -57 °C. The probe temperature was calibrated with a methanol thermometer before and after the

polymerization experiment and was maintained at ± 0.2 °C throughout data acquisition. The ^1H and ^{19}F NMR spectra of the sample were obtained at -57 °C. On the vacuum line the sample was frozen, degassed, and a measured gas volume of propene (0.34 mmol, 0.4 M, 44 equiv) was condensed into the tube at -196 °C. The frozen sample was removed from the -196 °C bath, positioned in the spinner, and *immediately* inserted into the NMR spectrometer. After thawing at the preset temperature of the probe, the sample was ejected, *quickly* mixed, and reinserted into the spectrometer without substantial warming. Following equilibration (5 to 10 minutes) to the probe temperature, disappearance of propene was monitored by ^1H NMR spectroscopy. Spectra were recorded at regular intervals until the reaction was $> 88\%$ complete. The volume of the reaction mixture was determined as V (mL) = $0.01384H - 0.006754$, where H is the solution height in millimeters.

Characterization of species observed upon addition of propene to solutions of **5**:

^1H NMR (500 MHz, C_7D_8 , 216 K): **7**: δ 5.60, 5.56 (br, C_5H_5 , 5H), 1.25, 1.19 (br, $\text{C}_5(\text{CH}_3)_5$, 15H), -0.10, -0.18 (br, $[\text{CH}_3\text{B}(\text{C}_6\text{F}_5)_3]^-$, 3H); **5**: δ 5.22 (s, C_5H_5 , 5H), 1.17 (s, $\text{C}_5(\text{CH}_3)_5$, 15H), 0.24 (s, CH_3 , 3H), -0.23 (br s, $[\text{CH}_3\text{B}(\text{C}_6\text{F}_5)_3]^-$, 3H); propene: δ 5.74 (m, $\text{CH}_2\text{CH}(\text{CH}_3)$, 1H), 5.03 (m, $\text{CH}_2\text{CH}(\text{CH}_3)$, 2H), 1.58 (m, $\text{CH}_2\text{CH}(\text{CH}_3)$, 3H); poly(propene): δ 1.81 (br, CH , 1H), 1.33, 1.05 (br, CH_2 , 2H), 0.99 (br, CH_3 , 3H). ^{19}F NMR (470 MHz, C_7D_8 , 216 K): **7**: δ -133.3, 133.6 (br, *o-F* $[\text{CH}_3\text{B}(\text{C}_6\text{F}_5)_3]^-$, 6F), -158.8 (br, *p-F* $[\text{CH}_3\text{B}(\text{C}_6\text{F}_5)_3]^-$, 3F), -164.1 (br, *m-F* $[\text{CH}_3\text{B}(\text{C}_6\text{F}_5)_3]^-$, 6F); **5**: δ -133.8 (d, *o-F* $[\text{CH}_3\text{B}(\text{C}_6\text{F}_5)_3]^-$, 6F, $^3J_{\text{FF}} = 20.8$ Hz), -158.8 (br, *p-F* $[\text{CH}_3\text{B}(\text{C}_6\text{F}_5)_3]^-$, 3F), -164.1 (br, *m-F* $[\text{CH}_3\text{B}(\text{C}_6\text{F}_5)_3]^-$, 6F).

Measurement of initiation kinetics for propene polymerization with $[(\eta^5\text{-C}_5\text{H}_5)(\eta^5\text{-C}_5\text{Me}_5)\text{Zr}(\text{CH}_2\text{SiMe}_3)]^+[\text{CH}_3\text{B}(\text{C}_6\text{F}_5)_3]^-$ (4**).**

In an inert atmosphere glovebox a 5mm thin-walled NMR tube with a J. Young valve was charged with **4** (0.009–0.010 mmol, 12–3 mM, 1 equiv), 50 μL stock solution Ph_2CH_2 (6.0 mg, 0.03 mmol) in toluene- d_8 as an internal standard, and 700 μL toluene- d_8 to generate a yellow solution. The sample was evacuated on the vacuum line at $-196\text{ }^\circ\text{C}$, then was thawed at $-78\text{ }^\circ\text{C}$ in a dry ice-acetone bath. The ^1H NMR spectrum of the sample was obtained at $-70\text{ }^\circ\text{C}$. On the vacuum line the sample was frozen, degassed, and a measured gas volume of propene (0.97 mmol, 1.2 M, 100 equiv) was condensed into the tube at $-196\text{ }^\circ\text{C}$. The NMR probe was pre-equilibrated at $-70\text{ }^\circ\text{C}$. The probe temperature was calibrated with a methanol thermometer before and after each kinetic experiment and was maintained at $\pm 0.2\text{ }^\circ\text{C}$ throughout data acquisition. The frozen sample was removed from the $-196\text{ }^\circ\text{C}$ bath, thawed and *rapidly* mixed at $-78\text{ }^\circ\text{C}$ in a dry ice-acetone bath, and positioned in the spinner. The sample was *immediately* frozen at $-196\text{ }^\circ\text{C}$, was inserted into the NMR spectrometer, and was thawed at the preset temperature of the probe. Following equilibration (5 to 10 minutes) to the probe temperature, disappearance of **4** and propene were monitored by ^1H NMR spectroscopy. Spectra were recorded at regular intervals until the reaction was $> 75\%$ complete. The integral of **4** ($\eta^5\text{-C}_5\text{H}_5$) resonance and propene $\text{CH}_2\text{CH}(\text{CH}_3)$ resonance (relative to Ph_2CH_2 as an internal standard) was calculated as a function of time. The volume of the reaction mixture was determined as $V\text{ (mL)} = 0.01384H - 0.006754$, where H is the solution height in millimeters. The observed rate constants, k_{obs} , were obtained from the slope of plots of $\ln([\mathbf{4}]_t[\text{propene}]_t/[\text{propene}]_0)$ versus time. The correction factor applied

to each data point is $[\text{propene}]_t/[\text{propene}]_0$ which accounts for the continuous disappearance of propene. The initiation rate constant, k_i , at 203 K was then calculated from the expression $k_i = k_{\text{obs}} \div [\text{propene}]_0$, where $[\text{propene}]_0$ represents the initial propene concentration. The value reported is the average of two kinetic measurements.

Characterization of species observed upon addition of propene to solutions of **4** (note: some resonances could not be reported with certainty due to overlap with **4**, propene, or poly(propene) resonances; resonances due to Ph_2CH_2 are omitted):

^1H NMR (500 MHz, C_7D_8 , 203 K): **6**: δ 5.59, 5.55 (br, C_5H_5 , 5H), 1.20, 1.18 (br, $\text{C}_5(\text{CH}_3)_5$, 15H), 0.13 (br, $\text{CH}_2\text{Si}(\text{CH}_3)_3$, 9H), -0.07, -0.11 (br, $[\text{CH}_3\text{B}(\text{C}_6\text{F}_5)_3]^-$, 3H); **4**: δ 5.55 (s, C_5H_5 , 5H), 1.42 (d, $\text{CH}_2\text{Si}(\text{CH}_3)_3$, 1H, $J = 8.5$ Hz), 1.26 (s, $\text{C}_5(\text{CH}_3)_5$, 15H), 0.39 (d, $\text{CH}_2\text{Si}(\text{CH}_3)_3$, 1H, $J = 8.5$ Hz), 0.023 (s, $\text{CH}_2\text{Si}(\text{CH}_3)_3$, 9H), -0.17 (br s, $[\text{CH}_3\text{B}(\text{C}_6\text{F}_5)_3]^-$, 3H); propene: δ 5.74 (m, $\text{CH}_2\text{CH}(\text{CH}_3)$, 1H), 5.04 (m, $\text{CH}_2\text{CH}(\text{CH}_3)$, 2H), 1.58 (m, $\text{CH}_2\text{CH}(\text{CH}_3)$, 3H); poly(propene): δ 1.83 (br, CH, 1H), 1.34, 1.10 (br, CH_2 , 2H), 1.00 (br, CH_3 , 3H).

Measurement of initiation kinetics for propene polymerization with $[(\eta^5\text{-C}_5\text{H}_5)(\eta^5\text{-C}_5\text{Me}_5)\text{Zr}(\text{CH}_3)]^+[\text{CH}_3\text{B}(\text{C}_6\text{F}_5)_3]^-$ (5**).**

In an inert atmosphere glovebox a 5mm thin-walled NMR tube with a J. Young valve was charged with **5** (0.011–0.014 mmol, 15–18 mM, 1 equiv), 50 μL stock solution Ph_2CH_2 (6.0 mg, 0.03 mmol) in toluene- d_8 as an internal standard, and 700 μL toluene- d_8 to generate a yellow solution. The sample was evacuated on the vacuum line at -196 $^\circ\text{C}$, then was thawed at -78 $^\circ\text{C}$ in a dry ice-acetone bath. The ^1H NMR spectrum of the sample was obtained at -70 $^\circ\text{C}$. On the vacuum line the sample was frozen, degassed,

and a measured gas volume of propene (1.1 mmol, 1.4 M, 83-93 equiv) was condensed into the tube at $-196\text{ }^{\circ}\text{C}$. The NMR probe was pre-equilibrated at $-70\text{ }^{\circ}\text{C}$. The probe temperature was calibrated with a methanol thermometer before and after each kinetic experiment and was maintained at $\pm 0.2\text{ }^{\circ}\text{C}$ throughout data acquisition. The frozen sample was removed from the $-196\text{ }^{\circ}\text{C}$ bath, thawed and *rapidly* mixed at $-78\text{ }^{\circ}\text{C}$ in a dry ice-acetone bath, and positioned in the spinner. The sample was *immediately* frozen at $-196\text{ }^{\circ}\text{C}$, was inserted into the NMR spectrometer, and was thawed at the preset temperature of the probe. Following equilibration (5 to 10 minutes) to the probe temperature, disappearance of **5** and propene were monitored by ^1H NMR spectroscopy. Spectra were recorded at regular intervals until the reaction was $> 75\%$ complete. The integral of **5** ($\eta^5\text{-C}_5\text{H}_5$) resonance and propene $\text{CH}_2\text{CH}(\text{CH}_3)$ resonance (relative to Ph_2CH_2 as an internal standard) was calculated as a function of time. The volume of the reaction mixture was determined as $V\text{ (mL)} = 0.01384H - 0.006754$, where H is the solution height in millimeters. The observed rate constants, k_{obs} , were obtained from the slope of plots of $\ln([\mathbf{5}]_t[\text{propene}]_t/[\text{propene}]_0)$ versus time. The correction factor applied to each data point is $[\text{propene}]_t/[\text{propene}]_0$ which accounts for the continuous disappearance of propene. The initiation rate constant, k_i , at 203 K was then calculated from the expression $k_i = k_{\text{obs}} \div [\text{propene}]_0$, where $[\text{propene}]_0$ represents the initial propene concentration. The value reported is the average of three kinetic measurements.

Characterization of species observed upon addition of propene to solutions of **5** (note: some resonances could not be reported with certainty due to overlap with propene or poly(propene) resonances; resonances due to Ph_2CH_2 are omitted):

^1H NMR (500 MHz, C_7D_8 , 203 K): **7**: δ 5.59, 5.55 (br, C_5H_5 , 5H), 1.20, 1.18 (br, $\text{C}_5(\text{CH}_3)_5$, 15H), -0.12, -0.19 (br, $[\text{CH}_3\text{B}(\text{C}_6\text{F}_5)_3]^-$, 3H); **5**: δ 5.55 (s, C_5H_5 , 5H), 1.17 (s, $\text{C}_5(\text{CH}_3)_5$, 15H), 0.23 (s, CH_3 , 3H), -0.26 (br s, $[\text{CH}_3\text{B}(\text{C}_6\text{F}_5)_3]^-$, 3H); propene: δ 5.74 (m, $\text{CH}_2\text{CH}(\text{CH}_3)$, 1H), 5.03 (m, $\text{CH}_2\text{CH}(\text{CH}_3)$, 2H), 1.58 (m, $\text{CH}_2\text{CH}(\text{CH}_3)$, 3H); poly(propene): δ 1.82 (br, CH , 1H), 1.35, 1.10 (br, CH_2 , 2H), 0.99 (br, CH_3 , 3H).

Addition of 2,3,3-trimethyl-1-butene to $[(\eta^5\text{-C}_5\text{H}_5)(\eta^5\text{-C}_5\text{Me}_3)\text{Zr}(\text{CH}_2\text{CMe}_3)]^+[\text{CH}_3\text{B}(\text{C}_6\text{F}_5)_3]^-$ (1**) catalyst.**

A solution of **1** (0.008 mmol, 10 mM, 1 equiv) and Ph_2CH_2 (0.035 mmol; used as an internal standard) in toluene- d_8 was prepared in a 5mm thin-walled screw-capped NMR tube fitted with a septum as described above. The sample was thawed at -78 °C in a dry ice-acetone bath and carefully mixed without warming the contents. Upon mixing a bright yellow solution was observed. The NMR probe was pre-equilibrated at -70 °C. The probe temperature was calibrated with a methanol thermometer and was maintained at ± 0.2 °C throughout data acquisition. The ^1H and ^{19}F NMR spectra of the sample were obtained at -70 °C. A measured volume of 2,3,3-trimethyl-1-butene [$\text{CH}_2\text{C}(\text{CH}_3)_2(\text{CMe}_3)$] (0.03-0.66 mmol, 4-82 equiv) was injected into the sample using a gas-tight microsyringe at -78 °C. After careful mixing of the sample in the -78 °C bath, it was reinserted into the pre-thermostatted spectrometer. Following equilibration (5 to 10 minutes) to the probe temperature, the species in solution were monitored by ^1H and ^{19}F NMR spectroscopy. The amount of **1** and $\text{CH}_2\text{C}(\text{CH}_3)_2(\text{CMe}_3)$ in solution was quantified by integration versus the Ph_2CH_2 internal standard.

Characterization of species observed upon addition of $\text{CH}_2\text{C}(\text{CH}_3)(\text{CMe}_3)$ to solutions of **1** (resonances due to Ph_2CH_2 are omitted):

After addition of four equivalents $\text{CH}_2\text{C}(\text{CH}_3)(\text{CMe}_3)$: ^1H NMR (500 MHz, C_7D_8 , 203 K): **1**: δ 5.64 (s, C_5H_5 , 5H), 1.80 (d, $\text{CH}_2\text{C}(\text{CH}_3)_3$, 1H, $J = 11.0$ Hz), 1.18 (s, $\text{C}_5(\text{CH}_3)_5$, 15H), 0.94 (s, $\text{CH}_2\text{C}(\text{CH}_3)_3$, 9H), -0.11 (br d, $\text{CH}_2\text{C}(\text{CH}_3)_3$ and $[\text{CH}_3\text{B}(\text{C}_6\text{F}_5)_3]^-$, 4H, $J = 11.0$ Hz); $\text{CH}_2\text{C}(\text{CH}_3)(\text{CMe}_3)$: δ 4.90 (s, $\text{CH}_2\text{C}(\text{CH}_3)(\text{CMe}_3)$, 1H), 4.82 (s, $\text{CH}_2\text{C}(\text{CH}_3)(\text{CMe}_3)$, 1H), 1.70 (s, $\text{CH}_2\text{C}(\text{CH}_3)(\text{CMe}_3)$, 3H), 1.04 (s, $\text{CH}_2\text{C}(\text{CH}_3)(\text{CMe}_3)$, 9H). ^{19}F NMR (470 MHz, C_7D_8 , 203 K): **1**: δ -130.5 (br, *o-F* $[\text{CH}_3\text{B}(\text{C}_6\text{F}_5)_3]^-$, 6F), -155.8 (br, *p-F* $[\text{CH}_3\text{B}(\text{C}_6\text{F}_5)_3]^-$, 3F), -161.0 (br, *m-F* $[\text{CH}_3\text{B}(\text{C}_6\text{F}_5)_3]^-$, 6F).

After addition of 82 equivalents $\text{CH}_2\text{C}(\text{CH}_3)(\text{CMe}_3)$: ^1H NMR (500 MHz, C_7D_8 , 203 K): **1**: δ 5.63 (s, C_5H_5 , 5H), 1.78 (d, $\text{CH}_2\text{C}(\text{CH}_3)_3$, 1H, $J = 11.5$ Hz), 1.18 (s, $\text{C}_5(\text{CH}_3)_5$, 15H), 0.92 (s, $\text{CH}_2\text{C}(\text{CH}_3)_3$, 9H), -0.14 (br d, $\text{CH}_2\text{C}(\text{CH}_3)_3$ and $[\text{CH}_3\text{B}(\text{C}_6\text{F}_5)_3]^-$, 4H, $J = 11.0$ Hz); $\text{CH}_2\text{C}(\text{CH}_3)(\text{CMe}_3)$: δ 4.88 (s, $\text{CH}_2\text{C}(\text{CH}_3)(\text{CMe}_3)$, 1H), 4.80 (s, $\text{CH}_2\text{C}(\text{CH}_3)(\text{CMe}_3)$, 1H), 1.70 (s, $\text{CH}_2\text{C}(\text{CH}_3)(\text{CMe}_3)$, 3H), 1.04 (s, $\text{CH}_2\text{C}(\text{CH}_3)(\text{CMe}_3)$, 9H). ^{19}F NMR (470 MHz, C_7D_8 , 203 K): **1**: δ -130.5 (br, *o-F* $[\text{CH}_3\text{B}(\text{C}_6\text{F}_5)_3]^-$, 6F), -155.9 (br, *p-F* $[\text{CH}_3\text{B}(\text{C}_6\text{F}_5)_3]^-$, 3F), -161.1 (br, *m-F* $[\text{CH}_3\text{B}(\text{C}_6\text{F}_5)_3]^-$, 6F).

Addition of 2,3,3-trimethyl-1-butene to $[(\eta^5\text{-C}_5\text{H}_5)(\eta^5\text{-C}_5\text{Me}_5)\text{Zr}(\text{CH}_2\text{SiMe}_3)]^+[\text{CH}_3\text{B}(\text{C}_6\text{F}_5)_3]^-$ (4**) catalyst.**

A solution of **4** (0.009 mmol, 11 mM, 1 equiv) and Ph_2CH_2 (0.035 mmol; used as an internal standard) in toluene- d_8 was prepared in a 5mm thin-walled screw-capped NMR tube fitted with a septum. Dissolution of the sample generated a deep yellow solution. The NMR probe was pre-equilibrated at -70 °C. The probe temperature was calibrated

with a methanol thermometer and was maintained at ± 0.2 °C throughout data acquisition. The ^1H and ^{19}F NMR spectra of the sample were obtained at -70 °C. A measured volume of 2,3,3-trimethyl-1-butene [$\text{CH}_2\text{C}(\text{CH}_3)(\text{CMe}_3)$] (0.01-0.88 mmol, 1-104 equiv) was injected into the sample using a gas-tight microsyringe. After mixing the sample was reinserted into the pre-thermostatted spectrometer. Following equilibration (5 to 10 minutes) to the probe temperature, the species in solution were monitored by ^1H and ^{19}F NMR spectroscopy. The amount of **4** and $\text{CH}_2\text{C}(\text{CH}_3)(\text{CMe}_3)$ in solution was quantified by integration versus the Ph_2CH_2 internal standard.

Characterization of species observed upon addition of $\text{CH}_2\text{C}(\text{CH}_3)(\text{CMe}_3)$ to solutions of **4** (resonances due to Ph_2CH_2 are omitted):

After addition of 1.2 equivalents $\text{CH}_2\text{C}(\text{CH}_3)(\text{CMe}_3)$: ^1H NMR (500 MHz, C_7D_8 , 203 K): **4**: δ 5.54 (s, C_5H_5 , 5H), 1.41 (d, $\text{CH}_2\text{Si}(\text{CH}_3)_3$, 1H, $J = 8.5$ Hz), 1.25 (s, $\text{C}_5(\text{CH}_3)_5$, 15H), 0.42 (d, $\text{CH}_2\text{Si}(\text{CH}_3)_3$, 1H, $J = 8.5$ Hz), 0.032 (s, $\text{CH}_2\text{Si}(\text{CH}_3)_3$, 9H), -0.144 (br s, $[\text{CH}_3\text{B}(\text{C}_6\text{F}_5)_3]^-$, 3H); $\text{CH}_2\text{C}(\text{CH}_3)(\text{CMe}_3)$: δ 4.90 (s, $\text{CH}_2\text{C}(\text{CH}_3)(\text{CMe}_3)$, 1H), 4.83 (s, $\text{CH}_2\text{C}(\text{CH}_3)(\text{CMe}_3)$, 1H), 1.70 (s, $\text{CH}_2\text{C}(\text{CH}_3)(\text{CMe}_3)$, 3H), 1.04 (s, $\text{CH}_2\text{C}(\text{CH}_3)(\text{CMe}_3)$, 9H). ^{19}F NMR (470 MHz, C_7D_8 , 203 K): **4**: δ -133.8 (br, *o-F* $[\text{CH}_3\text{B}(\text{C}_6\text{F}_5)_3]^-$, 6F), -158.8 (br, *p-F* $[\text{CH}_3\text{B}(\text{C}_6\text{F}_5)_3]^-$, 3F), -164.0 (br, *m-F* $[\text{CH}_3\text{B}(\text{C}_6\text{F}_5)_3]^-$, 6F).

After addition of 104 equiv $\text{CH}_2\text{C}(\text{CH}_3)(\text{CMe}_3)$: ^1H NMR (500 MHz, C_7D_8 , 203 K): **4**: δ 5.53 (s, C_5H_5 , 5H), 1.39 (d, $\text{CH}_2\text{Si}(\text{CH}_3)_3$, 1H, $J = 9.0$ Hz), 1.25 (s, $\text{C}_5(\text{CH}_3)_5$, 15H), 0.35 (d, $\text{CH}_2\text{Si}(\text{CH}_3)_3$, 1H, $J = 9.0$ Hz), 0.008 (s, $\text{CH}_2\text{Si}(\text{CH}_3)_3$, 9H), -0.205 (br s, $[\text{CH}_3\text{B}(\text{C}_6\text{F}_5)_3]^-$, 3H); $\text{CH}_2\text{C}(\text{CH}_3)(\text{CMe}_3)$: δ 4.90 (s, $\text{CH}_2\text{C}(\text{CH}_3)(\text{CMe}_3)$, 1H), 4.83 (s, $\text{CH}_2\text{C}(\text{CH}_3)(\text{CMe}_3)$, 1H), 1.70 (s, $\text{CH}_2\text{C}(\text{CH}_3)(\text{CMe}_3)$, 3H), 1.04 (s, $\text{CH}_2\text{C}(\text{CH}_3)(\text{CMe}_3)$,

9H). ^{19}F NMR (470 MHz, C_7D_8 , 203 K): **4**: δ -133.9 (br, *o*-F [$\text{CH}_3\text{B}(\text{C}_6\text{F}_5)_3$] $^-$, 6F), -158.9 (br, *p*-F [$\text{CH}_3\text{B}(\text{C}_6\text{F}_5)_3$] $^-$, 3F), -164.0 (br, *m*-F [$\text{CH}_3\text{B}(\text{C}_6\text{F}_5)_3$] $^-$, 6F).

Addition of 2,3,3-trimethyl-1-butene to $[(\eta^5\text{-C}_5\text{H}_5)(\eta^5\text{-C}_5\text{Me}_5)\text{Zr}(\text{CH}_3)]^+[\text{CH}_3\text{B}(\text{C}_6\text{F}_5)_3]^-$ (5**) catalyst.**

A solution of **5** (0.010 mmol, 13 mM, 1 equiv) and Ph_2CH_2 (0.035 mmol; used as an internal standard) in toluene- d_8 was prepared in a 5mm thin-walled screw-capped NMR tube fitted with a septum. Dissolution of the sample generated a yellow solution. The NMR probe was pre-equilibrated at -70 °C. The probe temperature was calibrated with a methanol thermometer and was maintained at ± 0.2 °C throughout data acquisition. The ^1H and ^{19}F NMR spectra of the sample were obtained at -70 °C. A measured volume of 2,3,3-trimethyl-1-butene [$\text{CH}_2\text{C}(\text{CH}_3)_2(\text{CMe}_3)$] (0.03-0.85 mmol, 3-83 equiv) was injected into the sample using a gas-tight microsyringe. After mixing the sample was reinserted into the pre-thermostatted spectrometer. Following equilibration (5 to 10 minutes) to the probe temperature, the species in solution were monitored by ^1H and ^{19}F NMR spectroscopy. The amount of **5** and $\text{CH}_2\text{C}(\text{CH}_3)_2(\text{CMe}_3)$ in solution was quantified by integration versus the Ph_2CH_2 internal standard.

Characterization of species observed upon addition of $\text{CH}_2\text{C}(\text{CH}_3)_2(\text{CMe}_3)$ to solutions of **5** (resonances due to Ph_2CH_2 are omitted):

After addition of 2.75 equivalents $\text{CH}_2\text{C}(\text{CH}_3)_2(\text{CMe}_3)$: ^1H NMR (500 MHz, C_7D_8 , 203 K): **5**: δ 5.19 (s, C_5H_5 , 5H), 1.17 (s, $\text{C}_5(\text{CH}_3)_5$, 15H), 0.26 (s, CH_3 , 3H), -0.23 (br s, [$\text{CH}_3\text{B}(\text{C}_6\text{F}_5)_3$] $^-$, 3H); $\text{CH}_2\text{C}(\text{CH}_3)_2(\text{CMe}_3)$: δ 4.90 (s, $\text{CH}_2\text{C}(\text{CH}_3)_2(\text{CMe}_3)$, 1H), 4.82 (s, $\text{CH}_2\text{C}(\text{CH}_3)_2(\text{CMe}_3)$, 1H), 1.70 (s, $\text{CH}_2\text{C}(\text{CH}_3)_2(\text{CMe}_3)$, 3H), 1.04 (s, $\text{CH}_2\text{C}(\text{CH}_3)_2(\text{CMe}_3)$,

9H). ^{19}F NMR (470 MHz, C_7D_8 , 203 K): **5**: δ -133.7 (br, *o-F* [$\text{CH}_3\text{B}(\text{C}_6\text{F}_5)_3$] $^-$, 6F), -158.6 (br, *p-F* [$\text{CH}_3\text{B}(\text{C}_6\text{F}_5)_3$] $^-$, 3F), -164.0 (br, *m-F* [$\text{CH}_3\text{B}(\text{C}_6\text{F}_5)_3$] $^-$, 6F).

After addition of 83 equivalents $\text{CH}_2\text{C}(\text{CH}_3)(\text{CMe}_3)$: ^1H NMR (500 MHz, C_7D_8 , 203 K):

5: δ 5.19 (s, C_5H_5 , 5H), 1.17 (s, $\text{C}_5(\text{CH}_3)_5$, 15H), 0.26 (s, CH_3 , 3H), -0.28 (br s, [$\text{CH}_3\text{B}(\text{C}_6\text{F}_5)_3$] $^-$, 3H); $\text{CH}_2\text{C}(\text{CH}_3)(\text{CMe}_3)$: δ 4.90 (s, $\text{CH}_2\text{C}(\text{CH}_3)(\text{CMe}_3)$, 1H), 4.82 (s, $\text{CH}_2\text{C}(\text{CH}_3)(\text{CMe}_3)$, 1H), 1.70 (s, $\text{CH}_2\text{C}(\text{CH}_3)(\text{CMe}_3)$, 3H), 1.04 (s, $\text{CH}_2\text{C}(\text{CH}_3)(\text{CMe}_3)$,

9H). ^{19}F NMR (470 MHz, C_7D_8 , 203 K): **5**: δ -133.9 (br, *o-F* [$\text{CH}_3\text{B}(\text{C}_6\text{F}_5)_3$] $^-$, 6F), -158.8 (br, *p-F* [$\text{CH}_3\text{B}(\text{C}_6\text{F}_5)_3$] $^-$, 3F), -164.1 (br, *m-F* [$\text{CH}_3\text{B}(\text{C}_6\text{F}_5)_3$] $^-$, 6F).

Summary of Propene Initiation Kinetic Data

Table 4. Temperature dependence of propene initiation kinetics with **1**(toluene-*d*₈)

T (K)	[1] ₀ (M)	[propene] ₀ (M)	$k_{\text{obs}} \times 10^5$ (s ⁻¹)	$k_i \times 10^3$ (M ⁻¹ s ⁻¹)
182.9	0.0115	0.187	34(1)	1.8(6)
183.6	0.0115	0.247	63(2)	2.6(6)
183.6	0.0115	0.205	59(2)	2.9(6)
192.8	0.0113	0.126	73(1)	6(1)
192.8	0.0114	0.127	85(2)	7(1)
193.1	0.0107	0.129	104(2)	8(1)
194.8	0.0100	0.121	90(4)	7(1)
202.6	0.0104	0.084	120(2)	14(1)
202.8	0.0104	0.087	101(3)	12(1)

Table 5. Propene initiation kinetics for various alkylzirconocene initiators (203 K, toluene-*d*₈)

Initiator	[Zr] ₀ (M)	[propene] ₀ (M)	$k_{\text{obs}} \times 10^5$ (s ⁻¹)	$k_i \times 10^3$ (M ⁻¹ s ⁻¹)
1	0.0104	0.087	101(3)	12(1)
1	0.0104	0.084	120(2)	14(1)
5	0.0146	1.35	7.9(1)	0.058(5)
5	0.0166	1.38	8.3(2)	0.060(5)
5	0.0176	1.40	9.25(8)	0.066(5)
4	0.0121	1.22	5.58(6)	0.046(3)
4	0.0130	1.22	5.02(5)	0.041(3)

References

1. Brintzinger, H. H.; Fischer, D.; Mulhaupt, R.; Rieger, B.; Waymouth, R. M. *Angew. Chem., Int. Ed. Engl.* **1995**, *34*, 1143-1170.
2. Jordan, R. F. *Adv. Organomet. Chem.* **1991**, *32*, 325-387.
3. Coates, G. W.; Hustad, P. D.; Reinartz, S. *Angew. Chem., Int. Ed. Engl.* **2002**, *41*, 2236-2257.
4. Herfert, N.; Fink, G. *Makromol. Chem., Macromol. Symp.* **1993**, *66*, 157-178.
5. Mehrkhodavandi, P.; Bonitatebus, P. J.; Schrock, R. R. *J. Am. Chem. Soc.* **2000**, *122*, 7841-7842.
6. Liu, Z. X.; Somsook, E.; White, C. B.; Rosaaen, K. A.; Landis, C. R. *J. Am. Chem. Soc.* **2001**, *123*, 11193-11207.
7. Landis, C. R.; Rosaaen, K. A.; Sillars, D. R. *J. Am. Chem. Soc.* **2003**, *125*, 1710-1711.

8. Zhou, J. M.; Lancaster, S. J.; Walker, D. A.; Beck, S.; Thornton-Pett, M.; Bochmann, M. *J. Am. Chem. Soc.* **2001**, *123*, 223-237.
9. Beswick, C. L.; Marks, T. J. *J. Am. Chem. Soc.* **2000**, *122*, 10358-10370.
10. Moore, J. W.; Pearson, R. G. *Kinetics and Mechanism*; Wiley-Interscience: New York, 1981.
11. Burger, B. J.; Thompson, M. E.; Cotter, W. D.; Bercaw, J. E. *J. Am. Chem. Soc.* **1990**, *112*, 1566-1577.
12. Yang, X. M.; Stern, C. L.; Marks, T. J. *J. Am. Chem. Soc.* **1994**, *116*, 10015-10031.
13. gNMR, v3.6 for Macintosh, Cherwell Scientific Publishing Ltd.: Oxford Science Park, Oxford OX4 4GA, England.
14. Beck, S.; Lieber, S.; Schaper, F.; Geyer, A.; Brintzinger, H. H. *J. Am. Chem. Soc.* **2001**, *123*, 1483-1489.
15. Horton, A. D. *Organometallics* **1996**, *15*, 2675-2677.
16. Bryndza, H. E.; Fong, L. K.; Paciello, R. A.; Tam, W.; Bercaw, J. E. *J. Am. Chem. Soc.* **1987**, *109*, 1444-1456.
17. Dean, J. A. *Lange's Handbook of Chemistry and Physics*; 14th ed.; McGraw-Hill, INC.: New York, 1992.
18. Perrin, L.; Maron, L.; Eisenstein, O.; Lappert, M. F. *New J. Chem.* **2003**, *27*, 121-127.
19. Coughlin, E. B.; Henling, L. M.; Bercaw, J. E. *Inorg. Chim. Acta* **1996**, *242*, 205-210.
20. Zubris, D. L. Ph.D. Thesis, California Institute of Technology, 2001.
21. Burger, B. J.; Bercaw, J. E. *New Developments in the Synthesis, Manipulation, and Characterization of Organometallic Compounds*; American Chemical Society: Washington, DC, 1987; Vol. 357.
22. Pangborn, A. B.; Giardello, M. A.; Grubbs, R. H.; Rosen, R. K.; Timmers, F. J. *Organometallics* **1996**, *15*, 1518-1520.
23. Marvich, R. H.; Brintzinger, H. H. *J. Am. Chem. Soc.* **1971**, *93*, 2046-2048.
24. Wendt, O. F.; Bercaw, J. E. *manuscript in preparation*.
25. Massey, A. G.; Park, A. J. *J. Organomet. Chem.* **1964**, *2*, 245-250.

Appendix 1

Crystallographic Parameters and Tables

Table 1. Crystal data and structure refinement for Compound 1

Empirical formula	C ₂₅ H ₄₂ Zr
Formula weight	433.81
Crystallization Solvent	Pentane
Crystal Habit	Chunks
Crystal size	0.26 x 0.20 x 0.19 mm ³
Crystal color	Pale yellow

Data Collection

Preliminary Photos	Rotation	
Type of diffractometer	Bruker SMART 1000	
Wavelength	0.71073 Å MoK α	
Data Collection Temperature	98(2) K	
θ range for 27315 reflections used in lattice determination	2.33 to 28.81°	
Unit cell dimensions	a = 9.7467(4) Å b = 25.9839(12) Å c = 10.2031(5) Å	β = 116.6710(10)°
Volume	2309.07(18) Å ³	
Z	4	
Crystal system	Monoclinic	
Space group	P2 ₁ /c	
Density (calculated)	1.248 Mg/m ³	
F(000)	928	
Data collection program	Bruker SMART v5.054	
θ range for data collection	1.57 to 28.37°	
Completeness to θ = 28.37°	94.2 %	
Index ranges	-12 \leq h \leq 12, -33 \leq k \leq 33, -13 \leq l \leq 13	
Data collection scan type	ω scans at 7 ϕ settings	
Data reduction program	Bruker SAINT v6.022	
Reflections collected	46222	
Independent reflections	5440 [R _{int} = 0.0466]	
Absorption coefficient	0.482 mm ⁻¹	
Absorption correction	None	
Max. and min. transmission	0.9140 and 0.8849	

Table 1 (cont.)**Structure solution and Refinement**

Structure solution program	SHELXS-97 (Sheldrick, 1990)
Primary solution method	Direct methods
Secondary solution method	Difference Fourier map
Hydrogen placement	Difference Fourier map
Structure refinement program	SHELXL-97 (Sheldrick, 1997)
Refinement method	Full matrix least-squares on F^2
Data / restraints / parameters	5440 / 0 / 403
Treatment of hydrogen atoms	Unrestrained
Goodness-of-fit on F^2	2.059
Final R indices [$I > 2\sigma(I)$, 4770 reflections]	$R1 = 0.0247$, $wR2 = 0.0475$
R indices (all data)	$R1 = 0.0305$, $wR2 = 0.0480$
Type of weighting scheme used	Sigma
Weighting scheme used	$w = 1/\sigma^2(F_o^2)$
Max shift/error	0.001
Average shift/error	0.000
Largest diff. peak and hole	0.473 and -0.323 e. \AA^{-3}

Special Refinement Details

Refinement of F^2 against ALL reflections. The weighted R-factor (wR) and goodness of fit (S) are based on F^2 , conventional R-factors (R) are based on F , with F set to zero for negative F^2 . The threshold expression of $F^2 > 2\sigma(F^2)$ is used only for calculating R-factors(gt) etc. and is not relevant to the choice of reflections for refinement. R-factors based on F^2 are statistically about twice as large as those based on F , and R-factors based on ALL data will be even larger.

All esds (except the esd in the dihedral angle between two l.s. planes) are estimated using the full covariance matrix. The cell esds are taken into account individually in the estimation of esds in distances, angles and torsion angles; correlations between esds in cell parameters are only used when they are defined by crystal symmetry. An approximate (isotropic) treatment of cell esds is used for estimating esds involving l.s. planes.

Table 2. Crystal data and structure refinement for Compound 2

Empirical formula	C ₂₃ H ₄₂ Si ₂ Zr
Formula weight	465.97
Crystallization Solvent	Pentane
Crystal Habit	Block
Crystal size	0.26 x 0.26 x 0.21 mm ³
Crystal color	Colorless

Data Collection

Preliminary Photos	Rotation	
Type of diffractometer	Bruker SMART 1000	
Wavelength	0.71073 Å MoK α	
Data Collection Temperature	98(2) K	
θ range for 29725 reflections used in lattice determination	2.28 to 28.24°	
Unit cell dimensions	a = 9.9621(5) Å b = 26.8264(13) Å c = 10.4769(5) Å	β = 116.3020(10)°
Volume	2510.0(2) Å ³	
Z	4	
Crystal system	Monoclinic	
Space group	P2 ₁ /c	
Density (calculated)	1.233 Mg/m ³	
F(000)	992	
Data collection program	Bruker SMART v5.054	
θ range for data collection	1.52 to 28.36°	
Completeness to θ = 28.36°	95.3 %	
Index ranges	-13 ≤ h ≤ 13, -35 ≤ k ≤ 35, -13 ≤ l ≤ 13	
Data collection scan type	ω scans at 7 ϕ settings	
Data reduction program	Bruker SAINT v6.022	
Reflections collected	51027	
Independent reflections	5985 [R _{int} = 0.0515]	
Absorption coefficient	0.539 mm ⁻¹	
Absorption correction	None	
Max. and min. transmission	0.8953 and 0.8726	

Table 2 (cont.)**Structure solution and Refinement**

Structure solution program	SHELXS-97 (Sheldrick, 1990)
Primary solution method	Direct methods
Secondary solution method	Difference Fourier map
Hydrogen placement	Difference Fourier map
Structure refinement program	SHELXL-97 (Sheldrick, 1997)
Refinement method	Full matrix least-squares on F^2
Data / restraints / parameters	5985 / 0 / 403
Treatment of hydrogen atoms	Unrestrained
Goodness-of-fit on F^2	2.088
Final R indices [$I > 2\sigma(I)$, 5352 reflections]	$R_1 = 0.0302$, $wR_2 = 0.0514$
R indices (all data)	$R_1 = 0.0362$, $wR_2 = 0.0518$
Type of weighting scheme used	Sigma
Weighting scheme used	$w = 1/\sigma^2(F_o^2)$
Max shift/error	0.001
Average shift/error	0.000
Largest diff. peak and hole	0.480 and -0.327 e. \AA^{-3}

Special Refinement Details

Refinement of F^2 against ALL reflections. The weighted R-factor (wR) and goodness of fit (S) are based on F^2 , conventional R-factors (R) are based on F , with F set to zero for negative F^2 . The threshold expression of $F^2 > 2\sigma(F^2)$ is used only for calculating R-factors(gt) etc. and is not relevant to the choice of reflections for refinement. R-factors based on F^2 are statistically about twice as large as those based on F , and R-factors based on ALL data will be even larger.

All esds (except the esd in the dihedral angle between two l.s. planes) are estimated using the full covariance matrix. The cell esds are taken into account individually in the estimation of esds in distances, angles and torsion angles; correlations between esds in cell parameters are only used when they are defined by crystal symmetry. An approximate (isotropic) treatment of cell esds is used for estimating esds involving l.s. planes.

Table 3. Crystal data and structure refinement for Compound 6

Empirical formula	C ₂₀ H ₃₁ ClZr
Formula weight	398.12
Crystallization Solvent	Diethylether/petroleum ether
Crystal Habit	Fragment
Crystal size	0.36 x 0.26 x 0.26 mm ³
Crystal color	Yellow

Data Collection

Type of diffractometer	Bruker SMART 1000	
Wavelength	0.71073 Å MoK α	
Data Collection Temperature	100(2) K	
θ range for 22335 reflections used in lattice determination	2.37 to 45.84°	
Unit cell dimensions	a = 8.9772(2) Å b = 13.5673(4) Å c = 17.2242(5) Å	α = 101.6260(10)° β = 104.3560(10)° γ = 100.4190(10)°
Volume	1930.85(9) Å ³	
Z	4	
Crystal system	Triclinic	
Space group	P-1	
Density (calculated)	1.370 Mg/m ³	
F(000)	832	
Data collection program	Bruker SMART v5.054	
θ range for data collection	1.58 to 46.45°	
Completeness to $\theta = 46.45^\circ$	83.0 %	
Index ranges	-18 \leq h \leq 18, -27 \leq k \leq 27, -32 \leq l \leq 35	
Data collection scan type	ω scans at 7 ϕ settings	
Data reduction program	Bruker SAINT v6.45	
Reflections collected	54797	
Independent reflections	28459 [R _{int} = 0.0515]	
Absorption coefficient	0.704 mm ⁻¹	
Absorption correction	None	
Max. and min. transmission	0.8382 and 0.7857	

Table 3 (cont.)**Structure solution and Refinement**

Structure solution program	SHELXS-97 (Sheldrick, 1990)
Primary solution method	Direct methods
Secondary solution method	Difference Fourier map
Hydrogen placement	Geometric positions
Structure refinement program	SHELXL-97 (Sheldrick, 1997)
Refinement method	Full matrix least-squares on F^2
Data / restraints / parameters	28459 / 0 / 413
Treatment of hydrogen atoms	Riding
Goodness-of-fit on F^2	1.157
Final R indices [$I > 2\sigma(I)$, 18839 reflections]	$R1 = 0.0390$, $wR2 = 0.0748$
R indices (all data)	$R1 = 0.0668$, $wR2 = 0.0786$
Type of weighting scheme used	Sigma
Weighting scheme used	$w = 1/\sigma^2(F_o^2)$
Max shift/error	0.004
Average shift/error	0.000
Largest diff. peak and hole	1.282 and -0.693 e. \AA^{-3}

Special Refinement Details

Refinement of F^2 against ALL reflections. The weighted R-factor (wR) and goodness of fit (S) are based on F^2 , conventional R-factors (R) are based on F , with F set to zero for negative F^2 . The threshold expression of $F^2 > 2\sigma(F^2)$ is used only for calculating R-factors(gt) etc. and is not relevant to the choice of reflections for refinement. R-factors based on F^2 are statistically about twice as large as those based on F , and R-factors based on ALL data will be even larger.

All esds (except the esd in the dihedral angle between two l.s. planes) are estimated using the full covariance matrix. The cell esds are taken into account individually in the estimation of esds in distances, angles and torsion angles; correlations between esds in cell parameters are only used when they are defined by crystal symmetry. An approximate (isotropic) treatment of cell esds is used for estimating esds involving l.s. planes.

Table 4. Crystal data and structure refinement for Compound 22

Empirical formula	C ₁₉ H ₃₀ Zr
Formula weight	349.65
Crystallization Solvent	Pentane
Crystal Habit	Block
Crystal size	0.26 x 0.19 x 0.15 mm ³
Crystal color	Pale yellow

Data Collection

Preliminary Photos	Rotation	
Type of diffractometer	CCD area detector	
Wavelength	0.71073 Å MoK α	
Data Collection Temperature	98(2) K	
θ range for 19519 reflections used in lattice determination	2.38 to 28.50°	
Unit cell dimensions	a = 17.658(3) Å b = 8.2098(13) Å c = 25.878(4) Å	β = 109.532(2)°
Volume	3535.7(10) Å ³	
Z	8	
Crystal system	Monoclinic	
Space group	P2/c	
Density (calculated)	1.314 Mg/m ³	
F(000)	1472	
Data collection program	Bruker SMART	
θ range for data collection	1.71 to 28.52°	
Completeness to $\theta = 28.52^\circ$	94.4 %	
Index ranges	-22 \leq h \leq 23, -10 \leq k \leq 10, -34 \leq l \leq 34	
Data collection scan type	ω scans at 9 ϕ settings	
Data reduction program	Bruker SAINT v6.2	
Reflections collected	81002	
Independent reflections	8478 [R _{int} = 0.2107]	
Absorption coefficient	0.613 mm ⁻¹	
Absorption correction	None	
Max. and min. transmission	0.9148 and 0.8575	

Table 4 (cont.)**Structure solution and Refinement**

Structure solution program	SHELXS-97 (Sheldrick, 1990)
Primary solution method	Patterson method
Secondary solution method	Difference Fourier map
Hydrogen placement	Geometric positions
Structure refinement program	SHELXL-97 (Sheldrick, 1997)
Refinement method	Full matrix least-squares on F^2
Data / restraints / parameters	8478 / 0 / 369
Treatment of hydrogen atoms	Riding
Goodness-of-fit on F^2	1.217
Final R indices [$I > 2\sigma(I)$, 5799 reflections]	$R1 = 0.0571$, $wR2 = 0.0876$
R indices (all data)	$R1 = 0.0991$, $wR2 = 0.0958$
Type of weighting scheme used	Sigma
Weighting scheme used	$w = 1/\sigma^2(F_o^2)$
Max shift/error	0.002
Average shift/error	0.000
Largest diff. peak and hole	1.045 and -1.567 e. \AA^{-3}

Special Refinement Details

Refinement of F^2 against ALL reflections. The weighted R-factor (wR) and goodness of fit (S) are based on F^2 , conventional R-factors (R) are based on F , with F set to zero for negative F^2 . The threshold expression of $F^2 > 2\sigma(F^2)$ is used only for calculating R-factors(gt) etc. and is not relevant to the choice of reflections for refinement. R-factors based on F^2 are statistically about twice as large as those based on F , and R-factors based on ALL data will be even larger.

All esds (except the esd in the dihedral angle between two l.s. planes) are estimated using the full covariance matrix. The cell esds are taken into account individually in the estimation of esds in distances, angles and torsion angles; correlations between esds in cell parameters are only used when they are defined by crystal symmetry. An approximate (isotropic) treatment of cell esds is used for estimating esds involving l.s. planes.